UNIVERSIDAD DE MURCIA

ESCUELA INTERNACIONAL DE DOCTORADO

TESIS DOCTORAL

Reset control of multiple-input single-output systems

Control reseteado de sistemas con múltiples entradas y una sola salida

D. José Francisco Sáez Pérez

2023

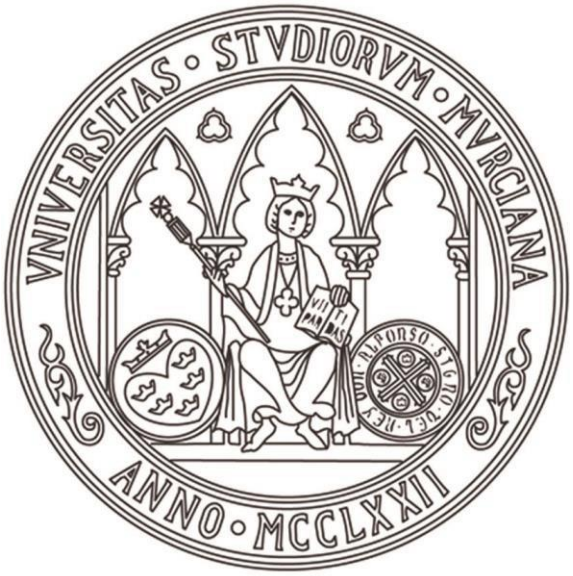

UNIVERSIDAD DE MURCIA

ESCUELA INTERNACIONAL DE DOCTORADO

TESIS DOCTORAL

Reset control of multiple-input single-output systems

Control reseteado de sistemas con múltiples entradas y una sola salida

Autor: D. José Francisco Sáez Pérez

Director/es: D. Alfonso Baños Torrico

UNIVERSIDAD DE MURCIA

DECLARACIÓN DE AUTORÍA Y ORIGINALIDAD DE LA TESIS PRESENTADA EN MODALIDAD DE COMPENDIO O ARTÍCULOS PARA OBTENER EL TÍTULO DE DOCTOR

Aprobado por la Comisión General de Doctorado el 19-10-2022

D./Dña. José Francisco Sáez Pérez

doctorando del Programa de Doctorado en

Informática

de la Escuela Internacional de Doctorado de la Universidad Murcia, como autor/a de la tesis presentada para la obtención del título de Doctor y titulada:

Reset control of multiple-input single-output systems /
Control reseteado de sistemas con múltiples entradas y una sola salida

y dirigida por,

D./Dña. Alfonso Baños Torrico

D./Dña.

D./Dña.

DECLARO QUE:

La tesis es una obra original que no infringe los derechos de propiedad intelectual ni los derechos de propiedad industrial u otros, de acuerdo con el ordenamiento jurídico vigente, en particular, la Ley de Propiedad Intelectual (R.D. legislativo 1/1996, de 12 de abril, por el que se aprueba el texto refundido de la Ley de Propiedad Intelectual, modificado por la Ley 2/2019, de 1 de marzo, regularizando, aclarando y armonizando las disposiciones legales vigentes sobre la materia), en particular, las disposiciones referidas al derecho de cita, cuando se han utilizado sus resultados o publicaciones.

Además, al haber sido autorizada como compendio de publicaciones o, tal y como prevé el artículo 29.8 del reglamento, cuenta con:

- *La aceptación por escrito de los coautores de las publicaciones de que el doctorando las presente como parte de la tesis.*
- *En su caso, la renuncia por escrito de los coautores no doctores de dichos trabajos a presentarlos como parte de otras tesis doctorales en la Universidad de Murcia o en cualquier otra universidad.*

Del mismo modo, asumo ante la Universidad cualquier responsabilidad que pudiera derivarse de la autoría o falta de originalidad del contenido de la tesis presentada, en caso de plagio, de conformidad con el ordenamiento jurídico vigente.

En Murcia, a 11 de marzo de 2023

Fdo.: José Francisco Sáez Pérez

Esta DECLARACIÓN DE AUTORÍA Y ORIGINALIDAD debe ser insertada en la primera página de la tesis presentada para la obtención del título de Doctor.

Información básica sobre protección de sus datos personales aportados	
Responsable:	Universidad de Murcia. Avenida teniente Flomesta, 5. Edificio de la Convalecencia. 30003; Murcia. Delegado de Protección de Datos: dpd@um.es
Legitimación:	La Universidad de Murcia se encuentra legitimada para el tratamiento de sus datos por ser necesario para el cumplimiento de una obligación legal aplicable al responsable del tratamiento. art. 6.1.c) del Reglamento General de Protección de Datos
Finalidad:	Gestionar su declaración de autoría y originalidad
Destinatarios:	No se prevén comunicaciones de datos
Derechos:	Los interesados pueden ejercer sus derechos de acceso, rectificación, cancelación, oposición, limitación del tratamiento, olvido y portabilidad a través del procedimiento establecido a tal efecto en el Registro Electrónico o mediante la presentación de la correspondiente solicitud en las Oficinas de Asistencia en Materia de Registro de la Universidad de Murcia

Agradecimientos

Me gustaría agradecer ante todo a mi director de tesis, Alfonso Baños, por su excelente guía y consejo durante el desarrollo de mis estudios de doctorado. También quiero expresar mi gratitud a Aurelio Arenas, cuyos conocimientos técnicos ha sido de gran ayuda sobre todo en el apartado experimental. También me gustaría dar las gracias a mis antiguos compañeros de doctorado, Pedro, Cristian, Ovidio y Pedro Gil, por su gran espíritu de trabajo y compañerismo.

Agradecer también a los miembros de los distintos grupos de investigación con los que he tenido el placer de colaborar, José Luis Guzmán, José Carlos Moreno, Manuel Berenguel, Juan Ignacio Mulero, Antonio Barreiro, Emma Delgado, Miguel Díaz-Cacho, Pablo Falcón y Miguel Cerdeira.

Finalmente, quisiera dar las gracias a mi familia y a mis amigos por apoyarme durante todo este periodo, en especial a mi hermana, cuyo apoyo incondicional en los momentos difíciles ha sido inmejorable.

Financiación

Dar las gracias al Ministerio de Ciencia e Innovación por parte de la financiación de esta tesis doctoral bajo los proyectos DPI2016-79278-C2-1-R y PID2020-112709RB-C22 y el subprograma de formación de personal investigador (FPI), y a la Fundación Séneca por parte de la financiación de esta tesis bajo la ayuda a la realización de proyecto n. 20842/PI/18.

Abstract

This thesis is concerned with reset control and hybrid reset-based control strategies for multiple-input single-output systems. Reset control, a kind of hybrid control where controllers instantaneously update (reset) their state in response to certain events, first appeared in the 1950s as a way to overcome fundamental limitations on the performance of linear time-invariant control systems. A great deal of research has been published during the last three decades showing the potential benefits of reset control, and developing a mathematical theory that appropriately models the behavior of reset systems. However, only a few works so far have dealt with the reset control of multivariable systems.

Multiple-input single-output systems, or MISO for short, are a particular type of multivariable system in which several degrees of freedom are available to control a single objective variable. MISO control strategies are usually focused on sharing the control load among different controllers in order to decrease wear on actuators, surpass limitations in range or provide a more robust control.

The practical motivation of considering MISO reset control systems lies in the design of new strategies obtaining a higher performance than possible with linear strategies while keeping a simple design and implementation, which leads to a higher potential applicability. Another motivation lies in advancing the theory of reset control, since the collection of such strategies and associated theoretical developments represents an important step towards the most general case of multiple-input multiple-output (MIMO) reset control systems.

In this context, the main objectives considered during the development of this work are the following. In first place, to formalize the reset controller, as well as different types of MISO reset control system, in the formalism of Hybrid Inclusions (HI). Secondly, to embark in a study of the theoretical properties of these systems,

including stability and robustness. Thirdly, to explore new reset-based strategies aimed especially at improving performance, and, whenever possible, systematically derive sets of tuning rules and design methodologies appropriate for MISO systems under different configurations and control objectives. Particular focus has been given to those design strategies that extend previously known methods valid for single-input single-output (SISO) systems. Finally, to apply these developments to a practical system, namely a heat exchanger in a food processing pilot plant.

After an introduction to the Hybrid Inclusions formalism, a robust model for the Clegg integrator (a basic building block of a reset controller) as a hybrid system with inputs is introduced, followed by a discussion of the resetting laws to be used. Next, a model for a general reset controller and a particular specialization of such, the PI+CI controller, are provided, considering a modification of the latter with a varying reset ratio. After that, closed loop models for SISO and MISO reset control systems are developed, focusing on the parallel control configuration (in which every controller receives the same input signal), and distinguishing between synchronous and asynchronous resetting laws. Possible extensions to these models are also addressed, which account for various phenomena such as exogenous inputs, derivative filters and time regularization.

An important property of a hybrid model in the HI formalism is well-posedness, which is related to a robust existence and uniqueness of solutions. Well-posedness is studied and proven for the previous closed loop MISO reset control system models. Similarly, the stability of the closed loop models is analyzed, resulting in a set of stability conditions determining when such a MISO reset control system is stable. These conditions are derived from a Lyapunov function, and are stated in the form of linear matrix inequalities (LMI), which is useful for computation. A different kind of stability condition is proposed for systems where only a finite number of reset actions are enabled.

Systems with time delays are crucial in the field of control systems, as most practical systems feature some kind of delay, either in the underlying physical process or in the acquisition and transmission of data. The presence of delays requires an extension to the Hybrid Inclusions formalism to systems with memory. After an introduction to this formalism is provided, a new reset-based control strategy, the reset-and-hold strategy, is introduced for the control of SISO and MISO systems with time delay. The properties of the proposed strategy are studied in the frequency domain by means of a

describing function analysis, and the model for a general reset-and-hold controller is next provided. Finally, the full closed loop models for (SISO and MISO) reset-and-hold systems with time delays are built, and their well-posedness and stability properties are investigated. The latter results in two main sets of LMI stability conditions, derived by means of a Lyapunov-Krasovskii method: one that doesn't take into account time delays, and another one that depends on their specific values.

In order to develop design rules, a time domain-based design methodology is followed, which is based on postulating a transient response to a step disturbance or set-point change with a finite settling time ("flat response") after a single reset action, and from there deriving the conditions that the controllers must satisfy in order to achieve this response. Doing this with a parallel control architecture featuring PI+CI controllers for a first order MISO plant results in a simple set of tuning rules for the reset ratios once the remainder of the PI+CI parameters have been fixed. In this way, previously known tuning rules for SISO first order plants have been successfully extended to the multiple input case. Some guidelines and limitations of the derived rules are discussed, such as the necessity of measuring or estimating the plant states in order to arrive at the tuned reset ratios; finally, some examples are presented which show to what extent the flat response property is preserved in the presence of noise or parameter uncertainty.

In the case of higher order MISO plants, a flat response to a step input can be seen to be unachievable with a single reset action, and so a different on-line tuning method featuring a variable band resetting law and variable reset ratios is proposed, based on minimizing an estimation of the integrated squared error between two reset instants. This also constitutes an extension of the previously known methods for SISO plants. The use of the resulting algorithm is exemplified with a second order plant.

For first order plants with delay, the previous PI+CI design methodology is used in combination with the reset-and-hold mechanism to find flat response-producing tuning rules for the relevant parameter set. A significant limitation in the presence of delays is the inability to react properly to two or more step inputs that occur very close together in time; a possible supervisory mechanism that avoids this is introduced. The simpler SISO case is treated and discussed first; the adaptation to the MISO case is then presented in an essentially identical way than in the nondelayed setting. The benefits of the reset-and-hold tuning method are showcased by means of examples.

Control strategies for other important kinds of SISO and MISO systems are proposed next: first, a PI+CI-based serial control architecture for first order MISO plants with two inputs is considered, following two approaches, one based on integrated squared error minimization, and another based on postulating a tuning rule identical to the SISO rule for one of the subplants. Afterwards, an extension of the PI+CI tuning rules to nonlinear first order plants is briefly explored. Finally, a reset-and-hold design method is applied to a PI+CI split-range control setup with a plant featuring possibly different time delays. Each of these strategies is supported by respective simulation examples.

The final part of this work is concerned with a practical application of the previous design methods, namely the parallel MISO PI+CI reset-and-hold control of a two-input single-output plant with time delay: the temperature control of a heat exchanger in a food processing pilot plant. The considered control inputs are the steam valve opening and the speed of the product pump. After a plant identification is performed, two experiments regarding reference tracking and disturbance rejection are performed, and the obtained data are presented and discussed. The results feature a good approximation of a flat response, and show significant improvements on several performance indices such as the integrated absolute error and maximum overshoot.

Resumen

Esta tesis se puede enmarcar en el área de control reseteado o reset, y concierne el desarrollo de nuevas estrategias de control híbridas basadas en reset para sistemas de múltiple entrada y una salida. El control reseteado, un tipo de control híbrido en el que los controladores modifican, o resetean, instantáneamente su estado en respuesta a determinados eventos, apareció por primera vez en los años 1950 como una manera de superar las limitaciones fundamentales en el rendimiento de los sistemas de control lineales e invariantes en el tiempo. En las últimas tres décadas se han publicado numerosos trabajos que han demostrado las potenciales ventajas del control reseteado y donde se ha desarrollado una teoría matemática que modela adecuadamente el comportamiento de estos sistemas. Sin embargo, hasta ahora solo unos pocos trabajos se han ocupado del control reseteado de sistemas multivariable.

Los sistemas de múltiple entrada y una única salida (MISO, por sus siglas en inglés) son un tipo particular de sistema multivariable en el que se dispone de varios grados de libertad para controlar una única variable objetivo. Las estrategias de control MISO suelen centrarse en repartir la carga de control entre diferentes controladores con el fin de disminuir el desgaste de los actuadores, superar las limitaciones de rango o proporcionar un control más robusto, entre otras cosas.

La motivación práctica de considerar sistemas de control de reajuste MISO radica en diseñar nuevas estrategias que consigan un rendimiento superior al posible con estrategias lineales, manteniendo un diseño e implementación sencillos, lo que va ligado a una mayor aplicabilidad en potencia. Otra de las motivaciones está en avanzar la teoría del control reseteado, ya que el conjunto de tales estrategias y de los desarrollos teóricos asociados representarían un paso importante a la hora de lidiar con el caso más general de sistemas de control reseteado con múltiples entradas y múltiples salidas (MIMO).

En este contexto, los principales objetivos considerados durante el desarrollo de este trabajo son los siguientes. En primer lugar, establecer una formulación matemática robusta del controlador reseteado, así como los diferentes tipos de sistema de control de reset MIMO, en el formalismo de Inclusiones Híbridas (HI). En segundo lugar, embarcarse en un estudio de las propiedades teóricas de estos sistemas, incluyendo la estabilidad y robustez. En tercer lugar, explorar nuevas estrategias basadas en reset dirigidas especialmente a mejorar el rendimiento y, siempre que sea posible, derivar reglas de sintonización y metodologías de diseño apropiadas para sistemas MISO bajo diferentes configuraciones y objetivos de control. Se ha prestado especial atención a las estrategias de diseño que extienden los métodos ya conocidos en trabajos previos, los cuales son válidos para sistemas de una sola entrada y una sola salida (SISO). Por último, se busca aplicar todos estos desarrollos a un sistema práctico, concretamente, a un intercambiador de calor en una planta piloto de procesamiento de alimentos.

Tras una introducción al formalismo de Inclusiones Híbridas, se presenta un modelo híbrido robusto para el integrador de Clegg (un componente básico de un controlador reseteado) como sistema híbrido con entradas, seguido de un análisis de las leyes de reseteo que se van a utilizar. A continuación, se proporciona el modelo híbrido de un controlador reseteado general y una especialización particular del mismo, el controlador PI+CI, considerando también una modificación de este último con un parámetro de reset variable. A continuación, se desarrollan modelos de lazo cerrado para sistemas de control reseteado SISO y MISO, centrándose en la configuración de control en paralelo (en la que cada controlador recibe la misma señal de entrada), y distinguiendo entre leyes de reseteo síncronas y asíncronas. También se abordan posibles ampliaciones de estos modelos, que tienen en cuenta diversos fenómenos, como entradas exógenas, filtros de derivadas o la regularización temporal.

Una propiedad importante de un modelo híbrido en el formalismo HI es el "buen condicionamiento" (*well-posedness* en inglés), un concepto relacionado con la existencia robusta y unicidad de las soluciones. Esta propiedad se estudiará y demostrará para cada uno de los modelos de lazo cerrado anteriores de sistema de control MISO reseteados. Del mismo modo, se analiza la estabilidad de los modelos de lazo cerrado, resultando en un conjunto de condiciones de estabilidad que determinan cuándo un sistema de control reseteado MISO será estable. Estas condiciones se derivan siguiendo el método de la función de Lyapunov, y se expresan en forma de desigualdades matriciales lineales (LMI), lo que resulta útil para su tratamiento computacional. También

se propone un tipo distinto de condición de estabilidad para sistemas en los que sólo se permite un número finito de acciones de reset.

El estudio de sistemas con retardos temporales es de crucial importancia en el campo de los sistemas de control, ya que la mayoría de los sistemas prácticos presentan algún tipo de retardo, ya sea en el proceso físico subyacente o en la adquisición y transmisión de datos. La presencia de retardos requiere de una extensión del formalismo de Inclusiones Híbridas para sistemas con memoria. Tras presentar una introducción a este formalismo, se presenta una nueva estrategia de control basada en reset, que se ha nombrado como *reset-and-hold* (resetear y mantener), para el control de sistemas SISO y MISO con retardo temporal. Esta estrategia se basa en la observación de que las estrategias de reseteo convencionales producen un subimpulso (*undershoot*) no deseado en sistemas con retardo en su(s) entrada(s), debido al efecto nocivo de la retroalimentación planta-controlador en el intervalo de tiempo comprendido entre la activación de una acción de reset y la recepción de esta acción por la planta; una manera de evitar esto es forzar al controlador a mantener una salida constante durante este tiempo, deshabilitando de forma efectiva esta retroalimentación durante el tiempo suficiente para evitar que se produzca subimpulso. Esto se puede conseguir con un control híbrido que conmute entre dos modos de operación: modo de reseteo y modo constante, de forma que el controlador cambie a modo constante tras cualquier acción de reset y vuelva a modo de reseteo al transcurrir un cierto tiempo, determinado por un nuevo parámetro (tiempo de permanencia o *holding time*). Tras estudiar las propiedades de la estrategia propuesta en el dominio de la frecuencia mediante un análisis de la función descriptora, se proporciona un modelo híbrido de un controlador reset-and-hold general. Por último, se construyen los modelos completos de lazo cerrado para sistemas reseteados con retardo (SISO y MISO), considerando en sistemas MISO una estrategia de control asíncrona (es decir, una estrategia donde cada controlador puede resetear de manera independiente de los otros), y al igual que en el caso anterior, se investigan las propiedades de *well-posedness* y de estabilidad. Este último análisis da lugar a dos conjuntos principales de condiciones de estabilidad expresadas por medio de desigualdades matriciales lineales (LMI), derivadas por medio del método del funcional de Lyapunov-Krasovskii: un conjunto de condiciones que no tiene en cuenta los retardos temporales, y otro menos conservador que sí depende del valor de dichos retardos.

Para el desarrollo de las reglas de diseño, se ha seguido una metodología basada en el dominio del tiempo, que consiste en postular una respuesta transitoria con un

tiempo de establecimiento finito a una perturbación escalón o cambio de consigna (lo que se ha denominado "respuesta plana") tras una única acción de reset; y a partir de aquí, derivar las condiciones que deben satisfacer los controladores para conseguir esta respuesta. Al hacer esto con una arquitectura de control en paralelo con controladores PI+CI para una planta MISO de primer orden, se obtiene un conjunto sencillo de reglas de ajuste para los coeficientes de reset una vez que se han fijado el resto de los parámetros del PI+CI. De este modo, las reglas de ajuste conocidas previamente para plantas SISO de primer orden se han conseguido extender con éxito al caso de múltiples entradas. Esta derivación va seguida de una discusión donde se detallan algunas indicaciones para el uso de las reglas derivadas y sus posibles limitaciones, tales como la necesidad de medir o estimar los estados de la planta para calcular los coeficientes de reseteo sintonizados o la posibilidad de obtener coeficientes de reseteo de magnitud alta al aplicar las reglas de ajuste en ciertas situaciones; finalmente, se presentan algunos ejemplos que muestran hasta qué punto se preserva la propiedad de respuesta plana en presencia de ruido o incertidumbre paramétrica.

En el caso de plantas MISO de orden superior, no es posible obtener una respuesta plana a una entrada de tipo escalón tras una única acción de reset, por lo cual se propone un método alternativo de sintonización en línea donde se combina una ley de reseteo de banda variable con coeficientes de reset variables en el tiempo. Este método está basado en la minimización de una estimación del error cuadrático integrado entre dos instantes de reset, que se obtiene tomando una señal de error ficticia obtenida desactivando todos los reseteos posteriores al primer instante considerado, aplicándole un peso exponencial definido por un cierto parámetro que depende del comportamiento frecuencial del sistema base, y calculando el error cuadrático integrado total de esta señal ficticia. Este método también constituye una extensión de los métodos previamente conocidos para plantas SISO. El uso del algoritmo resultante se ejemplifica en simulación con una planta de segundo orden.

Con respecto a plantas de primer orden con retardo, se utiliza la metodología de diseño PI+CI anterior en combinación con el mecanismo reset-and-hold para encontrar reglas de ajuste para el conjunto relevante de parámetros que produzcan una respuesta plana. En primer lugar se trata y discute el caso SISO, más sencillo; a continuación se presenta la adaptación al caso MISO, que discurre de forma esencialmente idéntica al escenario sin retardo. Una limitación significativa en presencia de retardos es la incapacidad de reaccionar adecuadamente a dos o más entradas escalón muy próximas en

el tiempo; para evitar este problema, se propone un posible mecanismo de supervisión añadido. Los beneficios de la estrategia reset-and-hold se muestran con ejemplos de simulación.

A continuación, se proponen estrategias de control para otros tipos importantes de sistemas SISO y MISO: en primer lugar, se considera una arquitectura de control en serie basada en PI+CI para plantas MISO de primer orden con dos entradas, donde se han seguido dos enfoques, uno de ellos basado en la minimización de una estimación del error cuadrático integrado (muy similar al método utilizado para plantas de orden alto), y otro basado en postular una regla de sintonía idéntica a la conocida regla SISO de primer orden para la rama de control con la dinámica más rápida, dejando el controlador de la otra rama sin resetear. Después, se explora brevemente una nueva extensión de las reglas de ajuste PI+CI para plantas no lineales de primer orden, enfocándose sobre todo en el caso SISO. Por último, se aplica un método de diseño reset-and-hold a una configuración de control de rango partido PI+CI en el caso de una planta MISO de primer orden que presenta retardos temporales potencialmente distintos, encontrándose que es necesario transformar la estrategia no colaborativa original en una colaborativa. Cada una de estas estrategias se apoya en ejemplos de simulación.

La parte final de este trabajo trata de una aplicación práctica de los métodos de diseño anteriores, que trata el control MISO en paralelo con controladores reset-and-hold de tipo PI+CI de un sistema de primer orden con dos entradas y una salida con retardo temporal: el control de la temperatura de un intercambiador de calor en una planta piloto de procesado de alimentos. Las entradas de control consideradas son la apertura de la válvula de vapor y la velocidad de la bomba de producto. Tras realizar una identificación de la planta, se llevan a cabo dos experimentos relativos al seguimiento de la referencia y al rechazo de perturbaciones donde se compara la estrategia reset-and-hold con una estrategia de reseteo convencional y con el sistema base lineal, y se presentan y discuten los datos obtenidos. Los resultados muestran una buena aproximación a una respuesta plana aun en presencia de retardos, con mejoras significativas en varios índices de rendimiento, tales como el error absoluto integrado y el sobreimpulso máximo.

Contents

List of Figures

List of Tables

Chapter 1

Introduction

This chapter introduces the two key concepts of reset control system and MISO control system, upon which this work is based. An updated (up to 2022) brief literature survey on reset control is included, together with a bibliographical analysis including the distribution of published works by type, by geographical location and by year of publication. The motivation and objectives of this work are then explained, followed by a list of publications derived from the thesis. Finally, an outline of the contents of the rest of the work is provided.

1.1 Preliminaries

A control system is a dynamical system which can roughly be separated into two interconnected parts, one of which -the *controller*- is used to govern or regulate the behavior of the other, usually called the *plant* or process. The controller is designed so as to maintain a certain desired steady-state and/or transient behavior in one or more process variables, also called *system outputs*; in order to achieve this, it has at its disposition a number of manipulated variables, or *control inputs*, which act on the system by means of respective actuators. Commonly, one of the control objectives is that the system's outputs follow a given reference output or setpoint.

In practice, there is always a degree of ignorance in the behavior of a system, which translates to model uncertainties. In addition, many physical processes feature unpredictable disturbances which affect the system's behavior; these are often modeled as signals that enter the system either at the plant's input(s) or its output(s). The necessity of a robust control strategy that works adequately even in the presence of

these problems leads to the use of feedback control loops. *Feedback control* is a kind of control where the input signal depends on one or more measured outputs. The measurements are made by sensors, which necessarily introduce some noise.

Traditionally, the design of control strategies has been focused on linear control strategies, in which both process and controller are modeled as linear time-invariant (LTI) systems, that is, systems which obey the superposition principle. This is mainly due to the easier mathematical treatment of these systems, which allows for the use of the Laplace transform (or the Z transform in the case of discrete systems) to reason about the system in the complex frequency domain by defining respective transfer functions $P(s)$ and $C(s)$ for the plant and controller, which are commonly rational functions of the variable s; the poles and zeros of these functions then determine the system's dynamics. Although few physical systems are truly linear, most of them possess a certain allowed range about a suitably selected operating point within which their behavior is well-approximated by a LTI system.

However, since the seminal work of Bode in the mid 20th century [67], it is known that there exist fundamental limitations on the maximum performance that LTI feedback control systems can realize. These limitations can be mathematically stated in many ways; one of the most well-known is Bode's integral formula

$$\int_0^\infty \log \left| \frac{1}{1 + C(i\omega)P(i\omega)} \right| d\omega = 0, \tag{1.1}$$

which holds for LTI feedback control systems under some conditions. Since the magnitude of the transfer function $(1 + C(s)P(s))^{-1}$ (called the sensitivity function) at real frequencies represents the amplification or attenuation of a sinusoidal disturbance of that frequency at the plant output, the above relationship means that it is impossible to design a LTI control strategy capable of regulating both low frequency disturbances (load disturbances) and high frequency disturbances (such as noise). Similar formulas exist limiting the magnitude of related transfer functions. In practice, these mean that there exist some performance specifications that no linear controller will be able to achieve.

In the control of systems featuring certain behaviors which are collectively called *nonminimum phase* phenomena, which include unstable poles, right-hand-plane zeros and time delays, these limitations become especially important [149], [328]. In partic-

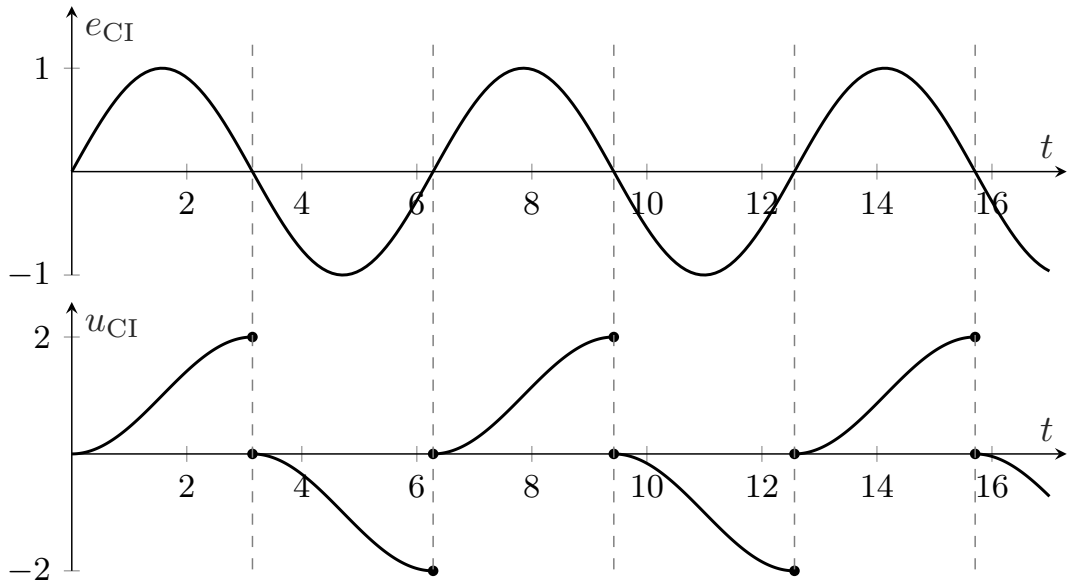

Figure 1.1: Illustration of the response of the state $u_{CI}(t)$ of the Clegg integrator to a sinusoidal input $e_{CI}(t)$.

ular, a *time-delayed system*, or delayed system for short, is a system whose current state is dependent on its past state in some way. Delayed systems are especially interesting, as they show up relatively often in control practice due to inherent physical limitations on both the speed of transport of matter (e.g. in process industry) and/or transmission of information (e.g. in networked systems). On the other hand, they are mathematically much more complicated to describe. Delayed systems can often be characterized by one or more parameters $h_1, h_2, \ldots$ (called *time delays* or dead times), so that the state at time t depends on the state at times $t - h_1, t - h_2$, etc.

Although some of the mentioned limitations are inherent to the plant and thus inescapable, many of them can be successfully transcended by going beyond linear control. As such, many kinds of nonlinear control strategies have been proposed in the last decades as a way to overcome the limitations of LTI control. This work deals with a particular kind of these strategies, namely reset control.

1.1.1 Reset control systems

Conceptually, *reset control* is a particular kind of hybrid control (i.e., a control modality involving both continuous time-based and discrete event-based evolution), in which some underlying *base controller* comes equipped with a mechanism for instantaneously changing their state back to a prescribed value, usually zero, according to a given

triggering event, the *resetting law*. Resetting laws can be based on an input reaching a given threshold value, a predefined sequence of time instants, etc. The jump itself is called a *reset action*, or just *reset* for short.

As a nonlinear control strategy, reset control is motivated by overcoming fundamental limitations inherent to LTI control. This possibility was already apparent to J. C. Clegg in 1958 [106], who, motivated by the relationship between stability and phase, introduced a modification of an integrator circuit whose state is reset to zero whenever the product of input and state becomes zero or negative, as shown in Figure 1.1. This was the first example of a reset controller, and evolved into what is now called the *Clegg integrator* (CI). Clegg performed a describing function analysis of the CI, and found an effective phase lead at all frequencies which violated Bode's integral formula, thus opening an avenue for the development of controllers pottentially better than any linear one in terms of performance.

This potential for reset control to surpass LTI control was explicitly demonstrated for the first time in the work of Beker *et al.* in 2001 [54], where it is shown that for the LTI feedback control of a plant with an integrator (i.e., a plant whose transfer function is of the form $P(s) = Q(s)/s$ for some $Q(s)$), under the assumption that the controller stabilizes, the error signal $e = y - y_{ref}$ due to a unit step reference change must satisfy

$$\int_0^\infty e(t)dt = \frac{1}{k}, \tag{1.2}$$

where $k = \lim_{s\to 0} sC(s)P(s)$. This is shown to imply that a performance specification for which (i) the rise time t_r (the time taken for the output to reach the reference value) is slower than $2/k$ and (ii) the overshoot (the amount over which the output exceeds the reference after reaching it) is zero cannot be met by any $C(s)$. The authors show that a FORE controller, a reset extension of a first order linear controller introduced earlier in 1975 by Horowitz and collaborators [197], can meet these specifications, thus demonstrating the advantages of reset control.

In the last two decades, the discipline of reset control has proven very fruitful, seeing the development of several research lines and the establishment of a solid mathematical foundation, as well as a multitude of practical applications in various areas. However, the field is far from finished, and there still exist many open questions and avenues for further research.

1.1.2 Multiple-input single-output systems

Systems featuring multiple variables have occupied a prominent place in the field of control engineering since its beginnings. A *multiple-input multiple-output* system (MIMO) is a system featuring more than one input and/or more than one output. MIMO systems arise often in control practice, due to the fact that the parts of a system very frequently interact with each other due to natural or man-made interconnections, in such a way that the system cannot be separated into independent one-variable subsystems, also called *single-input single-output* (SISO) subsystems in this context. The most studied kind of MIMO system is the square or $n \times n$ system, where there is the same number of inputs as there are outputs (n). In these systems, the number of control degrees of freedom exactly matches the number of manipulated variables, which makes the analysis easier in some respects.

However, non-square $m \times n$ systems with $m \neq n$ are also found in many physical processes. These can be divided into two kinds:

- *Under-actuated systems* ($m < n$): systems which have less control inputs than outputs. These systems are necessarily limited in their ability to manipulate the system. The extreme case is that of *single-input multiple-output* (SIMO) systems, where only one input is available to control several outputs.
- *Over-actuated systems* ($m > n$): systems with more available inputs than system outputs. In this kind of system, there exist redundant degrees of freedom which are not strictly necessary in order to control all outputs. In particular, *multiple-input single-output* (MISO) systems feature several control inputs and only one output.

The structure of a typical MISO plant P is depicted in Figure 1.2: the n inputs are labelled u_1 to u_n, and the output is y. Note that if the MISO system is linear and time invariant, it can be regarded as the sum of n subsystems $P_1, \ldots, P_n$.

The control of MISO systems will be the main focus of this work. The availability of several control inputs provides a certain flexibility due to the existence of more control degrees of freedom than variables one wishes to control. These extra degrees of freedom can then be utilized for various purposes, e.g. to reduce the control action of one or more controllers (in order to minimize the corresponding operational cost), to

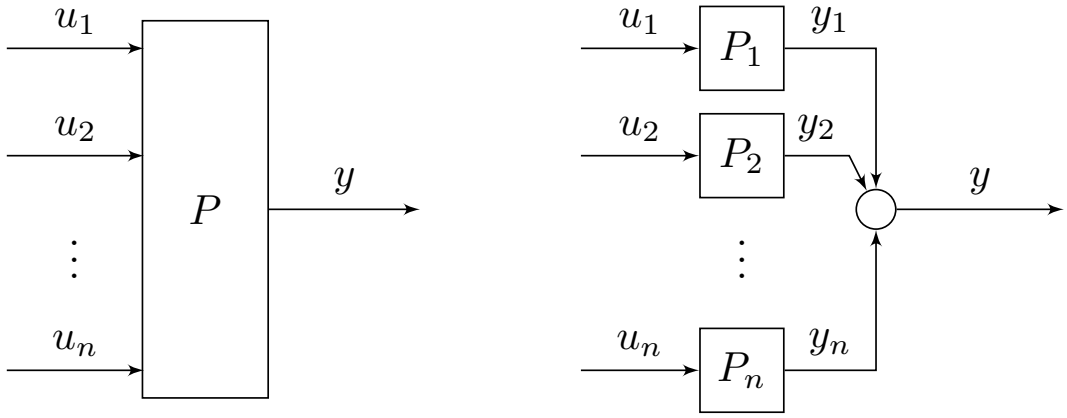

Figure 1.2: Left: structure of a MISO system. Right: a LTI MISO plant can be decomposed as the sum of n subplants.

add robustness against failure (by using redundant controllers), to allow for a greater actuation range, or to achieve a greater performance in the manipulated variable with regard to a given metric.

Due to the lack of a unified nomenclature and the disparity in control approaches in the literature, a classification of MISO control structures and strategies was proposed in [313] according to their properties; this classification will be adopted in the remainder of this work.

MISO control strategies can be divided into collaborative or noncollaborative. Noncollaborative strategies are based on the use of one control input at a time; in this way, the system can be controlled like if it were a SISO system, except in the possible transitions from one input to another. A characteristic example of a noncollaborative strategy is split-range control [13].

In contrast, in a collaborative strategy, several control inputs can be active at the same time, and the focus is on sharing the control effort among different controllers to achieve performance specifications and/or minimize the costs of feedback. Collaborative strategies can be further divided into parallel and serial according to the disposition of controllers [136]: essentially, in the parallel configuration, all controllers receive the same input, i.e. the tracking error signal associated to the plant output, while in the serial configuration, the controllers are ordered in advance according to their transient dynamics, and the input of each controller is related to the output of the one immediately faster in this ordering (only the first controller receives the tracking

error). This work will focus mainly on the parallel control structure, due mainly to its simplicity when it comes to building appropriate resetting laws, although a brief exploration of reset strategies for the serial structure is also included.

The reset control of feedback MIMO systems is not sufficiently explored, as the literature for reset control techniques applying specifically to MIMO systems [55, 246, 386, 403] is relatively scarce. An important question, yet not properly tackled, is how to find appropriate resetting laws in the case of plants with multiple outputs (and thus multiple error signals) [1]. The main approach in the former works is the use of sector-based laws; the exception is [403], where the considered resetting law is essentially the combination of several zero crossing reset laws associated to each independent error signal. However, the problem is also challenging if it is restricted to one output, i.e. for a multiple-input single-output (MISO) control problem.

1.2 Literature survey of reset control

The field of reset control can be said to initiate in 1958 with the seminal work of J. Clegg [106], who introduced the first reset controller, the Clegg integrator, as an operational amplifier circuit. Around a decade later, in 1974, Horowitz and others [235] noticed the potential benefits of resetting, and incorporated this idea into a fully developed control design strategy; the resetting condition of the CI, in which a reset is triggered whenever its input multiplied by its state becomes negative, was here simplified to a zero-crossing detection in the input, i.e., a reset is triggered when the input becomes zero. In order to be able to reach a zero steady state error, they developed a control setup combining in parallel a linear integrator and a CI, and showed that the use of this controller could lead to performance specifications not achievable by any linear controller.

A year later, Horowitz and Rosenbaum [197] devised the first order reset element (FORE) as a modification of the Clegg integrator, and considered a systematic control design method in which the base linear dynamics was tuned so as to meet performance and robustness specifications excluding overshoot, and then reset actions were used to separately handle an overshoot specification while preserving the others.

The previous developments were limited to specific cases. Lacking a general theory of reset control, the field lay essentially dormant (with the exception of the works [232]

and [66]) until the late 1990s, when Hu, Zheng, Chait, Hollot and others [94, 431] started a new research line with the aim of establishing a theoretical formalism for the modeling and analysis of general reset control systems (still using the same zero-crossing resetting law), including studies on stability, performance and robustness, culminating in the work [58] where the term "reset controller" was coined. One of the most important results is the H_β condition, which allows for checking the stability of a reset control system using properties of the base linear system in the frequency domain.

Another research line, started at around the same time by the works of Haddad *et al.* [77, 184], concerned the development of a framework for a more general class of reset systems, by simultaneously considering more general state-dependent or time-dependent resetting criteria, and allowing for partial resetting to a nonzero value. This generalization, based on the theory of impulsive differential equations, led to what is now known as the Impulsive Dynamical Systems (IDS) framework.

A little later in 2005, Zaccarian *et al.* introduced a new version of the Clegg integrator that uses the original implementation considered by Clegg, in which the CI resets to zero whenever its state and its input have different signs (now referred to as a "sector based" resetting law), motivated by the fact that the simplified model with zero crossing law suffers from a lack of robustness under noisy inputs, and leads to the existence of unphysical solutions. From this work derived an important research line which included the development of piecewise quadratic Lyapunov-based stability conditions [282, 283], LMI based approaches for performance analysis [2, 371], and further generalizations of the control structure in [146, 147]. A review of many of these results can be found in [308].

In 2009, an alternative framework for the modeling of general hybrid systems was developed by Goebel, Sanfelice and Teel [158, 159], now known as the Hybrid Inclusions (HI) framework [128]. This framework is based on treating continuous and discrete dynamics separately through the use of two respective parameters t and j, and the possibility of incorporating robustness properties automatically into the model by the use of set inclusions instead of equations.

On the other hand, under the IDS framework and based on the simplified zero crossing resetting law, Baños, Barreiro and collaborators carried out important foundational work for reset control systems, where their formalization was completed [18, 26],

including studies of existence of solutions, Zeno behavior, robustness, etc. and extended to different resetting laws [362], as well as to systems with inputs, time delays and with saturation [46, 84, 120]. This research line led to conditions for reset-times-dependent and delay-dependent closed loop stability, existence and uniqueness of solutions, continuous dependence on initial conditions, input-output stability, etc. A summary of some of these results can be found in the monograph [18]. Control design techniques based on the well-known proportional-integral (PI) controller have also been explored, resulting in the PI+CI controller [31]. Applications of this last controller include [118, 123, 132, 224, 277, 358, 359].

Some relevant research lines that have emerged during the last two decades are described next.

- **Reset control with fixed reset instants**: this research line, which originated in the year 2006 with the works [196, 249, 372], comprises the study of reset controllers for which the reset instants are fixed in advance, and the design problem is to choose the appropriate instants and after-reset states (which are not reset to zero, but are allowed to reset to some nonzero value) in an optimal way. A periodic sequence of reset instants is commonly considered. These works were followed by [154, 155, 172, 177, 178, 240, 243, 365, 429, 430], in which applications were found in the control of hard disk drives and piezoelectric actuators. Concretely, the work [241] deals with a hard disk drive control system modeled as a MISO plant, and controlled by a serial architecture. On a more theoretical note, [188] discusses stability and $\mathcal{L}_2$ gain properties, and a relaxation of the periodicity condition to nearly-periodic reset is studied in [193].

- **Reset observers**: this research line is based on the so-called impulsive or reset adaptive observers, in which the techniques inherent to reset control are applied to the design of observers for the estimation of process variables, thus overcoming the limitations inherent to linear adaptive observers. They were introduced in the work [292], and further developed in [289]. An extension to MIMO systems is considered in [293]. Further work is found in [39, 139, 163, 290, 293, 395, 413]. Applications include [4, 10, 39, 153, 319].

- **Discrete-time reset control**: a formulation of reset controllers adapted to discrete time evolution, suitable for digital controllers. A first application to

the control of hard disk drives was considered in [240, 242, 243] and a first formalization appears in [47], followed by the works [27, 28, 298, 299]. Stability has been considered e.g. in [169, 170, 383, 384] and in [87]. Further studies on this line have been carried out in [103, 166, 181, 338, 378, 419], including an extension to discrete-time MIMO systems proposed in [403].

- **Fractional reset control**: this research line consists of the combination of reset control and fractional order control (a linear control approach based upon the concept of fractional integration and differentiation). The properties of this system were studied in [202] and in the subsequent works [201, 205, 206], including a study of stability [203] and an application to the control of servomotors [204]. A fractional generalization of the FORE, the so-called generalized fractional order reset element (GFrORE), was introduced in [318] and applied to exhaust gas recirculation systems in [391]. Further works on fractional reset include [96, 97, 207, 231, 269–271, 327, 366, 368, 370].

- **Frequency based reset control**: this line of research involves the formulation of control analysis and synthesis methods for reset controllers based on the frequency domain, in order to achieve a better compatibility with common LTI control techniques more familiar to industrial control practice. The first results on this line were developed already by Beker, Hollot and coworkers [58, 59], including the H_β condition (which was further extended to systems with time delay in [18]). In the work of van Loon *et al.* in 2017 [354], a new frequency based method was devised for assessing the stability of reset controllers. Some other works on this line include [74, 111]. Another kind of development concerns the higher order sinusoidal input describing function (HOSIDF) [286], a certain extension of the describing function method, to describe reset controllers in the frequency domain [78, 209].

- **Generalized reset elements**: increasingly sophisticated generalizations of the Clegg integrator and the FORE, apart from the already mentioned PI+CI and GFrORE, are considered e.g. in [372] (reset integral derivative element, or RIDE), [185] (second order reset element, or SORE) and [402] (generalized first order reset element, or GFORE); the constant-in-gain lead-in-phase (CgLp) element was also introduced recently in [320]. Some further works which use this last

element include [5, 209, 319].

- **Reset control of fuzzy systems**: this recent research direction, consisting of the application of reset control to systems governed by fuzzy logic, was first considered in the early work [163], and picked up again in [61, 134, 304, 366, 382, 397], where it connects with the research line of reset observers.

- **Continuous approximation to reset**: this research line, also recent, focuses on the development of nonlinear control elements and implementations which constitute a continuous approximation of the behavior of reset controllers in a certain sense, avoiding in this way the drawbacks of dealing with discontinuous signals and the ambiguities in the traditional implementations of these controllers, while still preserving many of the performance benefits of reset control. This has been explored in [229], where a continuous version of the CgLp element is introduced, and in [239, 343], where a "soft-reset" implementation of a reset system is achieved using a differential inclusion.

- **Control of multiagent systems**: this research, pioneered by the work of Meng *et al.* in 2016 [262], is of practical nature and deals with the application of reset control to the leader-following problem in multiagent systems with the aim to obtain a better transient performance. This work has been further continued and generalized to different types of multiagent systems and strategies in [104, 105, 110, 211, 263, 264, 366, 367, 400, 401, 404–407].

Some selected examples of experimental applications for reset control systems are the following:

- Control of hard disk drives. [172, 173, 177, 178, 196, 240–243, 249, 365, 372, 433]
- Automotive brake systems [90, 91, 130, 141].
- Precision motion systems [6, 14, 50, 73, 229, 294, 320, 327].
- Power converters [95, 270, 277–279, 373, 374].
- Teleoperation [39, 140, 143, 144].

- Solar collectors [360].
- Wind turbines [88, 361].
- Two-stage chemical reactors [303].
- Temperature of a heat exchanger [275, 358] [ref to Article3].
- Liquid level of a tank [123].
- Combustion oscillation systems [216, 217].
- Biodiesel production [4].
- Proton exchange membrane fuel cell [151, 251].
- Exhaust gas recirculation valve [295, 296, 391].
- Cooking pot temperature [153].
- Gantry cranes [310].
- Servomotor speed [202].
- Microgrids [17, 346, 349].
- Aircraft flight control [10, 261, 394].
- Unmanned surface vessels [364, 396].
- Marine thrusters [15].
- Lens motion system [162].
- Piezoelectric actuators [319, 428, 430].
- Magnetic suspension system [213, 214].
- Tape speed control system [432].
- Dynamic bipedal robots [11].

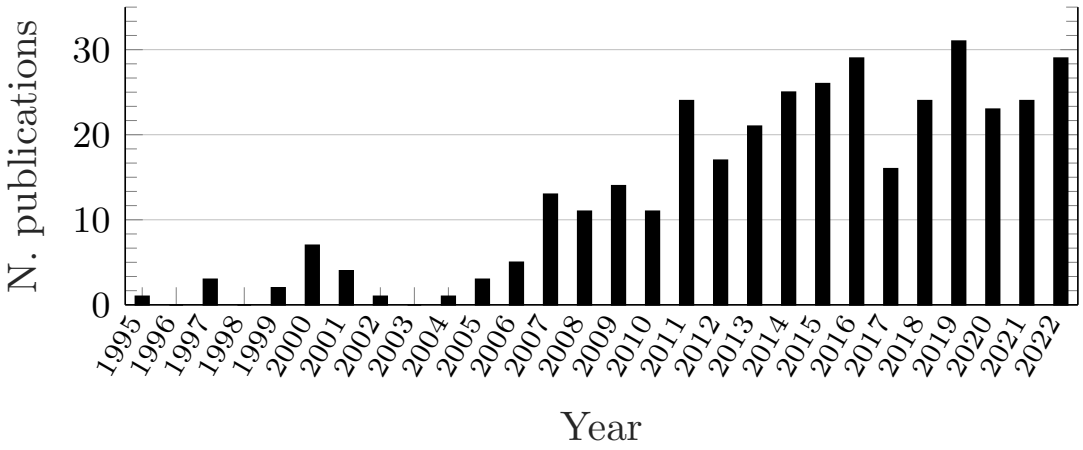

Figure 1.3: Number of publications per year in the field of reset control from 1995 to 2022 (PhD theses and books are excluded).

Bibliographical analysis

A bibliographical search for publications in the field of reset control has been performed using data gathered from Google Scholar and SCOPUS, as well as data from earlier bibliographical analyses made in [118] in the year 2015, and in the survey article [308] in the year 2018. The results have been summarized in Table 1.1, which details the authors, year and type (journal article, conference article, PhD thesis or book) of each bibliographical entry. In addition, Figure 1.3 shows the evolution of number of publications by year (excluding the small number of works before 1995), and Figure 1.3 shows the geographical distribution of publications by country. It can be deduced from this data that reset control is an active but still emerging discipline, comprising about 400 total published works as of 2022.

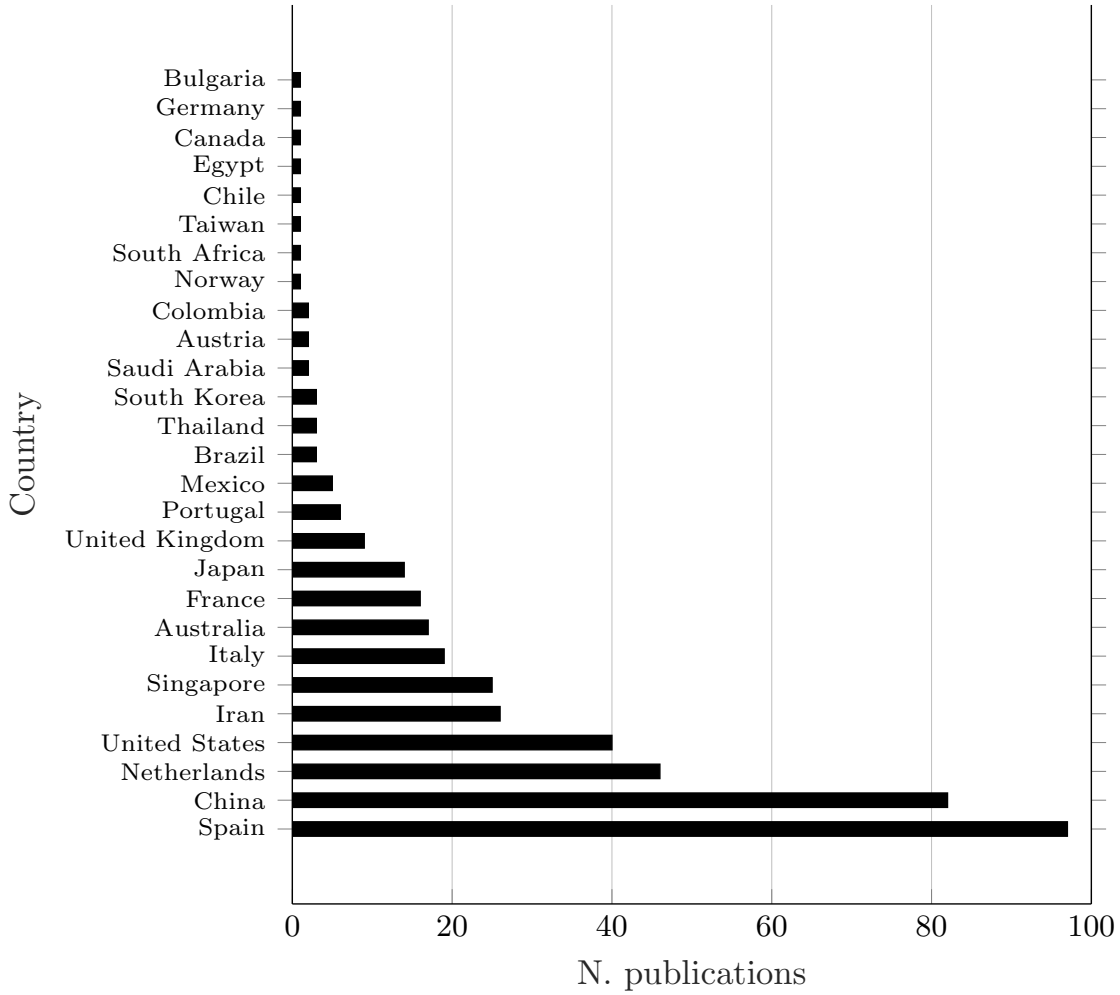

Figure 1.4: Number of publications per country in the field of reset control (PhD theses and books are excluded).

1.3 Motivation and objectives

The present work is developed within the research project DPI2016-79278-C2-1-R, which is a continuation of the coordinated project DPI2013-47100-C2-P, following a research line related to impulsive and reset control systems, also funded by Fundación Séneca (CARM) under grant 20842/PI/18.

The main motivation of considering reset control systems in general is threefold:

1. Overcoming performance limitations: surpassing the limits inherent to linear systems can be said to be the main and traditional motivation of considering reset control. Saving energy is becoming increasingly important in the 21st century with the challenges posed by climate change and geopolitical instability; consequently, the study of control techniques focused on performance and energy efficiency can help potentially lower economic and energy costs associated to industrial processes, and so provide resilience against these challenges.

2. Simplicity in design and implementation: although the underlying theoretical details can be highly nontrivial, the behavior of reset controllers themselves is simple to understand, and naturally leads to a simple modular design procedure; on the other hand, the ability to reset is already incorporated in many practical systems, and the versatility of reset strategies makes it easy to simply add an appropriate reset mechanism on top of an already designed LTI control system, and obtain in this way a better performance.

3. Theoretical significance: any advances in the study of reset control represent advances in the theory of impulsive or hybrid dynamical systems. This motivates the appropriate mathematical treatment of reset control systems by means of a sufficiently robust and versatile framework.

On the other hand, the motivation of extending reset control to MISO systems can be summarized as follows:

1. Beneficial effects of MISO: multiple-input systems allow for more flexibility in control and, in particular, a well-designed MISO control architecture for which the control effort is shared among multiple actuators can lead to a higher performance in cases where the individual control actions are limited (for example, by saturation), a potential decrease in the wearing down of the actuators, as

well as a redundancy that protects against possible controller failure. These advantages are inherent to MISO control schemes and are thus applicable to different kinds of controllers, including reset controllers.

2. Higher applicability: extending reset control techniques to multiple-input systems broadens the potential applicability of reset control, facilitating the adoption of these techniques by industry.

3. Theoretical significance: extending reset control to MISO systems is of theoretical importance in view of eventually tackling the full case of MIMO reset control systems, and already exhibits some of the potential problems expected to appear in MIMO systems, such as reset asynchronicity (a situation for which individual components of a reset control system are allowed to reset independently at different times). At the same time, the simplicity of only having to consider one error signal makes the MISO setting more tractable.

1.3.1 Objectives

The main objective of this thesis is the study of new reset control and hybrid control strategies for multiple-input single-output (MISO) systems. There are relatively very few works dealing with the reset control of multivariable systems in general; the main difficulties are the question of how to deal with multiple error signals and the treatment of independent resetting laws affecting different parts of a system. MISO systems, by the virtue of having a single output and thus only one error signal, are easier to treat than fully general MIMO systems in this regard. Thus, the development of new control strategies for these systems represents a nontrivial step towards the general multivariable case.

Derived objectives include:

- **A review of the literature concerning reset control systems**. A brief context is provided, together with a summary of historical developments and the most important research lines and applications derived from these. A short introduction to MISO control systems, putting them into context and detailing the main types and control techniques, is also included.

- **The formalization of different kinds of hybrid multiple-input single-output systems and control structures under the Hybrid Inclusions**

framework. This framework constitutes a powerful formalism for the mathematical treatment of hybrid control systems, and particularly reset control systems, in which important properties like robustness, existence of solutions, etc. are easy to deal with. However, especially in the case of systems with memory, not much work has been yet done on the appropriate formalization of reset control systems with time delay.

- **Theoretical developments concerning the stability and robustness (well-posedness) of these hybrid control systems**. As usual in the field of control, a study of stability and well-posedness of solutions is of crucial importance for any new control proposal. Specifically, the well-posedness and stability of different kinds of hybrid control systems (nondelayed MISO, delayed SISO or delayed MISO with or without the reset-and-hold strategy, with delay-independent or delay-dependent stability conditions) is considered.

- **The design of PI+CI-based tuning rules for the former MISO hybrid control systems**, generalizing known rules for SISO systems. Again the main focus will be on extending known phenomena such as the flat response property, and on recognizing in which situations this can be done, although practical considerations and limitations specific to MISO systems will also be explored.

- **The study of new hybrid control strategies focused on efficiency.** The existent PI+CI-based control design methods concerning SISO plants with time delay are not completely satisfactory, relying on either the plant being an integrator system with delay or on a Padé approximation to a second order system. Moreover, it can be shown that traditional resetting comes with certain limitations related to an overshoot-undershoot balance when delays are present. It is thus convenient to explore new hybrid (reset or reset-derived) methods, and develop associated design rules, specifically for first order systems with delay, with the aim of achieving a greater performance compared to previously known methods by overcoming this overshoot-undershoot balance.

- **A practical application of the previously developed strategies**, namely the MISO 2×1 temperature control of a heat exchanger in an experimental food processing pilot plant connected to a steam boiler. This will constitute an experimental demonstration of the performance of a new hybrid reset-based strategy for first order MISO systems with delay.

1.4 List of publications derived from this thesis

Some journal and conference publications derived from this work are gathered in the following list.

- J. F. Sáez and A. Baños. Reset control of parallel MISO systems. *MDPI Mathematics*, 9(15):1823, 2021 [315].
- J. F. Sáez, A. Baños, and A. Arenas. Reset-and-hold control of systems with time delay. *IEEE Access*, 10:101803–101813, 2022 [316].
- J. F. Sáez, A. Baños, and A. Arenas. Hybrid reset-based control of MISO Systems with delays. Submitted to *ISA Transactions* (under review).
- J. F. Sáez and A. Baños. Tuning rules for the design of MISO reset control systems. In 2020 6th International Conference on Event-Based Control, Communication, and Signal Processing (EBCCSP), Kraków, Poland, 23–25 September 2020; IEEE: New York, NY, USA, 2020; pp. 1–7 [314].
- J. F. Sáez, A. Baños, and A. Arenas. Multiple-Input Reset-and-Hold Control of Systems with Delay. Submitted to International Conference on Control, Decision and Information Technologies (CODIT), Rome, Italy, 03-06 July 2023 (under review).

1.5 Outline of contents

The remainder of this work is structured as follows.

In Chapter 2, the problem of reset control for a MISO system is studied. First, the Hybrid Inclusions framework is introduced, including its version for systems with inputs. Next, a definition of reset control system is provided, starting with its most basic building block, the Clegg integrator, for which a robust implementation in the HI framework is described. The different resetting laws are discussed, and the model of a general reset controller is defined. Subsequently, the PI+CI controller is introduced, and the variable reset ratio approach is described. A discussion about the different kinds of MISO control systems follows, leading to the definitions of closed loop models for a nondelayed parallel MISO control system in the synchronous and asynchronous cases. Possible extensions to these models that account for exosystems, derivative

filters and time regularization are provided next. Finally, an analysis of well-posedness and stability is performed.

Chapter 3 is devoted to the reset control of SISO and MISO systems with time delay. The HI framework for systems with memory is introduced, explaining all the relevant concepts. A novel hybrid control strategy, reset-and-hold strategy, is described next, and a describing function analysis is performed in order to better understand its benefits. Closed loop system models are defined, first in the simpler SISO case, and next in the fully general asynchronous MISO case. A final analysis of well-posedness and stability derives in a set of stability conditions for SISO and MISO reset-and-hold control systems; one delay-independent, and the other, less conservative, delay-dependent.

Chapter 4 deals with control design, i.e., the development of tuning rules and algorithms that achieve a desired performance in a given class of MISO reset and reset-and-hold control systems. Specifically, tuning rules that achieve a "flat response" are derived for parallel MISO first order reset control systems, and for SISO and parallel MISO first order reset-and-hold control systems, thus generalizing previously known rules for SISO first order plants. Similarly, a design algorithm is developed for higher order systems. Finally, the design methodology is applied to other kinds of MISO systems. Concretely, serial control of a MISO plant is considered, applying both the approach based on tuning rules and the algorithmic approach, and comparing their results; furthermore, the PI+CI tuning rules approach is extended to a wide class of nondelayed first order nonlinear plants, and in the delayed case, another set of tuning rules is derived for split-range PI+CI reset-and-hold control of first order plants. The chapter concludes with a brief summary of the developed design strategies.

In Chapter 5, the tuning rules for PI+CI parallel reset-and-hold MISO control systems are put to the text in an experimental application. First, an identification of the plant is made, obtaining a two-input single-output first order model with time delay. Next, a parallel reset-and-hold control system is designed using the tuning rules. Two experiments are performed, considering the respective control objectives of reference tracking and disturbance rejection. Finally, the obtained results are discussed.

Finally, a summary of the main results and contributions of this work, together with some concluding remarks, and followed by a list of suggested potential future research lines, can be found in the final Conclusions chapter.

Authors	**Year**	**T**	**Ref**
Clegg	1958	J	[106]
Khishnan, Horowitz	1974	J	[235]
Horowitz *et al.*	1975	J	[197]
Karybakas	1977	J	[232]
Bobrow, Jabbari *et al.*	1995	J	[66]
Hu, Zheng *et al.*	1997	C	[210]
Hollot, Zheng *et al.*	1997	C	[195]
Bupp, Bernstein *et al.*	1997	C	[75]
Zheng	1998	T	[431]
Beker, Hollot *et al.*	1999	C	[55]
Beker, Hollot *et al.*	1999	C	[59]
Bupp, Bernstein *et al.*	2000	J	[77]
Zheng, Chait *et al.*	2000	J	[432]
Chen, Hollot*et al.*	2000	C	[98]
Haddad *et al.*	2000	C	[184]
Chen, Hollot *et al.*	2000	C	[101]
Chen, Chait *et al.*	2000	C	[102]
Beker, Hollot *et al.*	2000	C	[56]
Chen	2000	T	[100]
Chen, Chait *et al.*	2001	J	[99]
Beker, Hollot *et al.*	2001	J	[54]
Beker, Hollot *et al.*	2001	C	[57]
Hollot, Beker *et al.*	2001	B	[194]
Beker	2001	T	[60]
Chait, Hollot	2002	J	[94]
Beker, Hollot *et al.*	2004	J	[58]
Zaccarian, Nešić *et al.*	2005	C	[387]
Nešić, Zaccarian *et al.*	2005	C	[282]
Li, G. Guo, Wang	2005	C	[248]
G. Guo, Yu, Ma	2006	J	[165]
Hong, Wong	2006	C	[196]
Baños, Barreiro	2006	C	[40]
Zaccarian, Nešić *et al.*	2006	C	[388]
Li, G. Guo, Wang	2006	C	[249]
Wu, G. Guo, Wang	2007	J	[372]
Baños, Vidal	2007	C	[48]
Baños, Carrasco *et al.*	2007	C	[41]
Baños, Vidal	2007	C	[31]
Baños, Barreiro	2007	C	[44]
Baños, Carrasco *et al.*	2007	C	[45]
Y. Guo, Wang, Xie	2007	C	[178]
Zaccarian, Nešić *et al.*	2007	C	[388]
J. Zheng *et al.*	2007	C	[429]

Authors	**Year**	**T**	**Ref**
Witvoet *et al.*	2007	C	[371]
Loquen *et al.*	2007	C	[257]
Y. Guo, Wang *et al.*	2007	C	[172]
Lahee	2007	C	[238]
Bakkeheim *et al.*	2008	J	[15]
J. Zheng *et al.*	2008	J	[430]
Nešić, Zaccarian *et al.*	2008	J	[280]
Aangenent *et al.*	2008	C	[2]
Nešić, Teel *et al.*	2008	C	[283]
Vidal, Baños	2008	C	[360]
Carrasco, Baños	2008	C	[86]
Carrasco, Baños *et al.*	2008	C	[84]
Vidal, Baños *et al.*	2008	C	[359]
Fernández *et al.*	2008	C	[143]
Loquen *et al.*	2008	C	[257]
Y. Guo *et al.*	2009	J	[175]
Baños, Barreiro	2009	J	[47]
Y. Guo, Wang, Xie	2009	J	[173]
Li, Du *et al.*	2009	J	[242]
Li, Du, Wang	2009	C	[240]
Li, Du *et al.*	2009	C	[243]
Vidal, Baños	2009	C	[357]
Baños, Dormido *et al.*	2009	C	[23]
Baños, Perez *et al.*	2009	C	[47]
Li, Du *et al.*	2009	C	[244]
K. El Rifai, O. El Rifai	2009	C	[138]
Raimúndez *et al.*	2009	C	[309]
Carrasco, Baños *et al.*	2009	C	[82]
Y. Guo, Wang *et al.*	2009	C	[175]
Carrasco	2009	T	[82]
Vidal	2009	T	[357]
Aangenent *et al.*	2010	J	[1]
Zheng, Fu	2010	J	[428]
Carrasco, Baños *et al.*	2010	J	[66]
Barreiro, Baños	2010	J	[33]
Vidal, Baños	2010	J	[358]
G. Guo	2010	J	[164]
Paesa, Franco *et al.*	2010	C	[292]
Polenkova *et al.*	2010	C	[301]
Loquen, Nešić *et al.*	2010	C	[255]
Baños, Perez *et al.*	2010	C	[27]
Li, Wang	2010	C	[245]
Loquen	2010	T	[256]

Authors	**Year**	**T**	**Ref**
Zaccarian, Nešić, Teel	2011	J	[389]
Baños, Carrasco *et al.*	2011	J	[19]
Fernández, Blas *et al.*	2011	J	[144]
Paesa, Franco *et al.*	2011	J	[293]
Baños, Dormido *et al.*	2011	J	[24]
Tarbouriech *et al.*	2011	J	[342]
Nešić, Teel *et al.*	2011	J	[281]
Forni, Nešić *et al.*	2011	J	[148]
Paesa, Baños, Sagues	2011	J	[289]
Li, G. Guo, Wang	2011	J	[250]
Li, Du, Wang	2011	J	[241]
Y. Guo, Wang *et al.*	2011	J	[176]
Perez, Baños *et al.*	2011	C	[297]
Barreiro, Baños *et al.*	2011	C	[36]
Y. Guo, Wei	2011	C	[171]
Y. Guo, Gui *et al.*	2011	C	[169]
Y. Guo, Gui, Yang	2011	C	[168]
Perez, Baños *et al.*	2011	C	[299]
Perez, Baños *et al.*	2011	C	[298]
Paesa, Carrasco *et al.*	2011	C	[291]
Hetel, Daafouz *et al.*	2011	C	[192]
Satoh	2011	C	[323]
Dormido, Baños *et al.*	2011	C	[133]
Paesa, Baños *et al.*	2011	C	[290]
Paesa	2011	T	[153]
Raimúndez *et al.*	2012	J	[310]
Baños, Vidal	2012	J	[49]
Suyama, Kosugi	2012	J	[339]
Paesa, Franco *et al.*	2012	J	[221]
Carrasco, Baños	2012	J	[83]
Y. Guo, Wang, Xie	2012	J	[174]
Barreiro, Baños	2012	J	[34]
Y. Guo, Gui *et al.*	2012	J	[170]
Baños, Mulero	2012	J	[25]
Valério, S. da Costa	2012	J	[350]
Baños, Davó	2012	C	[46]
Moreno *et al.*	2012	C	[274]
Prieto, Barreiro *et al.*	2012	C	[307]
Panni, Alberger *et al.*	2012	C	[295]
Y. Guo, Xie	2012	C	[179]
Davó, Baños	2012	C	[122]
Polenkova *et al.*	2012	C	[302]
Baños, Barreiro	2012	B	[18]
Moreno *et al.*	2013	J	[275]

Authors	**Year**	**T**	**Ref**
Guillen-Flores *et al.*	2013	J	[163]
HosseinNia *et al.*	2013	J	[204]
Prieto, Barreiro *et al.*	2013	J	[306]
Bras, Carapito *et al.*	2013	J	[71]
Hetel, Daafouz *et al.*	2013	J	[193]
Carrasco *et al.*	2013	J	[87]
Liu, Xum Wang	2013	J	[254]
Lu, Lee	2013	J	[258]
Li, Fen, Xinmin	2013	C	[246]
HosseinNia, Tejado	2013	C	[203]
Falcón, Barreiro *et al.*	2013	C	[140]
HosseinNia *et al.*	2013	C	[200]
Wu, Guo, Gui, Jiang	2013	C	[375]
Davó, Baños	2013	C	[124]
Mercader, Davó *et al.*	2013	C	[267]
Suyama, Kosugi	2013	C	[340]
Davó, Baños	2013	C	[123]
Mercader *et al.*	2013	C	[267]
Zhao, Nešić *et al.*	2013	C	[411]
Pérez	2013	T	[300]
Fichera	2013	T	[146]
HosseinNia	2013	T	[200]
Yuan, Wu	2014	J	[385]
Ghaffari *et al.*	2014	J	[154]
HosseinNia *et al.*	2014	J	[205]
Shakibjoo, Vasegh	2014	J	[332]
Panni, Waschl *et al.*	2014	J	[296]
Ghaffari *et al.*	2014	J	[155]
Zhao, Wang	2014	J	[413]
Ogura, Martin	2014	J	[287]
Baños, Davó	2014	J	[20]
Barreiro, Baños *et al.*	2014	J	[37]
Baños, Perez *et al.*	2014	J	[28]
Yuan, Wu	2014	C	[386]
HosseinNia *et al.*	2014	C	[206]
Delgado, Cacho *et al.*	2014	C	[129]
Y. Guo, Zhu	2014	C	[181]
Bragagnolo *et al.*	2014	C	[69]
Zhao, Wang, Li	2014	C	[424]
HosseinNia *et al.*	2014	C	[201]
Zhao, Nešić *et al.*	2014	C	[412]
Davó, Baños, Moreno	2014	C	[120]
Acho	2014	C	[3]
Zhao, Wang, Li	2014	C	[423]

Authors	**Year**	**T**	**Ref**
Vettori *et al.*	2014	C	[356]
Delgado *et al.*	2014	C	[131]
Yuan *et al.*	2014	C	[386]
Prieto	2014	T	[305]
Baños, Perez *et al.*	2014	B	[29]
Zhao, Wang	2015	J	[415]
Zhao, Wang	2015	J	[416]
Zhao, Wang *et al.*	2015	J	[425]
Yu, Y. Guo, Zhao	2015	J	[383]
Yu *et al.*	2015	J	[384]
Wang, Zhao	2015	J	[369]
Heemels *et al.*	2015	J	[188]
Zhao, Wang	2015	J	[417]
Ghaffari *et al.*	2015	J	[156]
Zhao, Wang	2015	J	[414]
Zhao *et al.*	2015	J	[425]
Amato *et al.*	2015	J	[9]
Heertjes *et al.*	2015	C	[190]
Mercader, Davó *et al.*	2015	C	[268]
Iwai, Ushio	2015	C	[218]
Meng *et al.*	2015	C	[265]
Cordioli *et al.*	2015	C	[107]
Satoh	2015	C	[324]
Shakibjoo *et al.*	2015	C	[331]
Delgado *et al.*	2015	C	[130]
McDonough *et al.*	2015	C	[261]
Wada	2015	C	[363]
HosseinNia *et al.*	2015	C	[207]
Davó	2015	T	[118]
Zhao, Wang	2016	J	[420]
Baños *et al.*	2016	J	[26]
Ghaffari *et al.*	2016	J	[157]
Hunnekens *et al.*	2016	J	[212]
Fichera *et al.*	2016	J	[147]
Zhao, Hua	2016	J	[402]
Shin *et al.*	2016	J	[334]
Zhao, Wang	2016	J	[419]
Seuret *et al.*	2016	J	[329]
Heertjes *et al.*	2016	J	[189]
Etienne *et al.*	2016	J	[139]
González *et al.*	2016	J	[161]
Shakibjoo *et al.*	2016	J	[333]

Authors	**Year**	**T**	**Ref**
Zhao *et al.*	2016	J	[426]
Davó, Baños	2016	J	[119]
Aguilar-Garnica *et al.*	2016	J	[4]
Guo	2016	J	[166]
Zhao, Wang	2016	J	[422]
Zhao, Wang	2016	J	[421]
Iwai, Ushio	2016	C	[219]
Cánovas *et al.*	2016	C	[81]
Meng *et al.*	2016	C	[263]
Zhao, Mi	2016	C	[408]
Hazeleger *et al.*	2016	C	[185]
Meng *et al.*	2016	C	[262]
Bisoffi *et al.*	2016	C	[65]
Shizuku, Ishida	2016	C	[335]
Costas *et al.*	2016	C	[108]
Cerdeira *et al.*	2016	C	[91]
van Loon	2016	T	[353]
Suyama, Sebe	2017	J	[341]
van Loon *et al.*	2017	J	[354]
Davó *et al.*	2017	J	[125]
Vidal *et al.*	2017	J	[361]
Scola *et al.*	2017	J	[326]
Davanipour *et al.*	2017	J	[115]
Zhang *et al.*	2017	J	[395]
Jin *et al.*	2017	C	[223]
Iwai	2017	C	[215]
Toochinda *et al.*	2017	C	[344]
Zhu *et al.*	2017	C	[433]
Zhao *et al.*	2017	C	[409]
Zhai *et al.*	2017	C	[392]
Saikumar *et al.*	2017	C	[318]
Zarghami *et al.*	2017	C	[391]
Cerdeira *et al.*	2017	C	[92]
Falcón *et al.*	2018	J	[141]
Aminzadeh *et al.*	2018	J	[10]
Bisoffi *et al.*	2018	J	[64]
Prieur *et al.*	2018	J	[308]
Li, Deng	2018	J	[247]
Mahmoud, Karaki	2018	J	[260]
Nair *et al.*	2018	J	[277]
Davanipour *et al.*	2018	J	[116]
Vafamand *et al.*	2018	J	[348]

Authors	**Year**	**T**	**Ref**
Davanipour *et al.*	2018	J	[117]
Subramanian *et al.*	2018	J	[338]
Pourdehi *et al.*	2018	J	[303]
Davó *et al.*	2018	J	[126]
Cerdeira *et al.*	2018	J	[89]
Chen, Guo	2018	C	[103]
Iwai	2018	C	[216]
Joraked *et al.*	2018	C	[224]
Zhao *et al.*	2018	C	[403]
Zhao *et al.*	2018	C	[399]
Chen *et al.*	2018	C	[96]
Nair *et al.*	2018	C	[278]
Beerens *et al.*	2018	C	[52]
Palanikumar *et al.*	2018	C	[294]
Carreño *et al.*	2018	C	[88]
Cerdeira *et al.*	2018	C	[93]
Mahmoud, Karaki	2018	C	[259]
Nikolov	2018	C	[285]
Beerens *et al.*	2019	J	[51]
Meng *et al.*	2019	J	[264]
Mercader *et al.*	2019	J	[266]
Zhao *et al.*	2019	J	[410]
Saikumar *et al.*	2019	J	[319]
Saikumar *et al.*	2019	J	[320]
Nair *et al.*	2019	J	[279]
Chen *et al.*	2019	J	[97]
Zhao *et al.*	2019	J	[405]
Zhao *et al.*	2019	J	[404]
Hosseini *et al.*	2019	J	[199]
Guo, Chen	2019	J	[167]
Vafamand *et al.*	2019	J	[349]
Akyüz *et al.*	2019	J	[6]
Ferrante, Zaccarian	2019	J	[145]
Barreiro, Delgado	2019	J	[39]
Campos *et al.*	2019	J	[80]
Xiao *et al.*	2019	J	[376]
Zhan *et al.*	2019	J	[393]
Arcos *et al.*	2019	J	[11]
Valério *et al.*	2019	J	[351]
Wang *et al.*	2019	J	[365]
Ishino *et al.*	2019	C	[213]
Iwai	2019	C	[217]
Gruntjens *et al.*	2019	C	[162]

Authors	**Year**	**T**	**Ref**
Doktian *et al.*	2019	C	[132]
Chen *et al.*	2019	C	[95]
Ban, Kim	2019	C	[16]
Saikumar *et al.*	2019	C	[321]
Ishino *et al.*	2019	C	[214]
Falcón *et al.*	2019	C	[142]
Bisoffi *et al.*	2020	J	[63]
van den Eijnden *et al.*	2020	J	[352]
Xu *et al.*	2020	J	[378]
Zhao *et al.*	2020	J	[406]
Xu *et al.*	2020	J	[377]
Weise *et al.*	2020	J	[370]
Bahnamiri *et al.*	2020	J	[14]
Yazdi, Khayatian	2020	J	[380]
Pourdehi *et al.*	2020	J	[304]
Yazdi, Khayatian	2020	J	[381]
Hosseini *et al.*	2020	J	[198]
Jaramillo *et al.*	2020	J	[221]
Jaramillo *et al.*	2020	J	[220]
Zaragoza *et al.*	2020	J	[390]
Banki *et al.*	2020	J	[17]
Echreshavi *et al.*	2020	C	[134]
Dastjerdi *et al.*	2020	C	[111]
Karbasizadeh *et al.*	2020	C	[227]
Hou *et al.*	2020	C	[209]
Sáez, Baños	2020	C	[314]
Zhang *et al.*	2020	C	[396]
Cai *et al.*	2020	C	[78]
Beerens	2020	T	[50]
Zhang *et al.*	2021	J	[394]
Barreiro *et al.*	2021	J	[35]
Saikumar *et al.*	2021	J	[317]
Dastjerdi *et al.*	2021	J	[113]
Echreshavi *et al.*	2021	J	[135]
Zhao, Hua	2021	J	[407]
Beerens *et al.*	2021	J	[53]
Wu *et al.*	2021	J	[373]
Yazdi *et al.*	2021	J	[382]
Bertollo *et al.*	2021	J	[62]
Zhao, Chui	2021	J	[400]
Wang *et al.*	2021	J	[367]
Karbasizadeh *et al.*	2021	J	[231]
Wang, Zhang	2021	J	[364]

Authors	**Year**	**T**	**Ref**
Sáez, Baños	2021	J	[315]
Cui *et al.*	2021	C	[110]
Le, Teel	2021	C	[239]
Brummelhuis *et al.*	2021	C	[73]
Dastjerdi *et al.*	2021	C	[114]
Kieft *et al.*	2021	C	[233]
Kieft *et al.*	2021	C	[234]
Sebastian *et al.*	2021	C	[327]
Benalcázar *et al.*	2021	C	[61]
Wu *et al.*	2021	C	[374]
Costas *et al.*	2021	C	[109]
Dastjerdi	2021	T	[5]
Kaczmarek *et al.*	2022	J	[225]
Wang *et al.*	2022	J	[368]
Hu *et al.*	2022	J	[211]
Tugal *et al.*	2022	J	[347]
Linli *et al.*	2022	J	[251]
Karbasizadeh *et al.*	2022	J	[229]
Gao *et al.*	2022	J	[151]
He *et al.*	2022	J	[186]
Dastjerdi *et al.*	2022	J	[112]
Karbasizadeh *et al.*	2022	J	[226]
Wang, Dong	2022	J	[366]
Tu *et al.*	2022	J	[346]
Baños, Barreiro	2022	J	[43]
Mohadeszadeh *et al.*	2022	J	[269]
Zhao *et al.*	2022	J	[401]
Mohadeszadeh *et al.*	2022	J	[270]
Ali, Mahmoud	2022	J	[7]
Shahbazzadeh *et al.*	2022	J	[330]
Mohadeszadeh *et al.*	2022	J	[271]
Cheng *et al.*	2022	J	[105]
Zhang *et al.*	2022	J	[397]
Teel	2022	J	[343]
Sáez, Baños, Arenas	2022	J	[316]
Karbasizadeh *et al.*	2022	C	[228]
Karbasizadeh *et al.*	2022	C	[230]
Mohan *et al.*	2022	C	[272]
Cheng, Hu	2022	C	[104]

Table 1.1: List of publications in the field of reset control (J: journal article, C: conference article, T: PhD thesis, B: book).

Chapter 2

Reset control of multiple-input single-output systems

This chapter introduces the mathematical background upon which the developments in this work are based. First, a basic introduction to the Hybrid Inclusions framework is given, describing as well its extensions to systems with inputs and systems with memory. Under this framework, a robust model of a Clegg integrator (CI) is introduced, which is then used as a building block for a general reset controller. A discussion of the various resetting laws and control strategies follows. The proportional-integral plus Clegg integrator (PI+CI) compensator is then introduced as a particular case of the general reset controller, based upon the well-known proportional-integral (PI) controller. Next, a theoretical introduction to the control of multiple-input single-output systems is given, focusing on collaborative control design and its two main associated control structures. Finally, a full closed loop model of a multiple-input single-output (MISO) reset control system as a hybrid system is given for both control structures.

2.1 Theoretical preliminaries

Reset control systems constitute an important class of hybrid systems. Roughly speaking, a *hybrid dynamical system*, or hybrid system for short, is a system whose time evolution can be both continuous (referred to as *flowing*) and discrete (referred to as *jumping*). Numerous practical systems (analog mechanisms controlled by digital inputs, physical processes featuring phase transitions, rigid body collisions, switching systems, signal sampling, etc.) feature characteristics of both continuous-time and discrete-time

dynamical systems, and are thus susceptible to be modeled as hybrid systems.

Since the advent of the theory of hybrid systems, a multitude of mathematical frameworks have been developed to deal with their modeling and analysis. The Impulsive Differential Systems (IDS) framework [183] constitutes one of the main such frameworks that have been successfully used in the context of hybrid control systems, and is the formalism where many previous works about reset control systems under the research line of Baños *et al.* (where this work also falls) have been formalized [18, 26].

Under the IDS framework, a model of a reset control system is based on a *resetting set* $\mathcal{M} \subset \mathbb{R}^n \times \mathbb{R}$, implementing a corresponding resetting law. Solutions of the system are certain functions $\mathbf{x} : \mathbb{R} \to \mathbb{R}^n$ which are left continuous with right limits (also called *càglàd*), i.e. for all $t \in \mathbb{R}$ it holds that $\mathbf{x}(t) = \lim_{\varepsilon \to 0^-} \mathbf{x}(t+\varepsilon)$, and the limit $\mathbf{x}(t^+) = \lim_{\varepsilon \to 0^+} \mathbf{x}(t+\varepsilon)$ exists. The model of a general closed loop reset control system (i.e. disregarding reference and disturbance inputs) is then given by

$$\begin{cases} \dot{\mathbf{x}}(t) = f(\mathbf{x}(t), t), & \text{if } (\mathbf{x}(t), t) \notin \mathcal{M}, \\ \mathbf{x}(t^+) = g(\mathbf{x}(t), t), & \text{if } (\mathbf{x}(t), t) \in \mathcal{M}, \end{cases} \tag{2.1}$$

where f, g are functions governing the respective continuous and discrete evolution of the system. Commonly in state-based reset control, the resetting set $\mathcal{M}$ is taken to be a hyperplane in $\mathbb{R}^n$ defined by the condition $C_R\mathbf{x} = 0$, for a covector C_R satisfying some properties.

In contrast, in the Hybrid Inclusions framework, the other main prevailing framework in the field of reset control, the models for reset control systems (and more general hybrid control systems) are based on a different kind of function, parametrized by two variables: continuous time and discrete number of jumps. In addition, f and g are upgraded to set-valued maps in order to take into account possible indeterminacies in the system's evolution. These models come equipped with good structural properties, especially those related to robustness and well-posedness against disturbances of various nature. For this reason, this framework has been the one chosen to formalize the results in this work. Hence, an important contribution of the present thesis consists of the restatement of some of the aforementioned results regarding the design, stability, etc. of reset control systems under the HI framework, with the aim to make them more accessible to a broader part of the reset control community (see also [43]).

2.1.1 The Hybrid Inclusions framework

Definition 2.1. A *hybrid system* Σ with state $\mathbf{x} \in \mathbb{R}^n$ is formally given by

$$\Sigma : \begin{cases} \dot{\mathbf{x}} \in f(\mathbf{x}), & \text{if } \mathbf{x} \in \mathcal{C}, \\ \mathbf{x}^+ \in g(\mathbf{x}), & \text{if } \mathbf{x} \in \mathcal{D}, \end{cases} \tag{2.2}$$

with the following four data:

- The flow map $f : \mathbb{R}^n \rightrightarrows \mathbb{R}^n$.
- The jump map $g : \mathbb{R}^n \rightrightarrows \mathbb{R}^n$.
- The flow set $\mathcal{C} \subseteq \mathbb{R}^n$.
- The jump set $\mathcal{D} \subseteq \mathbb{R}^n$.

Here, the maps f, g are *set-valued* functions, which send vectors $\mathbf{x} \in \mathbb{R}^n$ to sets $f(\mathbf{x})$, $g(\mathbf{x}) \subseteq \mathbb{R}^n$. Note that as a particular case, an ordinary function $h : X \to \mathbb{R}^n$ on some domain $X \subseteq \mathbb{R}^n$ can be equivalently thought of as a set-valued function $h_{\text{set}} : \mathbb{R}^n \to \mathbb{R}^n$ such that $h_{\text{set}}(\mathbf{x}) = \{h(\mathbf{x})\}$ when $\mathbf{x} \in X$ and $h_{\text{set}}(\mathbf{x}) = \varnothing$ if $\mathbf{x} \notin X$. In the following developments, the inclusion will be replaced by an equality in (2.2) when f or g are ordinary functions.

Definition 2.2. A *hybrid time domain* E is a subset of $\mathbb{R}_{\geq 0} \times \mathbb{N}$ consisting of a union of intervals of the form $[t_j, t_{j+1}] \times \{j\}$ for $j = 0, 1, 2, \ldots$ and some nondecreasing sequence $0 = t_0 \geq t_1 \geq t_2 \ldots$ of real numbers (finite or infinite), with the last interval (if it exists) being instead of the form $[t_J, T) \times \{J\}$, with either T finite or $T = \infty$.

Intuitively, given an element $(t, j) \in E$, the real variable t will represent the time elapsed so far, and the nonnegative integer j will count the number of jumps that have occurred. Thus, under this framework continuous and discrete evolution are treated on an equal footing, allowing e.g. for the possibility of two or more jumps in the same time instant.

Definition 2.3. A *hybrid arc* is a function $\phi(t, j)$ defined on some hybrid time domain $E = \operatorname{dom} \phi$ and taking values on $\mathbb{R}^n$, which is locally absolutely continuous on each interval of E.

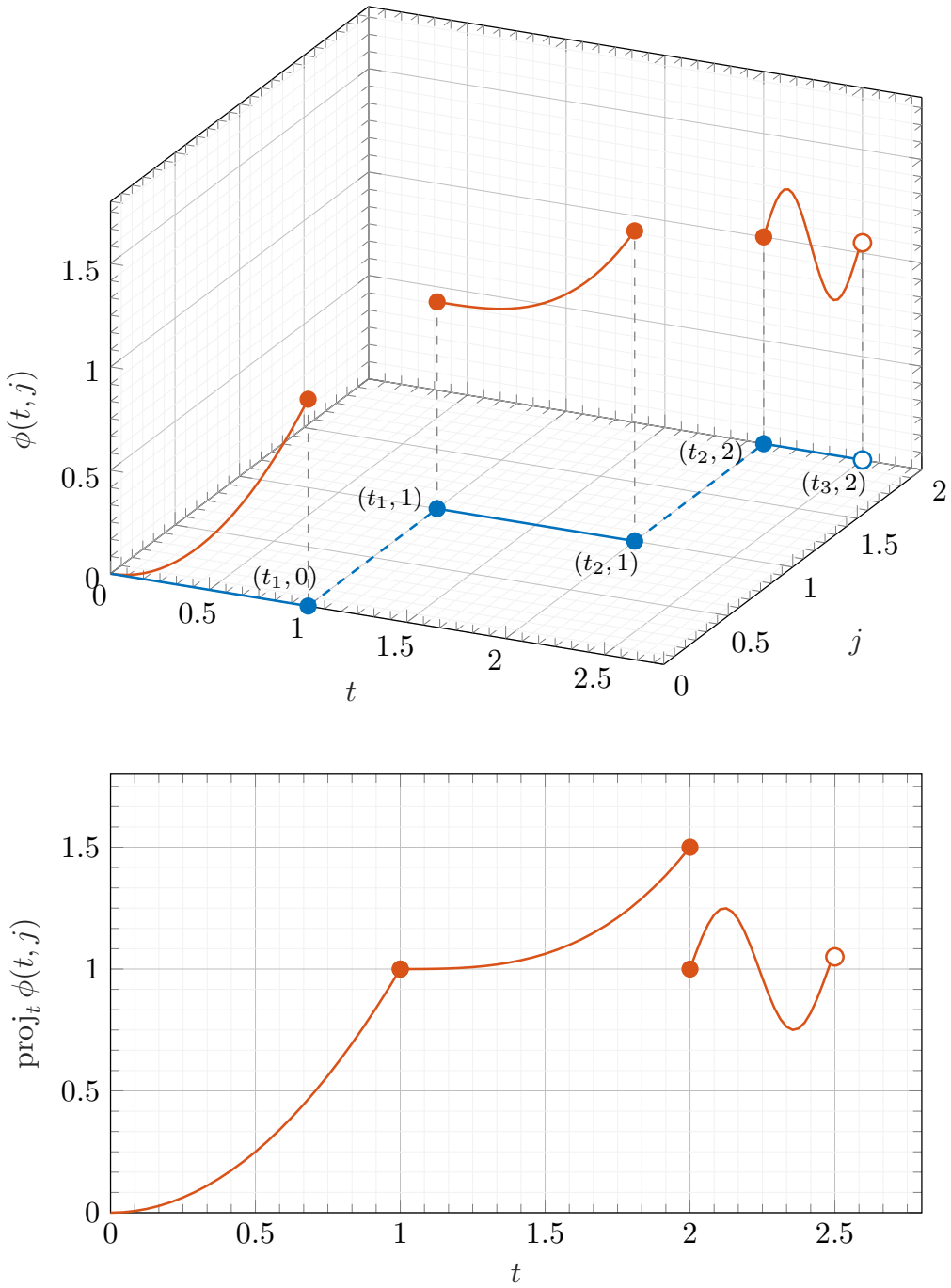

Figure 2.1: Above: representation of a hybrid arc ϕ (orange) and its associated hybrid time domain (blue) as a function of time t and the number of jumps j. Below: projection $\text{proj}_t\, \phi$ of the hybrid arc onto the continuous time domain.

Figure 2.1 depicts an example of a hybrid arc $\phi : E \to \mathbb{R}$, together with its time domain $E = \operatorname{dom} \phi$. In this case, the rightmost interval of E does not include its right endpoint; another valid choice of hybrid time domain would have been one with all intervals closed (this kind of domain is called *compact*). Note how the projection $\operatorname{proj}_t \phi$ of ϕ obtained by disregarding the parameter j is not the graph of a function, since at time $t = 2$ it achieves two different values. This kind of projection will be frequently used in this thesis to represent signals whenever the location of their jumps can be deduced from context.

Different kinds of hybrid arcs can be distinguished:

- *Complete hybrid arcs* are those whose domain is unbounded in the t-axis, the j-axis or both.
- *Zeno hybrid arcs* are those whose domain is unbounded in the j-axis but bounded in the t-axis. All Zeno hybrid arcs are complete.
- A hybrid arc is *continuous* if its domain is a subset of $\mathbb{R}_{\geq 0} \times \{0\}$, and discrete if its domain is contained in $\{0\} \times \mathbb{N}$.

Finally, solutions to the hybrid system Σ are defined to be particular hybrid arcs.

Definition 2.4. A *solution* to the hybrid system Σ given by (2.2) is a hybrid arc ϕ satisfying the following properties:

1. $\phi(t, j) \in \mathcal{C}$ for all (t, j) in any nonempty interval $I_j \subseteq \operatorname{dom} \phi$, and $d\phi(t, j)/dt \in f(\phi(t, j))$ for almost all (t, j) in the interior of I_j.
2. $\phi(t, j) \in \mathcal{D}$ and $\phi(t, j + 1) \in g(\phi(t, j))$ for all $(t, j) \in \operatorname{dom} \phi$ such that $(t, j + 1) \in \operatorname{dom} \phi$ (i.e., for all right endpoints of intervals).
3. $\phi(0, 0) \in \bar{\mathcal{C}} \cup \mathcal{D}$.

In other words, ϕ is a solution if it flows only when its image is in $\mathcal{C}$, jumps only when its image is in $\mathcal{D}$, and in each case its continuous and discrete evolution is governed by the respective maps f and g everywhere except possibly at a measure zero set in the interior of intervals.

Since the HI framework is based on inclusions instead of equations, a hybrid system will generally not have a unique solution, but a family of allowed solutions. This is

an important difference of the HI framework with respect to other formalisms such as IDS, and is motivated by robustness considerations, allowing for possible indeterminate behavior due to model uncertainty, noise or disturbances.

It is also important to take into account that the flow and jump sets $\mathcal{C}$ and $\mathcal{D}$ need not be disjoint, and in fact they frequently aren't, for reasons related to robustness. This is another source of indeterminate behavior: when $\phi(t, j) \in \mathcal{C} \cap \mathcal{D}$, there is the choice to either flow or jump, and both choices will generally define two different allowed solutions. We will come back later to these aspects of the formulation in Section 2.2, when we discuss its implications with respect to reset control design.

2.1.2 Hybrid systems with inputs

Any reset feedback controller is a system with inputs, since by definition of feedback, its behavior is dependent on one or more inputs (commonly an error signal). Thus, it is convenient to briefly recall another extension of the HI framework to systems with inputs [79], which will be used to state the definitions of various reset-based controllers and strategies.

Definition 2.5. A *hybrid system with inputs* Σ for a state $\mathbf{x} \in \mathbb{R}^{n_x}$ and an input $\mathbf{w} \in W$ for some set $W \subseteq \mathbb{R}^{n_w}$ is modeled by

$$\Sigma : \begin{cases} \dot{\mathbf{x}} \in f(\mathbf{x}, \mathbf{w}), & \text{if } (\mathbf{x}, \mathbf{w}) \in \mathcal{C}, \\ \mathbf{x}^+ \in g(\mathbf{x}, \mathbf{w}), & \text{if } (\mathbf{x}, \mathbf{w}) \in \mathcal{D}. \end{cases} \tag{2.3}$$

where as before $f : \mathbb{R}^{n_x} \times \mathbb{R}^{n_w} \rightrightarrows \mathbb{R}^{n_x}$ is the flow map, $g : \mathbb{R}^{n_x} \times \mathbb{R}^{n_w} \rightrightarrows \mathbb{R}^{n_x}$ is the jump map, and $\mathcal{C}, \mathcal{D} \subseteq \mathbb{R}^{n_x} \times \mathbb{R}^{n_w}$ are the flow and jump sets respectively.

A subtle point to consider is whether $\phi(t, j)$ or $\mathcal{A}_{[t,j]}\phi$ is required to belong to $\mathcal{C}$ *everywhere* or *almost everywhere* when flowing. Applying this requirement in the case of systems with inputs leads to two different concepts of solution, which [187] calls *e-solutions* and *ae-solutions*.

Following [187], we will not regard the allowed inputs $\mathbf{w}$ as hybrid arcs depending on (t, j), since otherwise their hybrid time domains must be known in advance, which is not realistic in practice; instead, the space of admissible inputs $\mathbf{w}(t)$ will be taken as the set of *càdlàg* functions from $\mathbb{R}_{\geq 0}$ to W, i.e., piecewise continuous functions which

are right-continuous and whose left limits exist for any point of discontinuity. Under this space of inputs, the two concepts of solution considered in [187] coincide, and the results about existence of solutions and completeness therein developed follow easily. Thus, it will be sufficient to state the definition of e-solution (with a third condition added for consistency with previous definitions):

Definition 2.6. For an Lebesgue measurable, locally bounded input signal $w \in W$, a *solution* to the hybrid system with inputs Σ given by (2.3) is a hybrid arc ϕ satisfying the following properties:

1. $(\phi(t,j), w(t)) \in \mathcal{C}$ for all (t,j) in the interior of any nonempty interval $I_j \subseteq \operatorname{dom}\phi$, and $d\phi(t,j)/dt \in f(\phi(t,j), w(t))$ for almost all (t,j) in the interior of I_j.

2. $(\phi(t,j), w(t) \in \mathcal{D}$ and $\phi(t,j+1) \in g(\phi(t,j), w(t))$ for all $(t,j) \in \operatorname{dom}\phi$ such that $(t,j+1) \in \operatorname{dom}\phi$ (i.e., for all right endpoints of intervals).

3. $(\phi(0,0), w(0)) \in \bar{\mathcal{C}} \cup \mathcal{D}$.

2.2 Reset control systems

In this section, the basics of reset control systems will be examined using the Hybrid Inclusions framework, providing robust models of the Clegg integrator and of a general reset controller, and introducing the PI+CI controller.

2.2.1 The Clegg integrator

The *Clegg integrator* (abbreviated CI) is a fundamental example of a reset controller, and the first one to be created. It was devised by Clegg in 1958 [106]. As will be seen later, a general reset controller can be built out of linear combinations of linear controllers and Clegg integrator blocks.

In plain words, the behavior of a CI is that of an ordinary, linear integrator as long as its input signal e is nonzero. Whenever the input signal reaches zero, the CI's state x instantaneously jumps (resets) to zero.

The simplest implementation of a CI in the HI framework is the following one:

$$\mathrm{CI}_{\mathrm{simple}} : \begin{cases} \dot{x} = e, & \text{if } e \neq 0, \\ x^+ = 0, & \text{if } e = 0. \end{cases} \tag{2.4}$$

An important drawback of this implementation is that it does not have robust zero crossing detection, in the sense that $\mathcal{D}$ is a set of measure zero, so adding an arbitrarily small noise to the input signal will almost surely cause the reset condition not to be triggered even for trajectories that nominally cross zero. Moreover, the fact that $\mathcal{C}$ is not a closed set prevents the model from being well-posed in the sense of [159]. For these reasons among others, a robust model, based on the original behavior of the circuit proposed by Clegg, was devised in [387]. It is referred to as a sector-based implementation:

$$\mathrm{CI}_{\mathrm{sector}} : \begin{cases} \dot{x} = e, & \text{if } x\, e \geq 0, \\ x^+ = 0, & \text{if } x\, e \leq 0. \end{cases} \tag{2.5}$$

Recently, due to similar motivations, another robust implementation of the Clegg integrator has been proposed in [43]. A simplified version of it is given by

$$\mathrm{CI}_{\mathrm{zcd}} : \begin{cases} \dot{x} = e, & \text{if } (e, q) \in \mathcal{C}, \\ \begin{pmatrix} x^+ \\ q^+ \end{pmatrix} = \begin{pmatrix} 0 & 0 \\ 0 & -1 \end{pmatrix} \begin{pmatrix} x \\ q \end{pmatrix}, & \text{if } (e, q) \in \mathcal{D}, \end{cases} \tag{2.6}$$

where $(x, q) \in \mathbb{R} \times \{1, -1\}$ is the state of the CI, and the jump and flow sets are given by

$$\mathcal{C} = \{(e, q) \in \mathbb{R} \times \{-1, 1\} \mid q\, e \geq 0\}, \tag{2.7a}$$

$$\mathcal{D} = \{(e, q) \in \mathbb{R} \times \{-1, 1\} \mid q\, e \leq 0\}, \tag{2.7b}$$

as shown in Figure 2.2. This implementation uses an additional discrete signal q to detect a zero crossing of the error signal e. As conventionally done in the HI framework for discrete variables, the trivial flow equation $\dot{q} = 0$ is omitted for simplicity. As with the sector-based model (2.5), it has the advantage of being robust against abrupt changes in e, due e.g. to measurement noise or numerical errors. Note that both $\mathcal{C}$ and $\mathcal{D}$ are closed sets whose union is the whole space, so the well-posedness results for hybrid systems are applicable, as will be seen in Section 2.5. The model (2.6)–(2.7) will be used throughout this thesis, due to its robustness properties and its easier

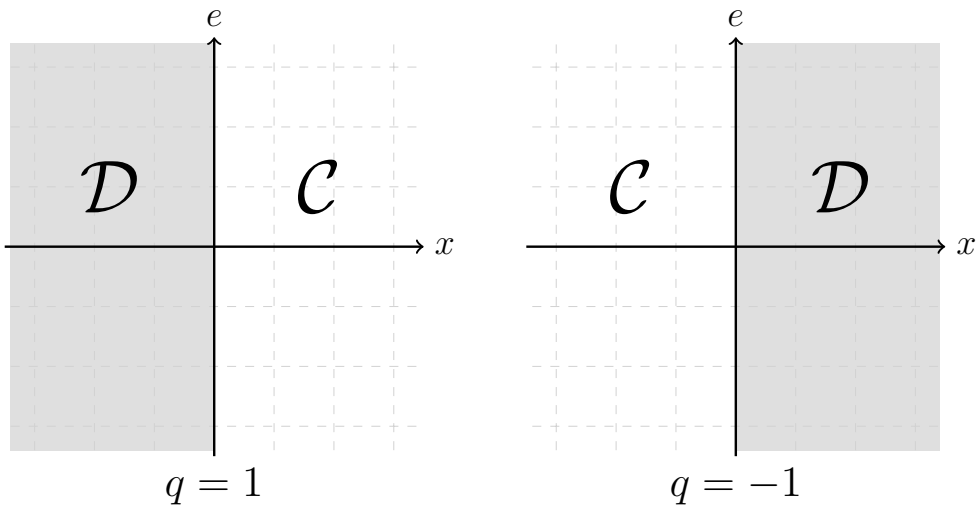

Figure 2.2: Jump and flow sets for the Clegg integrator with zero crossing detection.

applicability to multiple-input single-output systems (the sector-based implementation runs into problems when two or more controllers receive the same input but their control outputs have different signs, as commonly happens in MISO control. There exist ways to sidestep this issue, but the modifications are less straightforward).

For later developments, it will be convenient to also give the definition of a first order reset element (FORE), another basic example of reset controller first introduced in [197]. The FORE is a reset controller whose base linear system is a first order system with transfer function $1/(s + a_r)$, where $a_r > 0$ is a design parameter. An implementation of a FORE with robust zero crossing detection is given by

$$\text{FORE}_{\text{zcd}} : \begin{cases} \dot{x} = -a_r x + e, & \text{if } (e,q) \in \mathcal{C}, \\ \begin{pmatrix} x^+ \\ q^+ \end{pmatrix} = \begin{pmatrix} 0 & 0 \\ 0 & -1 \end{pmatrix} \begin{pmatrix} x \\ q \end{pmatrix}, & \text{if } (e,q) \in \mathcal{D}. \end{cases} \tag{2.8}$$

2.2.2 Resetting laws

A *resetting law* is a criterion upon which a reset action is performed. One of the simplest resetting laws, the *zero crossing law*, has already been mentioned: under this law, a reset action is triggered whenever the input crosses zero (or jump from a value to another with the opposite sign). Since the advent of reset control, various resetting laws have been proposed in the literature in order to achieve different objectives, such

as improving the performance or robustness of the system.

Resetting laws can be divided into several types [183]:

- Time-dependent resetting laws, in which the sequence of reset instants is totally or partially fixed in advance (for example, the sequence can be periodic where the period is a design parameter).
- State-dependent resetting laws, in which the triggering condition is defined in terms of the values of the states (for example, when a certain state reaches its saturation value).
- Input-dependent resetting laws, in which the triggering condition is defined in terms of the values of the inputs (the zero crossing law is an example).
- Resetting laws dependent on any combination of time, states and inputs.

In the Hybrid Inclusions formalism, any given resetting law may be used to define a corresponding jump set $\mathcal{D}$ as the set of all $(\mathbf{w}, \mathbf{x}, t)$ satisfying the law, and the flow set $\mathcal{C}$ as its complement. Some modifications such as taking closures can be then considered in order to achieve well-posedness properties. Note that state-dependent and input-dependent laws can be unified when the inputs are included within the model (e.g. as exosystems). Time-dependent laws will not be considered in this work.

As mentioned above, the Clegg integrator is a basic example of a reset controller implemented by using variations of the zero crossing resetting law. However, reset controllers equipped with a zero crossing law have been found to produce bad results in plants featuring significant time delay, or plants with dynamics of order higher than one (which can be approximated by time delays). In fact, most of the time, the performance is worse than that of its equivalent linear controller. The reason is that because of the existence of delays, the effect of any reset action is received by the plant later than it should, producing an undesired undershoot.

Motivated by this phenomenon, *reset band laws* were developed in [362]–[358] with the objective of anticipating a zero crossing, so that resetting earlier would make the effect of reset reach the plant at the right moment. The *fixed band law* [362] was a first attempt to solve this problem: under this law, a reset action is applied when either $e = -\delta$ and $\dot{e} > 0$ or $e = \delta$ and $\dot{e} < 0$, where $\delta \in \mathbb{R}_{\geq 0}$ is a parameter with the

same dimensions as e. In this way, the reset is triggered once the input signal enters a given band around zero (but not when it leaves the band, hence the condition on the sign of its derivative). An important drawback of this law is that a proper choice for the parameter δ is dependent on the magnitude of a typical reference change or disturbance, and thus it is not appropriate for cases in which there is a lot of variation in the magnitude of these signals.

For this reason, a *variable band law* was introduced in [358]. This law is based on a parameter $\theta \in \mathbb{R}_{\geq 0}$, the *variable band*, with dimensions of time. Under the variable band law, a reset action is triggered when the quantity $e + \theta\dot{e}$ reaches zero. There are various ways of interpreting this law. One of them is that it defines a reset band whose magnitude $\delta(t) = \theta\dot{e}(t)$ is time-varying (hence its name). Another, perhaps more illuminating interpretation, is that it anticipates a zero crossing of the input by means of a first order approximation; indeed, considering for simplicity the input as a differentiable function of time, it holds that $e(t) + \theta\dot{e}(t) \simeq e(t + \theta)$. In this way, if h denotes the effective delay of a process, choosing a reset feedback loop with $\theta = h$ will make the reset action reach the plant approximately when the true error crosses zero, avoiding some of the undershooting caused by resetting (but not all, as will be explained later).

Note that when using the variable band resetting law in practice, a filter must be added to prevent undesired early reset actions due to the presence of noise, which affects the calculation of the derivative of the input $\dot{e}$. A first order low-pass filter with the transfer function

$$F_{\mathrm{f}}(s) = \frac{1}{1 + \gamma\theta s}$$

is commonly considered, where γ is an extra dimensionless design parameter. In [118], the design choice $\gamma = 0.4$ is proposed; this value will be implicitly adopted in the developments that follow, if not otherwise specified.

To handle the different resetting laws, it is convenient, as in [43], to separate the *input signal* that is integrated (for which the notation e is kept) from the *reset signal* that triggers the reset actions (which will be called σ). The new model preserves the robust zero crossing detection, while allowing for more flexibility with regard to how the reset actions are determined. This generalized CI is what will be used in the next section to build a general reset controller admitting an arbitrary resetting law.

Definition 2.7. The *generalized Clegg integrator* with input signal (σ, q) is given by

$$\mathrm{CI}: \begin{cases} \dot{x} = e, & \text{if } (\sigma, q) \in \mathcal{C}, \\ \begin{pmatrix} x^+ \\ q^+ \end{pmatrix} = \begin{pmatrix} 0 & 0 \\ 0 & -1 \end{pmatrix} \begin{pmatrix} x \\ q \end{pmatrix}, & \text{if } (\sigma, q) \in \mathcal{D}, \end{cases} \tag{2.9}$$

where $\mathcal{C}, \mathcal{D}$ are as in (2.7), with e replaced by σ:

$$\mathcal{C} = \{(\sigma, q) \in \mathbb{R} \times \{-1, 1\} \mid q\,\sigma \geq 0\}, \tag{2.10a}$$

$$\mathcal{D} = \{(\sigma, q) \in \mathbb{R} \times \{-1, 1\} \mid q\,\sigma \leq 0\}. \tag{2.10b}$$

There is a minor issue worth mentioning. When a stationary state with zero σ is achieved (for the zero crossing and variable band resetting laws, this will occur when e becomes identically zero after a reset action, a phenomenon called *flat response* in Chapter 4), there exist solutions to the system where the reset laws force the state to be continually resetting, thus in the worst case no continuous time evolution can take place (this is an example of a Zeno solution in the terminology of the Hybrid Inclusions framework, and is also sometimes called *beating* or *livelock* to distinguish it from "genuinely Zeno" solutions where the sequence of reset instants is convergent but not eventually constant).

Note that in the absence of noise or numerical errors, this is really only a problem with the particular implementation of the resetting mechanism within a practical controller (cf. the discussion in Section 3.2 of [43]): when presented with the alternative between flowing and jumping (i.e., when $\phi(t, j) \in \mathcal{C} \cap \mathcal{D}$), these particular Zeno solutions will only arise if the number of times the controller takes the choice of flowing is finite (this happens e.g. if the chosen rule is to always jump). In any other case, the solution will be clearly unbounded in the time domain. However, it is important to notice that even if an implementation is chosen accordingly so as to avoid this problem in the nominal case, the presence of random-like noise and numerical fluctuations will mean that any state sufficiently close to a stationary state with $\sigma = 0$ will generically still suffer an infinite number of jumps, which might cause wearing out of the actuator depending on how the reset actions are physically performed.

When this is a concern, there are multiple ways to solve this issue; perhaps the simplest one consists of modifying the jump and flow sets by adding a small hysteresis,

i.e., substituting a small negative value $-\varepsilon$ instead of 0 in their definition (2.10), for which no stationary solutions with $\sigma = -\varepsilon$ exist. Another common solution is to use time regularization. A third possibility, which will be also considered in the stability analysis in Section 2.5, is to impose a maximum allowed number of jumps during a given control experiment (in practice, a counter state can be added which restarts upon the detection of a new reference change or disturbance; evidently this will only be an acceptable solution if these are known to come sufficiently spaced in time). Since this problem is minor and does not affect the theoretical treatments that follow, the choice is made not to discuss it further in order to keep the notation less cumbersome.

The strategies developed in the following will all use either the zero crossing or the variable band laws.

2.2.3 The general reset controller

Consider now a general reset controller, having a total of n_r independent states. Without loss of generality, a basis of the state space may be adopted for which n_ρ of the states are set to zero when a reset action is triggered, whereas the other states remain entirely unaffected. If $n_\rho = n_r$, the controller is said to be a *full reset* controller; if instead $0 < n_\rho < n_r$, it is said to be a *partial reset* controller. Define additionally $n_{\bar{\rho}} = n_r - n_\rho$, and let $\mathcal{O}^{n_r} = \mathbb{R}^n_r \times \{-1, 1\}$.

Definition 2.8. A *general reset controller* with state $(\mathbf{x}_r, q) \in \mathcal{O}^{n_r}$ and input $(e, \sigma) \in \mathbb{R}^2$ is given by the following hybrid system with inputs:

$$R : \begin{cases} \dot{\mathbf{x}}_r = A_r \mathbf{x}_r + B_r e, & \text{if } (\sigma, q) \in \mathcal{C}, \\ \begin{pmatrix} \mathbf{x}_r^+ \\ q^+ \end{pmatrix} = \begin{pmatrix} A_\rho & 0 \\ 0 & -1 \end{pmatrix} \begin{pmatrix} \mathbf{x}_r \\ q \end{pmatrix}, & \text{if } (\sigma, q) \in \mathcal{D}, \\ u = C_r \mathbf{x} + D_r e, \end{cases} \tag{2.11}$$

where $\mathbf{x}_r \in \mathbb{R}^{n_r}$, A_r, B_r, C_r, D_r are constant matrices of the appropriate dimensions, and the jump and flow sets are again given by (2.10).

It will be assumed in the following that $\sigma = S(e)$, where S is the output of some possibly nonlinear transformation of e implementing a corresponding resetting law. For example, the zero crossing law is given by $S(e) = e$, and the variable band law is given by $S(e) = e + \theta \dot{e}$.

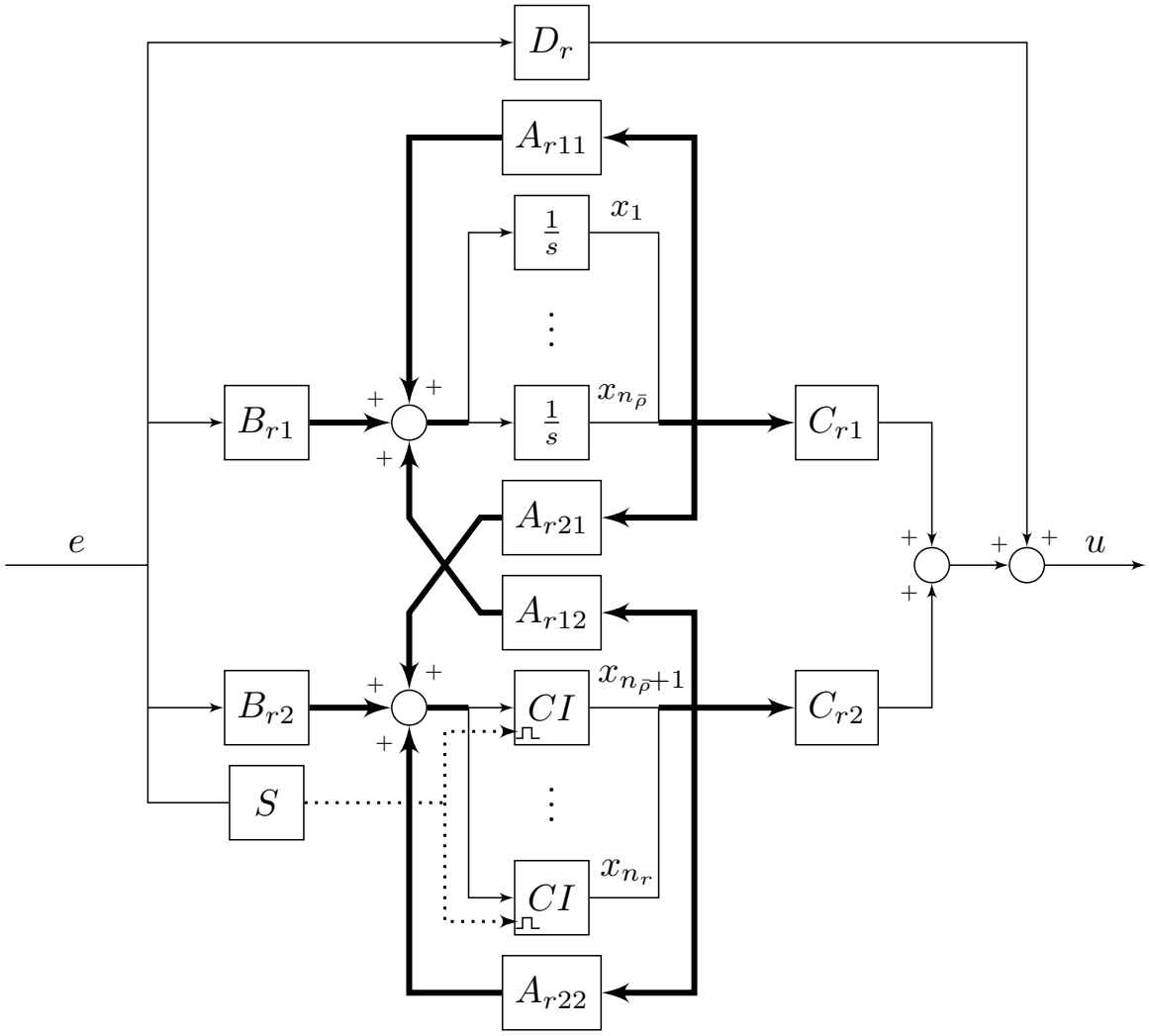

Figure 2.3: Block diagram of the general reset controller given by (2.11). Thick lines represent vector signals of the appropriate dimension, and the dotted line represents the reset signal σ.

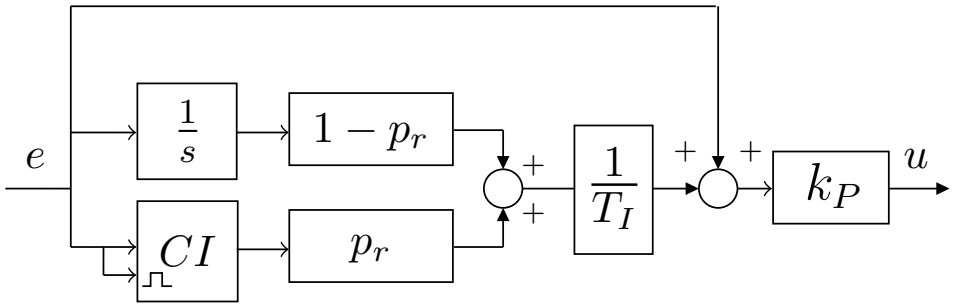

Figure 2.4: Block diagram of a PI+CI controller (the zero crossing law $\sigma = S(e) = e$ is depicted for simplicity).

The matrix A_ρ is partitioned into blocks as follows:

$$A_\rho = \begin{pmatrix} I_{n_{\bar{\rho}}} & 0 \\ 0 & 0 \end{pmatrix}, \tag{2.12}$$

where I_n denotes a $n \times n$ identity matrix, and the zero blocks are of the appropriate dimension. Furthermore, A_r, B_r and C_r can be partitioned as

$$A_r = \begin{pmatrix} A_{r11} & A_{r12} \\ A_{r21} & A_{r22} \end{pmatrix}, \quad B_r = \begin{pmatrix} B_{r1} \\ B_{r2} \end{pmatrix}, \quad C_r = \begin{pmatrix} C_{r1} & C_{r2} \end{pmatrix}, \tag{2.13}$$

again with blocks of appropriate dimension. Figure 2.3 shows how this general reset controller can be built using generalized Clegg integrator blocks, as given by (2.9), together with ordinary linear integrators and appropriate gain matrices. Note how all the Clegg integrator blocks within the reset controller receive the same reset signal σ, and so all of them necessarily reset at the same time instants; this will be referred to as *synchronous reset*, a concept which will be useful in the multivariable setting.

2.2.4 The PI+CI controller

Due to their simplicity and versatility, proportional-integral-derivative (PID) controllers nowadays constitute the most widespread control structure in industry. It is a well-known fact that over 95% of the existent feedback control loops in industrial processes use PID controllers. In an IFAC survey [322] about the perceived industrial success of different control technologies, respondents were in unanimous agreement that PID was the control strategy with the highest perceived impact in industry (in contrast, the area of hybrid dynamical systems, together with robust control, was the lowest rated in terms of perceived impact). Moreover, the derivative action is frequently avoided in practice, because of its poor behavior in presence of high frequency noise.

Given this, it is desirable to explore hybrid variants of PI control, so as to overcome the performance limitations inherent to linear time invariant systems, while preserving as much as possible its simple design and its applicability, which opens the door to an increased acceptance of hybrid-based methods in industry.

Motivated by this, the *proportional-integral plus Clegg integrator* controller, or PI+CI controller, was devised in [32]. This controller, whose block diagram is shown in Figure 2.4, is a hybrid extension of the PI controller in which the integral term is replaced with a linear combination of a linear integrator and a Clegg integrator. In addition to the parameters k_P and T_I inherited from the base PI, it has a new dimensionless design parameter $p_r \in \mathbb{R}$, called the *reset ratio*, which determines the weight of the CI state in the total output. In the interval between two consecutive reset actions, the behavior of the PI+CI controller is identical to that of a PI controller with the same proportional gain k_P and integral time T_I. On the other hand, if a zero crossing of $\sigma(t, j)$ is detected, the state of the Clegg integrator is immediately reset to zero, in such a way that the overall control output u jumps to a certain value depending on p_r.

The notation $\mathbf{x}_r = (x_I, x_{CI})$ is introduced, where x_I is the linear integrator state and x_{CI} the Clegg integrator state. Explicitly, an implementation of the PI+CI controller is given by the following system with inputs:

$$\text{PI} + \text{CI}: \begin{cases} \dot{\mathbf{x}}_r = \begin{pmatrix} 1 \\ 1 \end{pmatrix} e, & \text{if } (\sigma, q) \in \mathcal{C}, \\ \begin{pmatrix} \mathbf{x}_r^+ \\ q^+ \end{pmatrix} = \begin{pmatrix} A_\rho & 0 \\ 0 & -1 \end{pmatrix} \begin{pmatrix} \mathbf{x}_r \\ q \end{pmatrix}, & \text{if } (\sigma, q) \in \mathcal{D}, \end{cases} \tag{2.14}$$

where the jump and flow sets are again given by (2.10). Note that the PI+CI can be modeled as a particular case of the general reset controller, by setting $n_r = 2$ and

$$A_r = 0, \;\; B_r = \begin{pmatrix} 1 \\ 1 \end{pmatrix}, \; A_\rho = \begin{pmatrix} 1 & 0 \\ 0 & 0 \end{pmatrix}, \;\; C_r = (\frac{k_P}{T_I}(1 - p_r), \frac{k_P}{T_I} p_r), \;\; D_r = k_P. \tag{2.15}$$

Note also that when $p_r = 0$, the behavior of the underlying linear PI controller is recovered (the system still jumps when σ crosses zero, but these jumps have no effect on the value of u and may be disregarded). Despite its simplicity, the PI+CI controller has already been proven to be useful in several practical control applications [18, 118].

2.2.5 Variable reset ratio

In addition to the consideration of different resetting laws, a further design improvement specific to the PI+CI controller, which has been found to produce a better behavior in the control of second order or delayed plants, is the so-called *variable reset ratio*.

The concept of variable reset ratio, introduced in [357], consists of replacing the constant p_r in (2.14) by a time-varying function $\mathcal{P}_r(t, j)$. The motivation of doing this lies in the fact that a reset ratio that produces an acceptable response when applied in the first reset instant is not guaranteed to continue doing so in subsequent reset instants; in fact, these further reset actions can be shown to produce undershoot in the response when the plant is not first order. Allowing for the value of the reset ratio to change permits more flexibility in its design, and constitutes a way of reducing the undershoot without abandoning the traditional reset mechanism. However, note that with this modification, the PI+CI controller's base system becomes a *linear time variant* system, whose mathematical treatment is more complicated.

In most applications, the function $\mathcal{P}_r$ will be recalculated according to some algorithm only after each jump, i.e., $\mathcal{P}_r(t, j) = \mathcal{P}_r(j)$ can be assumed to depend only on j.

2.3 Multiple-input single-output systems

A *multiple-input single-output system*, or MISO system, refers to a process whose output signal can be simultaneously manipulated by more than one input signal. MISO systems are examples of over-actuated systems, in which the number of available control inputs is higher than the number of system outputs.

This interesting feature allows for the possibility of collaborative control strategies where the controllers may share the control load, with the aim of improving closed loop performance or robustness, avoiding controller saturation or out-of-range nonlinearities of the actuators, and reducing the cost of feedback with respect to single-input strategies [313].

Collaborative MISO control design structures can be divided into two main classes: parallel control and serial control.

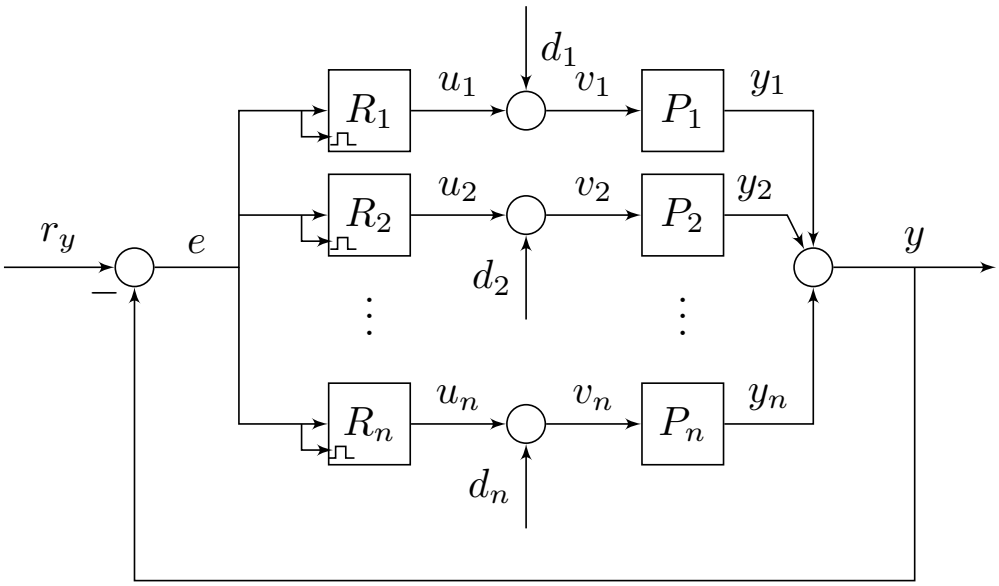

Figure 2.5: Block diagram of the parallel control structure.

2.3.1 Parallel and serial structures

The *parallel control* structure, also known as *centralized control* or *load-sharing control*, constitutes one of the two main classes of MISO control structure considered in the literature. This structure is a generalization of the one proposed in Brosilow *et al.* [72], and has been studied e.g. in [8, 136, 191, 312, 325]. As depicted in Figure 2.5, it consists of applying independent controllers (here denoted as $R_1, \ldots, R_n$) to each one of the inputs of the plant P, which in the LTI case can be considered as the sum of n sub-plants $P_1, \ldots, P_n$. Applications of this structure can be found, among others, in the idle speed control of an engine [222], the control of temperature [137], the control of aero-electric power stations [182] or the control of spacecrafts [152].

This type of MISO control structure is commonly used in cases where no clear hierarchy exists distinguishing between plants with faster and slower dynamics [313]. In some treatments, a master controller R_m is explicitly considered as part of the parallel control structure; however, from a mathematical perspective this controller can be treated as a part of the other controllers by means of the redefinitions $R_i \to R_m R_i$ (where juxtaposition denotes a connection in series).

The other main class of MISO control structure is called *serial control* structure or *cascade control*, depicted in Figure 2.6. As the parallel structure, it consists of n

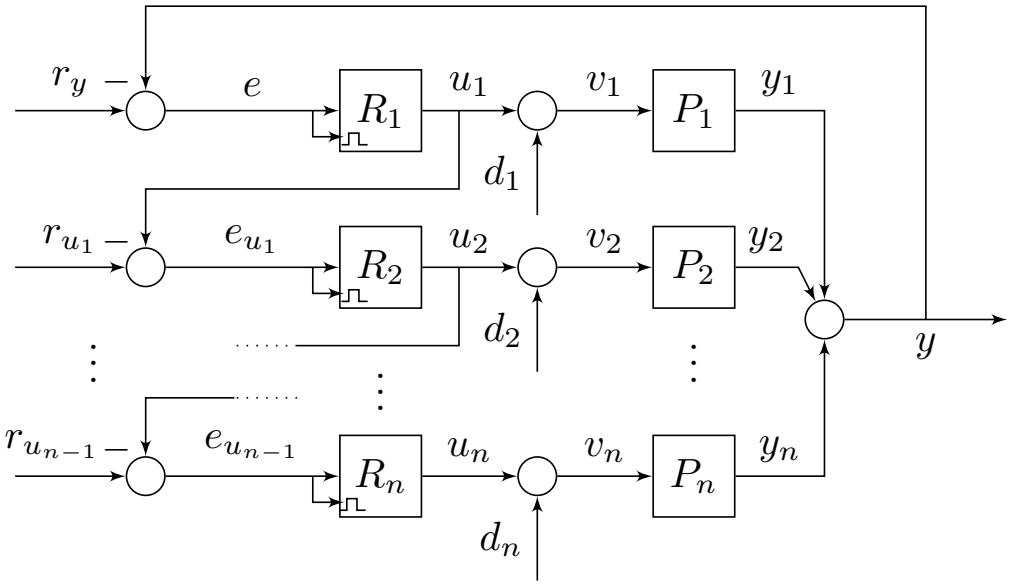

Figure 2.6: Block diagram of the serial control structure.

sub-plants of the form (2.16), controlled by n respective reset controllers of the form (2.11). However, in this case, there exist additional reference signals $r_{u1}, r_{u2}, \ldots, r_{u\,n-1}$ for $n-1$ of the controllers, and corresponding error signals $e_{u1}, e_{u2}, \ldots, e_{u\,n-1}$. This control structure is usually employed in cases where the controller-plant loops can be ordered according to how fast their dynamics are: the objective is to minimize the use of fast but expensive control actuators by letting slower and cheaper actuators take charge of low frequency behavior [312]. In this way, the fastest loop (corresponding to R_1 and P_1) governs the high frequency, transient behavior and is responsible for performance; the second loop (corresponding to R_2 and P_2) then acts to drive the first controller towards its reference value, and so on in sequence, until the control effort is transferred to the slowest loop (corresponding to R_n and P_n) governing the steady state behavior. Note that this last controller does not have a prescribed reference signal, as it needs to accommodate any changes in the set point of y.

In both control structures, the feedback connection is achieved by setting $e = r_y - y$ and $v_i = u_i + d_i$ for all i; in the serial case, one also sets $e_{u_i} = r_{u_i} - u_i$ for $1 \leq i < n$. A disturbance at the output d_o can also be considered, but note that from a modeling point of view it can be treated as part of the reference signal by redefining $r_y \to r_y - d_o$.

2.4 Closed loop system models

In this section, closed loop models of the main hybrid control systems used in this work will be developed under the Hybrid Inclusions framework, considering two cases: a synchronous MISO system and an asynchronous MISO system. Some extensions to these model that account for different phenomena such as exogenous inputs, filtered derivative states for the variable band resetting law, and the time regularization mechanism, will be considered.

2.4.1 Model of a parallel MISO control system: synchronous case

The closed loop model of a parallel MISO control system in the case of a LTI plant without time delays is introduced in this section. It is not treated as a special case of the delayed parallel MISO control system because both the mathematical details of the model (and thus the well-posedness and stability results from Section 2.5) and the control strategy used to develop design rules in Chapter 4 are different.

An LTI MISO system consisting of n plants is controlled by respective reset controllers R_i, $i = 1, \ldots, n$, of the form (2.11). The ith plant is described by

$$P_i : \begin{cases} \dot{\mathbf{x}}_{pi} = A_{pi}\mathbf{x}_{pi} + B_{pi}v_i \\ y_i = C_{pi}\mathbf{x}_{pi}, \end{cases} \tag{2.16}$$

and the subscript i will be added to all variables in (2.11) associated with the ith controller except the variable q, which will be shared among all of them (as mentioned in previous sections, this corresponds to a synchronous reset). The total output is defined by $y = \sum_{i=1}^{n} y_i$. Finally, the feedback connection is achieved by setting $e = r_y - y$, where r_y is a reference signal, and $v_i = u_i + d_i$, for input disturbances d_i, for $i = 1, 2, \ldots$. The closed-loop state is defined as

$$\mathbf{z} = (\mathbf{x}, q) = (\mathbf{x}_{p1}, \ldots, \mathbf{x}_{pn}, \mathbf{x}_{r1}, \ldots, \mathbf{x}_{rn}, q),$$

whereas n_{CL} is defined as $\sum_{i=1}^{n}(n_{pi} + n_{ri})$. For the case of no exogenous inputs (reference and disturbances), the closed loop reset control system is then described as the hybrid system

$$\Sigma : \begin{cases} \dot{\mathbf{x}} = A\mathbf{x}, & \text{if } (\mathbf{x}, q) \in \mathcal{C}, \\ \begin{pmatrix} \mathbf{x}^+ \\ q^+ \end{pmatrix} = \begin{pmatrix} A_R\mathbf{x} \\ -q \end{pmatrix}, & \text{if } (\mathbf{x}, q) \in \mathcal{D}, \end{cases} \tag{2.17}$$

where the matrices $A \in \mathbb{R}^{n_{CL}\times n_{CL}}, A_R \in \mathbb{R}^{n_{CL}\times n_{CL}}$ and the sets $\mathcal{C}$ and $\mathcal{D}$ are determined uniquely from A_{ri}, A_{pi}, B_{ri}, etc. Namely, A is given by

$$A = \begin{pmatrix} A_{p1}-B_{p1}D_{r1}C_{p1} & \cdots & -B_{p1}D_{r1}C_{pn} & B_{p1}C_{r1} & \cdots & 0 \\ \vdots & \ddots & \vdots & \vdots & \ddots & \vdots \\ -B_{pn}D_{rn}C_{p1} & \cdots & A_{pn}-B_{pn}D_{rn}C_{pn} & 0 & \cdots & B_{pn}C_{rn} \\ -B_{r1}C_{p1} & \cdots & -B_{r1}C_{pn} & A_{r1} & \cdots & 0 \\ \vdots & \ddots & \vdots & \vdots & \ddots & \vdots \\ -B_{rn}C_{p1} & \cdots & -B_{rn}C_{pn} & 0 & \cdots & A_{rn} \end{pmatrix} \tag{2.18}$$

and A_R by

$$A_R = \begin{pmatrix} I & \cdots & 0 & 0 & \cdots & 0 \\ \vdots & \ddots & \vdots & \vdots & \ddots & \vdots \\ 0 & \cdots & I & 0 & \cdots & 0 \\ 0 & \cdots & 0 & A_{\rho 1} & \cdots & 0 \\ \vdots & \ddots & \vdots & \vdots & \ddots & \vdots \\ 0 & \cdots & 0 & 0 & \cdots & A_{\rho n} \end{pmatrix}. \tag{2.19}$$

The resetting law will be given by the jump and flow sets

$$\mathcal{D} = \{(\mathbf{x}, q) \in \mathbb{R}^n \times \{1, -1\} : q\, C_R\, \mathbf{x} \leq 0\}, \tag{2.20a}$$

$$\mathcal{C} = \{(\mathbf{x}, q) \in \mathbb{R}^n \times \{1, -1\} : q\, C_R\, \mathbf{x} \geq 0\}, \tag{2.20b}$$

for some matrix (or matrix function) $C_R \in \mathbb{R}^{1\times m}$. That is, $\sigma = C_R\mathbf{x}$ is imposed. The zero crossing resetting law corresponds to

$$C_R = C = \begin{pmatrix} -C_{p1} & \cdots & -C_{pn} & 0 & \cdots & 0 \end{pmatrix}, \tag{2.21}$$

whereas it is easy to see that a *synchronous* variable band resetting law, where it is assumed that all controllers have the same variable band θ, can be modeled by choosing

$$C_R = C(I + \theta A) \tag{2.22}$$

(this is the ideal case with no filtering; the addition of a filtered state is discussed in Section 2.4.3).

Note that in the case of LTI controllers, it is readily seen that a serial MISO system is equivalent to a parallel MISO system with the same plants and with controllers given by $R_i \leftarrow (-1)^{i-1} \prod_{j=1}^{i} R_j$, for all i. Thus, we can obtain the closed loop system matrices (A, B, C, D, A_R) for the serial control structure by making the appropriate replacements in the previous expressions. As a result, the serial MISO control structure could be approached as a particular case of the parallel structure if the reset signals of all controllers depend only on e; however, if one allows for the reset signals to also depend on e_{u_i}, the problem becomes inequivalent in general.

2.4.2 Model of a parallel MISO control system: asynchronous case

A more general resetting law could be considered in principle, namely an asynchronous resetting law for which each controller R_i has its own variable band parameter θ_i, but in such a case the reset control system's model must be adapted accordingly. Note that allowing for individual reset actions will cause asynchronous jumping at different times, and this switching-like behavior cannot be captured by a single hyperplane-crossing detection as in (2.22): instead, one needs to consider a separate discrete variable q_i for each controller, and distinguish between $2^n - 1$ different cases to account for the fact that several reset actions may be in principle triggered at the same time.

Define the vector $\mathbf{q} = (q_1, \ldots, q_n)$. The discrete evolution of both $\mathbf{x}$ and $\mathbf{q}$ is now dependent on which controller is triggered; to account for this, the jump and flow sets will be taken as the union of n respective subsets, defined as follows:

$$\mathcal{D} = \bigcup_{i=1}^{n} \mathcal{D}_i, \tag{2.23a}$$

$$\mathcal{D}_i = \{(\mathbf{x}, q) \in \mathbb{R}^n \times \{1, -1\} : q\, C_{Ri}\, \mathbf{x} \leq 0\}, \tag{2.23b}$$

$$\mathcal{C} = \bigcup_{i=1}^{n} \mathcal{C}_i, \tag{2.23c}$$

$$\mathcal{C}_i = \{(\mathbf{x}, q) \in \mathbb{R}^n \times \{1, -1\} : q\, C_{Ri}\, \mathbf{x} \geq 0\}, \tag{2.23d}$$

where the covector C_{Ri} implements the ith variable band law:

$$C_{Ri} = C(I + \theta_i A). \tag{2.24}$$

Note that a related multiple variable band configuration was studied in [306] in the context of SISO systems due to its favorable phase lead properties; multiple reset conditions were also considered in [403] in the context of MIMO systems. Now, let A_{Ri} be the block diagonal matrix whose jth block is the identity if $j \neq \sum_{k=1}^{n} n_{pk} + \sum_{k=1}^{i} n_{rk}$ and $A_{\rho i}$ if $j = \sum_{k=1}^{n} n_{pk} + \sum_{k=1}^{i} n_{rk}$. Similarly, let A_{qi} be the diagonal matrix whose jth diagonal entry is 1 if $j \neq i$ and -1 if $j = i$. These matrices define the discrete evolution of $\mathbf{x}, \mathbf{q}$ when the ith controller's resetting law is triggered.

Finally, in order to model the possibility of two or more controllers being reset at the same time, the set-valued variable J is used which runs over the $2^n - 1$ nonempty subsets of $\{1, \ldots, n\}$. The model of the asynchronous parallel MISO control system is

$$\Sigma : \begin{cases} \dot{\mathbf{x}} = A\mathbf{x}, & \text{if } (\mathbf{x}, q) \in \mathcal{C}, \\ \begin{pmatrix} \mathbf{x}^+ \\ \mathbf{q}^+ \end{pmatrix} = \begin{pmatrix} \left(\prod_{i \in J} A_{Ri}\right) \mathbf{x} \\ \left(\prod_{i \in J} A_{qi}\right) \mathbf{q} \end{pmatrix}, & \text{if } (\mathbf{x}, q) \in \bigcap_{i \in J} \mathcal{D}_i, \end{cases} \tag{2.25}$$

Note that the matrices $\{A_{Ri}\}_{i=1}^{n}$ are mutually commuting, so the product is well-defined. The same applies to $\{A_{qi}\}_{i=1}^{n}$.

2.4.3 Model extensions

In this section, several extensions to the previously described models will be studied, in which the state space is augmented so as to account for various situations arising in their practical implementation, such as the modeling of external inputs such as disturbances, the reference signal and sensor noise as exosystems (something necessary in the delayed case), the filtering of the error derivative in the variable band resetting law, and the use of time regularization to guarantee that no solution to the system is Zeno.

- **Exogenous inputs as exosystems**:

  Exogenous inputs are crucial in feedback control, since they are an essential component both in tracking and regulation. In particular, a reference signal r_y, disturbance signals d_i and a sensor noise signal η will be considered here. Recall the equations $e = r_y - y$ and $v_i = u_i + d_i$, valid in the noiseless case. In the

presence of noise, the measured output y_m must be distinguished from the real plant output y. Their relation is $y_m = y+\eta$. Thus, the equation defining the error is modified to $e = r_y - y_m = (r_y - \eta) + y$. Note that the signal η could as well be used to model a disturbance at the output of the plant, so far not considered here.

The reason for treating these exogenous input as exosystems is twofold: first, the HI frameworks for systems with memory and for systems with inputs have not yet been combined in the literature, so this approach is necessary for the modeling of exogenous inputs in the case of delayed systems. Secondly, one of the design rules in Chapter 4 for nondelayed systems will be based on an implementation of the base linear closed loop system which includes exosystem models of the reference and disturbances.

In all three cases, LTI exosystems without time delay will be considered for simplicity. These exosystems are known to produce continuous-time solutions consisting of *Bohl functions* [345], that is, real-valued linear combinations of complex functions of the form $t^m e^{\xi t} U(t)$ for $m \in \mathbb{N}$ and $\xi \in \mathbb{C}$, where $U(t)$ is a Heaviside step function. These are sufficiently general to capture most practical common behaviors of signals such as step changes, ramps or sinusoidal waves. The exosystem model for all three signals, with state $\mathbf{x}_e = (\mathbf{x}_{e1}, \mathbf{x}_{e2}, \mathbf{x}_{e3})$, is given by

$$E : \begin{cases} \dot{\mathbf{x}}_e = \begin{pmatrix} A_{e1} & 0 & 0 \\ 0 & A_{e2} & 0 \\ 0 & 0 & A_{e3} \end{pmatrix} \mathbf{x}_e \\ \begin{pmatrix} r_y \\ \mathbf{d} \\ \eta \end{pmatrix} = \begin{pmatrix} C_{e1} \\ C_{e2} \\ C_{e3} \end{pmatrix} \mathbf{x}_e, \end{cases} \tag{2.26}$$

where $\mathbf{d} = (d_1, \ldots, d_n)$, and C_{e2} is a block diagonal matrix with entries the covectors C_{e2i}. As for the new closed loop system, consider the nondelayed MISO case first. The new state is $(\mathbf{x}, \mathbf{x}_e)$. If A_{old} denotes the continuous time evolution matrix (2.18) associated to the original system, the new one is given by

$$A = \begin{pmatrix} A_{\text{old}} & B_{\text{ref}} & B_{\text{dist}} & B_{\text{noise}} \\ 0 & A_{e1} & 0 & 0 \\ 0 & 0 & A_{e2} & 0 \\ 0 & 0 & 0 & A_{e3} \end{pmatrix}, \tag{2.27}$$

where

$$B_{\text{ref}} = \begin{pmatrix} B_{p1}D_{r1}C_{e1} \\ \vdots \\ B_{pn}D_{rn}C_{e1} \\ B_{r1}C_{e1} \\ \vdots \\ B_{rn}C_{e1} \end{pmatrix}, B_{\text{dist}} = \begin{pmatrix} C_{e21} \\ \vdots \\ C_{e2n} \\ 0 \\ \vdots \\ 0 \end{pmatrix}, B_{\text{noise}} = \begin{pmatrix} -B_{p1}D_{r1}C_{e3} \\ \vdots \\ -B_{pn}D_{rn}C_{e3} \\ -B_{r1}C_{e3} \\ \vdots \\ -B_{rn}C_{e3} \end{pmatrix}. \tag{2.28}$$

Similarly, if C_{old} denotes (2.21), then the new C is

$$C = \begin{pmatrix} C_{\text{old}} & C_{e3} & 0 & -C_{e3} \end{pmatrix}. \tag{2.29}$$

The augmented model is then given by (2.17), (2.20) with the new definitions of A and C (the reset matrix A_R is extended in the obvious way so that it acts as the identity on the new states).

- **Derivative filters**:

In full generality, consider the asynchronous reset-and-hold control system model (3.24) applied to a MISO plant. Since the model is asynchronous, it is assumed that each controller has its own independent filter, and thus the model will be augmented with n new filtered derivative states $x_{d1}, \ldots, x_{di}$.

In order to define the augmented model, the following replacements are performed (recall that $\gamma_i\theta_i$ is the ith filter's time constant, which is assumed to be greater than zero for simplicity):

$$\mathbf{x} \leftarrow \begin{pmatrix} \mathbf{x} \\ x_{d1} \\ \vdots \\ x_{dn} \end{pmatrix}, \quad A \leftarrow \begin{pmatrix} A & 0 & \cdots & 0 \\ CA & -1/(\gamma_1\theta_1) & \cdots & 0 \\ \vdots & \vdots & \ddots & \vdots \\ CA & 0 & \cdots & -1/(\gamma_n\theta_n) \end{pmatrix},$$
$$C \leftarrow \begin{pmatrix} C & 0 & \cdots & 0 \end{pmatrix} \tag{2.30}$$

$$C_{Ri} \leftarrow \begin{pmatrix} C & 0 & \cdots & \theta_i & \cdots & 0 \end{pmatrix}. \tag{2.31}$$

The closed loop system is then given by (2.25) with the jump and flow subsets (2.24), with the new definitions of A, C, C_{Ri}, and with A_R extended to act as the identity matrix on the new states. The equations for a synchronous resetting law ($\theta_i = \theta$ for all i) are obtained in the obvious way by adding just one state x_d. Similarly, if one or more of the variable bands is zero, the corresponding states can be removed. Recall that as explained in Section 2.2.2, all the parameters γ_i will be taken as 0.4 unless otherwise specified.

- **Time regularization**:

Time regularization is a standard method in reset control, used to avoid the existence of defective solutions where the sequence of reset times converges to a finite value $t_{\max} < \infty$. The method consists of using a timer variable $\tau_{TR} \in [0, \infty]$, initialized to 0 after a jump, and that prevents the system from performing a new jump until $\tau_{TR} \geq D$, where $D > 0$ is a design parameter (the *minimum dwell-time*).

Given any model Σ, the time-regularized hybrid system Σ_{TR} is defined by

$$\Sigma_{TR} : \begin{cases} \begin{pmatrix} \dot{\mathbf{x}} \\ \dot{\tau}_{TR} \end{pmatrix} \in \begin{pmatrix} f(\mathbf{x}) \\ 1 \end{pmatrix}, & \text{if } (\mathbf{x}, \tau_{TR}) \in \mathcal{C}_{TR}, \\ \begin{pmatrix} \mathbf{x}^+ \\ \tau_{TR}^+ \end{pmatrix} \in \begin{pmatrix} g(\mathbf{x}) \\ 0 \end{pmatrix}, & \text{if } (\mathbf{x}, \tau_{TR}) \in \mathcal{D}_{TR}, \end{cases} \tag{2.32}$$

where the new flow and jump sets are given in terms of the old ones by

$$\mathcal{C}_{TR} = (\mathcal{C} \times [0, \infty)) \cup (\mathcal{D} \times [0, D]), \tag{2.33}$$

$$\mathcal{D}_{TR} = \mathcal{D} \times [D, \infty). \tag{2.34}$$

2.5 Well-posedness and stability

2.5.1 Well-posedness

The well-posedness of a hybrid system is a robust version of the property of existence of solutions and their continuous dependence on initial conditions. Intuitively, a hybrid system is *nominally well-posed* if the limit of a convergent sequence of hybrid arcs satisfying a certain boundedness property is also a solution, whereas convergent sequences of hybrid arcs lacking that property lead to a solution that diverges in finite time, and it is *well-posed* if these statements still hold true under arbitrarily small perturbations ([159]). It will not be necessary to state the full definition of well-posedness here, which is nontrivial and requires a preliminary definition of convergence for hybrid arcs; instead, the following theorem will be used, that describes a set of simple conditions that a system must satisfy in order to be well-posed:

Theorem 2.9. *A hybrid system Σ is well-posed if these conditions (the* basic hybrid conditions*) are satisfied (Theorem 6.30 in [159]):*

- *The sets $\mathcal{C}$ and $\mathcal{D}$ are closed subsets of $\mathbb{R}^n$.*
- *The set-valued function f is outer semicontinuous and locally bounded relative to $\mathcal{C}$, and has nonempty, convex image at every point in $\mathcal{C}$.*
- *The set-valued function g is outer semicontinuous and locally bounded relative to $\mathcal{D}$, and has nonempty image at every point in $\mathcal{D}$.*

Proof. See [159].

Consider the nondelayed MISO reset control system Σ as given by (2.16)–(2.20). Well-posedness of Σ directly follows from the fact that $f(\mathbf{x}) = A\mathbf{x}$ and $g(\mathbf{x}) = A_R\mathbf{x}$ are continuous maps, and the flow and map sets $\mathcal{F}_{CL}$ and $\mathcal{J}_{CL}$ are closed sets, and thus Σ_{CL} satisfies the basic hybrid conditions. Well-posedness in this sense [159] is a less restrictive condition than the one considered in [26]. Nevertheless, it still implies some

important properties regarding robustness, stability and the nature of solutions (we refer the reader to [159] for technical details).

2.5.2 Stability analysis

In the nondelayed setting, the distinction between synchronous and asynchronous resetting laws becomes of importance. Many stability results in the literature regarding reset control systems in the IDS formalism [18, 37] have been designed to be applicable to any reset system where the continuous and discrete evolution is linear and the resetting law is given in the form of a hyperplane crossing; in a synchronous MISO system, both zero crossing and variable band resetting laws can be stated in this form, as shown in (2.20). This means that all the aforementioned stability conditions can be applied to this kind of system simply by adapting the relevant statements and proofs to the Hybrid Inclusions framework. In contrast, an asynchronous MISO system (for example, one with independent variable band resetting laws such as (2.23)), most of the previous results do no longer apply without substantial modification, and consequently new stability conditions must be developed to appropriately handle this kind of system.

The following preliminary definitions will be needed to state the stability conditions.

Definition 2.10. A function $\alpha : \mathbb{R}_{\geq 0} \to \mathbb{R}_{\geq 0}$ is called class-$\mathcal{K}_\infty$ if it is a continuous, unbounded, strictly increasing function with $\alpha(0) = 0$.

Definition 2.11. A function $\rho : \mathbb{R}_{\geq 0} \to \mathbb{R}_{\geq 0}$ is called positive definite if $\rho(0) = 0$ and $\rho(x) > 0$ for all $x > 0$.

Definition 2.12 (Uniform global pre-asymptotic stability)**.** A closed set $\mathcal{A}$ is called uniformly globally pre-asymptotically stable for the hybrid system Σ if there exists a class-$\mathcal{K}_\infty$ function α such that $|\varphi(t,j)|_\mathcal{A} \leq \alpha(|\varphi(0,0)|_\mathcal{A})$ for any solution φ and $(t,j) \in \operatorname{dom}\varphi$, and for all $\varepsilon > 0$ and $r > 0$ there exists $T > 0$ such that any solution φ with $|\varphi(0,0)|_\mathcal{A} \leq r$ satisfies $|\varphi(t,j)|_\mathcal{A} \leq \varepsilon$ for all $(t,j) \in \operatorname{dom}\varphi$ such that $t + j \geq T$.

Here $|\mathbf{x}|_\mathcal{A}$ is defined as $\inf_{\mathbf{y}\in\mathcal{A}} |\mathbf{x} - \mathbf{y}|$.

Definition 2.13 (Local pre-asymptotic stability)**.** A compact set $\mathcal{A}$ is called locally pre-asymptotically stable for the hybrid system Σ if for every $\varepsilon > 0$ there exists $\delta > 0$ such that any solution φ to the system with $|\varphi(0,0)|_\mathcal{A} \leq \delta$ satisfies $|\varphi(t,j)|_\mathcal{A} \leq \varepsilon$

for any $(t, j) \in \operatorname{dom}\varphi$, and if there exists $\mu > 0$ such that any solution satisfying $|\varphi(0,0)|_{\mathcal{A}} \leq \mu$ is bounded and, if φ is complete, $\lim_{t+j\to\infty} |\varphi(t,j)|_{\mathcal{A}} = 0$.

Note that uniform global pre-asymptotic stability implies local pre-asymptotic stability. A sufficient condition for uniform pre-asymptotic stability is the existence of a Lyapunov function. Assume that Σ satisfies the hybrid basic conditions, and that there exists a candidate Lyapunov function V with $\mathcal{C} \cup \mathcal{D} \cup g(\mathcal{D}) \subset \operatorname{dom} V$, that is continuously differentiable on an open set containing f. The following theorem from [159] defines sufficient conditions for stability in terms of V.

Theorem 2.14. *A closed set $\mathcal{A}$ is uniformly globally pre-asymptotically stable for the hybrid system Σ if there exists a candidate Lyapunov function V, $\alpha_1, \alpha_2 \in \mathcal{K}_\infty$ and a continuous positive definite function ρ such that the three following conditions are satisfied:*

$$\alpha_1(|\mathbf{x}|_{\mathcal{A}}) \leq V(\mathbf{x}) \leq \alpha_2(|\mathbf{x}|_{\mathcal{A}}) \quad \forall \mathbf{x} \in \mathcal{F} \cup \mathcal{J} \cup g(\mathcal{J}), \tag{2.35a}$$

$$\langle \nabla V(\mathbf{x}), f(\mathbf{x}) \rangle \leq -\rho(|\mathbf{x}|_{\mathcal{A}}) \quad \forall \mathbf{x} \in \mathcal{F}, \tag{2.35b}$$

$$V(g(\mathbf{x})) - V(\mathbf{x}) \leq -\rho(|\mathbf{x}|_{\mathcal{A}}) \quad \forall \mathbf{x} \in \mathcal{J}. \tag{2.35c}$$

Proof. See [159].

Moreover, the following theorem, also taken from [159], will apply in those instances in which there is a finite number of jumps for any given initial condition.

Theorem 2.15. *A closed set $\mathcal{A}$ is uniformly globally pre-asymptotically stable for the hybrid system Σ if conditions* (2.35a) *and* (2.35b) *hold for some V, there exists $\lambda \in \mathcal{K}_\infty$ such that*

$$V(g(\mathbf{x})) \leq \lambda(V(\mathbf{x})) \quad \mathbf{x} \in \mathcal{J}, \tag{2.36}$$

and there exist some $\gamma \in \mathcal{K}_\infty$ and $J > 0$ such that for any solution ϕ to the system, $(t, j) \in \operatorname{dom}\phi$ implies

$$j \leq \gamma(|\phi(0,0)|_{\mathcal{A}}) + J. \tag{2.37}$$

Proof. See [159].

Stability for the closed-loop synchronous reset control system Σ (2.17) of the set $\mathcal{A} = \{\mathbf{0}\} \times \{-1, 1\}$ is analyzed in the following. The set $\mathcal{A}$ consists of two equilibrium states with $\mathbf{x} = 0$, one for each value of the variable q. The problem is approached by using a Lyapunov function satisfying the sufficient Lyapunov conditions (2.35) for $\mathcal{A}$ to be uniformly globally asymptotically stable for Σ.

Proposition 2.16 (Stability conditions #1, synchronous case)**.** *Consider the MISO reset control system* Σ (2.17) *equipped with a zero crossing resetting law. The set* $\mathcal{A}$ *is globally asymptotically stable for* Σ *if there exists a matrix* $P > 0$ *such that*

$$A^\top P + PA \leq -\varepsilon I, \tag{2.38a}$$

and

$$\Theta^\top (A_R P A_R - P)\Theta \leq -\varepsilon \Theta^\top \Theta, \tag{2.38b}$$

hold for some $\varepsilon > 0$ *and any matrix* Θ *such that* $\operatorname{Im}\Theta = \operatorname{Ker} C$.

Proof. Consider the state $(\mathbf{x}, q)$ of the MISO reset control system Σ. The quadratic Lyapunov function $V(\mathbf{x}, q) = \mathbf{x}^\top P \mathbf{x}$ is postulated. The result will follow after checking the sufficient Lyapunov conditions (2.35).

Condition (2.35a) is easily satisfied by taking $\alpha_1(|(\mathbf{x}, q)|_{\mathcal{A}}) = \lambda_{\min} |\mathbf{x}|^2$ and $\alpha_2(|(\mathbf{x}, q)|_{\mathcal{A}}) = \lambda_{\max} |\mathbf{x}|^2$, where $\lambda_{\min}$ and $\lambda_{\max}$ are respectively the minimum and maximum eigenvalues of P, both positive real numbers since $P > 0$.

As for the condition (2.35b), it holds that

$$\langle \nabla V(x, q), f(\mathbf{x}, q) \rangle = \mathbf{x}^T (A^T P + PA)\mathbf{x}; \tag{2.39}$$

now taking $\rho(|(\mathbf{x}, q)|_{\mathcal{A}}) = \varepsilon |\mathbf{x}|^2$, (2.38a) directly implies (2.35b). The fulfilment of condition (2.35c) is a bit more involved. First, it is shown that (2.35c) can be relaxed to

$$V(g(\mathbf{x},q)) - V((\mathbf{x},q)) \leq -\varepsilon\|\mathbf{x}\|^2, \quad \forall \mathbf{x} \in \partial\mathcal{J} = \{(\mathbf{x},q) \in \mathbb{R}^n \times \{1,-1\} : C\mathbf{x} = 0\} \quad (2.40)$$

since no solution to the system (2.17) takes values in the region $\mathcal{J}_{\text{CL}}^{\circ} = \{(\mathbf{x},q) \in \mathbb{R}^n \times \{1,-1\} : q\,C\mathbf{x} < 0\}$ except possibly at the initial instant $(0,0)$. In order to obtain a contradiction, assume that there exists some solution $\phi = (\mathbf{x},q)$ such that $\phi(t,j) \in \mathcal{J}^{\circ}$ satisfies (2.35c) for some $(t,j) \neq (0,0)$, and thus $q(t,j)C\mathbf{x}(t,j) < 0$. There are two possibilities:

- $(t,j-1) \in \operatorname{dom}\phi$, and then $\phi(t,j-1) \in \mathcal{J}$. This means that $\mathbf{x}(t,j) = A_R\mathbf{x}(t,j-1)$, and one must have both $q(t,j-1)C\mathbf{x}(t,j-1) \leq 0$ and $q(t,j)CA_R\mathbf{x}(t,j-1) < 0$. But this is impossible, since $CA_R = C$ and $q(t,j-1) = -q(t,j)$.
- (t,j) belongs to a connected component of $\operatorname{dom}\phi$ which is not a singleton, that is, there exists $\varepsilon > 0$ such that $(t-\tau,j) \in \operatorname{dom}\phi$ for all $0 < \tau < \varepsilon$, and hence $\phi(t-\tau,j) \in \mathcal{F}$ for almost all such τ. Since $\mathcal{J}^{\circ}$ is an open set, τ can be chosen small enough such that $\phi(t-\tau,j) \in \mathcal{J}^{\circ} \cap \mathcal{F}$. But this is a contradiction, since $\mathcal{J}^{\circ} \cap \mathcal{F}$ is empty.

Finally, since $V(g(\mathbf{x},q)) - V((\mathbf{x},q)) = \mathbf{x}^{\top}(A_RPA_R - P)\mathbf{x}$, considering Θ to be any full-rank right annihilator of C, that is, any matrix satisfying $\operatorname{Im}\Theta = \operatorname{Ker} C$, from (2.38b) condition (2.39) and thus (2.35c) follow, ending the proof.

For the case of a variable band resetting law, corresponding to the flow and jump sets given by (2.20) and (2.22), stability does not follow from (2.38), since in this case $C_RA_R \neq C_R$. However, a more conservative version of Proposition 2.16 holds for this resetting law if one replaces (2.38b) by the condition

$$A_R^{\top}PA_R - P \leq -\varepsilon I. \quad (2.41)$$

Note that both conditions in Proposition 2.16, and the modified condition (2.41), are stated in the form of linear matrix inequalities (LMI) [68], which is useful for computational purposes.

Stability of $\mathcal{A}_{\text{async}} = \{\mathbf{0}\} \times \{-1,1\}^n$ is now considered for the closed loop reset control system Σ (2.25) with an asynchronous resetting law, such as one consisting of

independent variable band laws.

Proposition 2.17 (Stability conditions #1, asynchronous case)**.** *Consider the asynchronous MISO reset control system* (2.25)*. The set $\mathcal{A}_{async}$ is globally asymptotically stable for this system if there exists a matrix $P > 0$ such that*

$$A^\top P + PA \leq -\varepsilon I, \tag{2.42a}$$

and for all $i = 1, \ldots, n$,

$$A_{Ri} P A_{Ri} - P \leq -\varepsilon I, \tag{2.42b}$$

hold for some $\varepsilon > 0$.

Proof. The *ansatz* $V(\mathbf{x}, q) = \mathbf{x}^\top P \mathbf{x}$ is again considered. The result will follow after showing that the sufficient Lyapunov conditions (3.31) hold.

Conditions (2.35a) and (2.35b) are easily checked as in the proof of Proposition 2.16. As for (2.35c), its relaxed version

$$V(g(\mathbf{x}, \mathbf{q})) - V((\mathbf{x}, \mathbf{q})) \leq -\varepsilon \|\mathbf{x}\|^2, \quad \forall (\mathbf{x}, \mathbf{q}) \in \bigcup_i \{(\mathbf{x}, \mathbf{q}) \in \mathbb{R}^n \times \{1, -1\}^n : C_{Ri}\mathbf{x} = 0\} \tag{2.43}$$

can be again shown to hold for (2.25) except possibly at the initial instant $(0, 0)$. The same reasoning as in the proof of Proposition 2.16 can be used to show that the Lyapunov function of any trajectory will decrease after each jump in any possible case; note that cases where two or more controllers are reset at the same time are automatically included, since e.g. $A_{Ri} P A_{Ri} - P \leq -\varepsilon I$ and $A_{Rj} P A_{Rj} - P \leq -\varepsilon I$ imply that $A_{Ri} P A_{Ri} < P$ and $A_{Rj} P A_{Rj} < P$, and thus that $A_{Ri} A_{Rj} P A_{Rj} A_{Ri} < P$ by transitivity of $<$. This last inequality implies that there exists some ε' such that $A_{Ri} A_{Rj} P A_{Rj} A_{Ri} - P \leq \varepsilon' I$. The same reasoning can be extended to an arbitrary product of reset matrices, completing the proof.

The following alternative stability conditions, applicable to both the synchronous and asynchronous configurations, correspond to the case of a reset control system

which performs a finite number of jumps and whose base system is stable.

Proposition 2.18 (Stability conditions #2)**.** *Consider the MISO reset control system* Σ *given by either* (2.17) *or* (2.25)*. The set* $\mathcal{A}$ *is globally asymptotically stable for* Σ *if there exists a matrix* $P > 0$ *such that* (2.38a) *is satisfied, and in addition there exist some* $\gamma \in \mathcal{K}_\infty$ *and* $J > 0$ *such that for any solution* ϕ *to the MISO system,* $(t, j) \in \operatorname{dom} \phi$ *implies*

$$j \leq \gamma(|\phi(0,0)|_{\mathcal{A}}) + J. \tag{2.44}$$

Proof. The proof follows directly from Theorem 2.15, since conditions 2a, 2b and 4 of the stability result are satisfied with a quadratic Lyapunov function $V(\mathbf{x}) = \mathbf{x}^\top P \mathbf{x}$. As for condition 3, it can be checked to hold by considering the function $\lambda(s) = (\lambda^R_{\max}/\lambda_{\min})s$, where $\lambda^R_{\max} > 0$ is the largest eigenvalue of $A_R^\top P A_R$ and $\lambda_{\min} > 0$ is the smallest eigenvalue of P.

To illustrate the use of the stability conditions developed in this section, a simple example is considered.

Example 2.19 (Stability of a 2×1 serial MISO system)**.** This example consists of a 2×1 MISO reset control system under a serial configuration (Figure 2.6), with the two LTI subplants given by

$$P_1(s) = \frac{1}{1+s}, \qquad P_2(s) = \frac{1}{1+10s}, \tag{2.45}$$

and the two respective controllers are PI+FORE, that is, PI+CI controllers where the Clegg integrator is replaced with a FORE with a small damping term a_r. The resetting law is the zero crossing law. The parameters are

$$k_{P1} = T_{I1} = 0.5, p_{r1} = 0.5, \qquad k_{P2} = -1, T_{I2} = 10, p_{r2} = 0.005, \tag{2.46}$$

and the FORE damping term is $a_r = 0.001$ for both controllers. The stability conditions (2.38) are applied, finding respective solutions

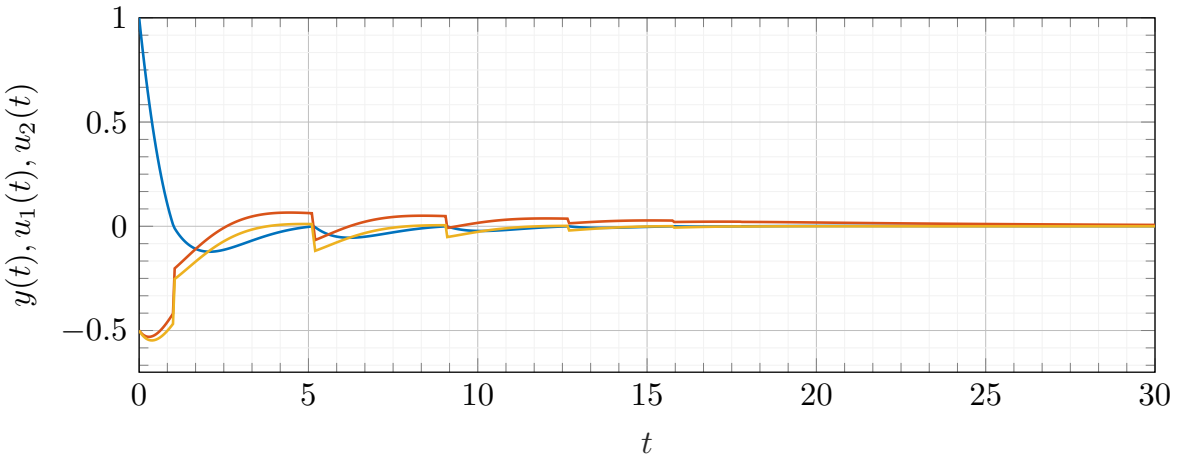

Figure 2.7: Evolution of the closed loop system and controller outputs y, u_1, u_2 (blue, orange and yellow) in Example 2.19, with the initial condition $x_{p1} = 1, x_{p2} = \mathbf{x}_{r1} = \mathbf{x}_{r2} = 0$.

$$P = 10^9 \cdot \begin{pmatrix} 0.1074 & 0.0363 & -0.0030 & -0.0000 & 0.0010 & 0.0000 \\ 0.0363 & 1.3486 & -0.0410 & -0.0000 & 0.0562 & 0.0000 \\ -0.0030 & -0.0410 & 0.0797 & 0.0000 & -0.0061 & -0.0000 \\ -0.0000 & -0.0000 & 0.0000 & 0.0749 & 0.0000 & -0.0000 \\ 0.0010 & 0.0562 & -0.0061 & 0.0000 & 0.0084 & -0.0000 \\ 0.0000 & 0.0000 & -0.0000 & -0.0000 & -0.0000 & 0.0000 \end{pmatrix} \tag{2.47}$$

in the synchronous case, and

$$P = 10^8 \cdot \begin{pmatrix} 0.8787 & 0.3806 & -0.0346 & 0.0000 & 0.0122 & 0.0000 \\ 0.3806 & 9.2570 & -0.0660 & -0.0000 & 0.3672 & -0.0000 \\ -0.0346 & -0.0660 & 0.6696 & 0.0000 & -0.0264 & -0.0000 \\ 0.0000 & -0.0000 & 0.0000 & 0.6885 & -0.0000 & -0.0000 \\ 0.0122 & 0.3672 & -0.0264 & -0.0000 & 0.0622 & -0.0000 \\ 0.0000 & -0.0000 & -0.0000 & -0.0000 & -0.0000 & 0.0001 \end{pmatrix} \tag{2.48}$$

in the asynchronous case. Hence, the closed loop system is stable under all resetting laws for nondelayed MISO systems considered in this work (zero crossing and variable band). The evolution of the closed loop system with a zero crossing law has been simulated with the initial condition $x_{p1} = 1, x_{p2} = \mathbf{x}_{r1} = \mathbf{x}_{r2} = 0$ (and $q_i = 1$). Figure 2.7 depicts the evolution of the signals y, u_1 and u_2, clearly showing their convergence to

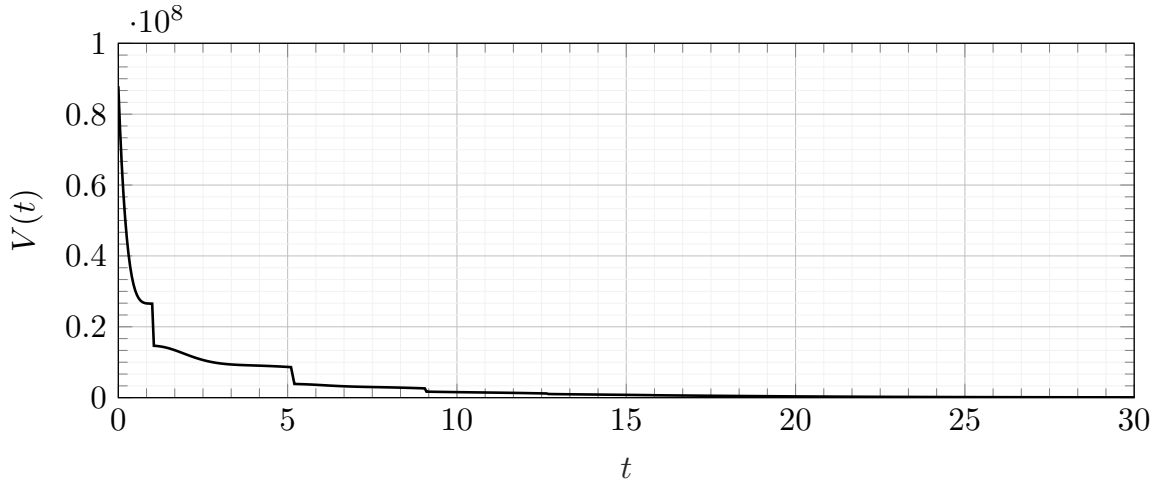

Figure 2.8: Evolution of the Lyapunov function V in Example 2.19, with the initial condition $x_{p1} = 1, x_{p2} = \mathbf{x}_{r1} = \mathbf{x}_{r2} = 0$.

the zero equilibrium state. Moreover, Figure 2.8 shows the values of the corresponding Lyapunov function $V = \mathbf{x}^\top P\mathbf{x}$ evaluated at the previous trajectory; as expected, it is decreasing both under flowing and under jumping.

Chapter 3

Hybrid and reset control of MISO and SISO systems with time delay

First, an introduction to the Hybrid Inclusions framework for systems with memory is described. A discussion of the various resetting laws and control strategies follows, including a novel development, called the *reset-and-hold strategy*, designed for the control of processes with time delay. Next, a theoretical introduction to the control of multiple-input single-output systems with delay is given. Finally, a full closed loop model of a multiple-input single-output (MISO) reset control system as a hybrid system with memory is given for both control structures.

3.1 Hybrid systems with memory

The HI framework presented in the previous chapter is unable to model systems having time delays, so an extension of the formalism is needed to account for the possible dependence on past states. This extension has been developed in [252]. The main difference of this modified framework with respect to the original one is that the domains of the solutions now extend into the past, over both the t-axis and the j-axis, and that both the flow and jump maps and the flow and jump sets are allowed to depend on the past values of solutions.

Definition 3.1. A *hybrid time domain with memory* E is a subset of $\mathbb{R} \times \mathbb{Z}$, consisting of an union of intervals of the form $[t_j, t_{j+1}] \times \{j\}$ for $j = \ldots, -1, 0, 1, \ldots$ and some nondecreasing sequence $\{t_j\}_j$ of real numbers (finite or infinite on either side) such that $(0, 0) \in E$, with the last interval (if it exists) possibly being of the form $[t_J, T) \times \{J\}$ with T finite or infinite and $J \geq 0$, and the first interval (if it exists) possibly being of

the form $(T', t_{J'}] \times \{J'\}$ with T' finite or infinite and $J' \leq 0$. A hybrid time domain with memory can be partitioned as $E = E_{\geq 0} \cup E_{\leq 0}$, where $E_{\geq 0} = E \cap (\mathbb{R}_{\geq 0} \times \mathbb{Z}_{\geq 0})$ and $E_{\leq 0} = E \cap (\mathbb{R}_{\leq 0} \times \mathbb{Z}_{\leq 0})$; if the former of these sets is empty, E is called a *hybrid memory domain*. (Note that in [252], [253] the notation s_k for $k = 1, \ldots$ is used for what we call t_{-k+1}, and t_0 is instead defined to be 0).

To simplify later definitions, we will define the *length* of a hybrid memory domain E to be either $-(T + J)$ where the infimum $(T, J) = \inf_{t,j}\{(t, j) \in E\}$ exists (note that this is always a nonnegative number), or ∞ when this infimum doesn't exist.

Definition 3.2. A *hybrid arc with memory* is a function $\phi(t, j)$ defined on a hybrid time domain $E = \operatorname{dom} \phi$ and taking values on $\mathbb{R}^n$, which is locally absolutely continuous on each interval of E. If $E = E_{\leq 0}$ is a hybrid memory domain, ϕ is referred to as a *hybrid memory arc*.

Hybrid memory arcs are used to represent both the initial conditions and the past history of a hybrid system with memory. Let $\mathcal{M}^\Delta$ be the set of all hybrid memory arcs whose domain's length lies between Δ and $\Delta + 1$, both inclusive. Figure 3.1 shows an example of a hybrid memory domain such that any hybrid memory arc with that domain is in in $\mathcal{M}^\Delta$ for $\Delta = 3$, as well as two examples of hybrid memory domains all of whose associated hybrid memory arcs fail to be in $\mathcal{M}^\Delta$.

Now we can state the definition of a hybrid system with memory:

Definition 3.3. A *hybrid system* Σ *with memory of size* Δ and state $\mathbf{x}$ is given by

$$\Sigma : \begin{cases} \dot{\mathbf{x}} \in f(\mathbf{x}), & \text{if } \mathbf{x} \in \mathcal{C}, \\ \mathbf{x}^+ \in g(\mathbf{x}), & \text{if } \mathbf{x} \in \mathcal{D}. \end{cases} \tag{3.1}$$

where $f : \mathcal{M}^\Delta \rightrightarrows \mathbb{R}^n$ is the flow map, $g : \mathcal{M}^\Delta \rightrightarrows \mathbb{R}^n$ is the jump map, and $\mathcal{C}, \mathcal{D} \subseteq \mathcal{M}^\Delta$ are the flow and jump sets respectively.

Note that the domains of f and g, as well as the sets $\mathcal{C}$ and $\mathcal{D}$, are now subsets of the space of hybrid memory arcs, instead of merely subsets of $\mathbb{R}^n$; this is meant to model the dependence on the past history of the system.

Definition 3.4. For any (t, j) in the domain of a hybrid arc ϕ, we define the *shift operators* $\mathcal{A}_{[t,j]} : (\operatorname{dom} \phi)_{\geq 0} \to \mathcal{M}^\Delta$, which satisfy

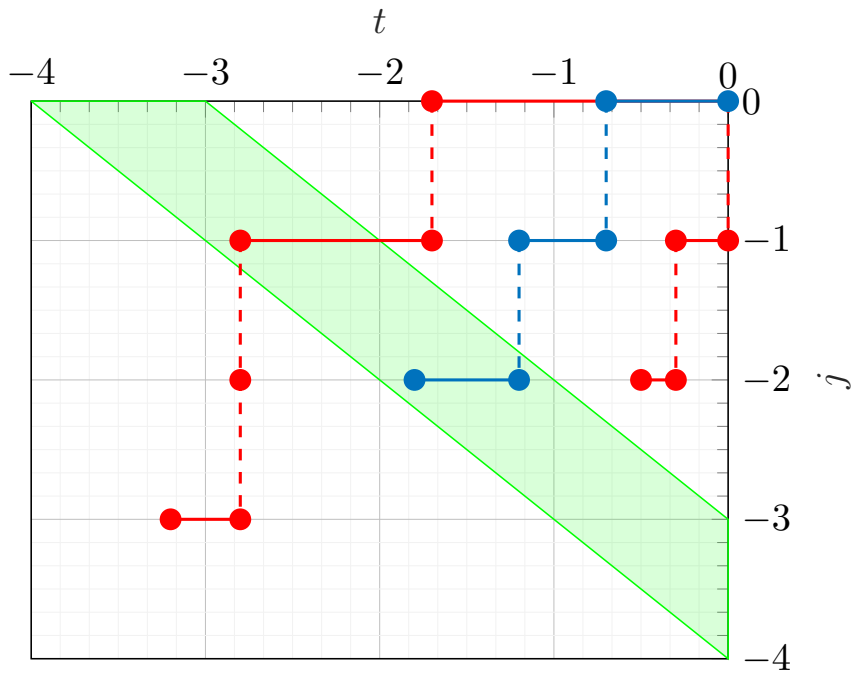

Figure 3.1: Example of a hybrid memory domain E such that any hybrid memory arc with domain E is in $\mathcal{M}^3$ (blue), together with two examples of hybrid memory domains such that hybrid memory arcs with those domains fail to be in $\mathcal{M}^3$ (red). Note that hybrid arcs with the leftmost domain will become elements of $\mathcal{M}^3$ after applying the shift operator $\mathcal{A}_{[0,0]}$, since the portion of the domain strictly below the line $t + j = -3$ is discarded.

$$(\mathcal{A}_{[t,j]}\phi)(s,k) = \phi(s+t, k+j) \tag{3.2}$$

for any $(s,k) \in \mathbb{R}_{\leq 0} \times \mathbb{Z}_{\leq 0}$ with $s + k > -\Delta$ for which the right hand side of the equality is defined.

The intuition is that $\mathcal{A}_{[t,j]}\phi$ represents the distributed state at (t,j), that is, the portion of the hybrid arc that extends backwards from (t,j) over a domain of total length at most Δ, considered as a hybrid memory arc in $\mathcal{M}^{\Delta}$. To simplify the notation, when $\mathbf{x}$ is a hybrid arc representing some (sub-)state of a reset control system, we will sometimes employ the shorthand notation $\mathbf{x}_{[t,j]}$ instead of $\mathcal{A}_{[t,j]}\mathbf{x}$.

A hybrid system with memory Σ is described in terms of the same four data $(f, g, \mathcal{C}, \mathcal{D})$ as ordinary hybrid systems, but the solutions are now defined by means of the above defined shift operators. The conditions a solution must satisfy are analogues of those in Definition 2.4.

Definition 3.5. A solution of Σ given by (3.1) is a hybrid arc satisfying the following properties:

1. $\mathcal{A}_{[t,j]}\phi \in \mathcal{C}$ and $d\phi(t,j)/dt \in f(\mathcal{A}_{[t,j]}\phi)$ for almost all (t,j) in the interior of any nonempty interval $I_j \subseteq (\operatorname{dom}\phi)_{\geq 0}$.

2. $\mathcal{A}_{[t,j]}\phi$ is in $\mathcal{D}$ and $\phi(t,j+1) \in g(\mathcal{A}_{[t,j]}\phi)$ for all $(t,j) \in (\operatorname{dom}\phi)_{\geq 0}$ such that $(t,j+1) \in (\operatorname{dom}\phi)_{\geq 0}$.

3. $\mathcal{A}_{[0,0]}\phi \in \bar{\mathcal{C}} \cup \mathcal{D}$.

A notion of convergence, called *graphical convergence*, can be defined on the space of hybrid arcs with memory; as the details are somewhat involved, the reader is referred to [252] for its definition.

For $\Delta, b, \lambda \in \mathbb{R}_{\geq 0}$, $\mathcal{M}^{\Delta}_{b,\lambda}$ is defined as the space of λ-Lipschitz hybrid memory arcs of size Δ whose pointwise norms are bounded by b. The space $\mathcal{M}^{\Delta}_{b}$ is defined in a similar manner by dropping the condition associated to λ. It is proven in [253] that $\mathcal{M}^{\Delta}_{b,\lambda}$ is a closed subset of $\mathcal{M}^{\Delta}$ under the topology induced by graphical convergence. The definition of these spaces is motivated by well-posedness and stability considerations, as will be seen in Section 3.4.

The results of the HI formalism for systems with inputs have not yet been extended (to the knowledge of the author) to account for systems with both memory and inputs; however, this will not represent an important problem in the following developments, since the controllers themselves are not subject to time delays. As for the full closed loop control system in the delayed case, any exogenous inputs such as disturbances, references and noise can be either assumed to be zero, or be included within the model description in the form of exosystems.

3.2 Reset-and-hold strategy

In this section, a new hybrid control strategy, referred to as *reset-and-hold* strategy, is introduced. This strategy is inspired in the distributed state resetting approach of [167], and will be shown to be especially useful for systems with time delays.

The main motivation of this strategy, as will be seen in Chapter 4, is to overcome the performance of ordinary reset control for systems with time delays. This is essentially due the fact that the performance improvement due to resetting crucially depends on a balance between the after-reset states of the plant and the controller. However, the presence of delay in the feedback path destroys that balance, typically producing an undesired undershooting, which in turn limits the potential performance improvement. In order to avoid this problem, the essential idea is to augment the resetting mechanism so as to keep the control signal constant after every reset action during a time interval of prescribed length, a mechanism which will be referred to as *holding*.

The holding mechanism was used in the work [316] with reset controllers for which $A_r = 0$ (namely, PI+CI controllers), and there are two different ways of extending it to the general reset controller with nonzero A_r: one is based on keeping the control output u constant, and the other is based on forcing the controller to evolve as if its control input were zero, ignoring the actual input e. Although the first choice was used in [316], a more general implementation that includes both of these extensions will be considered in the following.

Definition 3.6. The *reset-and-hold controller* R_H, with state $(\mathbf{x}_r, q, m, \tau) \in \mathcal{O}^H := \mathcal{O}^{n_r} \times \{0, 1\} \times \mathbb{R}_{\geq 0}$ and input $(e, \sigma) \in \mathbb{R}^2$, is defined as a hybrid system with inputs

given by:

$$R_H : \begin{cases} \begin{pmatrix} \dot{\mathbf{x}}_r \\ \dot{\tau} \end{pmatrix} = \begin{pmatrix} (mA_r + (1-m)A_r')\mathbf{x}_r + mB_r e \\ 1 \end{pmatrix}, (\mathbf{x}_r, q, m, \tau, \sigma) \in \mathcal{C}_H \\ \begin{pmatrix} \mathbf{x}_r^+ \\ q^+ \\ m^+ \\ \tau^+ \end{pmatrix} = \begin{pmatrix} A_\rho \mathbf{x}_r \\ (1-2m)q \\ 1-m \\ 0 \end{pmatrix}, \qquad (\mathbf{x}_r, q, m, \tau, \sigma) \in \mathcal{D}_H \end{cases} \tag{3.3}$$

where the output is $u = C_r\mathbf{x}_r + mD_re$, the flow set is defined as $\mathcal{C}_H = \mathcal{C}_{H_0} \cup \mathcal{C}_{H_1}$, being

$$\mathcal{C}_{H_0} = \{(\mathbf{x}_r, q, m, \tau, e) \in \mathcal{O}^H \times \mathbb{R} : m = 0, \tau \leq \tau_H\}, \tag{3.4a}$$
$$\mathcal{C}_{H_1} = \{(\mathbf{x}_r, q, m, \tau, e) \in \mathcal{O}^H \times \mathbb{R} : m = 1, q\,\sigma \geq 0\}, \tag{3.4b}$$

and the jump set is defined as $\mathcal{D}_H = \mathcal{D}_{H_0} \cup \mathcal{D}_{H_1}$, being

$$\mathcal{D}_{H_0} = \{(\mathbf{x}_r, q, m, \tau, e) \in \mathcal{O}^H \times \mathbb{R} : m = 0, \tau \geq \tau_H\}, \tag{3.5a}$$
$$\mathcal{D}_{H_1} = \{(\mathbf{x}_r, q, m, \tau, e) \in \mathcal{O}^H \times \mathbb{R} : m = 1, q\,\sigma \geq 0\}. \tag{3.5b}$$

As in (2.9), it is assumed that $\sigma = S(e)$ for some function S. In comparison with the reset controller (2.11), R_H includes an extra discrete state $m \in \{0, 1\}$, that will be used to switch between two operating modes, and a timer τ which will be in charge of regulating the time interval in which the controller output is held constant after every jump due to reset. The two operating modes are:

- *Resetting mode* ($m = 1$): the controller output corresponds to that of the base linear controller (A_r, B_r, C_r, D_r). Jumps are enabled only when the resetting law $q\,s \leq 0$ is triggered: a crossing is detected and thus the sign of q is changed, $\mathbf{x}_r$ is reset to $A_\rho\mathbf{x}_r$, the timer is reset to zero, and m switches to 0 (holding mode).

- *Holding mode* ($m = 0$): several cases can be distinguished depending on the matrix A_r'. If $A_r' = 0$, the state $\mathbf{x}_r$ is kept constant (note that $\dot{\mathbf{x}}_r = 0$ from (3.3)),

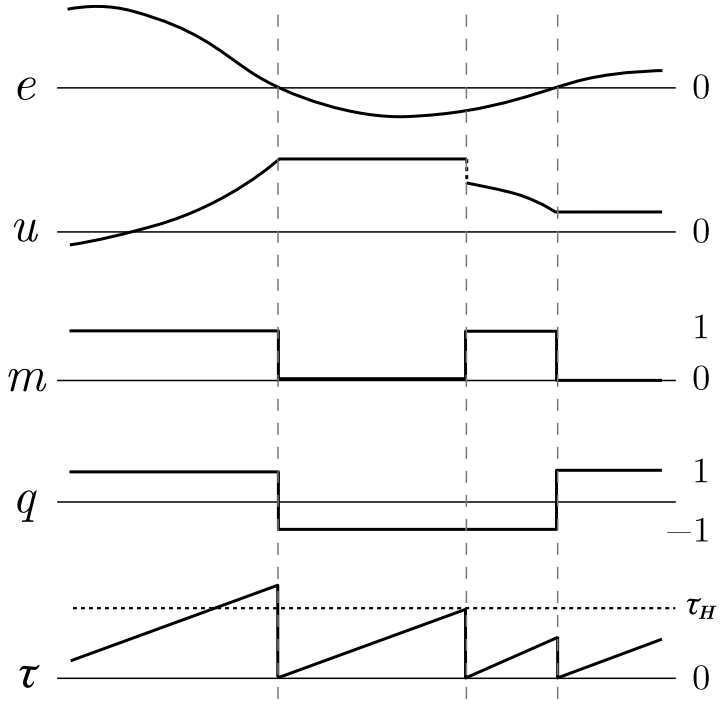

Figure 3.2: Reset-and-hold controller state and output response for a given input e, under a zero crossing resetting law.

and thus, since $u = C_r\mathbf{x}_r + mD_re = C_r\mathbf{x}_r$, then the control output is constant in this mode. On the other hand, if $A_r' = A_r \neq 0$, the state $\mathbf{x}_r$, and thus the output u, will evolve as if the control input were zero. In general, A_r' can be chosen arbitrarily, and the controller output will correspond to that of the linear system $(A_r', 0, C_r, 0)$. In any case, the timer τ is activated, and when it reaches the value $\tau = \tau_H$ a jump is enabled. After jumping, m switches to 1 (resetting mode), the timer τ is initialized to zero, and the rest of states are kept identical.

Figure 3.2 shows an example of a state and output response for a given controller input (with $A_r' = 0$), where both operating modes are represented. Moreover, note that the behavior of the ordinary reset controller R, as given by (2.11), can be recovered from (3.3) simply by making $\tau_H = 0$.

In summary, the essential idea behind the reset-and-hold strategy is to temporarily disable the feedback path during the intervals of time $[t_j, t_j + \tau_H]$ after some reset action at time t_j, until the effect of reset is able to properly reach a plant with time delay. This strategy is especially useful in cases where reset actions aim to drive this plant to a steady state where $e \to 0$ in a finite time, as will be seen in Chapter 4.

3.2.1 Describing function analysis

The describing function method [237] consists of considering the response of a nonlinear system to a sinusoidal input of frequency ω and amplitude E, and approximating the eventual output as $t \to \infty$ by its fundamental frequency component, that is, neglecting higher order terms in its Fourier series. Taking this component gives a two-parameter function $H(E, i\omega)$ dependent on the input's amplitude and frequency, which is analogous to the usual frequency response $H(i\omega)$ associated to a LTI system. Specifically, one has

$$H(E, i\omega) = \frac{2i\omega}{\pi E} \int_I F(E \sin(\omega t)) e^{-i\omega t} dt, \tag{3.6}$$

where $F(E \sin(\omega t))$ denotes the nonlinear system's output to an input $E \sin(\omega t)$, and the integral is evaluated over a time interval I of length π/ω. Although the describing function method does not give complete information about the behavior of a nonlinear system and may lead to mistaken impressions if not interpreted carefully, it can be used to capture some of its important features in a qualitative way, and allow for an easier comparison with closely related LTI systems.

To showcase the benefits of reset control and the reset-and-hold strategy with respect to linear control, the describing function method will be used to analyze the Clegg integrator with the zero crossing law, the variable band law, and the reset-and-hold strategy, and compare it to a linear integrator. The describing functions in all cases turn out to be independent of the amplitude E due to the linearity of the base system and the homogeneity of reset actions, so there is no loss of generality in assuming $E = 1$.

The describing function of the Clegg integrator with zero crossing law is known to be [106]

$$CI_{\mathrm{ZC}}(i\omega) = \frac{1 + 4i/\pi}{i\omega} \simeq \frac{1.619 e^{-i38.15^\circ}}{\omega}. \tag{3.7}$$

In comparison with the frequency response $I(i\omega) = \frac{1}{i\omega} = \frac{e^{-i90^\circ}}{\omega}$ of a linear integrator, it has a slightly bigger gain of 1.619, and a phase lead of about 51.85 degrees. These gain and phase values can be shown to be linked to various performance improvements compared to the linear integrator which are known to be unattainable for LTI systems (due to limitations such as e.g. Bode's gain-phase relationship), and is in fact one of

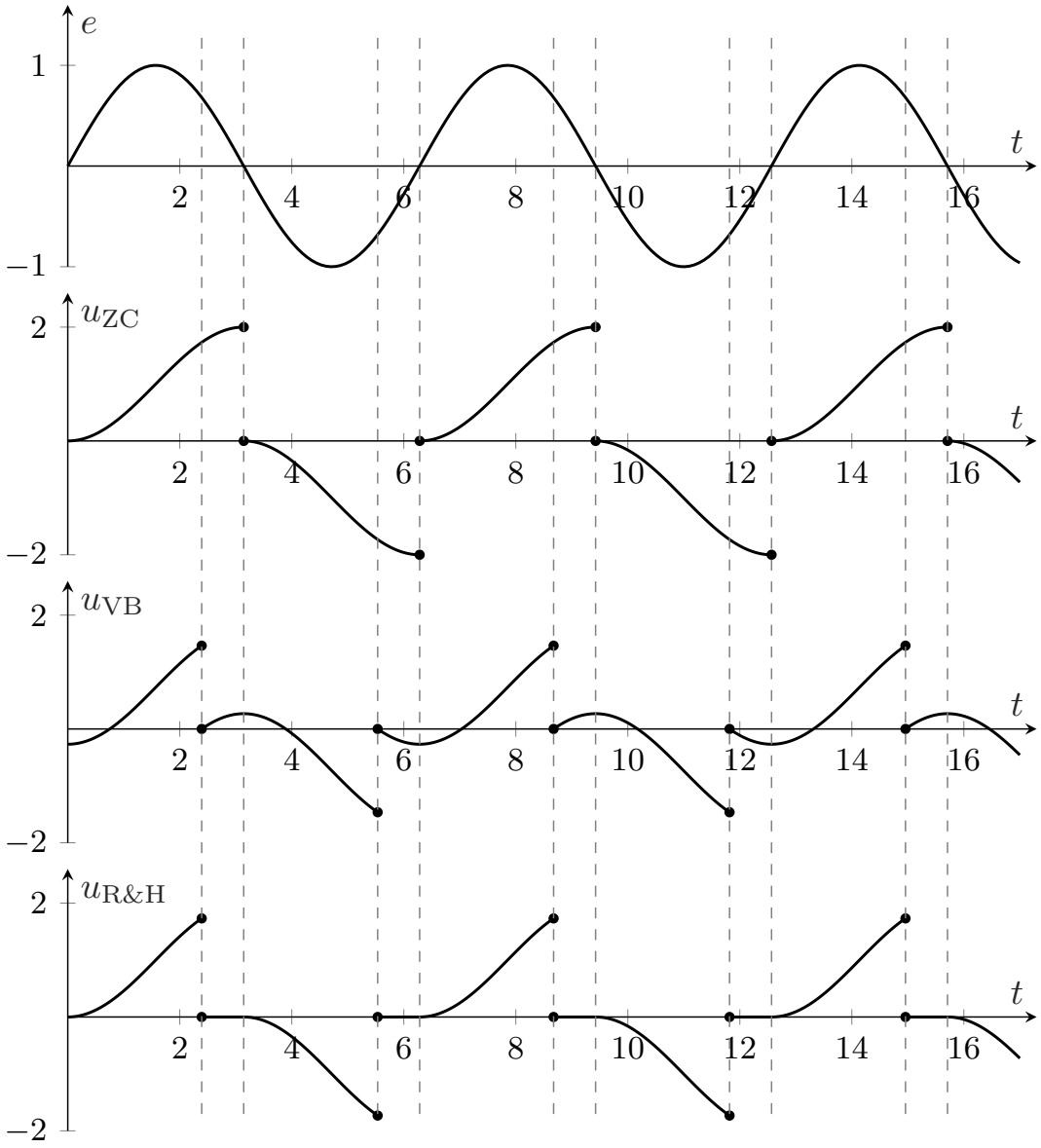

Figure 3.3: Illustration of the responses of the zero crossing, variable band, and reset-and-hold Clegg integrators to a sinusoidal input.

the original motivations for reset control.

The describing function of the Clegg integrator with variable band law is computed in [358]; the expression given therein can be further simplified to

$$CI_{\mathrm{VB}}(i\omega) = \frac{1}{i\omega}\left(1 + \frac{4i/\pi}{(1 - i\omega\theta)}\right). \tag{3.8}$$

Finally, the describing function for the reset-and-hold Clegg integrator is given by the integral (3.6) evaluated in the interval $[t_1, t_2]$ where $t_1 = \arctan(-\theta\omega)$ is the first instant at which the variable band law is first triggered, and $t_2 = t_1 + \pi/\omega(1 + \lfloor \omega\tau_H/\pi \rfloor)$ (where $\lfloor x \rfloor$ is the greatest integer lower or equal to x) is the second such instant. Recalling that the output is zero in the intervals $[t_k, t_k + \tau_H]$ because of holding (see Figure 3.3), this integral reduces to

$$CI_{\mathrm{RH}}(i\omega) = \frac{-i\int_{(\arctan(-\theta\omega)-\pi\lfloor\omega\tau_H/\pi\rfloor)/\omega+\tau}^{(\arctan(-\theta\omega)+\pi)/\omega} e^{-i\omega}\frac{\cos(\omega t)-\cos(\arctan(-\theta\omega)-\pi\lfloor\omega\tau_H/\pi\rfloor+\omega\tau)}{\omega}dt}{1 + \lfloor\omega\tau_H/\pi\rfloor}, \tag{3.9}$$

which is integrable by usual elementary methods, and readily evaluates to the piecewise-defined function

$$CI_{\mathrm{RH}}(i\omega) = \begin{cases} -\dfrac{A(i\omega) + B(i\omega)}{2i\omega(1 - i\omega\theta)\pi N(\omega)}, & N(\omega) \text{ even}, \\ \dfrac{A(i\omega) - B(i\omega)}{2i\omega(1 - i\omega\theta)\pi N(\omega)}, & N(\omega) \text{ odd}, \end{cases} \tag{3.10}$$

where $N(\omega) = \lfloor \omega\tau_H/\pi \rfloor$, and

$$A(i\omega) = 3 + e^{-2i\omega\tau_H}(1 + i\omega\theta) + 2i\omega\tau_H - 2\pi i(1 + N(\omega)) - i\omega\theta, \tag{3.11}$$

$$B(i\omega) = -i\omega\theta(2i\omega\tau_H - 2\pi i N(\omega)) + 4\cos(\omega\tau_H) + 4\omega\theta\sin(\omega\tau_H). \tag{3.12}$$

Figure 3.4 shows the gain of each considered describing function in the interval $[0.01, 5\pi]$, as well as its phase in the interval $[0.01, \pi]$ (with $\theta = 1$ for the variable band Clegg integrator and $\theta = \tau_H = 1$ reset-and-hold CI). Note how the gain $1.619/\omega$ of the zero crossing CI is in fact an upper bound for the gains of the other hybrid integrators; this bound is an indication that the considered control strategies do not lead to any amplification of the high frequency components of the input signal, such as sensor

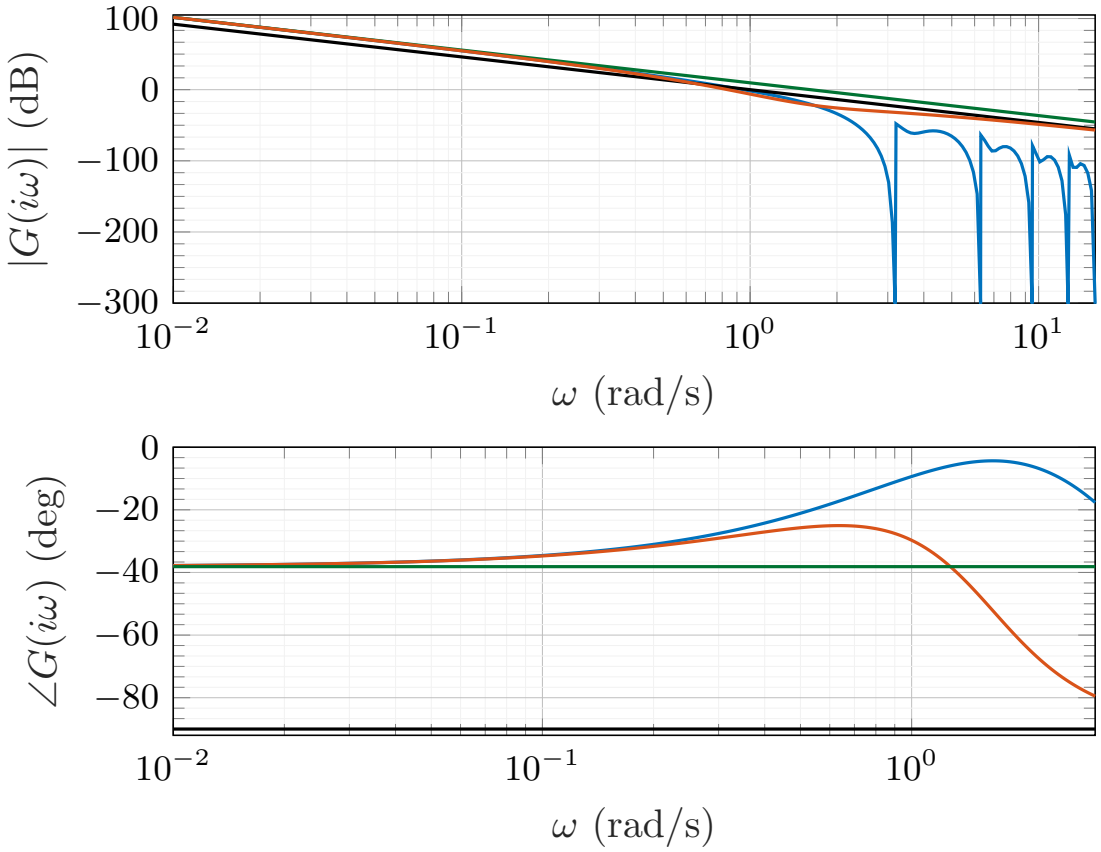

Figure 3.4: Bode plot of the describing functions for the Clegg integrator with the zero crossing law (green), the variable band law (orange) and the reset-and-hold mechanism (blue). The transfer function for a linear integrator is also shown in black for comparison purposes.

noise. Note also that the singularities appearing at $\omega = n\pi$ in the reset-and-hold case are due to the fact that sinusoidal signals with these periods are completely zeroed by the holding mechanism; this happens in the general case when $\omega = n\pi/\tau_H$.

With respect to the phases, focusing on the low-frequency interval $[0.01/\theta, \pi/\theta]$ the reset-and-hold CI features the biggest phase lead (up to 85.10° compared to the linear integrator), followed by the variable band CI (up to 64.96°). This lends credibility to the idea that variable band and (especially) reset-and-hold is well suited for compensating the phase lag associated to a process with time delay. Note that the addition of a filter for the variable band integrator is analyzed in [118], where it is shown not to degrade its useful phase lead properties provided the filter time constant is not greater than about 0.4θ.

Note that the describing function for a PI+CI controller is simply given by a weighted sum of a PI controller's frequency response function and the CI's describing function; the reset-and-hold PI+CI is slightly more complicated to describe, since holding also affects the linear integrator and the proportional part, but the qualitative behavior is similar to the reset-and-hold CI.

3.3 Closed loop system models

In this section, closed loop models of the main hybrid control systems used in this work will be developed under the Hybrid Inclusions framework, considering two cases: a delayed SISO system and a delayed MISO system.

3.3.1 Model of a SISO control system with time delay

Before dealing with the model of a fully general delayed MISO control system, it has been considered pertinent to first introduce the corresponding model specialized to delayed SISO systems, for the following reasons:

- The model of a parallel control system for a general delayed MISO LTI plant is mathematically quite complicated, so it is convenient to analyze the single-input case first, whose structure is somewhat simpler but has many shared features.
- To the knowledge of the author, there does not yet exist any full implementation, under the HI framework for systems with memory, of a SISO reset control system

for a delayed plant in the literature. Hence, the model developed here can be thought of as a separate contribution to the body of control knowledge.

- The design of a PI+CI based control setup using the newly developed reset-and-hold strategy, treated in Chapter 4, is also applicable to SISO systems. Moreover, there are certain limitations in the MISO case that are absent in the single-input case. Finally, from a practical perspective, examples of MISO control systems (especially under the parallel control structure) are less commonly found or studied than SISO control systems. Hence, it is important to deal with the SISO setting separately in view of its higher potential applicability.

A hybrid controller implementing the reset-and-hold strategy will be considered, since the model involving ordinary reset controllers can be recovered as a limiting case. Consider a linear time-invariant plant P with time delay h, defined by the delay-differential equation

$$P : \begin{cases} \dot{\mathbf{x}}_p(t) = A_p \mathbf{x}_p(t) + B_p v(t-h) \\ y = C_p \mathbf{x}_p(t). \end{cases} \tag{3.13}$$

with state $\mathbf{x} \in \mathbb{R}^{n_p}$, input $v \in \mathbb{R}$ and output $v \in \mathbb{R}$, and the feedback connection between P and a reset-and-hold controller R_H, given by $e = r_y - y$, where $r_y \in \mathbb{R}$ is a reference signal, and $v = u + d$, being u the controller output and $d \in \mathbb{R}$ a disturbance signal. The closed loop state is $\mathbf{z} \in \mathcal{O} := \mathbb{R}^{n_p} \times \mathcal{O}^H$, and is partitioned as $\mathbf{z} = (\mathbf{x}, \mathbf{s})$, where $\mathbf{x} = (\mathbf{x}_p, \mathbf{x}_r)$, and $\mathbf{s} = (q, m, \tau)$. From (3.3)–(3.5) and (2.16), the closed loop system (without exogenous inputs) is given informally by the evolution equations

$$\begin{aligned} \begin{pmatrix} \dot{\mathbf{x}} \\ \dot{q} \\ \dot{m} \\ \dot{\tau} \end{pmatrix} &= \begin{pmatrix} A_0(m)\mathbf{x} + A_h(m)\mathbf{x}(t-h) \\ 0 \\ 0 \\ 1 \end{pmatrix}, \quad (\mathbf{z}(t), \mathbf{z}(t-h)) \in \mathcal{C}_0 \\ \begin{pmatrix} \mathbf{x}^+ \\ q^+ \\ m^+ \\ \tau^+ \end{pmatrix} &= \begin{pmatrix} A_R \mathbf{x} \\ (1-2m)q \\ 1-m \\ 0 \end{pmatrix}, \qquad (\mathbf{z}(t), \mathbf{z}(t-h)) \in \mathcal{D}_0 \end{aligned} \tag{3.14}$$

where the flow and jump sets are given by

$$\begin{aligned}\mathcal{C}_0 = \quad & \{(\mathbf{z}_0, \mathbf{z}_1) \in \mathcal{O}^2 : m_0 = 0, \tau_0 \leq \tau_H\} \ \cup \\ & \{(\mathbf{z}_0, \mathbf{z}_1) \in \mathcal{O}^2 : m_0 = 1, \\ & \ qC((I + \theta A_0)\mathbf{x}_0 + \theta A_h \mathbf{x}_1)) \geq 0\}\end{aligned} \tag{3.15}$$

and

$$\begin{aligned}\mathcal{D}_0 = \quad & \{(\mathbf{z}_0, \mathbf{z}_1) \in \mathcal{O}^2 : m_0 = 0, \tau_0 \geq \tau_H\} \ \cup \\ & \{(\mathbf{z}_0, \mathbf{z}_1) \in \mathcal{O}^2 : m_0 = 1, \\ & \ qC((I + \theta A_0)\mathbf{x}_0 + \theta A_h \mathbf{x}_1)) \leq 0\}\end{aligned} \tag{3.16}$$

respectively, and

$$\begin{aligned}A_0(m) &= \begin{pmatrix} A_p & 0 \\ -mB_rC_p & mA_r + (1-m)A_r' \end{pmatrix}, \\ A_h(m) &= \begin{pmatrix} -mB_pD_rC_p & B_pC_r \\ 0 & 0 \end{pmatrix},\end{aligned} \tag{3.17}$$

$$A_R = \begin{pmatrix} I & 0 \\ 0 & A_\rho \end{pmatrix}, \quad C = \begin{pmatrix} -C_r & 0 \end{pmatrix}. \tag{3.18}$$

Now, consider a hybrid arc $\mathbf{z} = (\mathbf{x}, q, m, \tau)$ and let $\mathbf{z}_{[t,j]} \in \mathcal{M}^\Delta$ be its associated family of hybrid memory arcs at (t, j), partitioned as before. The closed loop hybrid system (3.14)–(3.18) can now be formally interpreted as a hybrid dynamical system with memory $\Sigma = (\mathcal{C}, \mathcal{D}, f, g)$ with the following data (similar but simpler examples are described in [252, 253]):

$$
\begin{aligned}
&\mathcal{C} = \{\phi \in \mathcal{M}^{\Delta} : (\phi(0,0), \phi(-h,-k_m)) \in \mathcal{C}_0\},\\
&f(\mathbf{z}_{[t,j]}) \in \begin{pmatrix} \overline{\text{conv}} \bigcup_{(-h,-k)\in \text{dom}\, \mathbf{x}_{[t,j]}} \{A_0\mathbf{x}(t,j) + A_h\mathbf{x}(t-h,j-k)\} \\ 0 \\ 0 \\ 1 \end{pmatrix},\\
&\mathcal{D} = \{\phi \in \mathcal{M}^{\Delta} : (\phi(0,0), \phi(-h,-k_m)) \in \mathcal{D}_0\},\\
&g(\mathbf{z}_{[t,j]}) = \begin{pmatrix} A_R\mathbf{x}(t,j) \\ (1-2m(t,j))q(t,j) \\ 1-m(t,j) \\ 0 \end{pmatrix},
\end{aligned}
\tag{3.19}
$$

where $k_m = \max\{k : (-h,k) \in \text{dom}\, \phi\}$. Note that the presence of the time delay h means that the flow evolution of $\mathbf{x}$ at $(t,j) \in \text{dom}\ \mathbf{x}$ depends on both $\mathbf{x}_{[t,j]}(0,0) = \mathbf{x}(t,j)$ and the value of $\mathbf{x}_{[t,j]}(-h,-k) = \mathbf{x}(t-h,j-k)$, and that due to the possibility of multiple instantaneous jumps at $t-h$, there can be more than one k satisfying $(-h,-k) \in \text{dom}\, \mathbf{x}_{[t,j]}$. The choice to take the convex hull of all those points is related to the fulfilment of regularity conditions (well-posedness) that guarantee robustness to small variations in the size of the delay [252], as will be shown in Section 3.4. In addition, the jumps also depend on $m_{[t,j]}(0,0) = m(t,j)$ and $q_{[t,j]}(0,0) = q(t,j)$. Moreover, the matrices A_0 and A_h implicitly depend on $m_{[t,j]}(0,0) = m(t,j)$, as shown in (3.17).

Note that the model corresponding to ordinary reset controllers (without the reset-and-hold mechanism) is recovered straightforwardly by setting $m = 1$ everywhere, taking out the conditions related to τ in the flow and jump sets (3.15) and (3.16), and finally removing both variables m, τ from the closed loop state and their associated evolution equations in (3.19).

3.3.2 Model of a parallel MISO control system with time delay

Consider now, in full generality, a linear and time invariant MISO system consisting of n plants P_i, $i = 1, \ldots, n$, with respective time delays $h_1, \ldots, h_n$. The ith plant is described by the linear delay-differential equation

$$P_i : \begin{cases} \dot{\mathbf{x}}_{pi}(t) = A_{pi}\mathbf{x}_{pi}(t) + B_{pi}v_i(t-h_i) \\ y_i(t) = C_{pi}\mathbf{x}_{pi}(t). \end{cases} \tag{3.20}$$

The plants are controlled by respective reset-and-hold controllers R_i. As usual, the subscript i is added to all variables in (2.11) associated with the ith controller. The total output is defined by $y = \sum_{i=1}^{n} y_i$. Finally, the feedback connection is achieved by setting $e = r_y - y$, where r_y is a reference signal, and $v_i = u_i + d_i$, for input disturbances d_i, for $i = 1, 2, \ldots$.

To arrive at the full closed-loop MISO system Σ, some more definitions are needed. The closed-loop state is now $\mathbf{z} \in \mathcal{O} := \prod_{i=1}^{n} \mathbb{R}^{n_{pi}} \times \mathcal{O}_i^H$, and is partitioned as $\mathbf{z} = (\mathbf{x}, \mathbf{s})$, where

$$\begin{aligned} \mathbf{x} &= (\mathbf{x}_{p1}, \ldots, \mathbf{x}_{pn}, \mathbf{x}_{r1}, \ldots, \mathbf{x}_{rn}) \in \mathbb{R}^N, \\ \mathbf{s} &= (\mathbf{q}, \mathbf{m}, \boldsymbol{\tau}) = (q_1, \ldots, q_n, m_1, \ldots, m_n, \tau_1, \ldots, \tau_n), \end{aligned}$$

and $N = \sum_{i=1}^{n}(n_{pi} + n_{ri})$. In order to state the flow equation, let the auxiliary matrix A be defined as

$$A = \begin{pmatrix} A_{p1} - m_1 B_{p1} D_{r1} C_{p1} & \cdots & -m_1 B_{p1} D_{r1} C_{pn} & B_{p1} C_{r1} & \cdots & 0 \\ \vdots & \ddots & \vdots & \vdots & \ddots & \vdots \\ -m_n B_{pn} D_{rn} C_{p1} & \cdots & A_{pn} - m_n B_{pn} D_{rn} C_{pn} & 0 & \cdots & B_{pn} C_{rn} \\ -m_1 B_{r1} C_{p1} & \cdots & -m_1 B_{r1} C_{pn} & m_1 A_{r1} & \cdots & 0 \\ \vdots & \ddots & \vdots & \vdots & \ddots & \vdots \\ -m_n B_{rn} C_{p1} & \cdots & -m_n B_{rn} C_{pn} & 0 & \cdots & m_n A_{rn} \end{pmatrix}. \tag{3.21}$$

Now let A_0 be the matrix obtained by formally setting $B_{pi} = 0$ in A for all i, and let A_i' for $i = 1, \ldots, n$ be the matrix obtained by setting $B_{pj} = 0$ in A for all $j \neq i$. Finally, define $A_i = A_i' - A_0$. Each of these matrices will be associated to a different source in the delay-differential flow equation for Σ: the matrix A_0 is applied to the non-delayed state, and A_i is applied to the state buffer delayed by h_i. Note that all matrices depend implicitly on the states $m_1, \ldots, m_n$.

Similarly, in order to describe the discrete evolution equation, for all $1 \leq i \leq n$ take A_{Ri} to be the $N \times N$ block diagonal matrix whose jth block equals the identity I if $j \neq \sum_{k=1}^{n} n_{pk} + \sum_{k=1}^{i} n_{rk}$ and $A_{\rho i}$ if $j = \sum_{k=1}^{n} n_{pk} + \sum_{k=1}^{i} n_{rk}$; take A_{qi} to be the diagonal matrix whose jth entry is 1 if $j \neq i$ and $1 - 2m_i$ if $j = i$; ; take A_{mi} to be the diagonal matrix whose jth entry is 1 if $j \neq i$ and -1 if $j = i$; and take M_i to be

the vector whose jth entry is 0 if $j \neq i$ and 1 if $j = i$. These matrices will govern the behavior of the closed loop system under a jump; note that the matrices with index i only affect the variables of the ith controller. The auxiliary vectors M_i will be needed to implement the affine evolution law $m_i \mapsto 1 - m_i$ in the multivariable case. Note that A_{qi} implicitly depends on m_i.

Next, let the covector C be given by

$$C = \begin{pmatrix} -C_{p1} & \cdots & -C_{pn} & 0 & \cdots & 0 \end{pmatrix}, \tag{3.22}$$

as in the nondelayed case, and define

$$C_{Ri0} = C(I + \theta_i A_0), \quad C_{Rij} = \theta_i C A_j \tag{3.23}$$

for $i, j = 1, \ldots, n$. This corresponds to an asynchronous variable band resetting law with variable band parameters θ_i; note that the separation of C_{Ri} into the $n + 1$ covectors C_{Ri0} and C_{Rij} $(1 \leq j \leq n)$ in the delayed case accounts for the fact that the time derivative of the error signal at time t depends on the system's state at the $n + 1$ different times t, $t - h_1$, $\ldots$, $t - h_n$.

The full closed loop delayed parallel MISO system Σ is then finally given by the following hybrid system with memory:

$$
\begin{aligned}
&\mathcal{C} = \textstyle\bigcup_{i=1}^{n} \mathcal{C}_i,\\
&\mathcal{C}_i = \{\varphi \in \mathcal{M}^{\Delta} : \{\varphi(-h_i, -k_{\max,\, i})\}_i \in \mathcal{C}_{0i}\},\\
&f(\mathbf{z}_{[t,j]}) \in \begin{pmatrix} \overline{\operatorname{conv}} \bigcup\limits_{(-h_i,-k_i)\in \operatorname{dom} \mathbf{x}_{[t,j]}} \{\sum_{i=0}^{n} A_i \mathbf{x}(t-h_i, j-k_i)\} \\ 0 \\ 0 \\ I \end{pmatrix},\\
&\mathcal{D} = \textstyle\bigcup_{i=1}^{n} \mathcal{D}_i,\\
&\mathcal{D}_i = \{\varphi \in \mathcal{M}^{\Delta} : \{\varphi(-h_i, -k_{\max,\, i})\}_i \in \mathcal{D}_{0i}\},\\
&g(\mathbf{z}_{[t,j]}) = \begin{pmatrix} (\prod_{i\in J} A_{Ri})\, \mathbf{x}(t,j) \\ (\prod_{i\in J} A_{qi})\, \mathbf{q}(t,j) \\ (\sum_{i\in J} M_i) + (\prod_{i\in J} A_{mi})\, \mathbf{m}(t,j) \\ 0 \end{pmatrix} \text{ if } \mathbf{z} \in \textstyle\bigcap_{i\in J} \mathcal{D}_i,
\end{aligned}
\tag{3.24}
$$

where J runs over the $2^n - 1$ nonempty subsets of $\{1, \ldots, n\}$. For convenience h_0 has been defined to be 0, and $k_{\max,\, i} = \max\{k \mid (-h_i, k) \in \operatorname{dom} \varphi\}$. Furthermore, to ease notation, the jump and flow sets have been split into n subsets, defined as

$$
\begin{aligned}
\mathcal{C}_{0i} = \; & \{\{\mathbf{z}_k\}_{k=0}^{n} \in \mathcal{O}^{n+1} : m_0 = 0, \tau_0 \le \tau_{Hi}\} \;\cup \\
& \{\{\mathbf{z}_k\}_{k=0}^{n} \in \mathcal{O}^{n+1} : m_0 = 1, \\
& \textstyle\sum_{k=0}^{n} q_0 C_{Rik} \mathbf{x}_k \ge 0\}
\end{aligned}
\tag{3.25}
$$

and

$$
\begin{aligned}
\mathcal{D}_{0i} = \; & \{\{\mathbf{z}_k\}_{k=0}^{n} \in \mathcal{O}^{n+1} : m_0 = 0, \tau_0 \ge \tau_{Hi}\} \;\cup \\
& \{\{\mathbf{z}_k\}_{k=0}^{n} \in \mathcal{O}^{n+1} : m_0 = 1, \\
& \textstyle\sum_{k=0}^{n} q_0 C_{Rik} \mathbf{x}_k \le 0\}.
\end{aligned}
\tag{3.26}
$$

The dynamics of jumps will be determined by which one of these jump subsets is hit by the state, i.e., by which variable band law is triggered. Note that the evolution of the system may be such that the state can belong to two or more jump subsets $\mathcal{D}_a, \mathcal{D}_b, \ldots$ at the same time (this may happen e.g. when $h_a = h_b = \ldots$ and $\theta_a = \theta_b = \ldots$), hence the use of the set-valued variable J. The appearance of a convex hull in f is due to well-posedness reasons, as in the single-input case.

Like in the nondelayed setting, this big leap in notational complexity with respect to the synchronous case arises from the fact that controllers may now perform asynchronous resetting at different times, so essentially one needs what amounts to n distinct resetting laws, in such a way that each set of controller variables is reset independently of the others whenever its associated condition is satisfied. The possible combinations of these laws leads to $2^n - 1$ situations to consider. In addition, the existence of n time delays with n associated continuous matrices further complicates the system's description.

Finally, the model for ordinary reset controllers is recovered through the same procedure as in the SISO case, by setting $m_i = 1, \tau_{Hi} = 0$ everywhere and then removing the states m_i, τ_i from the description of the system.

3.3.3 Model extensions

Similar formulas as for the model extensions considered in Section 2.4.3 apply in the case with time delays, with some minor changes described below.

For the exogenous-inputs extension to the model of a delayed MISO system with the reset-and-hold mechanism, let A_{old} denote the auxiliary matrix defined in (3.21). The new matrix is still given by (2.27), but now

$$B_{\text{ref}} = \begin{pmatrix} m_1 B_{p1} D_{r1} C_{e1} \\ \vdots \\ m_n B_{pn} D_{rn} C_{e1} \\ m_1 B_{r1} C_{e1} \\ \vdots \\ m_n B_{rn} C_{e1} \end{pmatrix}, B_{\text{dist}} = \begin{pmatrix} C_{e21} \\ \vdots \\ C_{e2n} \\ 0 \\ \vdots \\ 0 \end{pmatrix}, B_{\text{noise}} = \begin{pmatrix} -m_1 B_{p1} D_{r1} C_{e3} \\ \vdots \\ -m_n B_{pn} D_{rn} C_{e3} \\ -m_1 B_{r1} C_{e3} \\ \vdots \\ -m_n B_{rn} C_{e3} \end{pmatrix}. \tag{3.27}$$

The matrices A_0 and A_i for $i = 1, \ldots, n$ defining the delayed flow dynamics can then be obtained by the previously outlined process of formally setting some $B_{pi} = 0$ and subtracting. The new covector C is given by (2.29).

As for the derivative filter extension, the following replacements must be performed:

$$\mathbf{x} \leftarrow \begin{pmatrix} \mathbf{x} \\ x_{d1} \\ \vdots \\ x_{dn} \end{pmatrix}, \quad A_0 \leftarrow \begin{pmatrix} A_0 & 0 & \cdots & 0 \\ CA_0 & -1/(\gamma_1\theta_1) & \cdots & 0 \\ \vdots & \vdots & \ddots & \vdots \\ CA_0 & 0 & \cdots & -1/(\gamma_n\theta_n) \end{pmatrix},$$
$$A_j \leftarrow \begin{pmatrix} A_j & 0 & \cdots & 0 \\ CA_j & 0 & \cdots & 0 \\ \vdots & \vdots & \ddots & \vdots \\ CA_j & 0 & \cdots & 0 \end{pmatrix}, \quad C \leftarrow \begin{pmatrix} C & 0 & \cdots & 0 \end{pmatrix} \tag{3.28}$$

and

$$\begin{aligned} C_{Ri0} &\leftarrow \begin{pmatrix} C & 0 & \cdots & \theta_i & \cdots & 0 \end{pmatrix}, \\ C_{Rik} &\leftarrow \begin{pmatrix} 0 & 0 & \cdots & 0 & \cdots & 0 \end{pmatrix}. \end{aligned} \tag{3.29}$$

The closed loop system is then given by (3.24) with the jump and flow subsets (3.25), (3.26), with the new definitions of $A_0, A_j, C, C_{Ri0}, C_{Rik}$ (and with A_R extended to act as the identity matrix on the new states).

When using time regularization (with identical equations to the nondelayed case), the timer variable τ_{TR} would utilize a notation similar to the timer in the reset-and-hold strategy. However, note that time regularization becomes unnecessary once this strategy is implemented: in the SISO case, it is easy to see that the reset-and-hold system is guaranteed to have at most two jumps in any interval $[t, t+\tau_H)$, and similarly in the MISO case, at most $2n$ jumps will occur over the time interval $[t, t+\tau_{H,\min})$, where $\tau_{H,\min} = \min_{i=1}^{n} \tau_{Hi}$. In consequence, a situation does not arise where both strategies need to be used at the same time, thus avoiding the possible notational conflict.

3.4 Well-posedness and stability

3.4.1 Well-posedness

Like in the memoryless case, the well-posedness of a hybrid system with memory is a property related to the robust existence and maximality of solutions and their dependence on initial conditions. Since the full definition is mathematically involved and requires many other preliminary definitions, it is not reproduced here; the reader is instead referred to [253] for details.

Again, proving that a hybrid system with memory is well-posed reduces to checking whether some conditions are satisfied by the system's data, as indicated by the following theorem.

Theorem 3.7. *A hybrid system with memory Σ is well-posed if for every b and λ, these conditions (the* basic hybrid conditions *for systems with memory) are satisfied:*

- *The sets $\mathcal{C} \cap \mathcal{M}^{\Delta}_{b,\lambda}$ and $\mathcal{D} \cap \mathcal{M}^{\Delta}_{b,\lambda}$ are closed subsets of $\mathcal{M}^{\Delta}$.*
- *The set-valued function f is outer semicontinuous relative to $\mathcal{C} \cap \mathcal{M}^{\Delta}_{b,\lambda}$, locally bounded relative to $\mathcal{C} \cap \mathcal{M}^{\Delta}_{b}$, and has nonempty, convex image at every hybrid memory arc in $\mathcal{C} \cap \mathcal{M}^{\Delta}_{b,\lambda}$.*
- *The set-valued function g is outer semicontinuous relative to $\mathcal{D} \cap \mathcal{M}^{\Delta}_{b,\lambda}$, locally bounded relative to $\mathcal{D} \cap \mathcal{M}^{\Delta}_{b}$, and has nonempty image at every hybrid memory arc in $\mathcal{D} \cap \mathcal{M}^{\Delta}_{b,\lambda}$.*

Proof. See Theorem 3 of [253].

As in the nondelayed case, if Σ is well-posed in this sense, its solution sets inherit several properties, such as upper-semicontinuous dependence with respect to initial conditions, robustness against perturbations like measurement noise, and preservation of asymptotic stability under small perturbations (which is referred to as robust stability).

Proposition 3.8. *The hybrid system with memory Σ given by* (3.24) *is well-posed.*

Proof. From (3.24), it is clear that $\mathcal{C}$ and $\mathcal{D}$ are closed sets, and they remain closed after intersecting with the closed set $\mathcal{M}^{\Delta}_{b,\lambda}$. Moreover, from the definitions of f, g it

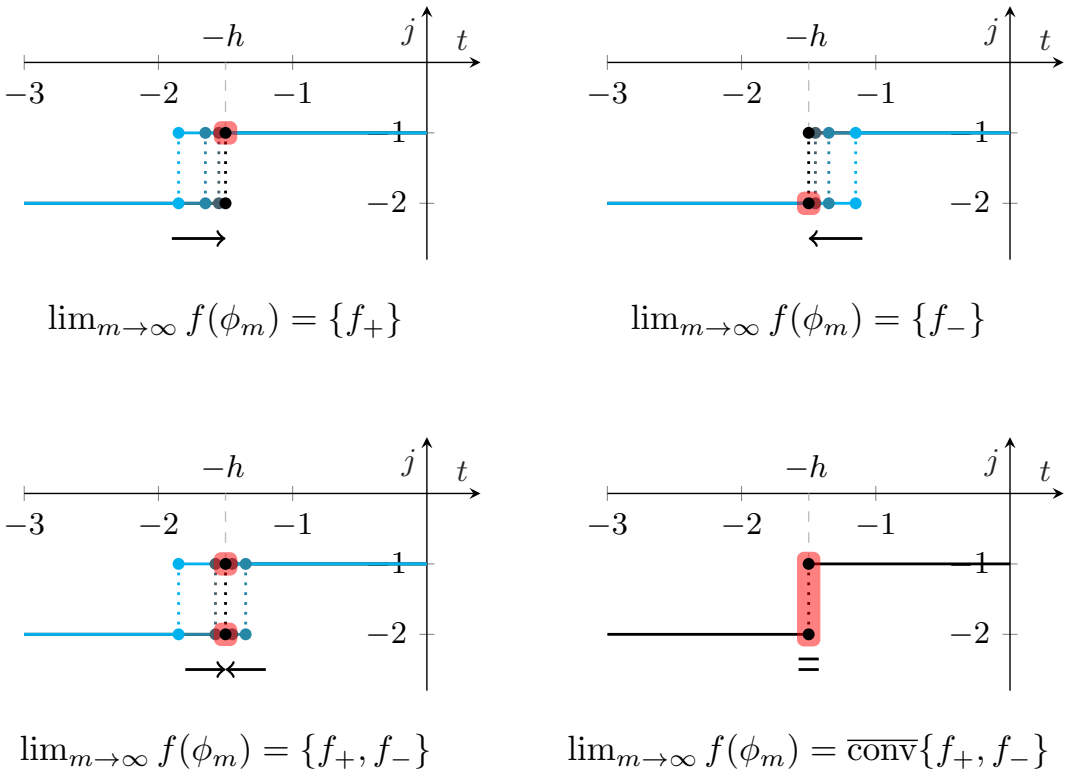

Figure 3.5: Some possible eventual behaviors of the domains $\operatorname{dom}\phi_m$ of a sequence of hybrid arcs converging to $\operatorname{dom}\phi$, which features a single jump at $t = -h = -1.5$: jumps approaching from the left (top left), from the right (top right), from both sides (bottom left) or an eventually constant sequence (bottom right). Here $f_\pm = A_0\phi(0,0) + A_h\phi(-h, k_\pm)$, where $k_- = -1$ and $k_+ = -2$; in every case, the limit equals f evaluated at the domain points highlighted in red.

follows that $f(\phi)$ is convex and nonempty for every $\phi \in \mathcal{D} \cap \mathcal{M}^{\Delta}_{b,\lambda}$, and that $g(\phi)$ is nonempty for every $\phi \in \mathcal{D} \cap \mathcal{M}^{\Delta}_{b,\lambda}$.

For the proof of local boundedness, recall from Section 3.3.2 that the state $\mathbf{z}$ is partitioned as $(\mathbf{x}, \mathbf{s})$. This induces a partition $\phi = (\mathbf{x}_\phi, \mathbf{s}_\phi)$ of an arbitrary hybrid memory arc $\phi \in \mathcal{M}^{\Delta}$ into two hybrid memory sub-arcs. Note that the hybrid memory sub-arc $\mathbf{s}_\phi : \operatorname{dom}\phi \to \{-1,1\}^n \times \{0,1\}^n \times \mathbb{R}^n_{\geq 0}$ is always pointwise bounded by $\sqrt{n \cdot 1^2 + n \cdot 1^2 + \sum_{i=1}^n \tau_{Hi}^2} = \sqrt{2n + n \max_{i=1}^n \tau_{Hi}^2}$. Hence, a bound for ϕ always implies a bound for $\mathbf{x}_\phi$, and vice versa.

Hence, suppose that $\mathbf{x}_\phi$ is bounded by some $b > 0$. By straightforward computation, a bound for $f(\phi)$ is given by

$$b_f = \left(\max_{\mathbf{m} \in \{0,1\}^n} (\sum_{i=0}^{n} ||A_i(\mathbf{m})|| \right) b,$$

and a bound for $g(\phi)$ is given by

$$b_g = \left(\max_{i=0}^{n} ||A_{Ri}|| \right) b;$$

thus f, g are locally bounded.

To prove outer semicontinuity of f, several cases can be distinguished. Recall that a set-valued map f is outer semicontinuous if for any sequence $\{\phi_m\}_m$, $m = 1, 2, \ldots$ of hybrid memory arcs converging to ϕ, $\lim_{\phi_m \to \phi} f(\phi_m) \subseteq f(\phi)$, where the limit for hybrid memory arcs is taken with respect to graphical convergence [252]. The SISO system (3.19) is analyzed here for simplicity; a similar argument works for arbitrary n.

- If the limit hybrid arc ϕ does not feature a jump at $t = -h$, then there exists $M \in \mathbb{Z}_{>0}$ such that for all $m > M$, f evaluated on ϕ_m is an ordinary function, and outer semicontinuity reduces to ordinary function continuity. Since f is composed of linear and quadratic functions of the state variables, it is continuous.

- If the limit hybrid arc ϕ features one or two jumps at $t = -h$ (as previously noted, there cannot be more than two jumps at a given time), there are several local behaviors for the domains of the sequence $\{\phi_m\}_m$ (see Figure 3.5): if the domains eventually only contain jumps at $t < -h$ which converge to the jump(s) of $\operatorname{dom} \phi$, the limit is equal to $A_0\phi(0,0) + A_h\phi(-h, k_+)$, where $k_- = \max_{(-h,k) \in \operatorname{dom} \phi} k$. Conversely, if the domains eventually only feature jumps at $t > -h$, the limit is $A_0\phi(0,0) + A_h\phi(-h, k_-)$, where $k_+ = \min_{(-h,k) \in \operatorname{dom} \phi} k$. If the domains of the sequence eventually feature jumps at $t < -h$ and $t > -h$ but not at $t = -h$, the limit is a subset of the set $\{A_0\phi(0,0) + A_h\phi(-h,k) \mid (-h,k) \in \operatorname{dom} \phi\}$ (there are again various behaviors depending on whether the limit arc ϕ features one or two jumps). Finally, if the domains eventually feature jumps at $t = -h$, the limit is equal to $f(\phi)$, i.e. the convex hull of the previous set. In all cases the limit is a subset of $f(\phi)$, proving that f is outer semicontinuous.

Finally, since g is an ordinary function of $\phi(0,0)$, outer semicontinuity is equivalent to ordinary continuity. Like in the nondelayed setting, since g is composed of linear and quadratic functions of the state variables, it is continuous.

Note that since the proof was stated for the most general asynchronous MISO reset-and-hold control system, the same proof applies for all possible variations (SISO/MISO, reset/reset-and-hold, synchronous/asynchronous) of the hybrid control system with time delay in Section 3.3, by reducing it to these special cases.

3.4.2 Delay-independent stability

In order to be able to develop sufficient stability conditions for delayed systems in the HI formalism, some definitions and results from [252] regarding the stability of hybrid systems with memory are recalled first.

A continuous function $f : [0,\infty) \to [0,\infty)$ belongs to class $\mathcal{K}_\infty$ (denoted $f \in \mathcal{K}_\infty$) if it is strictly increasing and unbounded, and $f(0) = 0$. If the unboundedness condition is dropped, it is said that f belongs to class $\mathcal{K}$. Similarly, continuous function $f : [0,\infty) \times [0,\infty) \to [0,\infty)$ belongs to class $\mathcal{KL}$ (denoted as $f \in \mathcal{KL}$) if it is strictly increasing with respect to the first variable, decreasing with respect to the second variable, and satisfies $f(0,y) = 0$ for any y and $\lim_{y\to\infty} f(x,y) = 0$ for any x. For a subset $\mathcal{W}$ of Euclidean space, the distance $|x|_\mathcal{W}$ from x to $\mathcal{W}$ is defined as $\inf_{y\in\mathcal{W}} |x-y|$. Furthermore, $||\phi||_\mathcal{W}$ is defined as $\sup_{\substack{(s,k)\in\operatorname{dom}\phi \\ s+k\geq-\Delta-1}} |\phi(s,k)|_\mathcal{W}$.

Definition 3.9. A compact set $\mathcal{W}$ is called $\mathcal{KL}$ pre-asymptotically stable for the hybrid system Σ if there is a $\mathcal{KL}$ function $\beta : \mathbb{R}_{\geq 0} \times \mathbb{R}_{\geq 0} \to \mathbb{R}_{\geq 0}$ such that any solution ϕ to the system satisfies

$$|\phi(t,j)|_\mathcal{W} \leq \beta(||\mathcal{A}_{[0,0]}\phi||_\mathcal{W}, t+j)$$

for any $(t,j) \in \operatorname{dom}\phi$.

To state sufficient stability conditions, a necessary standing assumption is that f satisfies the following property of local boundedness: for any $b > 0$ there exists $l > 0$ such that $|\xi| \leq l$ for all $\phi \in \mathcal{M}^\Delta \cap \mathcal{F}$ with $||\phi||_\mathcal{W}$ and all $\xi \in f(\phi)$. Under this assumption, a sufficient condition for $\mathcal{KL}$ pre-asymptotic stability is the existence of a Lyapunov-Krasovskii functional. To be able to state the condition in the most general case, one must first generalize the concept of time derivative to set-valued mappings.

This is achieved by the following definition:

Definition 3.10. Given any functional $V : \mathcal{M}^{\Delta} \to \mathbb{R}_{\geq 0}$, the upper right-hand derivative $\dot{V}$ at a hybrid memory arc ϕ along the solutions of the hybrid system Σ is defined as

$$\dot{V}(\phi) = \sup_{x \in \mathcal{S}_{\Sigma}(\phi)} \limsup_{t \to 0^+} \frac{V(\mathcal{A}_{[t,0]}x) - V(\mathcal{A}_{[0,0]}x)}{t}, \tag{3.30}$$

where $\mathcal{S}_{\Sigma}(\phi)$ denotes the set of maximal solutions of Σ with initial condition ϕ. Similarly, for a hybrid memory arc $\phi \in \mathcal{J}$ and $\gamma \in g(\phi)$, ϕ_{γ}^{+} denotes the hybrid memory arc such that $\phi_{\gamma}^{+}(0,0) = \gamma$ and for all $(s,k) \in \operatorname{dom}\phi$, $\phi_{\gamma}^{+}(s,k-1) = \phi(s,k)$; the set of all such ϕ_{γ}^{+} for all γ and ϕ is denoted $g^{+}(\mathcal{J})$.

Theorem 3.11. *A closed set $\mathcal{W}$ is $\mathcal{KL}$ pre-asymptotically stable for the hybrid system Σ if there exists a candidate Lyapunov-Krasovskii functional $V : \mathcal{M}^{\Delta} \to \mathbb{R}_{\geq 0}$, $\alpha_1, \alpha_2 \in \mathcal{K}_{\infty}$ and a continuous positive definite function ρ such that the three following conditions are satisfied:*

$$\alpha_1(|\phi(0,0)|_{\mathcal{W}}) \leq V(\phi) \leq \alpha_2(||\phi||_{\mathcal{W}}) \quad \forall \phi \in \mathcal{F} \cup \mathcal{J} \cup g^{+}(\mathcal{J}), \tag{3.31a}$$

$$\dot{V}(\phi) \leq -\rho(|\phi(0,0)|_{\mathcal{W}}) \quad \forall \phi \in \mathcal{F}, \tag{3.31b}$$

$$V(\phi_{\gamma}^{+}) - V(\phi) \leq -\rho(|\phi(0,0)|_{\mathcal{W}}) \quad \forall \phi \in \mathcal{J}, \gamma \in g(\phi). \tag{3.31c}$$

Proof. See [252].

In this section, the problem of $\mathcal{KL}$ pre-asymptotic stability is analyzed for the closed loop reset-and-hold system Σ (3.24) of the set given by $\mathcal{W} = \{\mathbf{0}\} \times \{-1,1\}^n \times \{0,1\}^n \times [0,\infty)^n$ (the third and fourth factors can be omitted if ordinary reset is considered), which corresponds to the set of possible equilibrium states for $\mathbf{x}$.

In the following, sufficient conditions for the stability of $\mathcal{W}$ with respect to Σ are provided for a reset-and-hold control system, with the ordinary reset system considered as a special case. The approach is based on postulating a quadratic Lyapunov-Krasovskii functional and deriving sufficient conditions for stability in the form of linear matrix

inequalities.

First, note that the assumption of local boundedness of f is satisfied for Σ: indeed, suppose that $||\phi||_{\mathcal{W}}$ is bounded by some $b > 0$. This means that $|\phi(-h_i, u_i)|_{\mathcal{W}} \leq b$ for any $u_i \in U_i$, and so $|A_i\phi(-h_i, u_i)|_{\mathcal{W}} \leq ||A_i||b$. Hence for any $\xi \in f(\phi)$, it holds that $|f| \leq l$ with $l = (\sum_{i=0}^{n} ||A_i||)b$. In consequence, the Lyapunov-Krasovskii conditions for stability can be applied to the closed loop system Σ.

Proposition 3.12 (Delay-independent stability conditions)**.** *Consider the parallel MISO control system Σ. The set $\mathcal{W}$ is $\mathcal{KL}$ pre-asymptotically stable for Σ under a reset-and-hold strategy if there exist $m \times m$ matrices $P > 0$ and $Q_i > 0$, $i = 1, \ldots, n$ such that the following conditions are satisfied:*

$$\begin{pmatrix} A_0(\mathbf{m}_0)^\top P + PA_0(\mathbf{m}_0) + \sum_i Q_i & PA_1(\mathbf{m}_1) & \cdots & PA_n(\mathbf{m}_n) \\ A_1(\mathbf{m}_1)^\top P & -Q_1 & \cdots & 0 \\ \vdots & \vdots & \ddots & \vdots \\ A_n(\mathbf{m}_n)^\top P & 0 & \cdots & -Q_n \end{pmatrix} \leq -\varepsilon I, \tag{3.32a}$$

for all possible vectors $\mathbf{m}_0, \mathbf{m}_1, \ldots, \mathbf{m}_n \in \{0, 1\}^n$, and

$$A_{Ri} P A_{Ri} - P \leq -\varepsilon I \tag{3.32b}$$

for all $i = 1, \ldots, n$. Furthermore, $\mathcal{W}$ is $\mathcal{KL}$ pre-asymptotically stable for Σ under an ordinary reset strategy if the previous conditions hold for the special case where $(\mathbf{m}_i)_j = 1$ for all i, j.

Proof. First, note that $|(\mathbf{x}, \mathbf{q}, \mathbf{m}, \boldsymbol{\tau})|_{\mathcal{W}} = |\mathbf{x}|$, so the analysis can be restricted to the evolution of the state $\mathbf{x}$.

Consider the quadratic Lyapunov-Krasovskii functional given on ϕ by

$$V(\phi) = \mathbf{x}_\phi(0, 0)^\top P \mathbf{x}_\phi(0, 0) + \int_{-h}^{0} \mathbf{x}_\phi(t, u_t)^\top Q \mathbf{x}_\phi(t, u_t) dt, \tag{3.33}$$

where u_θ is the value maximizing $|\mathbf{x}_\phi(\theta, j)|$ among the j such that $(\theta, j) \in \operatorname{dom} \phi$ (this choice is related to the supremum in the definition of the upper right hand derivative). Condition (3.31a) easily follows from the fact that this functional is positive

definite and radially unbounded.

The case of ordinary reset is analyzed first, i.e., $(\mathbf{m}_i)_j$ is set to identically 1 for all i, j and the corresponding states are removed from the model. Computing the upper right-hand derivative of V, it is readily found that

$$\begin{aligned}\dot{V}(\phi) = \mathbf{x}_\phi(0,0)^\top P \left(A_0 \mathbf{x}_\phi(0,0) + \sum_{i=1}^{n} A_i \mathbf{x}_\phi(-h_i, u_{-h_i}) \right) \\ + \left(A_0 \mathbf{x}_\phi(0,0) + \sum_{i=1}^{n} A_i \mathbf{x}_\phi(-h_i, u_{-h_i}) \right)^\top P \mathbf{x}_\phi(0,0) \\ + \sum_{i=1}^{n} (\mathbf{x}_\phi(0,0)^\top Q_i \mathbf{x}_\phi(0,0) - \mathbf{x}_\phi(-h_i, u_{-h_i})^\top Q_i \mathbf{x}_\phi(-h_i, u_{-h_i})); \quad (3.34)\end{aligned}$$

grouping terms together and putting the expression in matrix form, condition (3.32a) is shown to hold by taking $\rho(|(\mathbf{x}, \boldsymbol{\tau}, \mathbf{q}, \tau_{\mathrm{TR}})|_{\mathcal{W}}) = \varepsilon |\mathbf{x}|^2$. Analogously, a calculation shows that

$$V(\phi_\gamma^+) - V(\phi) = \phi(0,0)^\top (A_{Ri} P A_{Ri} - P) \phi(0,0) \quad (3.35)$$

where i depends on ϕ. Hence (3.32b) is obtained.

In the reset-and-hold case, one also needs to take into account the intervals of time in which the states and outputs of one or more controllers are being held constant. During such intervals, the evolution of $\mathbf{x}$ is given by an LTI delayed system with constant evolution matrices $A_i(\mathbf{m})$ (for some $\mathbf{m}$) when the system is flowing. The upper right hand derivative of V may thus be computed identically, arriving again at (3.32a).

3.4.3 Delay-dependent stability

Delay-independent stability conditions are often too restrictive in practice, since many practical examples of control systems are not stable for all possible values of the time delay(s); instead they are stable only when the delays lie within a certain range. For this reason, it is convenient to consider stability conditions which depend on the values of the delay. One of the simplest such conditions is based on the model transformation method, in which the delayed differential equation $\dot{\mathbf{x}}(t) = A_0 \mathbf{x}(t) + A_h \mathbf{x}(t-h)$ governing continuous evolution is transformed into a distributed-delay differential equation

$$\Gamma(m,m') = \begin{pmatrix} A_0(m)P+PA_0(m)^\top+Y+Y^\top+hA_0(m)^\top ZA_0(m)+Q & PA_h(m')^\top-Y+hA_0(m)^\top ZA_h(m') \\ A_h(m')^\top P-Y^\top+hA_h(m')^\top ZA_0(m) & -Q+hA_h(m')^\top ZA_h(m') \end{pmatrix} \tag{3.38}$$

$\dot{\mathbf{x}}(t) = (A_0 + A_h)\mathbf{x}(t) + \int_{-h}^{0}(A_0\mathbf{x}(t+\theta) + A_h\mathbf{x}(t+\theta-h))d\theta$, such that the stability of the system under this new equation implies the stability of the original system. In the case of a LTI base system, a set of stability conditions where the delay appears explicitly can be extracted from a Lyapunov-Krasovskii functional much like (3.33) with a single extra term.

The following lemma, which is Lemma 1 in [273], will be needed to obtain the stability conditions:

Lemma 3.13. *Given two vectors $\mathbf{a}(t) \in \mathbb{R}^n, \mathbf{b}(t) \in \mathbb{R}^m$ depending on a parameter $t \in \Omega$, the inequality*

$$-2\int_\Omega \mathbf{a}(t)^\top N\mathbf{b}(t)dt \leq \int_\Omega \begin{pmatrix}\mathbf{a}(t)\\ \mathbf{b}(t)\end{pmatrix}^\top \begin{pmatrix} X & Y-N \\ Y^\top - N^\top & Z\end{pmatrix}\begin{pmatrix}\mathbf{a}(t)\\ \mathbf{b}(t)\end{pmatrix} dt \tag{3.36}$$

holds for all matrices $N \in \mathbb{R}^{n\times m}, X \in \mathbb{R}^{n\times n}, Y \in \mathbb{R}^{n\times m}, Z \in \mathbb{R}^{m\times m}$ satisfying

$$\begin{pmatrix} X & Y \\ Y^\top & Z\end{pmatrix} \geq 0. \tag{3.37}$$

Proof. See [273].

The SISO case

In this section, stability of the closed loop hybrid system Σ, given by (3.19), is investigated (the SISO case is considered first for simplicity). More specifically, the $\mathcal{KL}$ pre-asymptotic stability of the set $\mathcal{W} = \{\mathbf{0}\} \times \{0,1\} \times \{-1,1\} \times \mathbb{R}_{\geq 0}$, which corresponds to the set of all the points $\mathbf{z} = (\mathbf{x}, q, m, \tau)$ such that $\mathbf{x} = 0$, is considered. The following proposition describes sufficient delay-dependent stability conditions for a SISO reset-and-hold system, and constitutes an adaptation and extension of the stability results in [123]. The approach is based on postulating a quadratic Lyapunov-Krasovskii functional and deriving sufficient conditions for stability in the form of linear matrix inequalities. Recall that A_0, A_h, as given by (3.17), depend on the discrete state $m \in \{0,1\}$.

Proposition 3.14 (Delay-dependent stability conditions for a SISO reset-and-hold system)**.** *Consider the reset-and-hold control system Σ given by* (3.19)*. The set $\mathcal{W}$ is asymptotically stable for Σ if there exist matrices $P > 0$, $Q > 0$, $X = X^\top$, Y and $Z > 0$ such that the following conditions are satisfied:*

1.

$$\Gamma(m, m') \leq -\varepsilon I, \tag{3.39}$$

for all combinations of $m, m' \in \{0, 1\}$ and for some $\varepsilon > 0$, where $\Gamma(m, m')$ is given by (3.38)*, and*

2.

$$\begin{pmatrix} X & Y \\ Y^\top & Z \end{pmatrix} \geq 0, \tag{3.40}$$

$$Y(A_R - I) = 0, \tag{3.41}$$

$$A_R P A_R - P \leq 0. \tag{3.42}$$

Proof. The proof is based on adapting the stability result in [123] for delayed reset control systems to the formalism of hybrid systems with memory. For a solution $\phi = (\mathbf{x}_\phi, \mathbf{s}_\phi)$ to Σ, consider the Lyapunov-Krasovskii functional

$$\begin{aligned} V(\phi) = \mathbf{x}_\phi(0,0)^\top P \mathbf{x}_\phi(0,0) + \textstyle\int_{-h}^{0} \mathbf{x}_\phi(t, u_t)^\top Q \mathbf{x}_\phi(t, u_t) dt \\ + \textstyle\int_{-h}^{0} \int_{t}^{0} \bar{f}(\phi)(t')^\top Z \bar{f}(\phi)(t') dt' dt, \end{aligned} \tag{3.43}$$

recalling that u_t is the value maximizing the norm $|\mathbf{x}_\phi(t, j)|$ among the j such that $(t, j) \in \operatorname{dom} \phi$ (or any such value if there is no unique choice), and for any $t \in (-h, 0)$ the functional $\bar{f}$ is defined as

$$\bar{f}(\phi)(t) = A_0(m_\phi(t, u_t))\mathbf{x}_\phi(t, u_t) + A_h(m_\phi(t - h, u_{t-h}))\mathbf{x}_\phi(t - h, u_{t-h}) \tag{3.44}$$

(note the difference with $f(\phi)$, as it is a single-valued mapping).

Now, (3.31a) easily follows from the fact that V, as given by (3.43), is positive definite and radially unbounded. Computing the upper right hand derivative of V and using Leibniz's rule, one obtains an expression consisting of a term depending on the states $x_\phi(0, 0)$ and $x_\phi(-h, u_{-h})$ plus an integral term. Following [123], Lemma 3.13 is applied to replace this integral with another expression in terms of $x_\phi(0, 0)$

and $x_\phi(-h, u_{-h})$. This step introduces new matrices X, Y satisfying (3.40), (3.41) in the stability conditions. Imposing condition (3.31b) results in the inequalities (3.39)–(3.41), by considering all four possible values for $m(0,0)$ and $m(-h, u_{-h})$. Finally, a straightforward application of (3.31c) results in the final condition (3.42).

The MISO case

In the following, the stability of $\mathcal{W} = \{\mathbf{0}\} \times \{-1, 1\}^n \times \{0, 1\}^n \times [0, \infty)^n$, corresponding to the set of all points $\mathbf{z} = (\mathbf{x}, \mathbf{q}, \mathbf{m}, \boldsymbol{\tau})$ such that $\mathbf{x} = 0$, is considered. A set of sufficient delay-dependent stability conditions are obtained for reset-and-hold MISO control systems with a LTI plant. The approach is again based on postulating an appropriate quadratic Lyapunov-Krasovskii functional and deriving sufficient conditions for stability in the form of LMIs, which take a similar form to the SISO case but involve a much greater number of matrices, since the inherent complexity of the model unavoidably implies the consideration of a large number of cases. Recall that $A_0, \ldots, A_n$, as given by (3.21), depend on the discrete state vector $\mathbf{m}$.

In order to simplify the treatment, the delay-dependent stability conditions will be stated in terms of a bound H satisfying

$$h_i \leq H. \tag{3.45}$$

for all $i = 1, \ldots, n$.

Proposition 3.15 (Delay-dependent stability conditions for a MISO reset-and-hold system)**.** *Consider the reset-and-hold control system Σ given by* (3.24)*. The set $\mathcal{W}$ is asymptotically stable for Σ if there exist matrices $P > 0$, $Q_i > 0$, $X_i = X_i^\top$, Y_i and $Z_i > 0$ such that the following conditions are satisfied:*

1.

$$\Gamma(\mathbf{m}_0, \ldots, \mathbf{m}_n) \leq -\varepsilon I, \tag{3.46}$$

for all combinations of $\mathbf{m}_0, \ldots, \mathbf{m}_n \in \{0, 1\}^n$ and for some $\varepsilon > 0$, and

2.

$$\begin{pmatrix} X_i & Y_i \\ Y_i^\top & Z_i \end{pmatrix} \geq 0, \tag{3.47}$$

$$Y_i(A_{Rk} - I) = 0, \tag{3.48}$$

$$A_{Ri} P A_{Ri} - P \leq 0. \tag{3.49}$$

for all $i, k = 1, \ldots, n$.

Here Γ *is defined as*

$$\Gamma(\mathbf{m}_0, \ldots, \mathbf{m}_n) = \begin{pmatrix} \Gamma_{\mathrm{I}} & \Gamma_{\mathrm{II}} \\ \Gamma_{\mathrm{II}}^\top & \Gamma_{\mathrm{III}} \end{pmatrix}, \tag{3.50}$$

where

$$\Gamma_{\mathrm{I}} = A_0(\mathbf{m}_0)^\top P + P A_0(\mathbf{m}_0) + \sum_{i=1}^{n} \left(H X_i + Y_i + Y_i^\top + H A_0(\mathbf{m}_0) Z_i A_0(\mathbf{m}_0)^\top + Q_i \right), \tag{3.51}$$

$$\Gamma_{\mathrm{II}} = \Bigg(P A_1(\mathbf{m}_1) - Y_1 + \sum_{i=1}^{n} H A_0(\mathbf{m}_0)^\top Z_i A_1(\mathbf{m}_1), \ldots, P A_n(\mathbf{m}_n) - Y_n + \sum_{i=1}^{n} H A_0(\mathbf{m}_0)^\top Z_i A_n(\mathbf{m}_n) \Bigg), \tag{3.52}$$

and

$$\Gamma_{\mathrm{III}} = \begin{pmatrix} -Q_1 + \sum_{i=1}^{n} H A_1(\mathbf{m}_1)^\top Z_i A_1(\mathbf{m}_1) & \cdots & \sum_{i=1}^{n} H A_1(\mathbf{m}_1)^\top Z_i A_n(\mathbf{m}_n) \\ \vdots & \ddots & \vdots \\ \sum_{i=1}^{n} H A_n(\mathbf{m}_n)^\top Z_i A_1(\mathbf{m}_1) & \cdots & -Q_n + \sum_{i=1}^{n} H A_n(\mathbf{m}_n)^\top Z_i A_n(\mathbf{m}_n) \end{pmatrix}. \tag{3.53}$$

Proof. The proof is based on following the approach in [379] for control systems featuring multiple time delays, and modifying it to account for the presence of resets as in the SISO case [123]. Consider the Lyapunov-Krasovskii functional

$$\begin{aligned} V(\phi) = \mathbf{x}_\phi(0,0)^\top P \mathbf{x}_\phi(0,0) + \textstyle\sum_{i=1}^{n} \int_{-h_i}^{0} \mathbf{x}_\phi(t, u_t)^\top Q_i \mathbf{x}_\phi(t, u_t) dt \\ + \textstyle\sum_{i=1}^{n} \int_{-h_i}^{0} \int_{t}^{0} \bar{f}(\phi)(t')^\top Z_i \bar{f}(\phi)(t') dt' dt, \end{aligned} \tag{3.54}$$

where

$$\bar{f}(\phi)(t) = A_0(m_\phi(t, u_t)) \mathbf{x}_\phi(t, u_t) + \sum_{i=1}^{n} A_i(m_\phi(t - h_i, u_{t-h_i})) \mathbf{x}_\phi(t - h_i, u_{t-h_i}), \tag{3.55}$$

with u_t defined as in the SISO case. As before, (3.31a) follows from the fact that the proposed functional is explicitly positive definite and radially unbounded.

Applying Leibniz's rule to the upper right-hand derivative of the first term gives

$$\mathbf{x}_\phi(0,0)^\top \sum_{i=0}^{n}(PA_i + A_i^\top P)\mathbf{x}_\phi(-h_i, u_{-h_i}) - \sum_{i=0}^{n}\int_{t-h_i}^{t} x(t,u_t)^\top (PA_i + A_i^\top P)\dot{x}(t', u_{t'})dt' - \sum_{i=1}^{n}\sum_{t_K\in[t-h,t)} x(t,u_t)^\top (PA_i(A_{RK}-I) + (A_{RK}-I)A_i^\top P)x(t_K,k), \quad (3.56)$$

where the variable t_K runs over the reset instants in the interval $[t-h, t)$ for which an unspecified A_{RK} (some nonempty product of reset matrices A_{Ri}) is applied depending on the solution ϕ. The form of the last integral term is suitable for applying Lemma 3.13 n times, with $N = A_i$, $i = 1, \ldots, n$ in each case. Doing this introduces new matrices X_i, Y_i satisfying condition (3.47), and after some simplification, the integral term in (3.56) for each i is replaced with a smaller integral which exactly cancels the integral coming from the upper right-hand derivative of the third term.

Moreover, imposing $Y_i A_{RK} = Y_i$ on the matrices Y_i for all A_{RK}, the sum over reset instants t_K cancels; it is then easily checked that condition (3.47) implies the former equality for all possible products of reset matrices A_{RK}. In this way, after using the inequality (3.45), the final expression can be put in the desired form $\dot{V} \leq \mathbf{X}^\top \Gamma \mathbf{X}$, where $\mathbf{X} = (\mathbf{x}_\phi(0,0), \mathbf{x}_\phi(-h_1, u_{-h_1}), \ldots, \mathbf{x}_\phi(-h_n, u_{-h_n}))^\top$ and Γ is given by (3.50). The inequalities (3.46)–(3.48) follow by considering all possible values for the discrete signal $\mathbf{m}_0, \ldots, \mathbf{m}_n$. Finally, after applying (3.31c) and simplifying, the final condition (3.49) is obtained.

Example 3.16 (Stability of a SISO reset-and-hold system with delay)**.** This example is adapted from Example 3.5 in [118], and is given by the feedback interconnection of the first order plant

$$P(s) = \frac{e^{-hs}}{0.5 + s} \quad (3.57)$$

and a reset-and-hold P+FORE controller (the sum of a proportional gain and a FORE) whose base linear system is

$$R_{\text{base}}(s) = 1 + \frac{1}{1+s}. \quad (3.58)$$

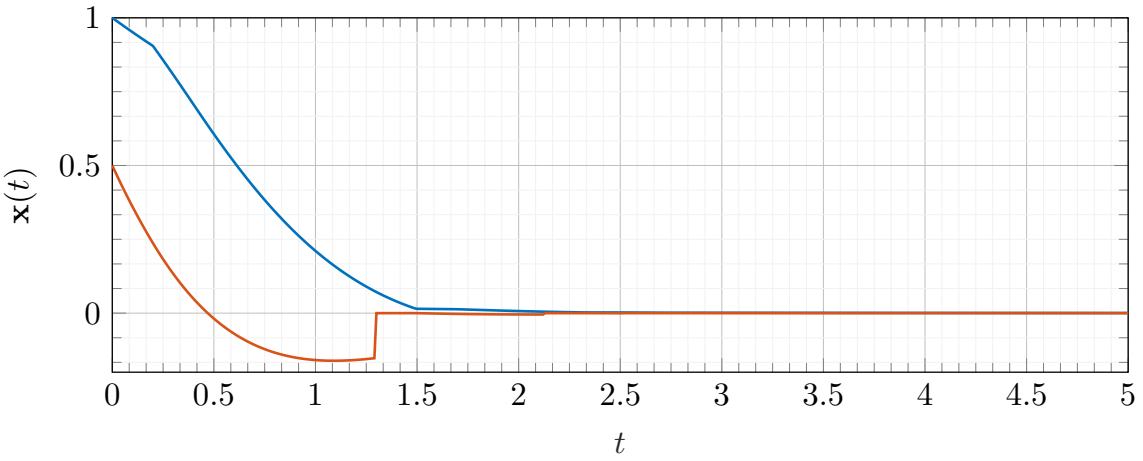

Figure 3.6: Evolution of the two closed loop system states $\mathbf{x} = (x_p, x_r)$ (blue and orange) in Example 3.16, with the initial condition $\mathbf{x}(0, 0) = (1, 0.5)$.

The holding modality where $A_r' = A_r$ in (3.3) is assumed, that is, the FORE damping term is not affected by the holding mechanism. The delay-dependent stability condition from Proposition 2 is applied to the closed loop system with the delay $h = 0.2$, resulting in the solution:

$$P = \begin{pmatrix} 2.6251 & -0.0000 \\ -0.0000 & 3.5911 \end{pmatrix}, \quad Q = \begin{pmatrix} 3.2457 & -0.2853 \\ -0.2853 & 2.1171 \end{pmatrix}, \quad X = \begin{pmatrix} 2.3959 & 0.5275 \\ 0.5275 & 2.6538 \end{pmatrix}, \tag{3.59}$$

$$Y = \begin{pmatrix} -1.8434 & 0 \\ -1.4698 & 0 \end{pmatrix}, \quad Z = \begin{pmatrix} 3.3594 & 0.0067 \\ 0.0067 & 2.9438 \end{pmatrix}. \tag{3.60}$$

Thus, the closed loop reset-and-hold system is stable under the variable band resetting law. In addition, the range of delays $h \in (0, h_{\max})$ for which the LMI system (3.31) is solvable has been computed using a binary search. The obtained bound for which the system is guaranteed to be stable is $h_{\max} = 0.770$.

The evolution of the closed loop system with the nominal delay $h = 0.2$ has been simulated with the initial condition $x_p = 1, x_r = 0.5$ (and $q_i = m_i = 1$). The resulting closed loop state $\mathbf{x} = (x_p, x_r)$ is shown in Figure 3.6, demonstrating its convergence to the equilibrium state. The Lyapunov-Krasovskii functional evaluated at the resulting trajectory is shown in Figure 3.7.

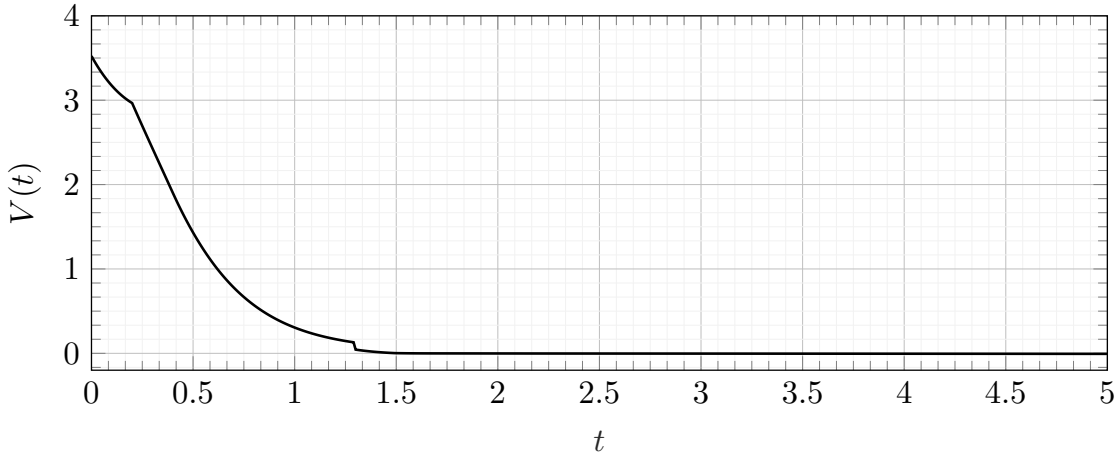

Figure 3.7: Evolution of the Lyapunov-Krasovskii functional V in Example 3.16, with the initial condition $\mathbf{x}(0,0) = (1, 0.5)$.

Example 3.17 (Stability of a MISO reset-and-hold system with delay)**.** This example is a combination of Examples 3.16 and 2.19. Consider a 2×1 MISO system with subplants

$$P_1(s) = \frac{e^{-h_1 s}}{1+s}, \quad P_2(s) = \frac{e^{-h_2 s}}{1+10s}, \tag{3.61}$$

controlled by respective reset-and-hold P+FORE controllers in serial configuration (Figure 2.6), whose base linear systems are

$$R_{1,\text{base}}(s) = 1 + \frac{1}{1+s}, \quad R_{2,\text{base}}(s) = \frac{1}{1+10s}. \tag{3.62}$$

(the second is a purely FORE controller with zero proportional part). Again it is assumed that the FORE damping terms are not affected by the holding mechanism. The delay-dependent stability condition from Proposition 3.15 is applied to the closed loop system with the bound $H = 0.4$ for the delays, resulting in the solution

$$P = \begin{pmatrix} 4.193 & 0.007 & 0.000 & 0.000 \\ 0.007 & 14.365 & 0.000 & 0.000 \\ 0.000 & 0.000 & 5.353 & 0.000 \\ 0.000 & 0.000 & 0.000 & 12.958 \end{pmatrix}, \quad Q_1 = \begin{pmatrix} 3.651 & -0.004 & 0.078 & -0.504 \\ -0.004 & 1.812 & 0.011 & 0.002 \\ 0.078 & 0.011 & 3.868 & 0.517 \\ -0.504 & 0.002 & 0.517 & 1.288 \end{pmatrix},$$

$$Q_2 = \begin{pmatrix} 1.969 & -0.005 & 0.525 & -0.136 \\ -0.005 & 1.810 & -0.010 & -0.005 \\ 0.525 & -0.010 & 1.648 & 0.040 \\ -0.136 & -0.005 & 0.040 & 1.150 \end{pmatrix}, X_1 = \begin{pmatrix} 4.737 & -0.003 & 0.319 & -0.168 \\ -0.003 & 1.375 & -0.003 & 0.001 \\ 0.319 & -0.003 & 1.118 & 0.112 \\ -0.168 & 0.001 & 0.112 & 0.325 \end{pmatrix},$$

$$X_2 = \begin{pmatrix} 1.511 & -0.036 & 0.443 & -0.086 \\ -0.036 & 1.374 & 0.012 & -0.003 \\ 0.443 & 0.012 & 1.171 & 0.097 \\ -0.086 & -0.003 & 0.097 & 0.326 \end{pmatrix}, \quad Y_1 = \begin{pmatrix} -3.114 & -0.014 & 0 & 0 \\ -0.008 & -0.840 & 0 & 0 \\ 0.332 & -0.001 & 0 & 0 \\ -0.026 & 0.001 & 0 & 0 \end{pmatrix},$$

$$Y_2 = \begin{pmatrix} -0.782 & -0.007 & 0 & 0 \\ 0.052 & -0.841 & 0 & 0 \\ 0.415 & -0.001 & 0 & 0 \\ -0.135 & 0.000 & 0 & 0 \end{pmatrix}, \quad Z_1 = \begin{pmatrix} 2.748 & 0.013 & 0.225 & 0.022 \\ 0.013 & 3.810 & 0.003 & 0.002 \\ 0.225 & 0.003 & 3.181 & -0.029 \\ 0.022 & 0.002 & -0.029 & 3.496 \end{pmatrix},$$

$$Z_2 = \begin{pmatrix} 1.565 & 0.000 & 0.202 & 0.011 \\ 0.000 & 3.813 & -0.001 & -0.000 \\ 0.202 & -0.001 & 3.179 & -0.033 \\ 0.011 & -0.000 & -0.033 & 3.488 \end{pmatrix}. \tag{3.63}$$

Consequently, the closed loop reset-and-hold system is stable for any time delays $h_1, h_2 \leq H$ under the asynchronous variable band resetting law. In addition, the maximum value $H_{\max}$ for which the LMI system is solvable has been computed using a binary search, obtaining the upper bound $H_{\max} = 0.7198$ for the system's stability.

The evolution of the closed loop system with the delays $h_1 = 0.2, h_2 = 0.4$ has been simulated with the initial condition $x_{p1} = x_{p2} = 0.1, x_{r1} = 0.5, x_{r2} = 0$ (and $q_i = m_i = 1$). The resulting closed loop state $\mathbf{x}$ is shown in Figure 3.8, demonstrating its convergence to the equilibrium state. The Lyapunov-Krasovskii functional evaluated at the resulting trajectory is shown in Figure 3.9.

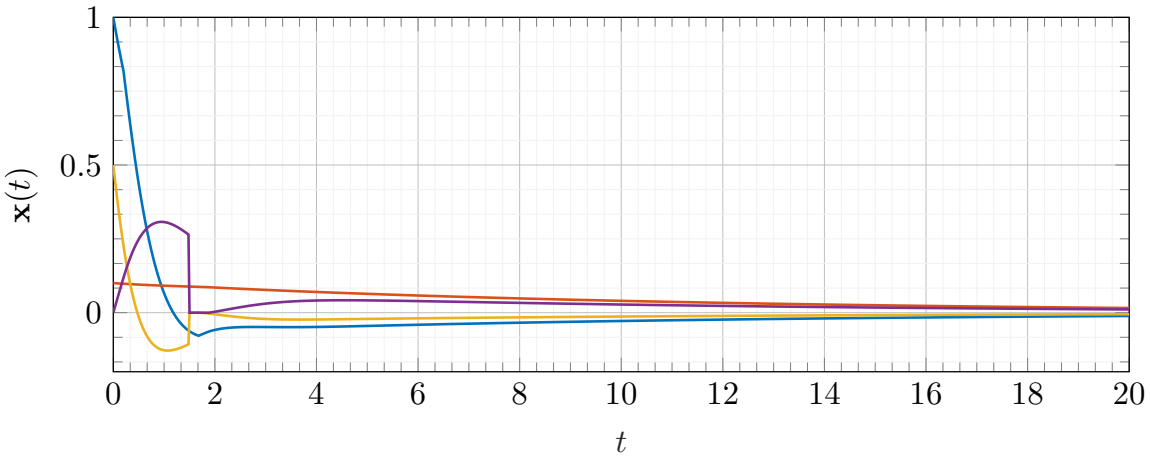

Figure 3.8: Evolution of the two closed loop system states $\mathbf{x} = (x_{p1}, x_{p2}, x_{r1}, x_{r2})$ (blue, orange, yellow and purple) in Example 3.17, with the initial condition $\mathbf{x}(0,0) = (1, 0.1, 0.5, 0)$.

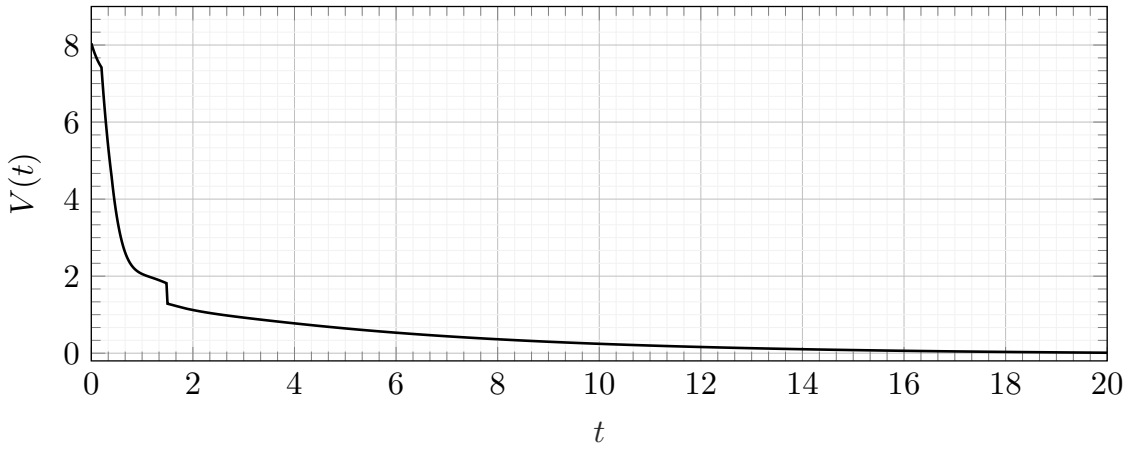

Figure 3.9: Evolution of the Lyapunov-Krasovskii functional V in Example 3.17, with the initial condition $\mathbf{x}(0,0) = (1, 0.1, 0.5, 0)$.

Chapter 4

Control design

This chapter will be focused on the development of design rules for the previous control systems. The PI+CI controller (2.14) will take a prominent role in these developments, due to its higher potential applicability. Note that when equipped e.g. with a variable band resetting law and the reset-and-hold mechanism, the PI+CI has almost thrice the number of design parameters $(k_P, T_I, p_r, \theta, \tau_h)$ compared to a linear PI controller (k_P, T_I). Given this greater complexity, it becomes especially important to find an appropriate set of tuning rules which will fix the values of these extra degrees of freedom.

The main objective will be to generalize the known results and techniques in the single-input setting to the MISO setting, and determine the control configurations for which it is possible to achieve them: a *flat response* in the case of first order systems after the first reset instant (the term "flat response" refers to a response for which the error signal becomes identically zero in finite time; this control modality is also known as *deadbeat control* or *finite settling time control* in other control subfields, and was first discussed in the works [54, 76] in the context of reset control), and an improved response with less overshoot in the case of high order systems. This is meant to constitute a first step towards the generalization of these strategies to the full multiple-input multiple-output (MIMO) setting.

As will be seen, incorporating reset elements into a MISO system will sometimes lead to an effective reduction on the degrees of freedom, since the generalization of known SISO design rules for maximum performance will be achieved only for a specific (parallel) configuration, which in some particular cases may be at odds with some other objectives relative to MISO systems, such as decreasing the total amount of control effort. However, an improvement on the performance is still possible by relaxing the

maximum performance (flat response) condition, as will be discussed.

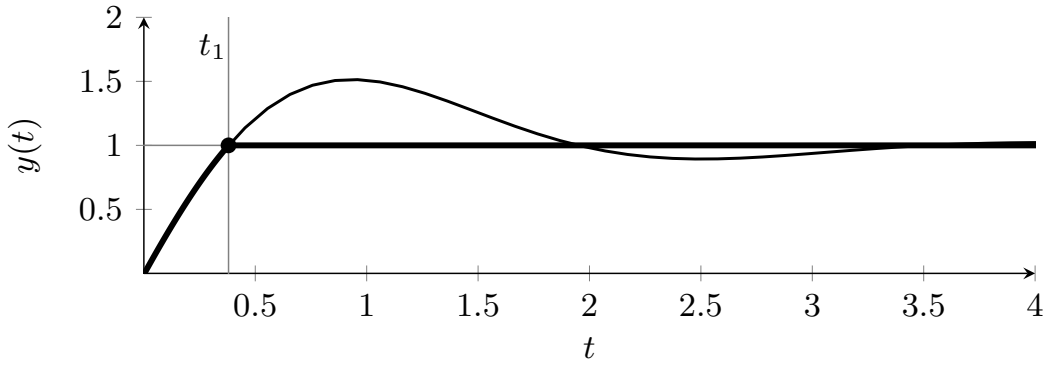

Figure 4.1: Illustration of a closed-loop flat step response y under a reference change: (thin line) PI controllers, (thick line) PI+CI controllers.

The reset-and-hold strategy (3.3), the novel hybrid design improvement previously described in Section 3.2, will be additionally applied to first order systems with time delay, obtaining a performance in both step reference tracking and disturbance rejection that further improves that of the known PI+CI-based design strategies developed so far even in the SISO case. Afterwards, a set of guidelines for proper tuning will be detailed, and some limitations of these basic strategies will be discussed, suggesting ways to overcome them. Finally, the performance of the proposed tuning rules, as well as their stability and their robustness to noise and parameter variation, will be shown by means of simulation examples.

Finally, some extensions of these rules will be explored for several other commonly considered control strategies, such as serial MISO control, split-range control and the control of nonlinear plants.

4.1 Parallel control of first order MISO plants

Up until now, the methodologies followed to find design rules for PI+CI compensation [46, 358] have mainly used frequency-based reasoning, based on the fact that a reset system's behavior is linear between two reset actions, and thus transfer functions $E_k(s)$ associated to the error signal after the kth reset instant can be defined using a Laplace transform.

However, a simple time-based approach will be shown to be best suited to systematically generate appropriate design rules that generalize the flat response property (or a good approximation of it) for a variety of control structures applied to first order systems (delayed and non-delayed), both in the SISO and parallel MISO cases. The strategies will be mainly based on the PI+CI controller due to its simplicity and applicability, although other more sophisticated partial-reset controllers can also be considered.

Here, the focus will be on the parallel control structure (2.17) applied to a non-delayed first order MISO process. The state space description of a first order plant reduces to

$$P_i : \begin{cases} \dot{\mathbf{x}}_{pi} = -a_i \mathbf{x}_{pi} + b_i v_i \\ y_i = \mathbf{x}_{pi}, \end{cases} \tag{4.1}$$

where $a_i, b_i \in \mathbb{R}$. Note that under this description, the gain of the ith subplant is b_i/a_i, and its time constant is $1/a_i$.

To begin with, a control strategy is assumed in which all controllers R_i are PI+CI controllers, and study whether the known analogous tuning rule for the single-input case can be generalized to this case. The zero crossing law will be used throughout this section.

4.1.1 Reference tracking

In this section, it is supposed that the system into consideration is initially at rest, and will analyze its behavior given a step reference input of height w_{10}, i.e., an input of the form $r_y(t) = w_{10}U(t)$, where $U(t)$ denotes a (càdlàg) Heaviside step function and $w_{10} \neq 0$ is a scaling factor. Alternatively, the reference signal can be taken as an exosystem (2.26) with $A_{e1} = A_{e2} = A_{e3} = C_{e2} = C_{e3} = 0$ and $C_{e1} = 1$.

Consider a solution $\mathbf{z}(t, j)$ to the system, and denote by t_1 the first reset instant; under the zero crossing law, this is the minimum $t_1 > 0$ such that $e(t_1) = 0$. From (2.17), the ith plant state $x_{pi}(t, j)$ flows in $[0, t_1] \times \{0\}$ according to the differential equation

$$\dot{x}_{pi}(t,j) = -a_i x_{pi}(t,j) + b_i k_{Pi}\left(e(t,j) + \frac{1}{T_{Ii}}((1-p_{ri})x_{Ii}(t,j) + p_{ri}x_{CIi}(t,j))\right). \quad (4.2)$$

Similarly, in the same interval the controller states x_{Ii} and x_{CIi} evolve as

$$x_{Ii}(t,j) = x_{CIi}(t,j) = \int_0^t e(t',j)\,dt' = x_I(t). \quad (4.3)$$

that is, the integrator and CI states of all controllers have an identical value, which will be notated as $x_I(t)$, up to the first reset instant. In particular, right before the jump this value is $x_{Ii}(t_1,0) = x_{CIi}(t_1,0) = x_I(t_1)$. Right after the jump, the integrator states keep their value $x_{Ii}(t_1,1) = x_I(t_1)$, and the CI states are reset to zero, $x_{CIi}(t_1,1) = 0$.

As for the plant states, one has $x_{pi}(t_1,1) = x_{pi}(t_1,0)$ and $e(t_1,1) = e(t_1,0) = 0$ (since the jump is produced at the instant in which the error signal is zero). Thus, from (4.2) it follows that

$$\dot{x}_{pi}(t_1,1) = -a_i x_{pi}(t_1,0) + b_i \frac{k_{Pi}}{T_{Ii}}(1-p_{ri})x_I(t_1). \quad (4.4)$$

For a flat response to be achieved, i.e. in order to achieve a stationary state $\dot{\mathbf{z}}(t_1,1) = 0$ instantaneously, the derivatives of the plant states must clearly satisfy $\dot{x}_{pi}(t_1,1) = 0$. From (4.4), it directly follows that the reset ratios p_{ri} must necessarily take the value

$$p_{ri} = 1 - \frac{a_i T_{Ii} x_{pi}(t_1,0)}{b_i k_{Pi} x_I(t_1)}. \quad (4.5)$$

On the other hand, the derivatives $\dot{x}_{Ii}(t_1,1) = \dot{x}_{CIi}(t_1,1) = e(t_1,1) = 0$ already vanish. The vanishing of $\dot{\mathbf{z}}(t,j)$ will evidently be preserved for all $t > t_1$, so a stationary state is indeed reached (disregarding the logical variable q).

In summary, in order to obtain a flat response, that is, a response so that $y(t,j) = w_{10}$ for any $t \geq t_1$, each PI+CI controller must have a different reset ratio p_{ri} given by (4.5), depending on the value of the plant state at the first jump $x_{pi}(t_1,0)$. Note that not all the p_{ri} are independent due to the fact that $y = \sum_{i=1}^n x_{pi}$ and $y(t_1,0) = w_{10}$. In particular, they satisfy

$$\sum_{i=1}^n \frac{b_i k_{Pi} x_I(t_1)(1-p_{ri})}{a_i T_{Ii}} = w_{10}. \quad (4.6)$$

Specializing (4.5) to the SISO case ($n = 1$), the tuning rule derived in [118] is recovered:

$$p_r = 1 - \frac{aT_I w_{10}}{bk_P x_I(t_1)}. \tag{4.7}$$

4.1.2 Disturbance rejection

Under the considered parallel control structure, different disturbances d_i may at any time enter the respective plants P_i. In full generality, the case of a family of step disturbances $d_i(t) = w_{20i}U(t)$ will be considered to act at the same time, where w_{20i} are nonzero arbitrary real numbers. An alternative description can be found by considering an exosystem (2.26) with $A_{e1} = A_{e2} = A_{e3} = C_{e1} = C_{e3} = 0$ and $C_{e2} = (w_{201}, \ldots, w_{20n})$. Note that the case where only some disturbance d_j is active, more common in practice, can be recovered by setting $w_{20i} = 0$ for all $i \neq j$.

In this case, the flow equation associated to the plant state x_{pi} is

$$\dot{x}_{pi}(t,j) = -a_i x_{pi}(t,j) + b_i k_{Pi}\Big(e(t,j) + \frac{1}{T_{Ii}}((1-p_{ri})x_{Ii}(t,j) + p_{ri}x_{CIi}(t,j))\Big) + b_i d_i(t,j). \tag{4.8}$$

Keeping the previous terminology, after the first reset action at $(t,j) = (t_1,1)$, one again has $x_{pi}(t_1,1) = x_{pi}(t_1,1)$, $e(t_1,1) = 0$, $x_{Ii}(t_1,1) = x_{Ii}(t_1,0) = x_I(t_1)$, and $x_{CIi}(t_1,1) = 0$, and thus (4.8) results in

$$\dot{x}_{pi}(t_1,1) = -a_i x_{pi}(t_1,0) + b_i \frac{k_{Pi}}{T_{Ii}}(1-p_{ri})x_I(t_1) + b_i w_{20i}. \tag{4.9}$$

After term rearrangement, one arrives at the tuning rule for the reset ratios p_{ri} that achieves a flat response (with $\dot{x}_{pi}(t_1,1) = 0$):

$$p_{ri} = 1 - \frac{(a_i x_{pi}(t_1,0) - b_i w_{20i})T_{Ii}}{b_i k_{Pi} x_I(t_1)}, \tag{4.10}$$

where again, since $y = \sum_{i=1}^{n} x_{pi}$ and $y(t_1,0) = 0$, the reset ratios satisfy a constraint given by

$$\sum_{i=1}^{n} \frac{b_i k_{Pi} x_I (1 - p_{ri})}{a_i T_{Ii}} = -\sum_{i=1}^{n} \frac{w_{20i}}{a_i}. \tag{4.11}$$

Again specializing (4.10) to the case $n = 1$ recovers the known reset ratio tuning rule developed in [118]:

$$p_r = 1 + \frac{w_{20} T_I}{k_P x_I(t_1)}. \tag{4.12}$$

4.1.3 Comments and guidelines

The tuning rules for a flat response (4.5) and (4.10) depend on $n - 1$ independent values related to the plant states after the first jump. In fact, they are expressed in terms of the n plant states $x_{pi}(t_1, 0)$, but one of them linearly depends on the others through (4.6) or (4.11). A reasonable way to obtain the values $x_{pi}(t_1, 0)$, without the necessity of using an analytical expression or relying on simulation, is to estimate them by using state observers. Note that since the integrator and CI states of all the controllers are identical up to the first jump, then

$$\begin{aligned} u_i(t,0) = k_{Pi} e(t,0) + \frac{k_{Pi}}{T_{Ii}} \Big((1 - p_{ri}) x_{Ii}(t,0) + p_{ri} x_{CIi}(t,0) \Big) \\ = k_{Pi} e(t,0) + \frac{k_{Pi}}{T_{Ii}} \int_0^t e(t,0)\, dt \end{aligned} \tag{4.13}$$

for $t \in [0, t_1]$, and thus it is only strictly necessary to tune the reset ratios p_{ri} just before the first jump at $t = t_1$. As a consequence, the controllers have a time interval $[0, t_1]$ to obtain a good estimate of $x_{pi}(t_1, 0)$.

An important fact is that although the tuning rules (4.5)–(4.6) explicitly depend on the amplitude w_{10} and w_{20i} of the reference change, it turns out that the resulting reset ratios p_{ri} take the same values independently of w_{10}. This is due to the fact that, before the first jump, the MISO reset control system flows like a linear (and time-invariant) system, and thus the values of $x_{pi}(t_1, 0)$ and x_I depend proportionally on the amplitude w_{10}. As a consequence, the values p_{ri} producing a flat response in reference tracking are *intrinsic* numbers of the MISO reset control system: the same values will produce flat responses for any step reference or disturbance signal of arbitrary amplitude. Therefore, once the reset ratios are tuned at the first jump, then

they may keep the same value afterwards.

Similarly, the tuning rules (4.10)–(4.11) for disturbance rejection can be shown to be invariant under simultaneous scaling of all w_{20i}; furthermore, given two independent disturbances w_{20i} and w_{20j} acting only on plants i and j, a convex linear combination of these disturbances is associated to a convex linear combination of the respective reset ratios. Taken together, these observations imply that in every possible case, the tuning rule will be determined by the set of n^2 invariant parameters $\{p_{ri,\text{dist1}}, p_{ri,\text{dist2}}, \ldots\}_{i=1}^{n}$ obtained by applying the rules (4.10)–(4.11) at each individual disturbance input.

Unlike in the SISO case, where the tuning rules always result in reset ratios between 0 and 1, the MISO tuning rules (4.5) or (4.10) (for $n > 1$) may result in large values of p_{ri} (positive or negative) in some cases. Since the proposed PI+CI controllers are equipped with a zero-crossing detection mechanism (by the use of the discrete state q), this is not a major issue even with small measurement noise, since $u_i(t_1, 1)$ can be shown to be reasonably bounded when resets occur close to a zero-crossing (it must be of the same order of $a_i x_{pi}(t_1, 0)/b_i$ due to (4.2), (4.8)). Nevertheless, whenever large reset ratios arise in practice, it might be an indication that either the base linear controllers are ill-designed or the plants have very different dynamics (for example, one is much slower than the others). In the latter situation, the PI+CI-based parallel control approach might be unsuitable, and one should consider a different control structure such as the serial structure. However, one way to deal with this problem without changing the control structure is to replace the requirement of a flat response by the requirement that all derivatives $\dot{x}_{pi}$ of the plant states are reduced by a factor $\chi \in [0, 1]$, that is, $\dot{x}_{pi}(t_1, 1) = \chi \dot{x}_{pi}(t_1, 0)$. This gives the modified design rules

$$p_{ri,\text{ref}} = 1 - (1 - \chi)\frac{a_i T_{Ii} x_{pi}(t_1, 0)}{b_i k_{Pi} x_I(t_1)}, \tag{4.14}$$

and

$$p_{ri,\text{dist}} = 1 - (1 - \chi)\frac{(a_i x_{pi}(t_1, 0) - b_i w_{20i}) T_{Ii}}{b_i k_{Pi} x_I(t_1)}. \tag{4.15}$$

Choosing $\chi = 0$ leads to the original tuning rules, and $\chi = 1$ recovers the base linear behavior. In general, χ can be chosen so that the reset ratios are appropriately bounded, while still obtaining an improved response compared to the linear case.

With regard to stability, the proposed parallel control architecture generically includes marginally stable modes for the flow dynamics if $n > 1$, due essentially to the underlying choice of base linear control. More specifically, consider a vector $\mathbf{v}$ defined as

$$\mathbf{v} = \begin{pmatrix} v_1 \\ v_2 \\ \vdots \\ v_n \\ \frac{a_1 v_1}{b_1 k_{I1}(1-p_{r1})} \\ 0 \\ \vdots \\ \frac{a_n v_n}{b_n k_{In}(1-p_{rn})} \\ 0 \end{pmatrix} \tag{4.16}$$

for some $v_1, \ldots, v_n \in \mathbb{R}$ such that $\sum_{i=1}^{n} v_i = 0$, and any $1 \neq p_{ri} \in \mathbb{R}$ $(i = 1, \cdots, n)$.

It follows that $A\mathbf{v} = 0$ and $A_R\mathbf{v} = \mathbf{v}$, and since $C_R\mathbf{v} = 0$, there exist solutions ϕ to the proposed control system with $\phi(t, j) \in \mathbf{v} \times \{1, -1\}$ for any $(t, j) \in \operatorname{dom} \phi$, corresponding to alternating flows and jumps of arbitrary length. Intuitively, this means that a steady state with zero error can be obtained for infinitely many choices of steady state values $u_1, \ldots, u_n$ of the control signals.

As a consequence, some modification is necessary for the PI+CI-based control strategy to achieve closed loop stability with respect to the equilibrium point $\{\mathbf{0}\} \times \{1, -1\}$. A simple way to avoid this problem is to slightly modify the PI+CI controller's structure by including a small FORE-like damping parameter ε affecting all the Clegg integrator blocks except possibly one of them, as follows:

$$\mathrm{CI}_\varepsilon : \begin{cases} \dot{x} = -\varepsilon x - e, & \text{if } (e, q) \in \mathcal{C}, \\ \begin{pmatrix} x^+ \\ q^+ \end{pmatrix} = \begin{pmatrix} 0 & 0 \\ 0 & -1 \end{pmatrix} \begin{pmatrix} x \\ q \end{pmatrix}, & \text{if } (e, q) \in \mathcal{D}, \end{cases} \tag{4.17}$$

The presence of the new design parameter ε prevents the appearance of marginal stability modes and leads to unique values for the control signals in the steady state, but in turn makes it impossible to achieve a perfect flat response with a zero-crossing law, since in general $\dot{x}_{Ii}(t_1, 1) = -\varepsilon x_{Ii}(t_1, 1) \neq 0$. However, a reasonable approximation in practice can still be obtained for small values of ε in comparison to the inverse of

the closed loop rise time.

It should be emphasized that in the SISO case [18, 32] corresponding to $n = 1$, the stability of PI+CI-based control for first order plants can easily be shown by taking advantage of the fact that the reset instants are always periodic. This special feature is particular to SISO systems (and first order plants), and it is generally no longer true in the multiple-input setting: in fact, it can be shown that in many cases the sequence of reset instants is chaotic [43]. Nonperiodicity makes the stability analysis essentially as difficult as the general case, thus one has to resort to more general results such as the stability conditions developed in Section 2.5.

Since in a well tuned control system the error signal will be very close to its steady state after a finite number of reset actions (usually, no more than 3–5 jumps will be sufficient for a good response, and allowing for more reset actions will not lead to a measurable increase in performance), the alternative stability conditions #2 can be directly used by imposing a maximum number of reset actions during the time in which the controller is working against any given disturbance or reference change.

Note that condition (2.44) is trivially satisfied, with J being the maximum number of jumps and $\gamma = 0$. Furthermore, the rest of the conditions are easily satisfied when the base system is stable.

4.1.4 Examples

Example 4.1 (Reference tracking in a 3×1 system)**.** Consider a parallel MISO reset control system, with the three plants given by the following transfer functions:

$$P_1(s) = \frac{0.5}{1+s}, \quad P_2(s) = \frac{1.5}{0.2+s}, \quad P_3(s) = \frac{3}{5+s}. \tag{4.18}$$

The base linear PI controllers are initially tuned according to the Skögestad Internal Model Control (SIMC) rule [337] (treating each plant-controller subbranch as a SISO system), and then the values of k_{Pi} and T_{Ii} are manually increased to produce a dominant oscillatory closed loop response, forcing reset actions to occur. The resulting parameters are

$$\begin{aligned} k_{P1} &= 2.00, \qquad T_{I1} = 0.333, \\ k_{P2} &= 0.67, \qquad T_{I2} = 0.067, \\ k_{P3} &= 0.33, \qquad T_{I3} = 1.667. \end{aligned} \tag{4.19}$$

For simplicity, the values of $x_{pi}(t_1, 0)$ and $x_I(t_1)$ have been obtained by simulating the step response of the MISO reset control system with the base PI controllers, and then obtaining the values of the plant states and integrator states at the first jump (in practice, a state observer should be used). Using (4.5)-(4.6) for $n = 3$ results in

$$p_{r1} = 0.531, \qquad p_{r2} = 0.942, \qquad p_{r3} = -2.482. \tag{4.20}$$

These reset ratios, jointly with (4.19), determine the three PI+CI controllers. The unit step response of the MISO reset control system has been simulated, for which a measurement noise signal consisting of a pseudo-random uniform signal of magnitude 0.025 has been added to the plant output. Figure 4.2 shows the expected flat response after the first jump; note that, in spite of the measurement noise, the overshooting has been completely eliminated in comparison with the base control system, and the settling time is also considerably reduced. It must be emphasized that the property of robustness to noise is formally guaranteed by the fact that the MISO reset control system (2.17) is well-posed, as shown in Section 2.5. Note also that the effect of sensor noise on the closed loop system is similar for both the base and the reset controllers, and does not significantly degrade the response after a reset action, even if this action may be triggered at a different time than the noiseless case.

Moreover, the controller outputs are shown in Figures 4.3(a), 4.3(b), and 4.3(c), showing how control signals achieve their steady state at the first reset instant. Finally, the closed loop stability of this MISO reset control system is analyzed. Once the modification (4.17) is performed on all PI+CI controllers, choosing $\varepsilon = 10^{-5}$, the stability conditions #1 from Section 2.5 are checked to be feasible by using the semidefinite programming solver CVX. The solution

$$P = 10^8 \cdot \begin{pmatrix} 0.09 & 0.09 & 0.09 & -0.01 & -0.01 & -0.00 & -0.03 & -0.00 & 0.00 \\ 0.09 & 0.09 & 0.09 & -0.01 & -0.01 & -0.00 & -0.03 & -0.00 & 0.00 \\ 0.09 & 0.09 & 0.10 & -0.01 & -0.01 & -0.00 & -0.03 & -0.01 & 0.00 \\ -0.01 & -0.01 & -0.01 & 17.4 & 0.00 & -6.75 & 0.00 & -10.3 & -0.00 \\ -0.01 & -0.01 & -0.01 & 0.00 & 28.1 & 0.00 & -20.4 & 0.00 & -7.44 \\ -0.00 & -0.00 & -0.00 & -6.75 & 0.00 & 16.3 & 0.00 & -9.45 & -0.00 \\ -0.03 & -0.03 & -0.03 & 0.00 & -20.4 & 0.00 & 33.3 & 0.00 & -11.8 \\ -0.00 & -0.00 & -0.01 & -10.3 & 0.00 & -9.45 & 0.00 & 19.8 & -0.00 \\ 0.00 & 0.00 & 0.00 & -0.00 & -7.44 & -0.00 & -11.8 & -0.00 & 19.2 \end{pmatrix}$$

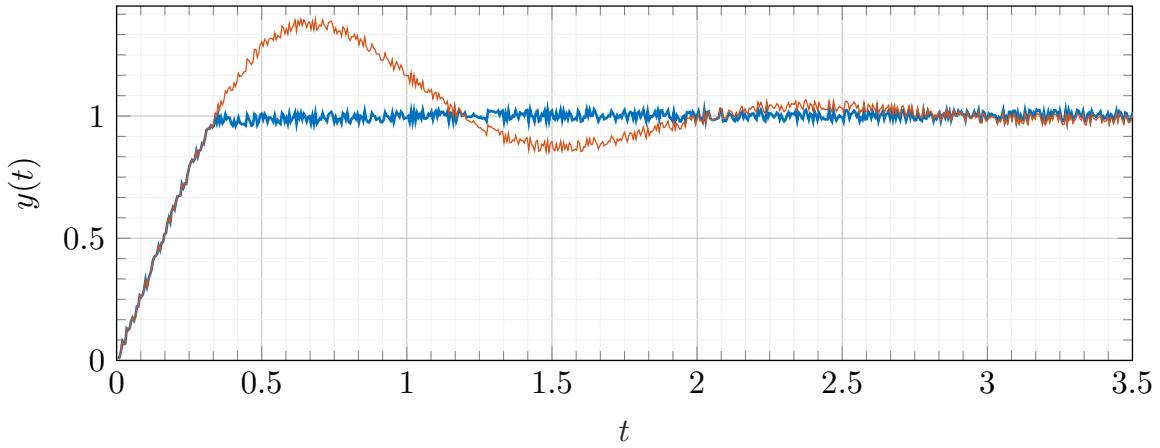

Figure 4.2: Closed-loop step response y under a reference change in Example 4.1: (orange) base PI controllers; (blue) PI+CI controllers.

is found, and thus the origin $\{\mathbf{0}\} \times \{1, -1\}$ is globally asymptotically stable for this control system.

Alternatively, by disabling reset actions after the first one, stability conditions #2 from Section 4.2 easily apply, since the base MISO system with $\varepsilon = 10^{-5}$ is stable (which can be easily proven by checking the eigenvalues of A).

Example 4.2 (Disturbance rejection in a 2×1 system)**.** In this example, a disturbance rejection problem with a two-input system is considered, where the two plants are given by the following transfer functions:

$$P_1(s) = \frac{1}{1+s}, \qquad P_2(s) = \frac{1.5}{1.5+s}. \tag{4.21}$$

The problem of disturbance rejection is considered for step disturbances at the input of the first plant. No measurement noise is explicitly considered in this case, as it has already been shown not to significantly affect the results. The corresponding PI controller parameters, tuned to obtain a fast oscillatory response in the same way as the previous example, are

$$\begin{aligned} k_{P1} &= 4, \qquad T_{I1} = 1/16, \\ k_{P2} &= 5, \qquad T_{I2} = 1/32. \end{aligned} \tag{4.22}$$

Reset ratios are obtained by using (4.10)–(4.11):

$$p_{r1} = -2.074, \qquad p_{r2} = 0.808. \tag{4.23}$$

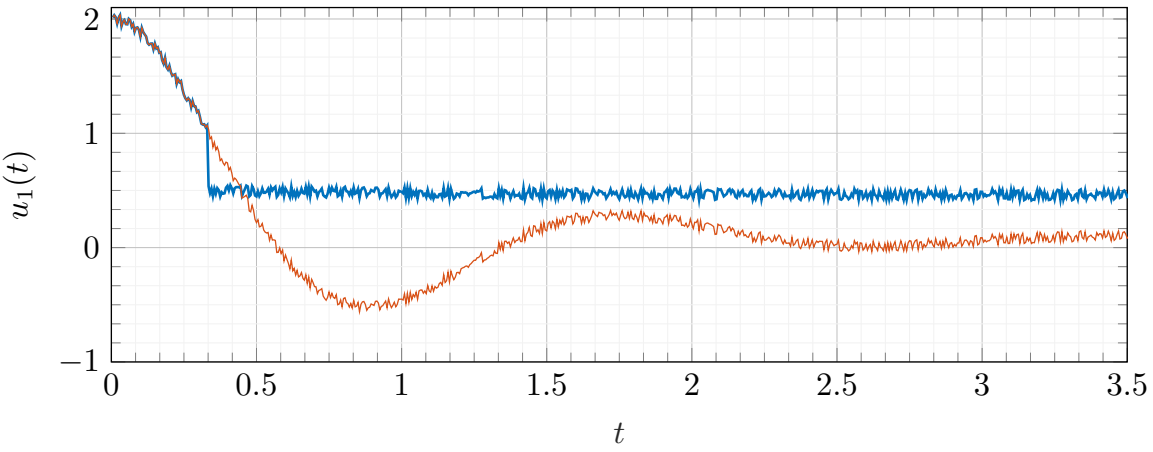

(a) Control output u_1.

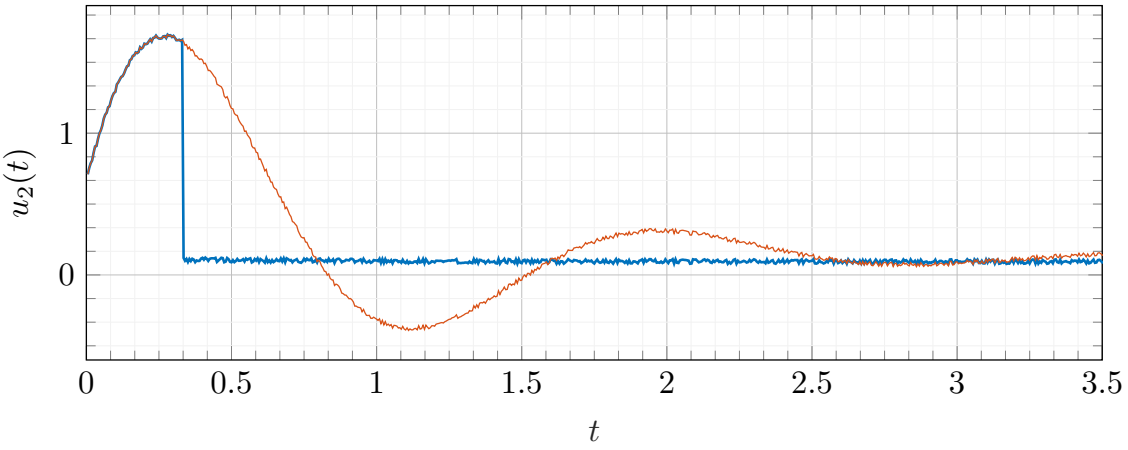

(b) Control output u_2.

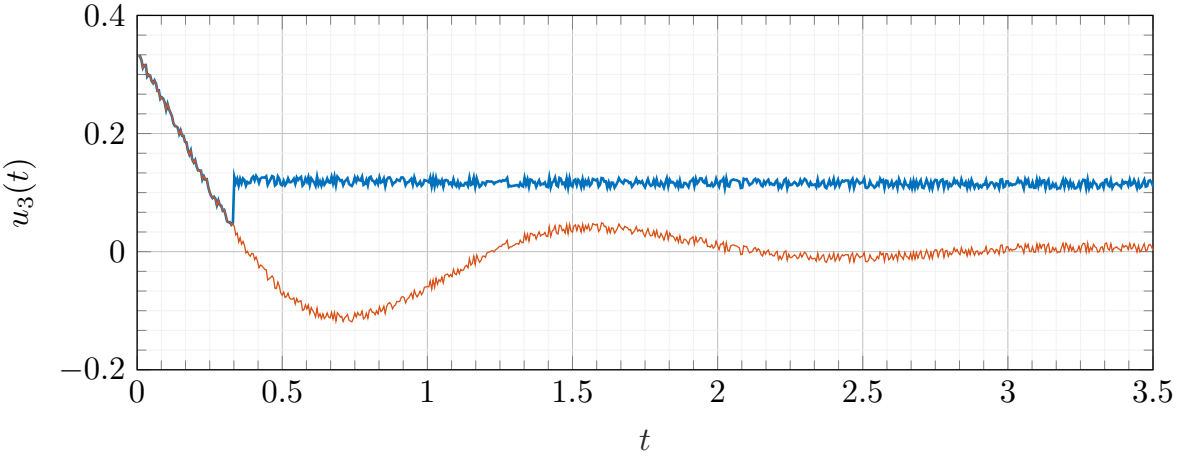

(c) Control output u_3.

Figure 4.3: Controller outputs for the reference change in Example 4.1: (orange) base PI controllers; (blue) PI+CI controllers.

A disturbance d_1 is considered ($d_2 = 0$), consisting of the sum of a unit step at $t = 0$ and a step of amplitude -0.5 at $t = 1$. As Figure 4.4 clearly shows, both disturbances are perfectly rejected by two respective reset actions (it is worth emphasizing that the values of p_{r1}, p_{r2} are constant and there is no need to update them after each reset). The controller outputs are shown in Figures 4.5(a) and 4.5(b).

Now, consider closed loop stability for this system. Again the modification (4.17) is performed on both PI+CI controllers, taking a small value $\varepsilon = 10^{-5}$. As before, solving the LMI stability conditions #1, the solution

$$P = 10^5 \cdot \begin{pmatrix} 0.0176 & 0.0175 & 0.0020 & -0.0071 & -0.0014 & 0.0122 \\ 0.0175 & 0.0175 & -0.0081 & -0.0071 & -0.0055 & 0.0122 \\ 0.0020 & -0.0081 & 3.0207 & -0.0000 & -0.6415 & 0.0000 \\ -0.0071 & -0.0071 & -0.0000 & 2.9706 & -0.0000 & -3.2296 \\ -0.0014 & -0.0055 & -0.6415 & -0.0000 & 1.4868 & 0.0000 \\ 0.0122 & 0.0122 & 0.0000 & -3.2296 & 0.0000 & 3.8922 \end{pmatrix}.$$

is found. As a result, the origin $\{\mathbf{0}\} \times \{1, -1\}$ is globally asymptotically stable for the MISO reset control system.

Note again that if resetting is inhibited after one reset action, the stability conditions #2 may be used to prove stability by directly checking that the eigenvalues of the matrix A are strictly in the left half plane.

4.2 Parallel control of higher order MISO plants

It is rare for processes to display exclusively first order behavior in control practice. Several commonly arising phenomena, such as resonance or oscillations, are linked to the existence of complex poles in the transfer function, and hence imply that the process has order at least two. Consequently, it is justifiable to consider the development of hybrid control strategies that are also applicable to higher order systems.

Even in the single-input case, a generic reset controller will be generally unable to achieve a flat response using a single reset action in the case of plants with orders higher than one, no matter which resetting law is applied (however, a flat response is achievable using more than one reset action [35]). This is due to the fact that the state

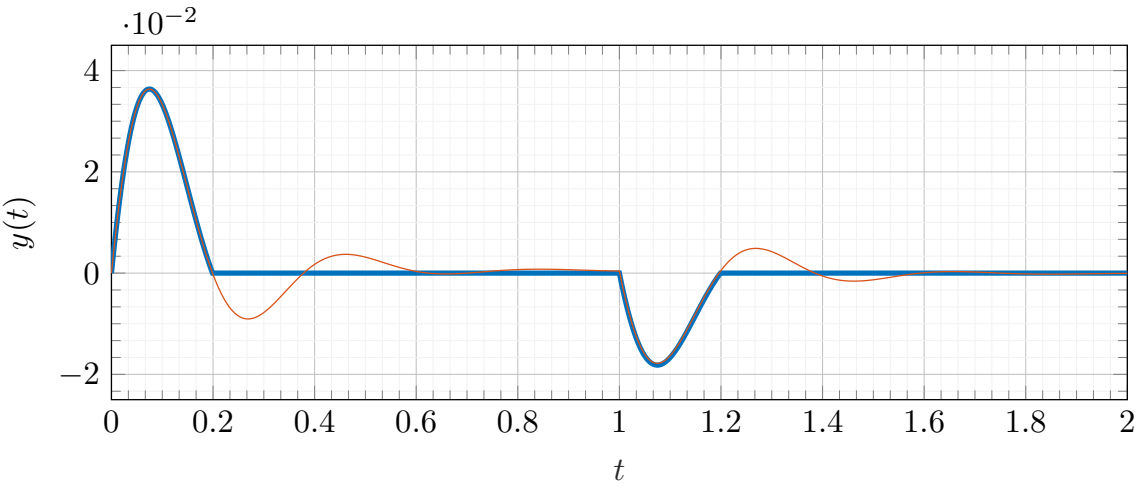

Figure 4.4: Closed-loop response y under a disturbance signal in Example 4.2: (orange thin line) base PI controllers; (blue thick line) PI+CI controllers.

space of higher order plants is of dimension greater than one, and through a similar reasoning to the above section, it can be shown to be impossible to simultaneously nullify the derivatives of all states in the ith plant by means of a single change to the value of u_i.

However, it is known that the PI+CI can still be used to achieve a significant performance improvement compared to its linear counterpart. In the following, an optimization-based approach will be developed for the case of a parallel MISO plant of arbitrarily high order, through the use of varying reset ratios combined with a variable band law with common variable band parameter θ. The followed methodology, which generalizes the on-line algorithm used in [46], does not produce an explicit formula except in the SISO case; instead, it will be based on solving a quadratic minimization problem and applying the solution at each reset instant. Similar algorithms have been used in the literature [386].

4.2.1 Variable reset ratios

Consider the same PI+CI based strategy as in the previous case, augmented by a variable reset ratio given by $\mathcal{P}_{ri}(t, j)$. The case will be considered where $\mathcal{P}_{ri}(t, j)$ depends only on the number of jumps, i.e., for any $(t_k, k-1) \in \operatorname{dom} \mathcal{P}_{ri}$, $\mathcal{P}_{ri}(t, k-1) = p_{ri}^{(k)}$ is constant for all $t \in [t_{k-1}, t_k]$.

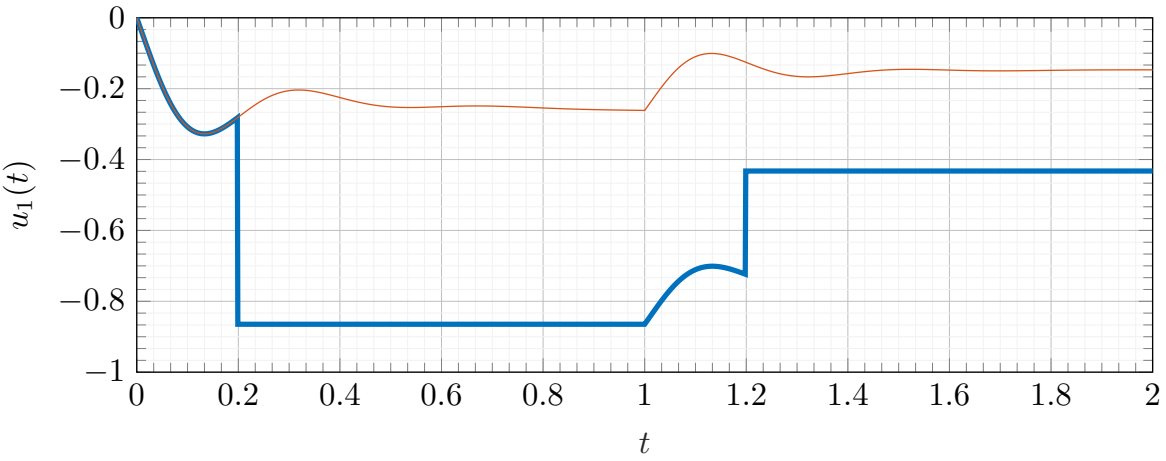

(a) Controller output u_1.

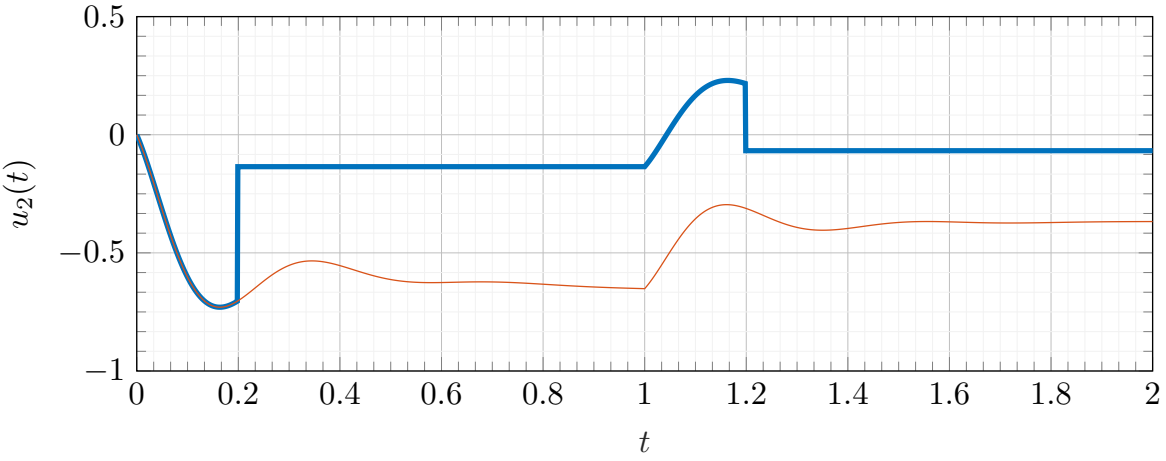

(b) Controller output u_2.

Figure 4.5: Controller outputs for the disturbance signal in Example 4.2: (orange thin line) base PI controllers; (blue thick line) PI+CI controllers.

Since obtaining a flat response is impossible with a PI+CI, a response that best approximates flatness according to some performance coefficient will be sought for. Two common metrics to measure the performance of a control strategy are the integrated absolute value of the error (IAE), defined on an interval $[T, T')$ as

$$\mathrm{IAE}_{[T,T')} = \int_T^{T'} |e(t,j)|dt,$$

and the maximum overshoot percentage, that can be defined on an interval $[T, T']$ by

$$M_{[T,T')} = \sup_{t\in[T,T')} \frac{|e(t,j)|}{w_0},$$

where w_0 is a parameter with the same dimension of e, typically the height of a step reference change or disturbance. A third metric, representing a kind of combination between the two former ones, is the integrated squared error (ISE), defined as

$$\mathrm{ISE}_{[T,T')} = \int_T^{T'} e(t,j)^2 dt;$$

note that an important difference with respect to the IAE is that the presence of a square penalizes situations with more overshooting. This performance coefficient will be the one chosen as the parameter to minimize.

However, as described in [20, 118], the corresponding minimization problem turns out to be analytically tractable only if the system is LTI and $T' = \infty$; in this case, one can easily compute the solution by solving a Lyapunov equation [336]. That is, for the purposes of minimization, one should consider the fictitious error signal $e_k(t)$ formed by extending $e(t,k)$ from the domain $[t_k, t_{k+1}] \times \{k\}$ to $[t_k, \infty) \times \{k\}$ using the flow equation, i.e. the signal one would obtain by disabling all reset actions after t_k (see Figure 4.6).

Since this signal contains spurious values in $[t_{k+1}, \infty)$ which negatively affect the minimization, a new modification of this strategy will be proposed in order to minimize the effect of these values. This will be achieved by multiplying the signal $e_k(t)$ by the exponential weight $e^{\alpha(t-t_k)}$, which will help suppress these spurious contributions located far from the instant t_k. This introduces a new design parameter α, with dimensions of inverse time.

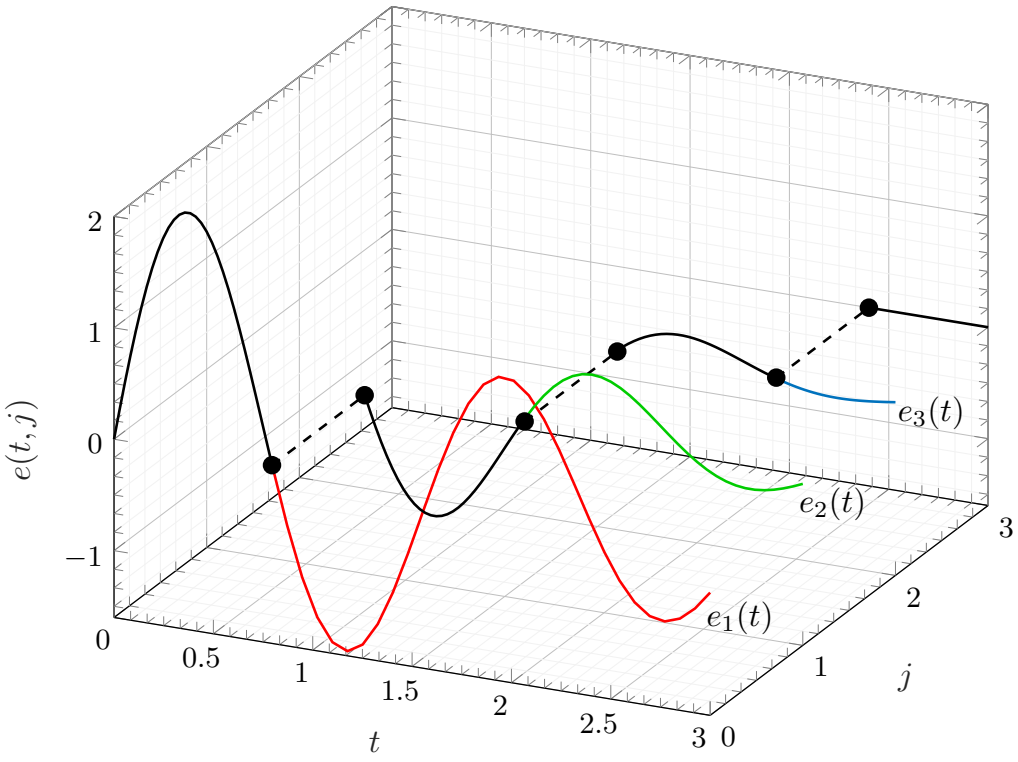

Figure 4.6: Example of an error signal $e(t, j)$ (black) featuring three jumps, with fictitious linear extensions $e_1(t)$ (red), $e_2(t)$ (green) and $e_3(t)$ (blue).

In summary, the sequence of reset ratios p_{ri}^1, $p_{ri}^2, \cdots$ will be calculated through an ISE minimization problem for the fictitious error $e_k(t)$ after each reset action, weighted by an exponential term. More specifically, $p_{ri}^{(k)}$ will be calculated by minimizing the value $\mathrm{ISE}_{[t_k,\infty),\alpha}$ defined by

$$\mathrm{ISE}_{[t_k,\infty),\alpha} = \int_{t_k}^{\infty} e_k(t)^2 e^{-2\alpha(t-t_k)}\, dt. \tag{4.24}$$

In general, a good rule of thumb is to take $\alpha \approx 0.5\tau^{-1}$, where τ denotes the average time interval between two consecutive zero crossings of the base system; in this way, $\mathrm{ISE}_{k,\alpha}$ is a good approximation of the integrated squared error between t_k and t_{k+1}, since at times $t \gg t_{k+1}$ the contribution will be exponentially suppressed. Following the method in [20], and considering the new exponential weighting factor, this quantity can be reexpressed as

$$\mathrm{ISE}_{[t_k,\infty),\alpha} = \mathbf{x}(t_k, k-1)^\top L \mathbf{x}(t_k, k-1). \tag{4.25}$$

Here $L > 0$ is a solution of the Lyapunov equation

$$(A - \alpha I)^\top L + L(A - \alpha I) + C^\top C = 0.$$

As before, two separate control design objectives are distinguished: reference tracking and disturbance rejection. For each case, it is assumed that the matrix A corresponds to a minimal realization of the base MISO control system, including the corresponding exosystem for reference or disturbances.

Since $\mathbf{x}(t_k, k-1)$ depends on $p_{ri}^{(k)}$ in an affine way, we arrive at a quadratic minimization problem whose objective function is of the form $\mathbf{x}(t_k, k-1)^\top L \mathbf{x}(t_k, k-1) = \mathbf{y}^\top M_k \mathbf{y} + \mathbf{b}_k^\top \mathbf{y} + c_k$ where $\mathbf{y} = (p_{r1}^{(k)}, \ldots, p_{rn}^{(k)})$. This minimization problem has an explicit solution given by $\mathbf{y}_{\min} = -\frac{1}{2} M_k^{-1} \mathbf{b}_k$. As a result, the proposed reset ratios for the m PI+CI controllers are obtained simply by

$$(p_{r1}^{(k)}, \cdots, p_{rn}^{(k)})^\top = -\frac{1}{2} M_k^{-1} \mathbf{b}_k, \tag{4.26}$$

where M_k and $\mathbf{b}_k$ are quadratic functions of $\mathbf{x}(t_k, k-1)$ with coefficients that depend only on the parameters of the plants and controllers.

4.2.2 Variable band resetting law

Since the zero crossing law is known to cause undershooting in plants not of first order, the previous optimization problem will be applied to a reset control system under a variable band law. The synchronous case will be considered first, with a single nonzero variable band θ.

In principle, a good idea would be to consider a time varying variable band parameter $\theta = \Theta(t, j)$ and calculate its optimal values $\theta^{(1)}, \theta^{(2)}, \ldots$ after each reset action by minimizing $\mathrm{ISE}_{[t_k,\infty),\alpha}$. In the second order SISO case, doing so leads to optimal values for the reset ratios and the variable band expressible as a simple formula. For a SISO second order plant given by $P(s) = b/(s^2 + as + a')$, for e.g. reference tracking the optimal values (with $\alpha = 0$) take the form [20]

$$p_{ri}^{(k)} = 1 - \frac{aT_I w_{10}}{bk_P x_I(t_1)} + \frac{\dot{e}(t_1, 0)}{a' x_I(t_1)}, \quad \theta^{(k)} = \theta_{\mathrm{opt}} = \frac{a'^2}{a'(a'^2 + a + bk_P) - bk_P T_I^{-1}}. \quad (4.27)$$

However, when $n > 1$, θ_k enters the objective function $ISE_{k,\alpha}$ in a rather complex way, which makes it very difficult, if not impossible, to solve the optimization problem on-line. The main issue is that the reset instant t_k at which optimization is performed implicitly depends on θ due to the variable band law, and this dependence cannot be calculated explicitly without essentially having access to the full solution to the kth fictitious linear system; even then, this solution is commonly not analytically invertible in a way that would allow to find an explicit expression for an optimal θ.

In consequence, a simple design method is proposed, considering a constant value for θ:

1. First, a value of θ is chosen. It should be taken low enough so that the error signal is, to a good approximation, linear in the time intervals spanning θ units of time before any zero crossing. In general, if the plants are approximated by first order systems with time delay, θ should be taken smaller than the lowest of the delays.

2. Secondly, the quadratic optimization problem (4.24) is solved to find optimal values for the reset ratios with respect to that constant value of θ as a function of the system's states and the step reference change or disturbance's height. The result is given by (4.26).

3. Finally, the reset ratios are updated on-line at each reset instant using (4.26) and the measured or estimated values of the plant and controller states.

In principle, if a more general asynchronous configuration is postulated with n independent variable bands $\theta_1, \ldots, \theta_n$, an identical $\mathrm{ISE}_{[t_k,\infty),\alpha}$ minimization procedure can be followed at each individual reset instant, giving rise to a total of $2^n - 1$ different optimization problems analogous to (4.24) in order to compute appropriate reset ratios in each possible case. Note that the complexity of this design method for asynchronous reset control systems increases exponentially with the number of plants: a simplifying assumption, if all variable bands θ_i are different, is to assume that no two controllers will be reset at exactly the same time, in which case only n optimization problems need to be considered.

Moreover, the justification of considering fictitious error signals in the asynchronous case is rather unclear, since the sequence of time intervals between any two reset instants can vary wildly in an essentially unpredictable way, making an appropriate choice of α extremely difficult, even if different values α_i were considered for each controller. In practice, acceptable results may be achieved by forcing a minimum time separation between reset actions through time regularization (2.32) with a time constant D, and then choosing $\alpha = 0.5D^{-1}$.

4.2.3 Comments and guidelines

In general, as in the first-order case, the obtained expression (4.26) depends on the plant and controller states at $(t, j) = (t_k, k-1)$. An online implementation of this algorithm requires knowing or estimating the values of the plant states, $x_{pi}(t_k, k), \dot{x}_{pi}(t_k, k), \ldots$ in real time (this is also true, particularly in the SISO case, where the reset ratio is an explicit function of $\dot{e}(t_k, k) = -\dot{x}_{p1}(t_k, k)$ [118]). Again, in a situation where state feedback is unavailable, a simple way to estimate plant states is to use a state observer and make use of the estimated values $\hat{x}_{pi}(t_k, k), \hat{\dot{x}}_{pi}(t_k, k)$, etc. Note that this will be more difficult if either the order of the number of plants is high, since a MISO $n \times 1$ mth order plant has in general a total of mn states.

An important difference with respect to both the MISO first order and SISO second order cases is that no explicit algebraic formula is available to calculate p_{ri}. However, as mentioned previously, it follows from the form of the minimization problem that $M_k = M(\mathbf{x}(t_k, k-1))$ and $\mathbf{b}_k = \mathbf{b}(\mathbf{x}(t_k, k-1))$, where M and $\mathbf{b}$ are exclusively

functions of the parameters of the plants and base controllers, and thus numerically computable *a priori* once the plant has been identified. Thus, updating the reset ratios online involves the evaluation of a known quadratic function at a vector $\mathbf{x}(t_k, k-1)$, which is not computationally expensive.

Another limitation, absent from the first order case, concerns the use of the variable band, which is based on the derivative of the error signal. Recall that this derivative must be filtered to avoid accidental early triggering of a reset action due to measurement noise; as specified in Section 2.2.2, a first order low pass filter is used with a time constant of 0.4θ by default.

Note that the results on stability based on LTI base plants are unavailable here, as the base linear system is time-varying. Hence, one must either resort to more general results applicable to linear plants, or else inhibit resetting after a certain number of reset actions is performed and apply the pertinent stability conditions (since the system becomes LTI after the last resetting).

Finally, the same considerations with regard to reset ratios of high magnitude for the first order reset strategy in Section 4.1 are also applicable here.

4.2.4 Examples

Example 4.3 (Reference tracking in a 2×1 second order system)**.** This example consists of a two-input single-output (TISO) plant that models a refrigeration system, and has been adapted from [311], where it comprises the cooling part of the temperature control system of a room.

Here, the two subplants (which correspond to an air conditioning unit and a cooling water input respectively) are approximated by second order systems, and the above design method is applied to design a parallel PI+CI control setup. The plants are given by the transfer functions

$$P_1(s) = \frac{-5}{(1+8s)(1+2s)}, \quad P_2(s) = \frac{-10}{(1+15s)(1+3s)}. \tag{4.28}$$

The two base PI controllers are first designed for a fast and oscillatory response, following the same method as in previous examples. Their parameters are:

$$\begin{aligned} k_{P1} &= -0.8, \qquad T_{I1} = 8, \\ k_{P2} &= -0.5, \qquad T_{I2} = 15. \end{aligned} \tag{4.29}$$

With these base parameters, the dominant complex eigenvalues of the closed loop base linear system can be checked to be $\lambda_{\pm} = -0.2209 \pm 0.5532i$, so the zero crossings of this system occur with an eventual semiperiod of $T = \pi/|\mathrm{Im}\lambda_{\pm}| = 5.68$ seconds. The corresponding α would be $0.5T^{-1} = 0.088$; the rounded-up value $\alpha = 0.1$ has been used.

Moreover, a variable band $\theta < h_{\min}$ should be used, where $h_{\min} = 2$ is the smallest plant delay [311]. After some trial and error, the value $\theta = 0.5$ is chosen.

Finally, the procedure (4.26) is used for the on-line computation of the values or $p_{ri}^{(k)}$, at $k = 1, 2, \ldots$; after simplifying, the resulting final formulas can be expressed as

$$(p_{r1}^{(k)}, p_{r2}^{(k)}) = (1,1) - \begin{pmatrix} \frac{1}{x_{I1}(t_k)} & 0 \\ 0 & \frac{1}{x_{I2}(t_k)} \end{pmatrix} \begin{pmatrix} 10.73 & -27.36 & 8.37 & -38.68 & 4.74 \\ -28.58 & 68.36 & -14.14 & 88.42 & -3.78 \end{pmatrix} \begin{pmatrix} w_{10} \\ x'_{p1} \\ x_{p1} \\ x'_{p2} \\ x_{p2} \end{pmatrix}, \tag{4.30}$$

where $\mathbf{x}_{pi} = (x'_{pi}, x_{pi})$. Here the reference input r_y is a step signal of amplitude $w_{10} = 2$ starting at $t = 1$. The reset actions have been disabled after three jumps (at $t = 11$ seconds) when the error signal is near its steady state.

As shown in Figure 4.7, in comparison with the base control system, the step response is clearly improved after the first reset action at $t \approx 4$, considerably decreasing both overshooting and the settling time. The two controller outputs are shown in Figures 4.8(a) and 4.8(b), and the two respective time-varying reset ratios are depicted in Figure 4.9.

Table 4.1 summarizes the ISE, IAE and overshoot metrics for the MISO reset control system as compared to the base LTI control system; the result is an improvement of 13.21% of the ISE, 26.70% of the IAE and 64.11% of the maximum overshoot percentage. Finally, closed loop stability easily follows by directly applying the stability conditions

	MISO system (PI)	**MISO system (PI+CI)**
ISE	7.015	6.088
IAE	6.835	5.010
Overshoot	29.26%	10.50%

Table 4.1: Integrated squared error (ISE), integrated absolute error (IAE), and maximum overshoot percentage, for the parallel MISO reset control system and its base system.

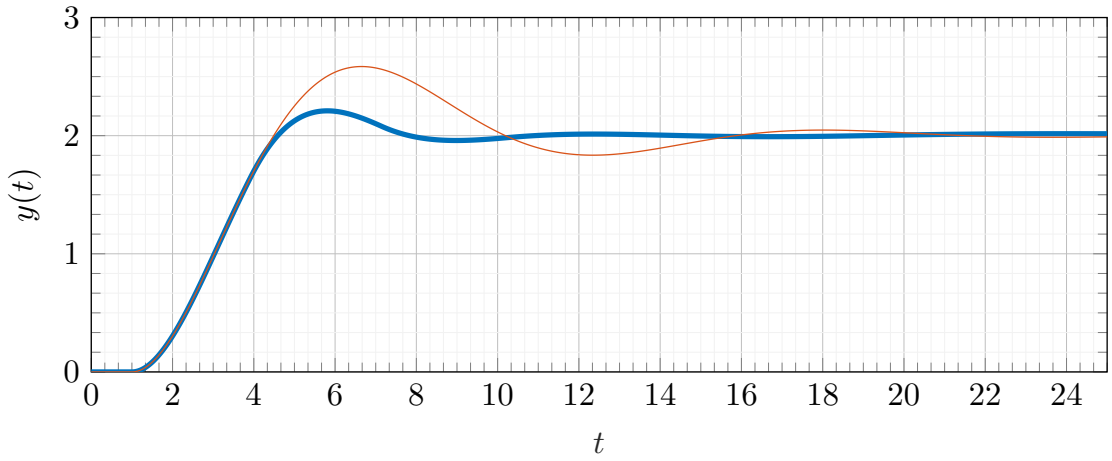

Figure 4.7: Closed loop step response output y in Example 4.3: (orange thin line) base PI controllers; (blue thick line) PI+CI controllers.

#2 with $J = 3$, provided the ε-modification is used to eliminate the marginally stable modes.

4.3 Control of first order SISO plants with delay

A possible strategy for the control of systems with delay, which has been used in the past, consists of treating the plant as if it were a nondelayed plant of second or higher order by means of a Padé approximation [288], and then applying the variable band and variable reset ratio method described in Section 4.2. However, especially in the case of MISO plants, the mentioned method's increased theoretical and practical complexity might make its implementation challenging; on the other hand, the suitability of the variable reset ratio method in an asynchronous configuration is doubtful, and the imposition of equal variable bands may be too strict of a limitation in practical cases. In this section and the next, an alternate hybrid control method for first order delayed plants based on the reset-and-hold strategy will be explored. The SISO case will be described first, since the proposed strategy is also new in this case.

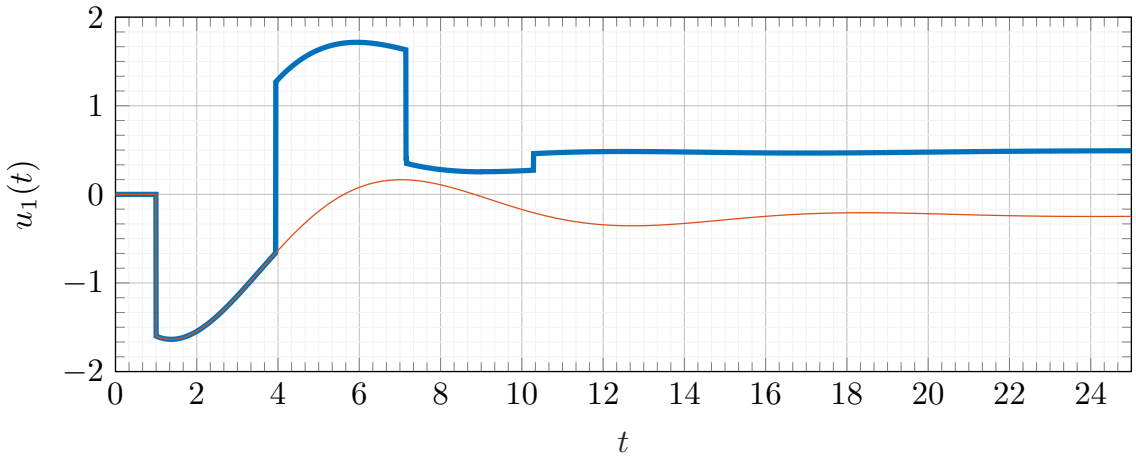

(a) Controller output u_1.

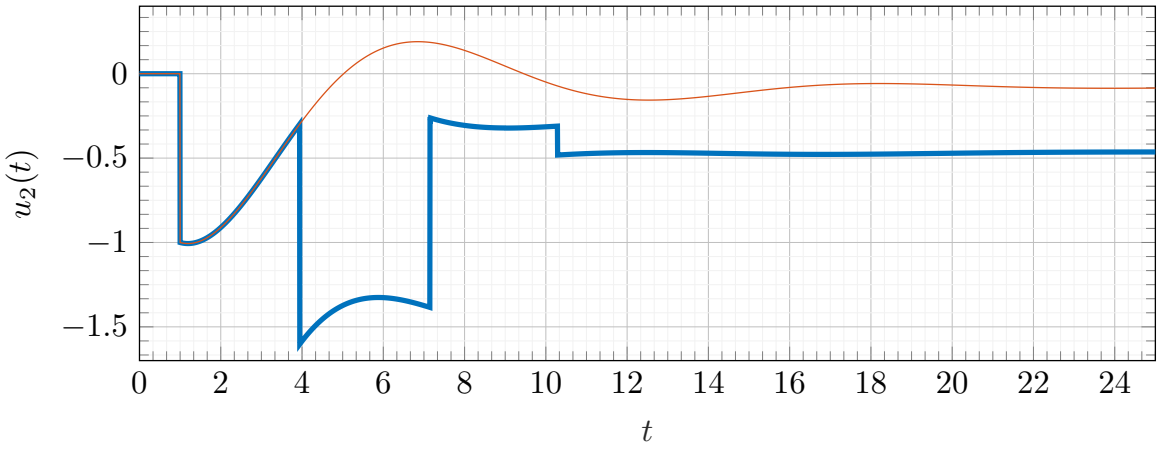

(b) Controller output u_2.

Figure 4.8: Controller outputs for the step response in Example 4.3: (orange thin line) base PI controllers; (blue thick line) PI+CI controllers.

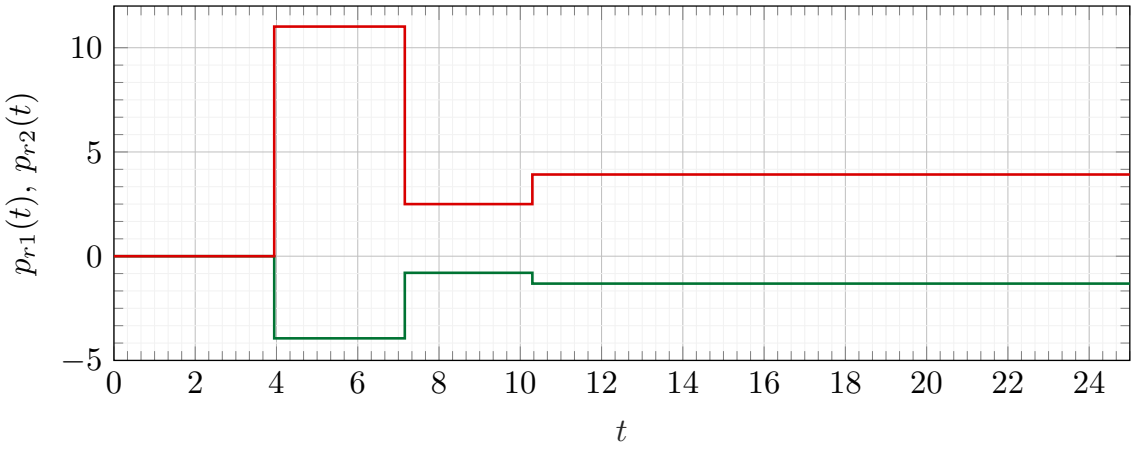

Figure 4.9: Projection onto the time domain of the time-varying reset ratios in Example 4.3: $p_{r1}(t,j)$ (green) and $p_{r2}(t,j)$ (red).

4.3.1 Reference tracking

This section will focus in the case $n = 1$ of the PI+CI control structure for the first order plant (3.13) with time delay h. For a first order plant, the matrices reduce to

$$A_p = -a, \quad B_p = b, \quad C_p = 1. \tag{4.31}$$

Consider again the situation where a step reference change r of amplitude w_{10} is applied to the system initially at rest. It will be instructive to follow the steps outlined in the nondelayed setting to find out where the argument that led to the tuning rules (4.7)–(4.12) fails, and how to make the according corrections.

A first difference with respect to the nondelayed case is that, because of the nonzero variable band, the instant $t = t_c$ in which the error signal crosses zero will in general be different from the instant $t = t_1$ at which the first reset action occurs. By direct substitution in (3.19), the value of $x_p(t,j)$ for $(t,j) \in [0,t_c) \times \{0\}$ is simply obtained from

$$\dot{x}_p(t,j) = -ax_p(t,j) + bk_P\Big(e(t-h,j) + \frac{1}{T_I}\Big((1-p_r)x_I(t-h,j) + p_r x_{CI}(t-h,j)\Big)\Big), \tag{4.32}$$

whereas the evolution of the controller states x_I, x_{CI} is still given by (4.3) (with $n = 1$).

The first design choice is to let the variable band be equal to the delay, i.e., to make $\theta = h$. In this way, the reset action will be triggered at $t_1 \approx t_c - h$, where the first order approximation $e(t + \delta, j) \approx e(t, j) + \delta\dot{e}(t, j)$, for $t \in [t_c - h, t_c]$ and $\delta \in [0, h]$ is assumed to hold to sufficient accuracy.

As a consequence, $x_I(t_1, 1) = x_I(t_c - h, 1) = x_I(t_1)$ and $x_{CI}(t_1, 1) = 0$, and substituting the expressions in (4.32) and (4.3), it follows that

$$\dot{x}_p(t_c, 1) = -ax_p(t_c, 1) + b\frac{k_P}{T_I}(1 - p_r)x_I(t_1) + bk_P e(t_1, 1), \tag{4.33}$$

At this point, an ultimately *incorrect* attempt to arrive at a flat response can be made by appropriately tuning the parameter p_r to set $\dot{x}_p(t_c, 1) = 0$; after rearranging terms, one is led to the value

$$p_{r,\text{incorrect}} = 1 - \frac{aT_I w_{10} - bk_P e(t_1, 1)}{bk_P x_I(t_1)}, \tag{4.34}$$

where the fact that $x_p(t_c, 1) = y(t_c, 1) = w_{10}$ has been used. However, this approach leads to a problem due to the delayed feedback loop. Indeed, this choice of reset ratio is able to momentarily set the derivative to zero at $t = t_c$. However, a further problem arises, namely that $\dot{x}_p(t, 1)$ will be driven away from zero in the subsequent interval $t \in (t_c, t_c + h)$. This is due to the fact that during this interval, the plant is receiving the delayed input of the controller $u(t - h, 1)$ evaluated at time $t - h \in (t_1, t_c)$, which in turn by (4.3) depends on the *nonzero past values* of the error at $t - h \in (t_1, t_c)$, and thus is not constant. Figure 4.10 illustrates this dependency.

This problem is what motivates the use of the reset-and-hold strategy. Recall that this strategy consists of keeping the controller output and states constant for τ_H units of time after each reset action. As suggested in the above paragraph, the appropriate design choice to avoid the delayed feedback problem is to make $\tau_H = h$. This choice will prevent the controller from reacting to the spurious input values $e(t', 1)$ for $t' \in (t_1, t_h)$, by forcing the controller output to hold a constant value $u(t', 1) = u(t_1, 1)$ until the plant has properly reacted to the effect of resetting (see Figure 4.10). The flow equation for the plant state at $(t_c, 1)$ is now

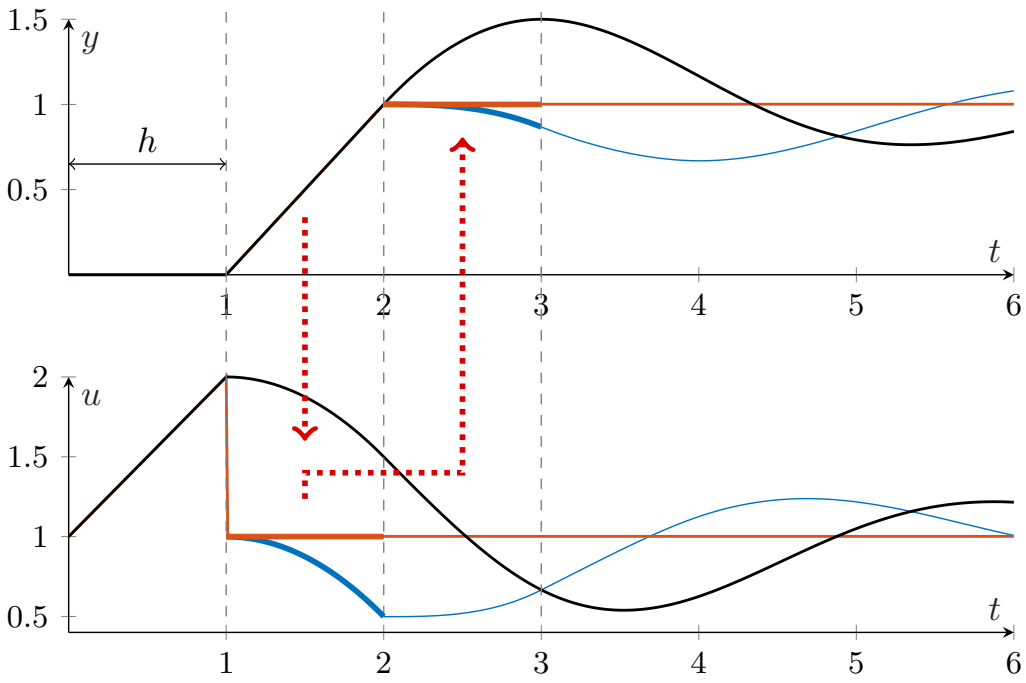

Figure 4.10: Illustration of reference tracking ($w_{10} = 1$) for a first order delayed plant under different control strategies: PI linear control (black), PI+CI reset control (blue), ideal PI+CI reset-and-hold control (orange). The detrimental dependency of $u(t)$ on $y(t)$ and of $y(t)$ on $u(t-h)$ is shown using red arrows, and the values for u in the interval $(t_1, t_c) = (1, 2)$ and y in $(t_c, t_c + h) = (2, 3)$ are emphasized using thickened lines.

$$\dot{x}_p(t_c, 1) = -ax_p(t_c, 1) + b\frac{k_P}{T_I}(1 - p_r)x_I(t_1), \tag{4.35}$$

recalling that the proportional part is crucially also zeroed out after a jump under the reset-and-hold strategy. Setting (4.35) equal to 0 leads to the following final design choice for the reset ratio:

$$p_r = 1 - \frac{aT_I w_{10}}{bk_P x_I(t_1)}. \tag{4.36}$$

With this set of parameters, the system will effectively reach a steady state, as all the time derivatives $\dot{x}_I(t, 1) = \dot{x}_{CI}(t, 1) = e(t, 1) = 0$ will remain zero for all $t > t_c$).

Note that the tuning rule (4.36) for the reset ratio is formally identical to the corresponding rule for first order systems *without* delay, despite the difference in approach between both strategies.

In summary, the resulting tuning rules for the reference tracking case are

$$(p_r, \theta, \tau_H) = (1 - \frac{aT_I w_{10}}{bk_P x_I(t_1)}, h, h). \tag{4.37}$$

4.3.2 Disturbance rejection

An analogous set of tuning rules can be found by starting with a step disturbance d of amplitude w_{20}. The reasoning is very similar to the reference tracking case, and will be skipped here for brevity. The obtained tuning rules for the disturbance rejection case are

$$(p_r, \theta, \tau_H) = (1 + \frac{T_I w_{20}}{k_P x_I(t_1)}, h, h). \tag{4.38}$$

4.3.3 Comments and guidelines

Note that although in (4.7) and (4.12) the amplitudes w_{10} and w_{20} appear explicitly, the reset ratios will not depend on these amplitudes, since $x_I(t_1)$ will be proportionally scaled due to the linearity of the base system. As a result, just like in the nondelayed setting, the tuned values for p_r are constant and intrinsic to the hybrid control system, i.e. they depend only on the plant and the base PI controller. Again, since an analytic computation is $x_I(t_1)$ is hard to obtain, in practice the value of p_r may be simply

calculated by using the value of the integrator state at the first reset instant, and stored for its later use.

Note also that the only source of error in this approach comes from the determination of the future time t_c such that $e(t_c, 1) = 0$ using the variable band resetting law; as the previous derivation implies, if t_c could be known in advance, a perfect flat response could in principle be attained by triggering the reset action at exactly $t = t_c - h$. More accurate higher order approximations of t_c could in principle be computed by generalizing the variable band rule to higher-order rules involving further derivatives of the error signal $\ddot{e}$, $\dddot{e}$, etc. Of course, usually this will not reliably work in practice, as these derivatives will be increasingly affected by measurement noise, preventing their accurate determination.

The reset-and-hold strategy is also applicable in cases where the delay h is not precisely known, but has a moderate degree of uncertainty. If it is known that $h \in [h_{\min}, h_{\max}]$, then the previous rules can be used assuming $h = (h_{\min} + h_{\max})/2$ (or using its nominal value if available). Another, more conservative approach is to take $\tau_H = \theta = h_{\min}$ and the same reset ratios than in (4.7) or (4.12); this choice will maximize the time the controller spends in flowing mode, producing a flat response only in the best case, but still improving the performance in nearly all cases with respect to more standard reset approaches. In addition, observe that the formulas for the reset ratios depend exclusively on the plant gain b/a, thus the design is in principle quite robust against uncertainty in the plant's time constant.

On that line, note that the unmodified reset-and-hold strategy may not be suitable in those cases in which the appearance of several disturbances or reference changes in a short time span, lower than the delay h, is expected. This is because the controller output is held constant during a fixed time interval, so it will not be able to react to any incoming disturbances until after this interval has passed. In such cases, an additional supervisory mechanism is needed so that holding can be disabled whenever a new disturbance or reference change is detected. A possible such mechanism is as follows: after each reset instant t_k, monitor the difference $|e(t) - e_E(t)|$ between the error signal $e(t)$ and its expected value, the linear approximation $e_E(t) = e(t_k)\left(1 - \frac{\tau(t)}{\theta}\right)$, and disable holding early as soon as this difference exceeds a certain percentage of $|e(t_k)|$ (which indicates that a significant disturbance is acting on the system). In the Hybrid Inclusions formalism, this amounts to redefining the sets (3.15) and (3.16) as

$$\begin{aligned}\mathcal{C}_0 = \; & \left\{(\mathbf{z}_0, \mathbf{z}_1) \in \mathcal{O}^2 : m_0 = 0, \tau_0 \leq \tau_H \vee \left|\tfrac{e}{e_r} - \left(1 - \tfrac{\tau}{\theta}\right)\right| \leq \beta\right\} \; \cup \\ & \{(\mathbf{z}_0, \mathbf{z}_1) \in \mathcal{O}^2 : m_0 = 1, \\ & \; qC((I + \theta A_0)\mathbf{x}_0 + \theta A_h \mathbf{x}_1)) \geq 0\}\end{aligned} \tag{4.39}$$

and

$$\begin{aligned}\mathcal{D}_0 = \; & \left\{(\mathbf{z}_0, \mathbf{z}_1) \in \mathcal{O}^2 : m_0 = 0, \tau_0 \geq \tau_H \wedge \left|\tfrac{e}{e_r} - \left(1 - \tfrac{\tau}{\theta}\right)\right| \geq \beta\right\} \; \cup \\ & \{(\mathbf{z}_0, \mathbf{z}_1) \in \mathcal{O}^2 : m_0 = 1, \\ & \; qC((I + \theta A_0)\mathbf{x}_0 + \theta A_h \mathbf{x}_1)) \leq 0\},\end{aligned} \tag{4.40}$$

where e_r is a new auxiliary state variable, updated as $\dot{e}_r = 0$ and $e_r^+ = e$, and $\beta > 0$ is a new design parameter representing the threshold after which holding is disabled (a choice that has been observed to give good results in simulation is $\beta = 0.2$). Note that this modification is also suited for situations where the shape of a disturbance signal is very different from that of a step function: resetting is still beneficial in many of these situations (intuitively, resetting removes "energy" from the system), but holding for too long is often inconvenient, especially in delay-dominant processes where $h \gg 1/a$.

4.3.4 Examples

To demonstrate the performance of the PI+CI reset-and-hold strategy, a simulation example is considered.

Example 4.4 (Reset-and-hold control of a SISO system)**.** Consider the first order delayed plant given by the transfer function

$$P(s) = \frac{e^{-0.3s}}{1 + s}. \tag{4.41}$$

The base PI controller's parameters have been chosen so as to produce an oscillating base linear closed-loop response in reference tracking mode. The chosen parameters are

$$k_P = 1, \qquad T_I = 1/3. \tag{4.42}$$

The tuning rules (4.37) have been used to determine the reset-and-hold parameters. The time $t_1 = 0.902$ at which the variable band law is triggered, and the corresponding averaged controller state $x_I(t_1)$, have been manually measured by simulating the unit step response of the system with the base PI controller. The resulting parameters are

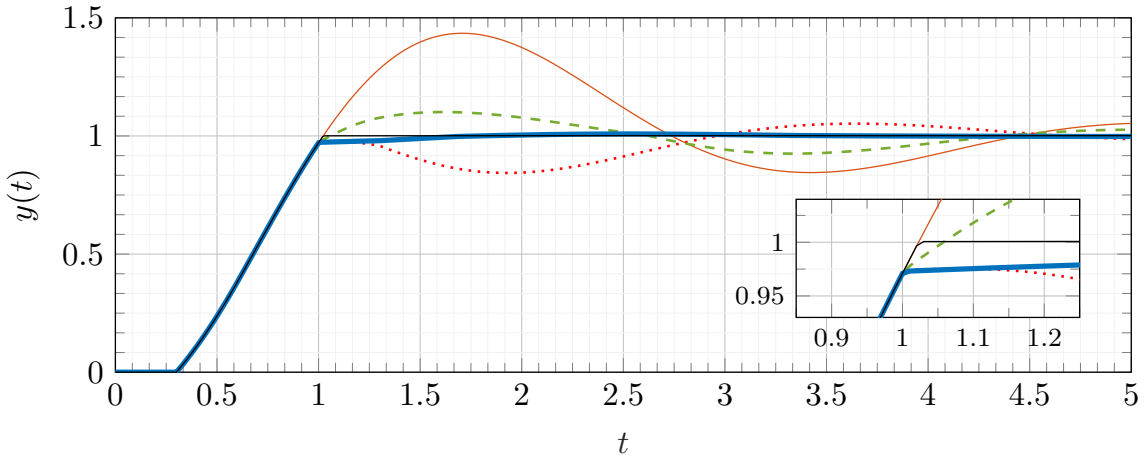

Figure 4.11: Closed-loop plant output $y(t)$ under a reference change in Example 4.4: (orange) base PI controllers; (green, dashed) ordinary reset PI+CI controllers with $p_r = 0.446$; (red, dotted) ordinary reset PI+CI controllers with $p_r = 0.702$; (blue, thick) reset-and-hold PI+CI controllers; (black) perfect tracking.

$$p_r = 0.446, \quad \theta = H = 0.3. \tag{4.43}$$

Figure 4.11 shows the unit step response of the closed-loop reset-and-hold system, together with the response of the base linear system. The output of the controller is shown in Fig. 4.12.

For the purposes of comparison, the response of the system with a single ordinary reset action (with the same variable band θ) is also shown, in two cases: 1) with the same value of p_r, and 2) with the tuning rule (4.34) that momentarily makes $\dot{x}_p(t_1 + \theta, 1) = 0$, namely

$$p_{r,\text{incorrect}} = 1 - \frac{aT_I w_{10} - k_P e(t_1, 1)}{b k_P x_I(t_1)} = 0.702. \tag{4.44}$$

As can be observed, the reset action in the first case is not sufficiently strong to flatten the error signal, as the proportional part has not been zeroed out, and so from (4.2) it follows that $\dot{x}_p(t_1 + \theta, 1) = -k_P e(t_1, 1) \neq 0$. In the second case, the reset action alone is indeed able to momentarily flatten the error signal, completely eliminating the initial overshoot; however, some undesired undershoot is produced, due to the delayed feedback loop preventing plant and controller achieving their stationary states at the same time. Finally, the reset-and-hold strategy prevents the former issues by both zeroing out the proportional part and forcing the controller to hold its output

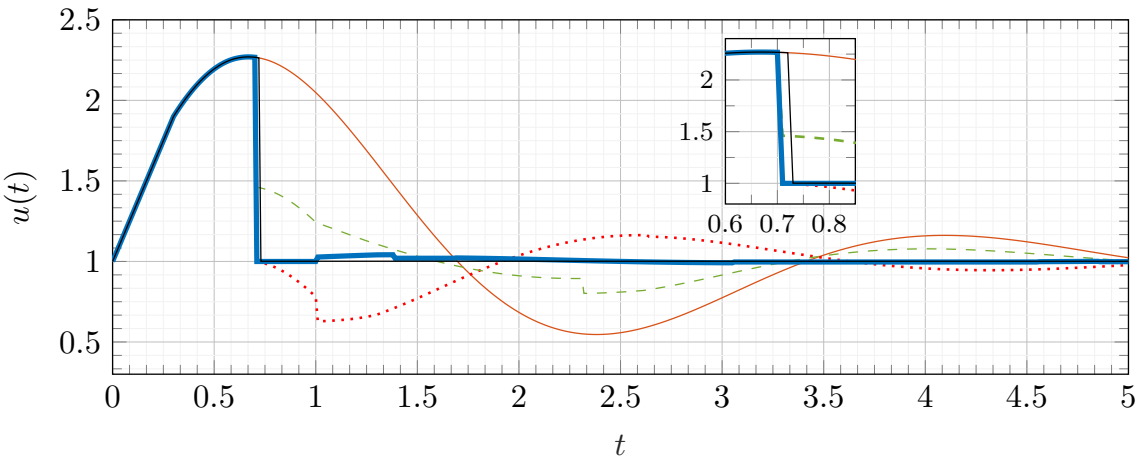

Figure 4.12: Controller output $u(t)$ for a reference change in Example 4.4: (orange) base PI controllers; (green, dashed) ordinary reset PI+CI controllers with $p_r = 0.446$; (red, dotted) ordinary reset PI+CI controllers with $p_r = 0.702$; (blue, thick) reset-and-hold PI+CI controllers; (black) perfect tracking.

constant until the effect of the resetting reaches the plant: as a consequence, a good approximation of a flat response is attained.

In addition, to demonstrate the assertion from the second paragraph of the Comments and Guidelines section, a variation of the strategy has been performed in which, instead of relying on a variable band to determine the time in which to perform the resetting, the reset action has been manually forced to occur at the optimal time instant $t_1' = t_c - 0.3 = 0.723$ (where t_c is again found by manual inspection of the base linear response), so that the resetting effect arrives to the plant exactly at the moment where the error crosses zero. The tuning rule (4.7) now gives the slightly different reset ratio $p_{r,\text{optimal}} = 0.4542$. In agreement with the aforementioned discussion, a perfect flat response is now observed after resetting (shown in black in the figures).

A further example featuring a combination of reference tracking and disturbance rejection is considered in order to demonstrate the robustness to noise and parameter variations.

Example 4.5 (Robustness to noise and variations in the delay)**.** Consider the control system (4.41)–(4.43) from the previous example. Two simulations are performed, considering respectively:

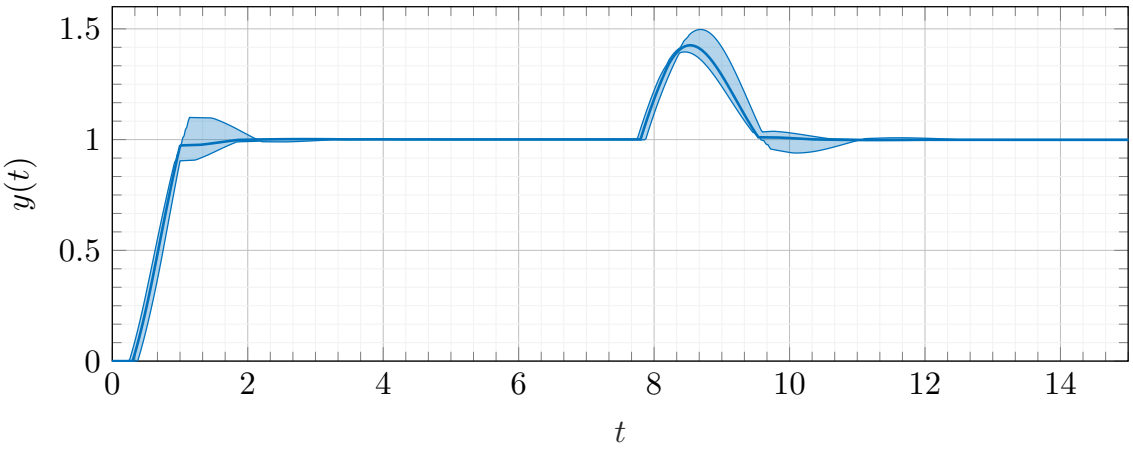

(a) Plant output y.

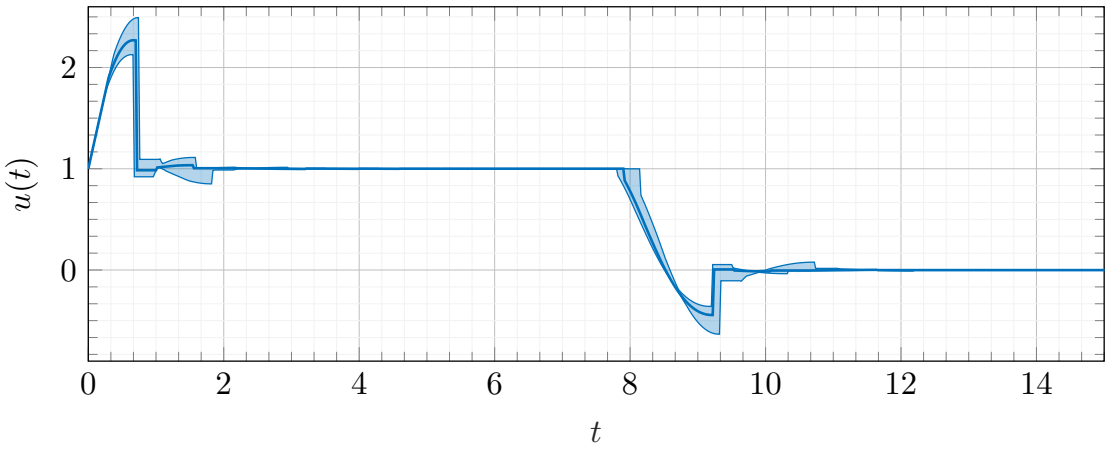

(b) Controller output u.

Figure 4.13: Closed-loop plant output $y(t)$ and controller output $u(t)$ under a combined reference change and disturbance in Example 4.5, with an uncertain delay $h \in [0.25, 0.375]$: nominal case (blue), envelope of six sampled cases (light blue).

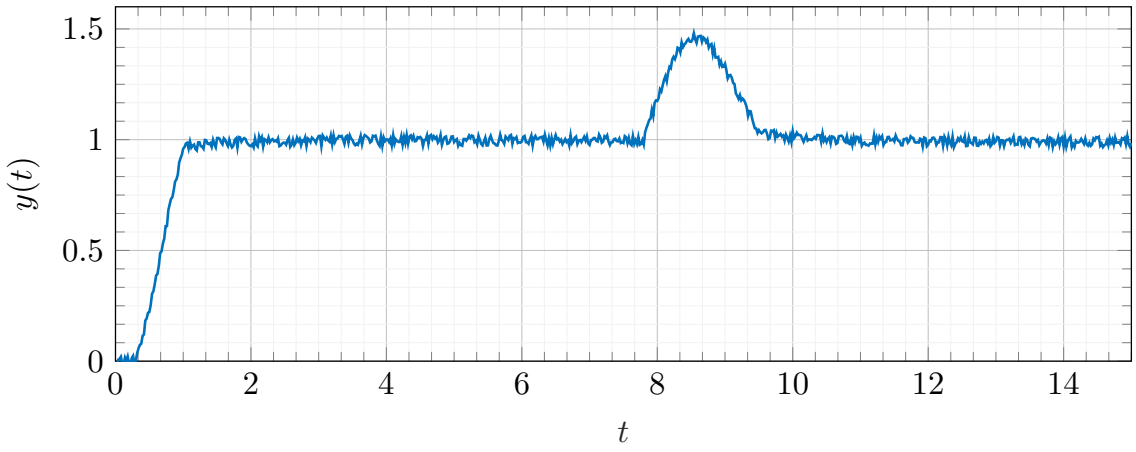

(a) Plant output y.

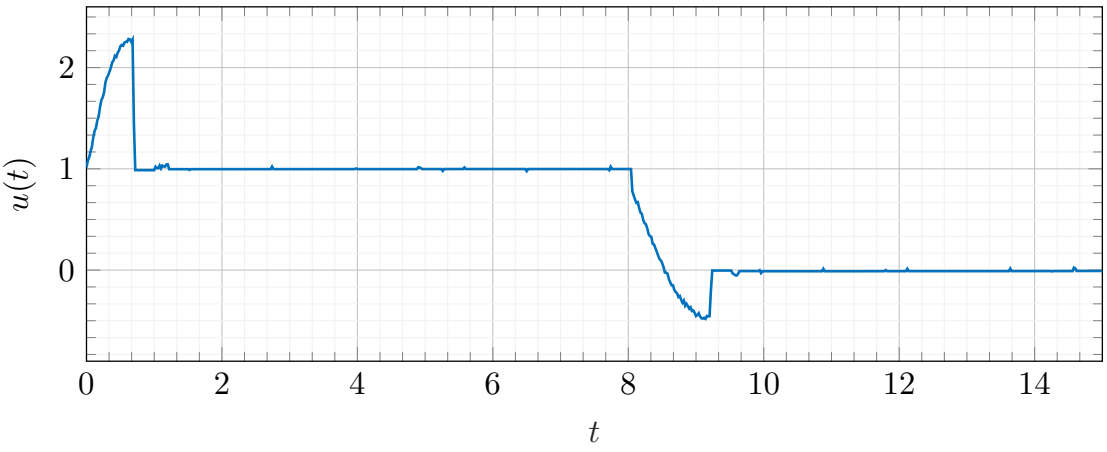

(b) Controller output u.

Figure 4.14: Closed-loop plant output $y(t)$ and controller output $u(t)$ under a combined reference change and disturbance in Example 4.5, in the presence of noise of amplitude 0.025.

- An uncertainty in the delay parameter h in the interval $h \in [0.25, 0.375]$. In each case, five simulations are performed with the six equally spaced values $h = 0.25, 0.275, 0.3, 0.325, 0.35, 0.375$, and the envelope of the resulting y, u signals is plotted together with the nominal signals for $h = 0.3$ (Figure 4.13(a)–4.13(b)).
- A pseudo-random sensor noise signal η of amplitude 0.025, with the nominal value $h_0 = 0.3$ (Figure 4.14(a)–4.14(b)). Note that this noise can be included in the system's model as an exosystem outputting a sinusoidal signal of sufficiently high frequency components.

The tuning rules for the nominal plant are used in both cases, with the step reference change starting at $t = 0$ and the step disturbance at $t = 7.5$. The controller parameters are the same as in the nominal case, except that the reset ratio p_r switches from its tracking value (4.43) to its disturbance rejection value $p_r = 0.223$ at $t = 7.49$.

Figures 4.13(a) and 4.14(a) clearly show that the performance of the response is not degraded too much in any case, revealing that the designed hybrid control strategy is robust to both small variations in the delay and sensor noise. An interesting observation is that in the example with delay variation, a nearly flat response seems to be obtained at the second reset instant in all tested cases.

A final example analyzes the situation where two step disturbances are acting almost simultaneously on the system, showing how the supervisory hold-disabling mechanism is to some extend able to avoid the degraded performance caused by the unmodified reset-and-hold strategy.

Example 4.6 (A hold-disabling mechanism)**.** For the plant

$$P(s) = \frac{e^{-s}}{1+s} \tag{4.45}$$

controlled by a reset-and-hold PI+CI controller with

$$k_P = 1, \qquad T_I = 1, \qquad \theta = \tau_H = 1, \tag{4.46}$$

a purposefully disfavourable situation is considered where a disturbance consisting of the sum of two unit step functions at $t = 0$ and $t = 2.5$ enters the system. As before, the base linear response is first simulated in order to obtain x_p, x_I at the first reset instant. The tuning rules for disturbance rejection then give

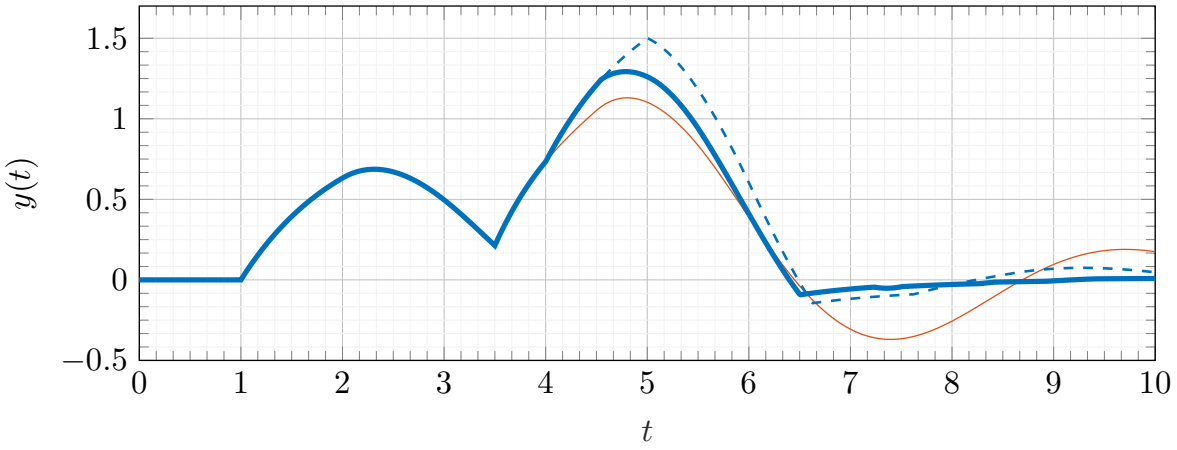

Figure 4.15: Closed-loop plant output $y(t)$ under two combined disturbances in Example 4.6: (orange) base PI controllers; (blue, dashed) reset-and-hold PI+CI controllers; (blue, thick) reset-and-hold PI+CI controllers with a supervisory hold-disabling mechanism ($\beta = 0.2$).

$$p_r = -0.049, \quad \theta = H = 1. \tag{4.47}$$

Figures 4.15 and 4.16 show the response to the disturbance, with and without the hold-disabling mechanism ($\beta = 0.2$), as well as the linear response for comparison purposes. Note how resetting and holding has a negative effect, obtaining an increased overshooting of the error signal in the interval $t \in [4, 6]$ compared to the linear response. The early deactivation of holding partially avoids this effect, letting the controller react as soon as the error signal deviates sufficiently from its expected behavior. Some of the increased error still remains, due mainly to the initial reset action; however, up to a certain point this increase cannot be prevented by further lowering β, as the controller has already reset its state by the time the second disturbance starts acting and this cannot be easily undone. In contrast, note that the overshooting generated by the linear response in the interval $t \in [6.5, 10]$ is greatly ameliorated by the reset-and-hold strategy, even when the disabling mechanism is in effect.

4.4 Parallel control of first order MISO plants with delay

4.4.1 Reference tracking and disturbance rejection

Finally, consider the control of a delayed MISO plant, with associated time delays $h_1, h_2, \ldots, h_n$, under the parallel PI+CI based strategy of previous sections. It is

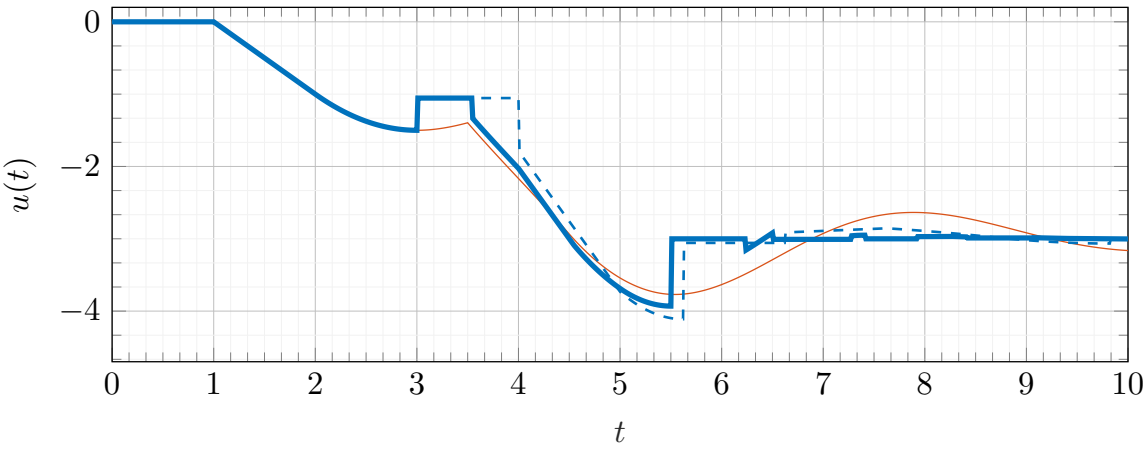

Figure 4.16: Controller output $u(t)$ for two combined disturbances in Example 4.6: (orange) base PI controllers; (blue, dashed) reset-and-hold PI+CI controllers; (blue, thick) reset-and-hold PI+CI controllers with a supervisory hold-disabling mechanism ($\beta = 0.2$).

supposed that the first order approximation $x_{pi}(t+\delta, j) \approx x_{pi}(t, j) + \delta \dot{x}_{pi}(t, j)$ holds to good accuracy for all $t \in [\min_i(t_{1i}), t_c]$, where $t_{1i} \simeq t_c - h_i$ is the time at which the ith Clegg integrator state performs a jump. A variable band resetting law is assumed in which each controller has an independent variable band θ_i; in addition, each controller is assumed to implement the reset-and-hold mechanism with time parameter τ_{Hi}. The derivation goes through analogously to the former ones, and is again omitted for brevity. The only important point to be kept in mind is that the expression for p_{ri} obtained by setting $\dot{x}_{pi} = 0$ at $t = t_c$ will come expressed in terms of $x_{pi}(t_c, 0)$, which is evaluated at a future time from the perspective of the controller performing the reset action, so in order to re-express it in terms of quantities evaluated at t_{1i}, the first order approximation $x_{pi}(t_c, 0) \simeq x_{pi}(t_{1i}, 0) + h_i \dot{x}_{pi}(t_{1i}, 0))$ is taken. The final results are the tuning rules $\theta_i = \tau_{Hi} = h_i$, and either

$$p_{ri} = 1 - \frac{a_i T_{Ii}(x_{pi}(t_{1i}, 0) + h_i \dot{x}_{pi}(t_{1i}, 0))}{b_i k_{Pi} x_I(t_{1i})}. \tag{4.48}$$

for the case of reference tracking, or

$$p_{ri} = 1 - \frac{a_i T_{Ii}(x_{pi}(t_{1i}, 0) + h_i \dot{x}_{pi}(t_{1i}, 0))}{b_i k_{Pi} x_I(t_{1i})} + \frac{w_{20i} T_{Ii}}{k_{Pi} x_I(t_{1i})}, \tag{4.49}$$

for the case of disturbance rejection. Note that specializing to $n = 1$ recovers the tuning rules for delayed SISO first order systems, and setting $h_i = 0$ for all i recovers the tuning rules for non-delayed MISO first order systems.

4.4.2 Comments and guidelines

Since the developed tuning rules for delayed first order MISO plants simply consist of a combination of the strategies for nondelayed first order MISO and delayed first order SISO plants, all previously discussed considerations and guidelines for these two cases (uniqueness of the reset ratios, necessity of estimating the plant states if they are inaccessible, early deactivation of holding, etc.) should also be taken into account here. The same considerations regarding stability also apply here, with the caveat that the FORE-like damping parameters in (4.17) must also be active in holding mode (i.e., $A_r' = A_r$ in the notation of (3.3)).

Note that achieving a good first order approximation of the error is a more delicate task when there are different delays in play, i.e. in an asynchronous reset configuration, since the effect of each controller will start reaching the total plant output y at a different times in a staggered way, causing abrupt changes in the slope of the error. Specifically, in order for the first order approximation to work properly, the resetting condition ought to be triggered when the plant has started receiving the input of all controllers. This is a limitation inherent to the variable band resetting law that is also present to some extent in the SISO case, which in practice translates into an effective limitation on the minimum achievable rise time for which a flat response can be properly obtained. In situations where a design specification includes a rise time much lower than the greatest of the delays, more sophisticated predictive control methods that abandon the basic PI+CI structure can be considered, such as a Smith predictor-based reset structure (some cases are studied in [275] for SISO systems and [333] for $n \times n$ MIMO systems).

4.4.3 Examples

Example 4.7 (Reference tracking in a 2×1 reset-and-hold system)**.** Consider the parallel TISO control system with plants

$$P_1(s) = \frac{e^{-0.5s}}{s+1}, \quad P_2(s) = \frac{3e^{-0.3s}}{s+1/3}. \tag{4.50}$$

As usual, the values of k_{Pi} and T_{Ii} are chosen to produce an oscillatory closed-loop response so that reset actions can be triggered. The corresponding parameters are

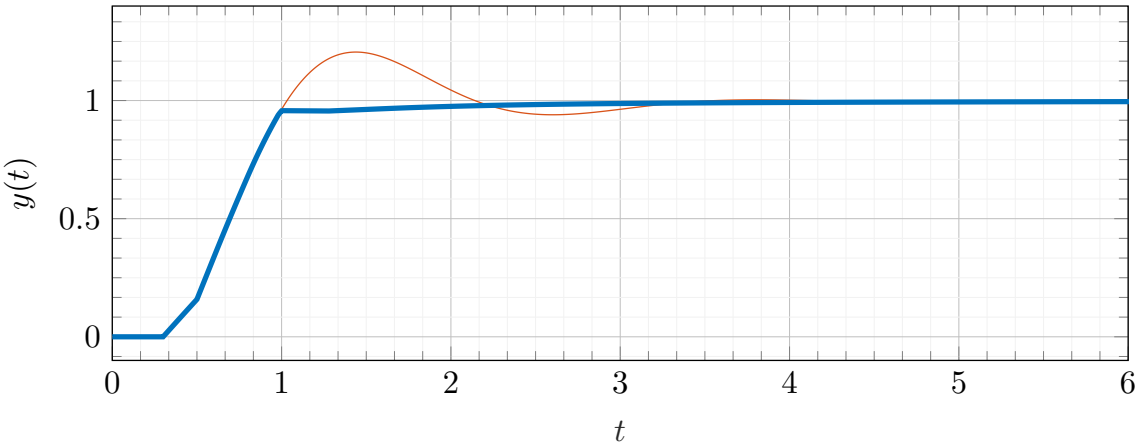

Figure 4.17: Closed-loop step response y under a reference change in Example 4.7: (orange) base PI controllers; (blue) PI+CI controllers.

$$\begin{aligned} k_{P1} &= 1, & T_{I1} &= 1, \\ k_{P2} &= 4/15, & T_{I2} &= 4. \end{aligned} \tag{4.51}$$

The values of x_{pi} and x_I at $t = t_{1i}$ have been again obtained by simulating the base linear system. Using (4.48) gives

$$p_{r1} = 0.0, \qquad p_{r2} = -0.25 \tag{4.52}$$

(remarkably, this means that a flat response for the first subplant can be obtained simply by holding without resetting; though note that the holding mechanism as defined in this work includes disabling the proportional part).

Figures 4.17 and 4.18 show the result of the simulation, where the expected almost-flat response appears. Note the staggered piecewise-like behavior in the interval $t \in [0, 0.5]$ due to the controller outputs reaching the plant at different times.

4.5 Other control strategies

4.5.1 Serial control structure

The serial control MISO structure, described in Section 2.3, constitutes one of the two types of collaborative MISO control structures. This control structure is predominantly

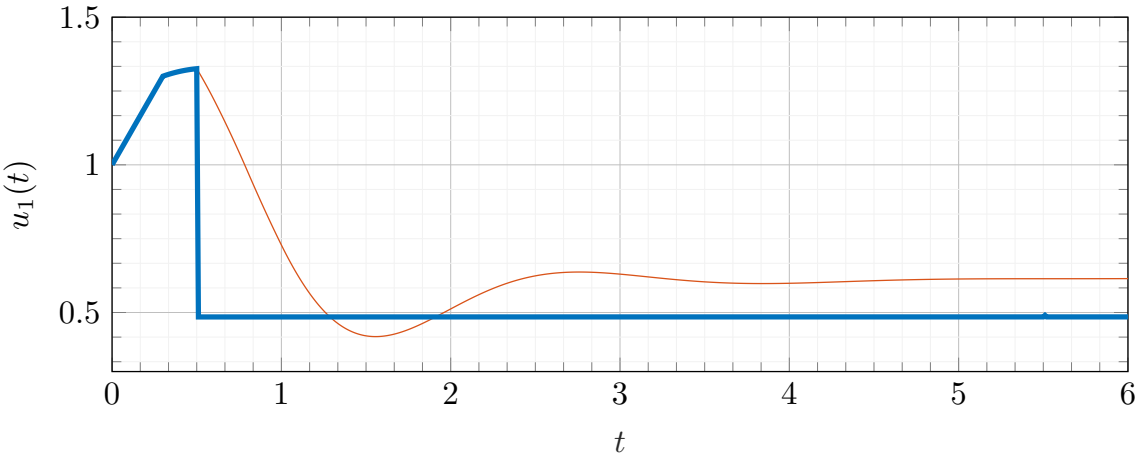

(a) Control output u_1.

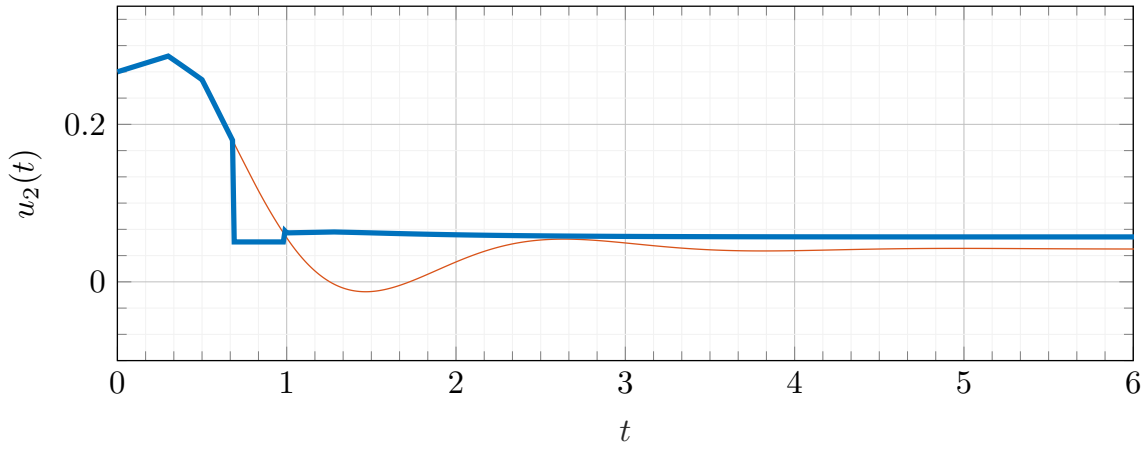

(b) Control output u_2.

Figure 4.18: Controller outputs for the reference tracking example in Example 4.7: (orange) base PI controllers; (blue) PI+CI controllers.

used in the case of TISO (2×1) systems, so only this case will be dealt with for simplicity.

Note that in this structure, it becomes manifest that there are actually two variables one wishes to control, namely the plant output y and the fast controller's output u_1. In this way, properly handling the design of tuning rules for this case would lead into the theory of multiple-input and *multiple-output* (MIMO) systems, which falls out of the scope of the current thesis. However, since the serial structure is more widely known and used compared to the parallel structure, it is convenient to understand whether the previous design methodologies can, under some simplifying assumptions, be extended to encompass serial MISO control.

One such assumption will be the use of the so-called *modified valve positioning control* (MVPC) strategy [13, 312] as the base linear control structure. Hence, the base linear controllers of R_1 and R_2 may both be taken as proportional-integral controllers.

In this case, two clear objectives can be distinguished: the first one is to keep a good performance (either in tracking or regulatory mode), and the second objective is to minimize the use of the fast controller R_1 by ensuring that it returns to its prescribed operating point in a specified time frame. The dynamic of the slow loop is usually such that it does not feature any oscillations. For that reason, as a simplifying assumption, in the following reset will only be considered to apply on the fast controller R_1.

With this in mind, two different approaches will be studied: the first one consists of minimizing a given objective function built out of the error signals e and e_{u_1}, and the second one is an adaptation of the tuning rules for the SISO case.

Weighted ISE + ISEU optimization

This method consists of using a variable reset ratio and computing its optimal value at each reset instant. The objective function to be minimized is a weighted combination of the integrated squared errors associated to the plant output and the first controller output (e and e_{u_1} respectively). Proceeding analogously to Section 4.2, the objective is to minimize the quantity $\text{ISE}\gamma = \gamma\,\text{ISE} + (1-\gamma)\,\text{ISEU}$ associated to the fictitious signals e_k and $e_{u_1,k}$ in the interval $[t_k, \infty)$, that is, to minimize

$$\int_{t_k}^{\infty} (\gamma e_k(t)^2 + (1-\gamma) e_{u_1,k}(t)^2) dt \;=\; \mathbf{x}(t_k, k-1)^\top L \mathbf{x}(t_k, k-1) \tag{4.53}$$

for each t_k, where the positive definite matrix L is now a solution to the Lyapunov equation $A^\top L + LA + \gamma C^\top C + (1-\gamma) C_{u_1}^\top C_{u_1} = 0$. Here A is again the evolution matrix of a minimal realization of the full system, including an exosystem for either the reference r_y or a disturbance signal d_i, and C_{u_1} is the covector such that $u_1(t,j) = C_{u_1}\mathbf{x}(t,j)$. The solution is formally the same as (4.26), though now it also depends on the optimization parameter γ.

Note that though it won't be considered here, this algorithm can be generalized in the obvious way to more than two plants, taking the objective function $\mathrm{ISE}_{\gamma_1\gamma_2\cdots}$ as a convex linear combination of the error signals attached to the total plant and to each controller, with design parameters γ_1, γ_2, etc. that determine the relative importance of each controller's output with respect to the plant output in the minimization.

SISO-like tuning rule

This approach consists of simply using the tuning rules (4.7) or (4.12) under a zero crossing law, the same as the ones for SISO first order plants. The effect is to produce an instantaneous flat response, where $\dot{e}(t_1 + \varepsilon, 1) \to 0$ as $\varepsilon \to 0^+$.

Even though this strategy is not optimal with respect to a given criterion, the tuning rule will still generally produce a good response with respect to the linear case, and it has the advantage of not needing any estimation of the plant states at the moment of reset. Moreover, unlike the previous approach, it does not produce any undershoot. The use of this method is justified if the dynamics of the second loop is slow enough to be approximated as constant relative to the first loop.

Example 4.8 (Reference tracking in a 2×1 first order serial system)**.** This example consists of the serial control of a 2×1 system given by the plants

$$P_1(s) = \frac{1}{1+s}, \qquad P_2(s) = \frac{1}{1+10s}. \tag{4.54}$$

The parameters for the controllers are

$$\begin{aligned} k_{P1} &= 0.5, \qquad T_{I1} = 0.5, \\ k_{P2} &= -1, \qquad T_{I2} = 10. \end{aligned} \tag{4.55}$$

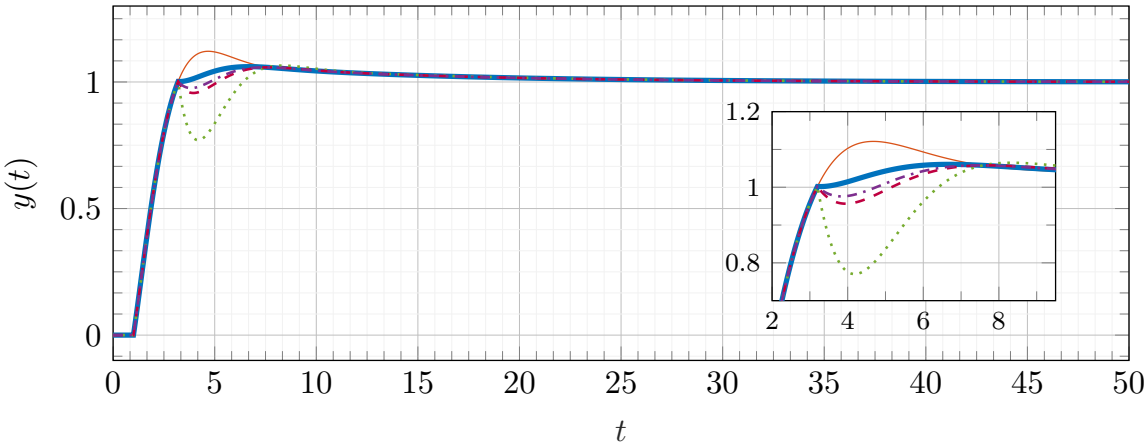

Figure 4.19: Total plant output $y(t)$ under a reference change for the base PI (orange) and PI+CI controllers under the SISO-like (blue, thick) and optimization ($\gamma = 0$: green, dotted; $\gamma = 0.5$: red, dashed; $\gamma = 1$: purple, dash-dotted) strategies in Example 4.8.

With these parameters for the base system, the error signal has an oscillating response. In reference tracking mode, a step reference change is applied of height $w_{10} = 1$. The optimization parameter γ is given the three values $\gamma = 0, 0.5, 1$ for the minimization approach, under a zero crossing law.

	Linear	**Reset (ISEγ opt., $\gamma = 0.5$)**	**Reset (SISO-like)**
ISE	0.639	0.642	0.612
ISEU	5.063	4.719	4.909
ISEγ	2.851	2.691	2.760
IAE	1.840	1.842	1.651
IAEU	9.924	9.919	9.922

Table 4.2: Integrated squared errors (ISE, ISEU, weighted mean) and integrated absolute errors (IAE, IAEU) for the reset vs. base linear controllers in Example 4.8.

The results are shown in Table 4.2 and Figures 4.19, 4.20(a) and 4.20(b). In the algorithmic case, reset has been inhibited after a single reset action for simplicity, as the obtained results are similar. It is observed that the algorithmic approach achieves the lowest ISEγ in every case as expected; however, it gives very poor results when γ is low, causing a considerable undershoot in the plant output without really achieving a faster return of u_1 to its operating point. It can be concluded that using a value of γ close to 1 will give the best results. In contrast, the SISO-like tuning rule produces only slightly worse performance indices than the $\gamma = 1$ approach, still improving the performance in every metric compared to the linear case without producing any

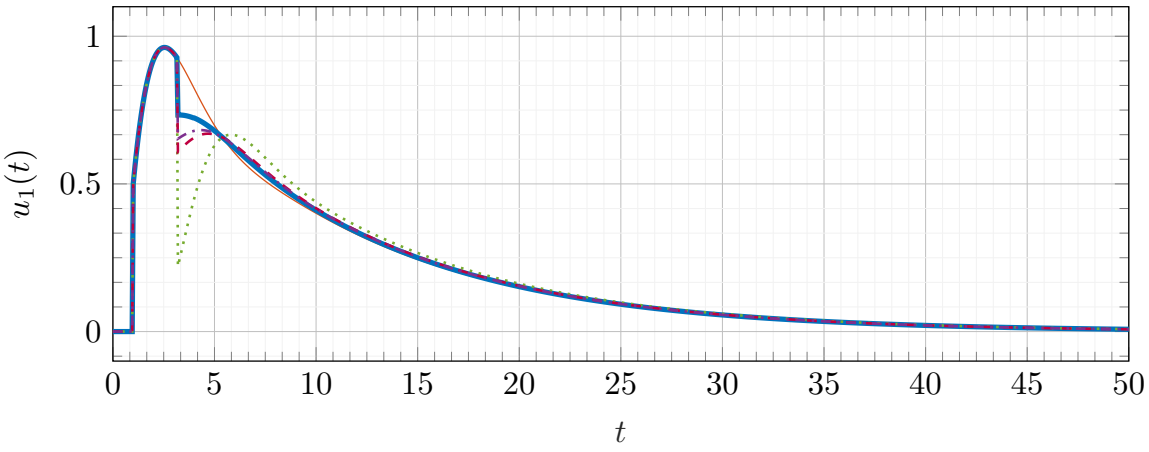

(a) First controller's output $u_1(t)$.

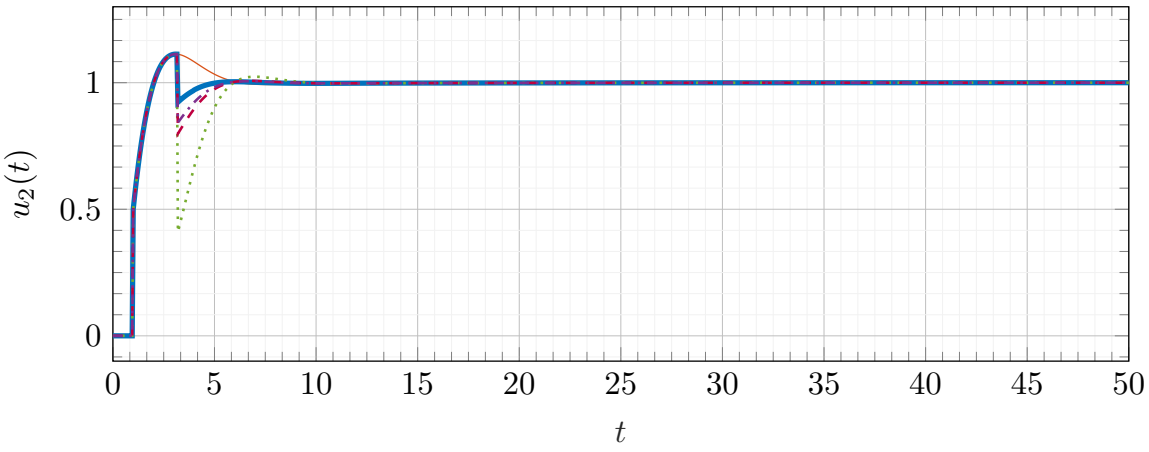

(b) Second controller's output $u_2(t)$.

Figure 4.20: Controllers' output under a reference change for the base PI (orange) and PI+CI controllers under the SISO-like (blue, thick) and optimization ($\gamma = 0$: green, dotted; $\gamma = 0.5$: red, dashed; $\gamma = 1$: purple, dash-dotted) strategies in Example 4.8.

undershoot. Interestingly, even when the second controller R_2 does not directly reset, the effect of the jump in the controller R_1 is nevertheless propagated to R_2 through e_{u_1}.

Note that in [241], a similar quadratic optimization method was successfully applied to the reset control of hard disk drives under a modified serial MISO structure. However, this method relies on a different resetting law based on a fixed periodic sequence of reset instants, for which only the period and first reset instant are design parameters. This law allows for an easy direct computation of $\mathrm{ISEU}_{[t_k,t_{k+1})}$ between two reset instants, instead of relying on an estimation like $\mathrm{ISEU}_{[t_k,\infty),\alpha}$; however, some flexibility is necessarily lost by imposing this rigid structure on the reset instants.

4.5.2 Extension to nonlinear plants

A possible advantage of the time-based approach to derive tuning rules for first order systems presented here, in comparison with former frequency-based approaches, is that it also applies with few modifications to certain *nonlinear* first order systems. Comparatively little work has been done that specifically deals with the reset control of nonlinear systems, with most studies mainly focusing on stability [85, 148, 334], so it is an interesting problem to explore from a design perspective.

Specifically, working in the $n = 1$ nondelayed setting for simplicity, let the nonlinear first order plant P be described by

$$P : \begin{cases} \dot{x}_p(t) = & f(x_p(t), v(t), t), \\ y(t) = & x_p(t), \end{cases} \tag{4.56}$$

and suppose it is connected to a PI+CI feedback controller with a zero crossing law. Assume the error signal crosses zero at some $t = t_1$, and let $F_{\mathrm{ref}}(u) = f(w_{10}, u, t_1)$ and $F_{\mathrm{dist}}(u) = f(0, u + w_{20}, t_1)$ for some constants w_{10}, w_{20}. If the nonlinear plant has the property that these functions are invertible in a neighborhood of zero, with respective inverses F_{ref}^{-1} and F_{dist}^{-1}, then

$$p_r = 1 - \frac{T_I F_{\mathrm{ref}}^{-1}(0)}{k_P x_I(t_1)} \tag{4.57}$$

and

$$p_r = 1 - \frac{T_I F_{\text{dist}}^{-1}(0)}{k_P x_I(t_1)} \tag{4.58}$$

can be easily shown to produce a flat response against step reference changes of height w_{10} and step disturbances of height w_{20} respectively. Note that here, due to the nonlinearity of the base system, the numerical value reset ratio is *not* an intrinsic value of the closed loop system anymore, since a single value of p_r will not in general produce flat responses for step inputs of different heights; instead, its value must be updated on-line for each new step reference or disturbance entering the system, using a variable reset ratio approach. This presents no particular problem in the SISO reference tracking case as long as $F_{\text{ref}}^{-1}(0)$ is computable, since the value $x_I(t_1)$ is directly accessible by the controller; in the disturbance rejection case, if the disturbance signal is not directly measurable, a disturbance observer, such as an unknown input observer [208], will be needed in order to obtain an estimation of w_{20}.

Analogous rules can be found for MISO first order systems with nonlinear flow equations of the form $\dot{x}_{pi}(t) = f_i(x_{pi}(t), v(t), t)$ under a parallel control structure:

$$p_{ri} = 1 - \frac{T_I F_{i,\text{ref}}^{-1}(0)}{k_P x_I(t_1)} \tag{4.59}$$

for reference tracking and

$$p_{ri} = 1 - \frac{T_I F_{i,\text{dist}}^{-1}(0)}{k_P x_I(t_1)} \tag{4.60}$$

for disturbance rejection, where $F_{i,\text{ref}}(u) = f_i(x_{pi}(t_1, 0), u_i, t_1)$ and $F_{i,\text{dist}}(u) = f_i(x_{pi}(t_1, 0), u_i + w_{20i}, t_1)$. Note that in the multivariable case the values $x_{pi}(t_1, 0)$ of the plant states will be required; since the on-line calculation of the reset ratios is necessary in the nonlinear setting, if these plant states aren't directly measurable, a state observer will be needed for their estimation (cf. the Comments and Guidelines from Section 4.1).

Example 4.9 (Application of tuning rules to a nonlinear first order SISO plant)**.** Consider the plant given by

$$P : \begin{cases} \dot{x}_p(t) = -x_p(t) + \frac{x_p(t)^3}{3} + v(t)\left(1 + \frac{x_p(t)}{10}\right), \\ y(t) \;=\; x_p(t), \end{cases} \tag{4.61}$$

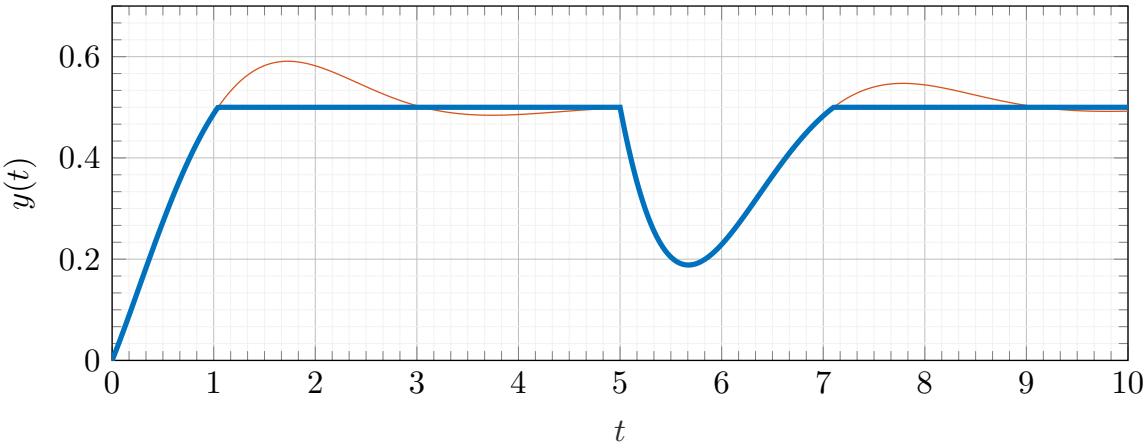

Figure 4.21: Closed loop step response output y in Example 4.9: (orange, thin) base PI controller; (blue, thick) PI+CI controller.

and a PI+CI controller with proportional gain $k_P = 1$ and integral time $T_I = 1/3$.

The rules (4.57)–(4.58) give respectively

$$p_r = 1 - \frac{w_{10} - w_{10}^3/3}{3(1 + w_{10}/10)\, x_I(t_1)} \tag{4.62}$$

for reference tracking and

$$p_r = 1 + \frac{w_{20}}{3x_I(t_1)} \tag{4.63}$$

for disturbance rejection, as a function of the heights w_{10} and w_{20}. Consider the response of the control system to a combination of a step reference change with $w_{10} = 0.5$ at $t = 0$ and a step disturbance with $w_{20} = -1$ at $t = 5$. The results are shown in Figures 4.21 and 4.22: as expected, a flat response appears in the output.

4.5.3 Split-range control

Split-range control is an example of a non-collaborative control strategy in which a single controller is tasked with coordinating two or more different control actions, corresponding to different ranges of the control signal. One of the most common examples in practice is in temperature control, where heating and cooling correspond to different actuators with possibly different dynamics. Another situation where split-range control is useful is when the controller in charge of the main dynamics has a limited actuation range; in such a case, an auxiliary plant can be activated whenever

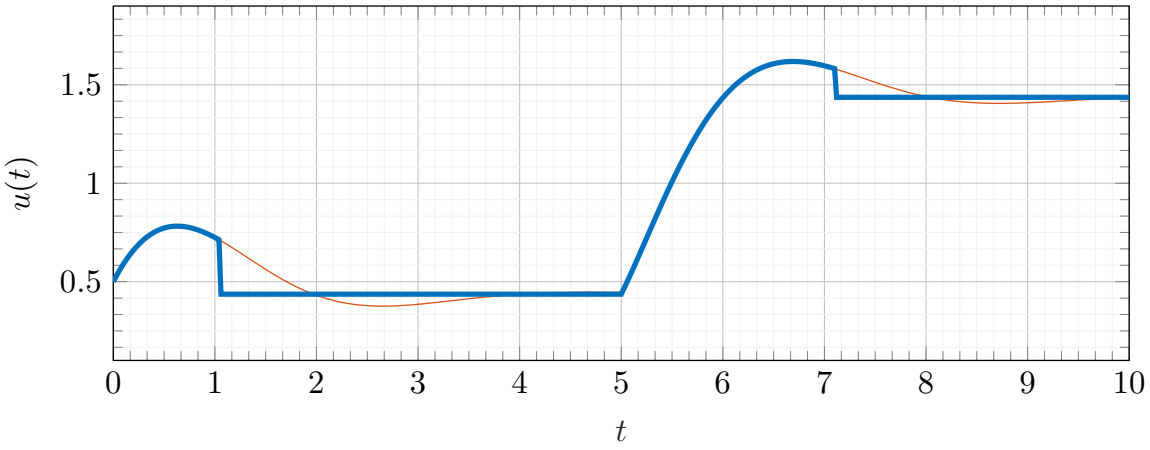

Figure 4.22: Controller output u in Example 4.9: (orange, thin) base PI controller; (blue, thick) PI+CI controller.

the first controller saturates, allowing for the total control signal to reach potentially higher values according to a given demand.

The basic structure of a split-range control system is depicted in Figure 4.23. For simplicity, we assume that the plants are ordered such that the control signal u_i satisfies $M_{i-1} \leq u_i \leq M_i$. Split-range control is implemented by means of a selector, which takes the control signal u as an input, determines which plant P_i will receive an input $u_i = k_{1i}u + k_{2i}$ for some $k_{1i}, k_{2i} \in \mathbb{R}$, and fixes all other values u_j with $j \neq i$ to constants, namely $u_j = M_j$ if $j < i$ and $u_j = M_{j-1}$ if $j > i$. E.g. in the temperature control example, with P_1 describing the heating dynamics and P_2 the cooling dynamics, whenever $u \geq 0$, the selector takes $u_1 = u, u_2 = 0$, and when $u < 0$, then $u_2 = -u, u_1 = 0$. In the auxiliary control example, say P_1 is the main plant and P_2 the auxiliary one, and let M denote the saturation value of the first controller. Then if $u \leq M$, one has $u_1 = u, u_2 = 0$, and if $u > M$, then $u_1 = M, u_2 = u - M$.

Split range PI+CI control of nondelayed first order plants can be thought of as a special case of the PI+CI control of nonlinear plants, by replacing the combination of the selector and the MISO plants $P_1, \ldots, P_n$ with a single nonlinear SISO plant P_{nl} whose evolution law is defined piecewise:

$$P_{\text{nl}}: \quad \dot{x}_p = -a(u)x_p + b(u)u, \tag{4.64}$$

such that $a(u) = a_i, b(u) = b_i$ for all u lying in the range for which the selector chooses plant P_i. The tuning rules (4.57)–(4.58) can thus be used, giving the expressions

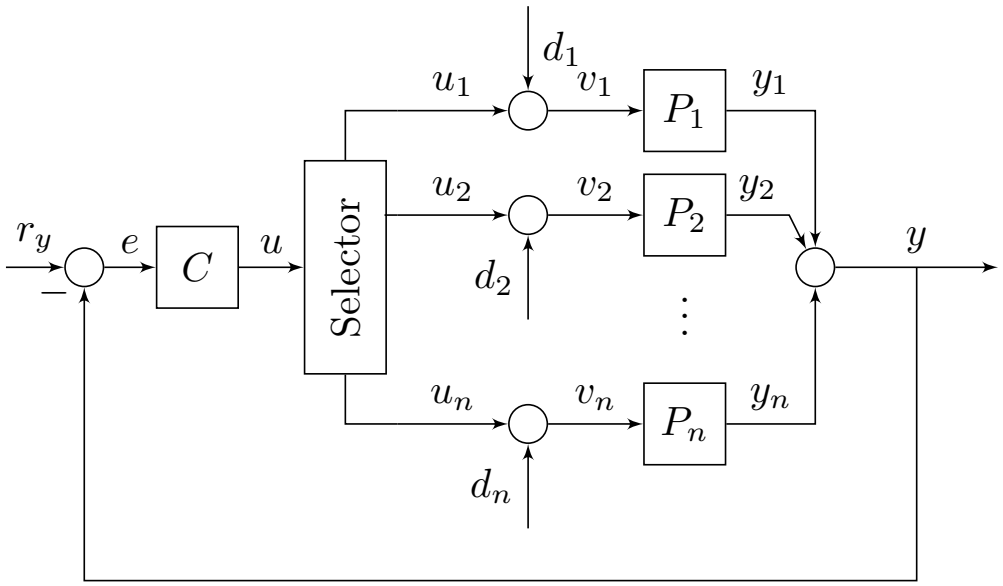

Figure 4.23: Block diagram of the split-range control structure.

$$p_{r,\text{ref}} = 1 - \frac{a_{j(i)} T_I w_{10}}{b_{j(i)} k_P x_I(t_1)}, \quad p_{r,\text{dist}} = 1 + \frac{T_I w_{20}}{k_P x_I(t_1)} \tag{4.65}$$

for the reset ratios whenever the ith input is active, where in the reference tracking case, $j(i)$ is the index closest to i such that $M_{j(i)-1} < a_{j(i)} w_{10}/b_{j(i)} < M_{j(i)}$.

On the other hand, in the delayed case, the split-range control system cannot in general be handled as if the process were a SISO nonlinear plant, since a delayed first order MISO plant features several time delays $h_1, h_2, \ldots$ which may be different, whereas the tuning rules for nonlinear systems are only applicable in case of a single delay h. The main problem is that when a reset action causes the control signal u to cross some saturation value, its effect will reach the plant at two different times because of the difference in delays, and this lack of coordination may prevent achieving a good performance. To solve this problem, the control signals u_i fed at the input of each subplant must be upgraded to independent signals, which can then be properly reset at different times using a different (variable band) resetting law; the equations $u_i = k_1 u + k_2, u_j = u_{j\pm}$ become conditions that are imposed at any time *except* in the intervals of length $|h_j - h_i|$ between two reset actions, in which some u_j may take a non-saturated value imposed by the corresponding tuning rule at the same time that u_i keeps evolving as normal (that is, two or more control signals may now be "active" simultaneously, like in collaborative strategies). One possible way to implement this

asynchronous strategy (though not the only way) is to replace the combination of a single PI+CI controller and a selector by n PI+CI controllers in a parallel configuration with the same parameters $k_{Pi} = k_P, T_{Ii} = T_I, p_{ri} = p_r$, but with possibly different θ_i and τ_{Hi}, and then impose the corresponding saturations.

With this in mind, the tuning rules for a flat response in first order delayed split-range PI+CI control systems can be taken to be (4.65) plus $\theta_i = \tau_{Hi} = h_i$.

Example 4.10 (Split-range reset-and-hold control of a delayed 2×1 system)**.** In this example, a two-input MISO system is considered consisting of a main plant and auxiliary plant, given respectively by

$$P_1(s) = \frac{e^{-0.5s}}{1+s}, \quad P_2(s) = \frac{e^{-0.3s}}{1+s}. \tag{4.66}$$

Note that the two plants share the same gain and time constant; this kind of situation can arise e.g. when the auxiliary plant has exactly the same characteristics as the main plant but is in a different physical location. The control inputs are assumed to be saturated according to the inequalities $u_1 < 1.5$ and $u_2 > 0$. The base PI parameters are chosen as

$$k_P = 1, \quad T_I = 1/2. \tag{4.67}$$

The response to the system to a unit step reference change is considered. The split-range reset-and-hold control system is tuned according to the rules (4.65), resulting in the values

$$p_r = 0.264, \quad \theta_1 = \tau_{H1} = 0.5, \quad \theta_2 = \tau_{H2} = 0.3. \tag{4.68}$$

Figure 4.24 shows the system output, together with the base linear response for comparison purposes. As expected, a flat response is observed to a good approximation. The controller outputs are shown in Figure 4.25; although u_1 and $u_2 + 1.5$ can be combined into a single signal u in the linear case, this is clearly not true for the reset-and-hold case, where in the interval $t \in [0.7, 0.9]$, u_1 has reset to a non-saturated value while u_2 is still evolving.

Thus, it is observed that the noncollaborative split-range strategy must be upgraded to a collaborative strategy, in which both plant inputs are simultaneously active, for a flat response to be achieved in the presence of two different delays (i.e., with reset

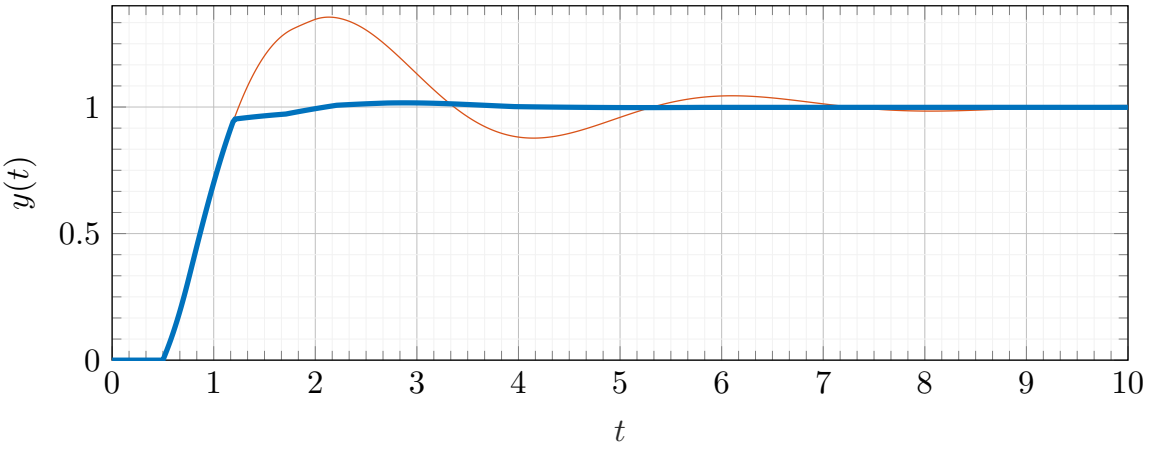

Figure 4.24: Closed loop step response output y in Example 4.10: (orange, thin) base PI split-range controller; (blue, thick) PI+CI split-range controller.

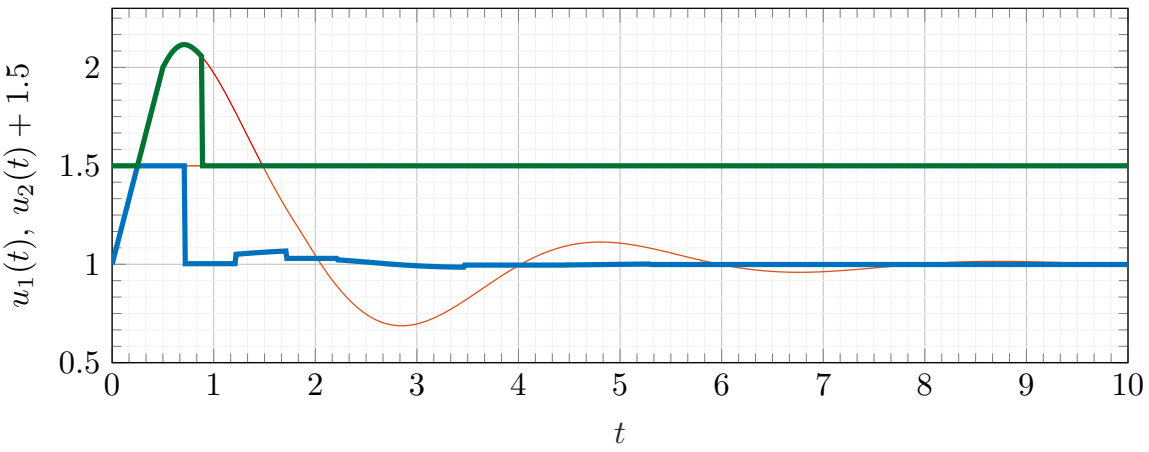

Figure 4.25: Controller outputs u_1 and $u_2 + 1.5$ in Example 4.10: (orange and red, thin) base PI split-range controller; (blue and green, thick) PI+CI split-range controller.

asynchronicity).

4.6 Summary of design strategies

Table 4.3 summarizes the tuning rules and algorithms proposed for all classes of PI+CI based control systems studied in this work. These rules can be classified into two main types: one of them concerns first order systems (with or without time delay), in which the focus has been on replicating the flat response property (or a lose approximation to it) in order to obtain a fast behavior preserving the rise time associated to the base system, but having little or no overshooting. This approach is based on extending the previously known tuning rules (4.7), (4.12) for first order nondelayed SISO systems, and is characterized by requiring only one reset action per disturbance or reference change. In the case of delayed systems, these rules depend on a new hybrid strategy, the reset-and-hold strategy, which is used to disable the detrimental plant-controller feedback loop in the crucial time interval from when the controller is reset to when the reset action arrives at the plant.

The other type of control design considered concerns higher order systems, or first order systems under a configuration that involves more than one error signal (the MISO serial structure). Since a perfect flat response is in general impossible to obtain in these systems, the focus has been on the use of more than one reset action to achieve an improved response, which minimizes an estimation of the integrated squared error in the interval between two consecutive reset actions. The result is an on-line algorithm where the reset ratios are updated with each jump, and can be seen as a generalization of the variable reset ratio algorithm proposed in [46].

Type	**Tuning rule**	**Comments**
MISO, FO, parallel	$p_{ri,\text{ref}} = 1 - \frac{a_i T_{Ii} x_{pi}(t_1,0)}{b_i k_{Pi} x_I(t_1)}$ $p_{ri,\text{dist}} = 1 - \frac{(a_i x_{pi}(t_1,0) - b_i w_{20i}) T_{Ii}}{b_i k_{Pi} x_I(t_1)}$	Unique values
MISO, HO, parallel	$(p_{r1}^{(k)}, \cdots, p_{rn}^{(k)})^\top = -\frac{1}{2} M_k^{-1} \mathbf{b}_k$	On-line algorithm
SISO, FOPDT	$p_{r,\text{ref}} = 1 - \frac{a T_I w_{10}}{b k_P x_I(t_1)}$ $p_{r,\text{dist}} = 1 + \frac{T_I w_{20}}{k_P x_I(t_1)}$ $\theta = \tau_H = h$	Unique values
MISO, FOPDT, parallel	$p_{ri,\text{ref}} = 1 - \frac{a_i T_{Ii}(x_{pi}(t_{1i},0) + h_i \dot{x}_{pi}(t_{1i},0))}{b_i k_{Pi} x_I(t_{1i})}$ $p_{ri,\text{dist}} = 1 - \frac{(a_i(x_{pi}(t_{1i},0) + h_i \dot{x}_{pi}(t_{1i},0)) - b_i w_{20i}) T_{Ii}}{b_i k_{Pi} x_I(t_{1i})}$ $\theta_i = \tau_{Hi} = h_i$	Unique values
MISO, FO, serial	$p_{r1,\text{ref}} = 1 - \frac{a T_I w_{10}}{b k_P x_I(t_1)}$ (I) $p_{r1,\text{dist}} = 1 + \frac{T_I w_{20}}{k_P x_I(t_1)}$ (I) $p_{r1}^{(k)} = -\frac{1}{2} M_k^{-1} \mathbf{b}_k$ (II)	(I): SISO-like rule (II): On-line alg.
SISO, FO, nonlinear	$p_{r,\text{ref}} = 1 - 1 - \frac{T_I F_{\text{ref}}^{-1}(0)}{k_P x_I(t_1)}$ $p_{r,\text{dist}} = 1 - \frac{T_I F_{\text{dist}}^{-1}(0)}{k_P x_I(t_1)}$	Depends on w_{10}, w_{20i}
MISO, FO, parallel, nonlin.	$p_{ri,\text{ref}} = 1 - \frac{T_I F_{i,\text{ref}}^{-1}(0)}{k_P x_I(t_1)}$ $p_{ri,\text{dist}} = 1 - \frac{T_I F_{i,\text{dist}}^{-1}(0)}{k_P x_I(t_1)}$	Dep. on plant states
MISO, FOPDT, split-range	$p_{r,\text{ref}} = 1 - \frac{a_{j(i)} T_I w_{10}}{b_{j(i)}}$ $p_{r,\text{dist}} = 1 + \frac{T_I w_{20}}{k_P x_I(t_1)}$ $\theta_i = \tau_{Hi} = h_i$	Independent u_i

Table 4.3: Summary of the proposed tuning rules (FO: first order, HO: higher order, FOPDT: first order plus dead time (delayed first order)).

Chapter 5

Applications

5.1 MISO control of a heat exchanger

In this section, the reset-and-hold control design results for first order MISO plants with delay derived in Chapter 4 are applied to a real experimental MISO plant.

The process to be controlled is part of a food processing pilot plant, pictured in Figure 5.1. A certain product fluid (in this case water) is circulated inside a heat exchanger, and interchanges heat with saturated steam coming from an electrically powered boiler at a given pressure, which is kept between 4.5 and 5 bar using on/off control. The flow of steam is controlled by an electropneumatic globe valve, and the flow of the fluid itself is controlled by means of an industrial helicoidal pump.

The heat exchanger is a HRS UNICUS model, consisting of two concentric, hollow, stainless steel tubes of length 3 m and respective diameters 10.4 and 7.62 cm; the product passes through the inner tube at a certain speed, and the saturated steam flows between both tubes in parallel to the product, transferring heat to the product; the condensed steam coming out of the heat exchanger is recirculated inside the boiler. In contrast, the product is continuously renewed from a local water supply network. The heated product is circulated through a second heat exchanger of identical specifications, where it is cooled by cooling water from a tank, and then it is returned to the water supply network. The installation also features pneumatically activated surface scrapers, which help homogenize the temperature of the fluid and prevent the buildup of impurities in the surface of the inner tube.

Figure 5.1: Image of the experimental food processing pilot plant.

The objective is to control the difference $y = \Delta T$ between the fluid's temperatures at the inlet and the outlet of the heat exchanger (measured in degrees Celsius). This temperature difference is obtained by two respective PT-100 thermocouples at the extremes of the heat exchanger.

The data is processed by an ABB programmable logic controller (PLC) connected to a supervisory control and data acquisition (SCADA) system (see Figure 5.2), which is in turn connected to MATLAB's environment Simulink, where the reset-and-hold MISO control setup is implemented. The two considered input variables are the valve opening $u_1 = V - V_0$ and the pump flow rate $u_2 = Q - Q_0$ (both measured as percentages), where V_0, Q_0 denote the nominal values. The control signals are then computed in real time and fed back to the PLC, which updates the actuators accordingly.

The temperature difference is related to the speed of heat transfer H by means of the equation

$$H = \dot{m}\, c_p\, \Delta T, \tag{5.1}$$

where $\dot{m}$ is the mass flow rate of the product fluid (determined by the pump speed), and c_p denotes its specific heat capacity at constant pressure. In turn, in the ideal case H can be shown to depend proportionally on the steam flow rate (as controlled by the valve opening) if the steam pressure is assumed constant. Thus, ΔT can be controlled

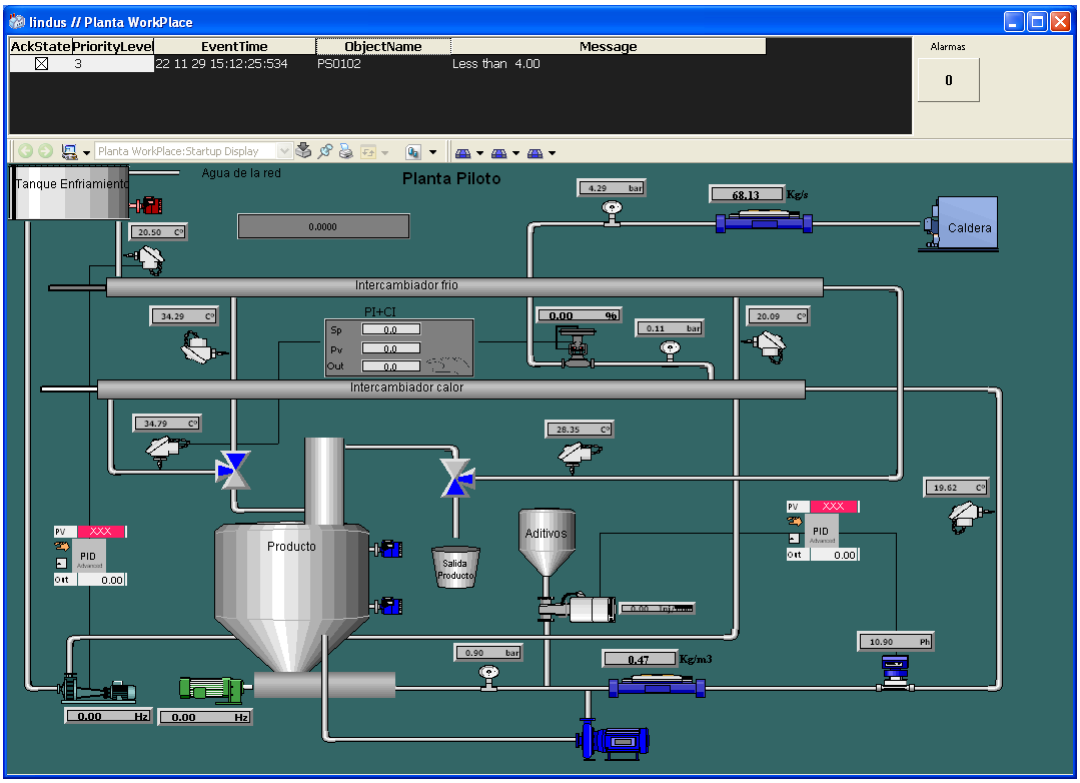

Figure 5.2: Image of the SCADA's human-machine interface.

by manipulating both the pump speed and the steam valve opening; however, since one cannot easily account for losses and time delays using a model from first principles, it becomes necessary to linearize the system about an operating point and perform a model identification first in order to design and implement the appropriate control strategy.

The chosen operating point, starting from which the linearization is performed, is

$$V_0 = 20\%, \qquad Q_0 = 40\%, \tag{5.2}$$

corresponding to a steady-state difference of temperatures of about $\Delta T = 12.4$ °C. Note that the range of the steam valve is restricted by design both from above (because an opening greater than about 30 % would cause a significant pressure decrease within the boiler, negatively affecting the performance) and from below (when the valve is opened less than 10 %, the effects of nonlinearity become much more noticeable and the LTI assumption ceases to be valid); similarly, the pump's range is also limited by nonlinearity, though only from below. Thus, it is justifiable to consider a collaborative MISO control strategy in which the control effort is shared between the valve and the

product pump, in order to be able to reach a wider scope of temperature differences whilst keeping the actuators within their appropriate ranges.

The plant has been identified by following two methods: first, applying a pseudo-random binary sequence signal at each of the plant inputs, and secondly, applying positive and negative step inputs at different operating points around the nominal point (the approaches followed are essentially the same as in [358], to which the reader is referred for details). The responses have been recorded and analyzed with MATLAB's Identification Toolbox. The experimental data has been fit to a first order linear process with delay. The results in the nominal case are as follows:

$$P_1(s) = 0.49\,\frac{e^{-139s}}{1+106s}, \tag{5.3}$$

$$P_2(s) = -0.32\,\frac{e^{-143s}}{1+90s}. \tag{5.4}$$

Note that the parameters of the obtained model are different to those of the identification performed in earlier works [275, 358], which also differ among themselves. As mentioned in the second reference, this could be partly attributed to the different chemical composition of the product water, and in this case, also to the different operating point for the product pump, which corresponds to a lower speed (about 200 liters per hour) that in turn leads to a slightly higher effective value for the delays.

An important thing to note is that the identified delays h_1 and h_2 have turned out to be very similar. As mentioned before, this allows for the possibility to use synchronous reset if a single delay $h = (h_1 + h_2)/2 = 141\,\text{s}$ is taken for the purposes of resetting, thus simplifying the treatment.

Two different experiments have been performed, dealing respectively with reference tracking and disturbance rejection.

5.1.1 Reference tracking

Consider a step change in the reference signal r_y of height 2 °C at $t = 30$ s. The parameters k_{P1}, k_{P2} and T_{I1}, T_{I2} of the base linear controllers have been initially tuned according to the Skögestad Internal Model Control (SIMC) rule [337] applied to

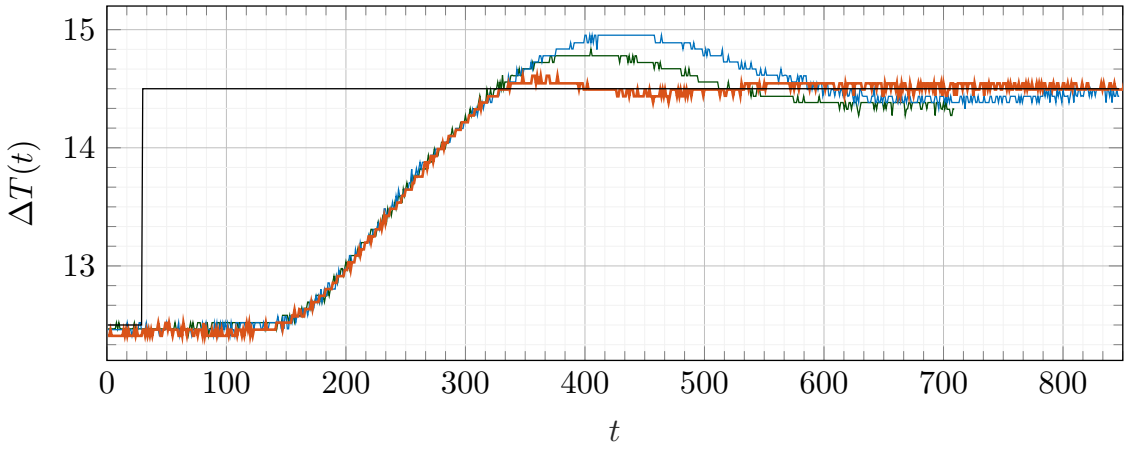

Figure 5.3: Temperature difference ΔT under a reference change: (blue) base PI controllers; (green) ordinary PI+CI controllers; (orange) reset-and-hold PI+CI controllers; (black) reference signal.

each independent controller, and have been further modified to obtain a sufficiently oscillating but not too aggressive base response. The resulting values are

$$\begin{aligned} k_{P1} &= 0.6465, \qquad T_{I1} = 118, \\ k_{P2} &= -1.130, \qquad T_{I2} = 126. \end{aligned} \tag{5.5}$$

The reset-and-hold strategy is implemented with the tuned reset ratios (4.48), using a state observer to determine the unknown values of the plant states and their derivatives. Both variable bands and dwelling times are taken as $\theta_i = H_i = h = 141$ s.

Figure 5.3 shows the resulting response of the reset-and-hold control system, together with that of the linear base system, as well as the response under a variable band, ordinary reset strategy with reset ratios $p_{r1} = 0.11, p_{r2} = 0.12$ which minimize the integral squared error in simulation (only one reset action is performed) for comparison purposes. As can be observed, a good approximation of a flat response is attained using reset-and-hold controllers, which significantly improves the response achievable by applying a traditional reset control method; note that the flatness is degraded due to many factors such as the measurement noise of the temperature sensors, the inaccuracies in the estimation of the plant states derived from using a state observer, the approximation inherent in the use of the variable band law to anticipate a zero crossing (as mentioned at the end of Section 4.3), the presence of physical noise induced by rapid oscillations in the steam flow due to the boiler's inner functioning, and the

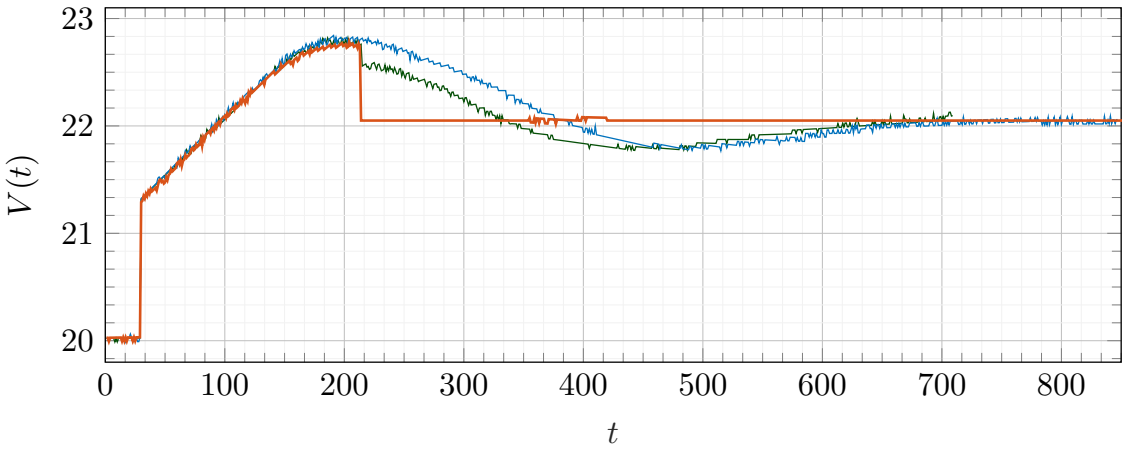

(a) Valve opening V.

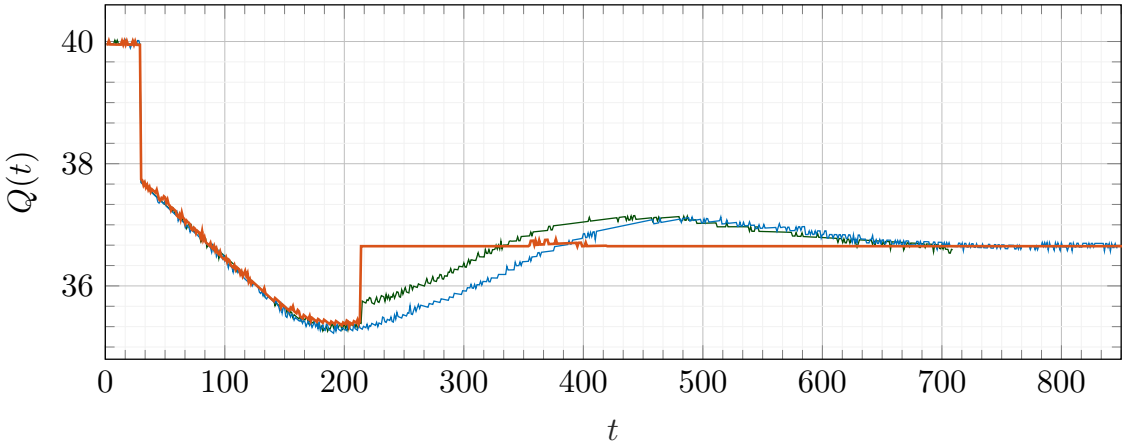

(b) Pump flow rate Q.

Figure 5.4: Controller outputs for the reference tracking example: (blue) base PI controllers; (green) ordinary PI+CI controllers; (orange) reset-and-hold PI+CI controllers.

fact that the system is not perfectly linear (which implies that the formulas (4.48), 4.49 are not completely accurate). However, this example shows how reset control, especially when augmented with a holding mechanism, is capable of achieving a greater performance than LTI control even in the presence of delays, as the overshooting has been eliminated for the most part without degrading the rise time. Figures 5.4(a) and 5.4(b) show the respective controller outputs (note the absence of noise in the intervals where the holding mechanism is active). Table 5.1 shows the ISE, IAE and maximum overshoot performance indices.

	Linear	**Reset**	**Reset-and-hold**
IAE ($^\circ$C $\cdot$ s)	565.28	537.01 (95%)	503.74 (89%)
ISE (($^\circ$C)^2 $\cdot$ s)	890.12	886.77 (99%)	865.13 (97%)
Overshoot (%)	22.654	16.817 (74%)	5.488 (24%)

Table 5.1: Integrated absolute error, integrated squared error and maximum overshoot percentage for the base linear, reset and reset-and-hold controllers in the reference tracking experiment. The percentages within brackets indicate the relative decrease with respect to the linear case.

5.1.2 Disturbance rejection

Consider now a step disturbance d_1 of magnitude 2% applied at $t = 30$ s, acting at the input of the first plant (corresponding to the valve opening). As the previous base controller parameters do not produce any oscillations in the error for this disturbance signal, the parameters k_{P1}, k_{P2} have been multiplied by a factor of 1.5 with respect to their values in reference tracking mode so as to obtain an oscillating base response, whereas T_{I1}, T_{I2} have not been changed. The modified values are

$$\begin{aligned} k_{P1} &= 0.9697, \qquad T_{I1} = 118, \\ k_{P2} &= -1.695, \qquad T_{I2} = 126. \end{aligned} \tag{5.6}$$

As before, the reset-and-hold strategy (4.49) is used with a state observer, maintaining the same values for the variable bands and dwelling times. Figure 5.5 shows the resulting output temperature difference. Similar comments than in the reference tracking case apply here. As one can see, the nonlinearity of the process is apparent in the fact that in the base PI response, the height of the second peak is of the same magnitude (and even higher) than that of the first trough: in physical terms, under the given experimental setup it is easier for the water to heat up than for it to cool down.

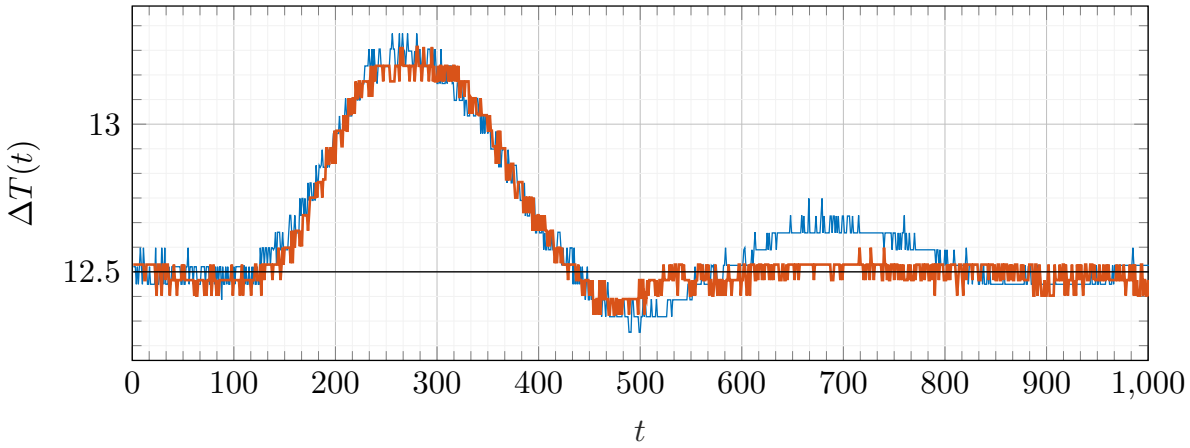

Figure 5.5: Temperature difference ΔT under a disturbance signal: (blue) base PI controllers; (orange) reset-and-hold PI+CI controllers; (black) reference signal.

Nevertheless, the reset-and-hold approach still works acceptably as in the previous case, producing an approximately flat response with considerably less overshoot. Figures 5.6(a) and 5.6(b) show the respective controller outputs, and Table 5.2 shows the corresponding ISE, IAE and overshoot performance indices.

	Linear	**Reset-and-hold**
IAE (°C · s)	178.05	151.56 (85%)
ISE $(°C)^2 \cdot s)$	79.081	72.299 (91%)
Overshoot (°C)	0.4022	0.2642 (66%)

Table 5.2: Integrated absolute error, integrated squared error and maximum overshoot for the base linear vs. reset-and-hold controllers in the disturbance rejection experiment. The percentages within brackets indicate the relative decrease with respect to the linear case.

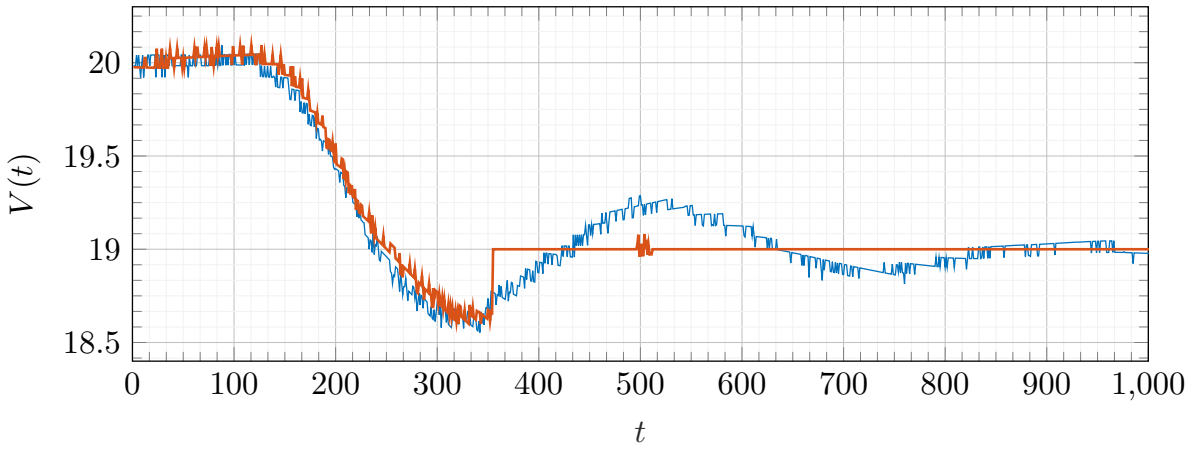

(a) Valve opening V.

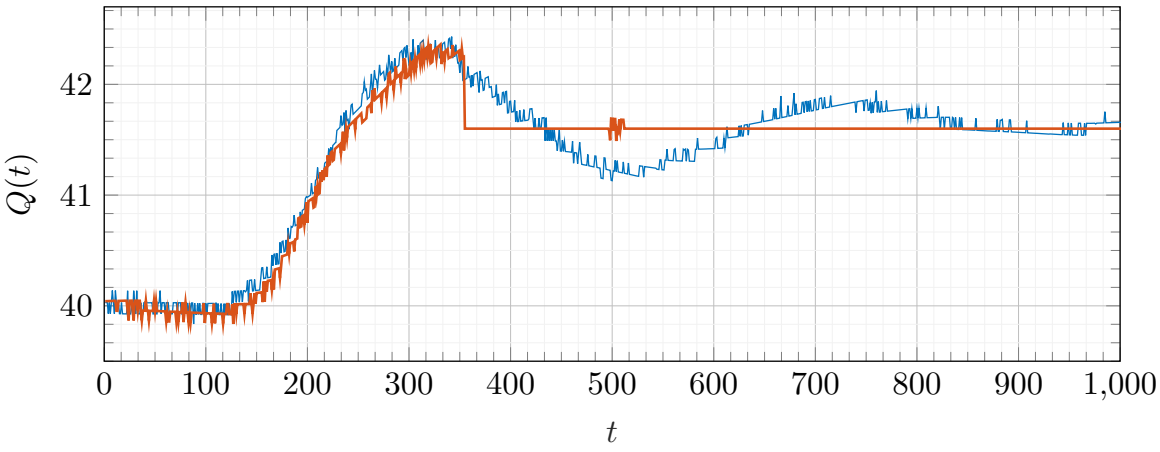

(b) Pump flow rate Q.

Figure 5.6: Controller outputs for the disturbance rejection example: (blue) base PI controllers; (orange) reset-and-hold PI+CI controllers.

Chapter 6

Conclusions

A mathematical formulation of MISO reset control systems and SISO/MISO reset-and-hold control systems has been developed in the Hybrid Inclusions formalism, allowing for their formal treatment. Concretely, robust models of the Clegg integrator, the FORE and the general reset controller have been provided, considering different resetting laws. The PI+CI controller and its modification with a variable reset ratio have been introduced next. The closed loop model for a nondelayed reset control system has been formulated, distinguishing between synchronous and asynchronous reset. Similarly, models for SISO and MISO delayed reset control systems have been formulated for the first time in the HI formalism for systems with memory. Various common model extensions have also been considered.

The well-posedness of the considered systems has been shown, and an analysis of stability has been performed, resulting in several sets of stability conditions for LTI base systems that comprise several kinds of systems: first, the well-posedness of the models for both nondelayed and delayed MISO hybrid control systems has been shown by checking that the basic hybrid conditions are fulfilled. Next, a simple set of LMI conditions for the stability of a nondelayed MISO reset control systems have been obtained using a Lyapunov-based approach. Similarly, two kinds of LMI conditions for delayed MISO reset-and-hold control systems have been derived, both based on a Lyapunov-Krasovskii functional: one more conservative set of conditions that holds irrespective of the time delay(s), and and a less conservative set of conditions that depends on a given delay bound. The use of the stability conditions has been demonstrated by means of respective examples.

Following a simple time domain-based design procedure, the tuning rules known in the SISO case have been successfully extended to a class of MISO systems, thus completing a major objective of this work. Concretely, tuning rules with the flat response property have been proposed for first order MISO reset control systems under a parallel configuration, and an on-line tuning algorithm, based on squared error minimization and the use of variable reset ratios, has been designed for an improved response in higher order MISO reset control systems under a parallel configuration, including a modification of the squared error minimization procedure used in previous works [20]. This last modification, based on an extra design parameter, constitutes a new performance improvement also applicable in the single variable case.

Furthermore, a new hybrid reset-based control strategy, the reset-and-hold strategy, has been developed specifically for systems with time delay. This strategy has been successfully applied in order to find PI+CI design rules achieving a good approximation of a flat response in both SISO and MISO delayed first order parallel plants. This constitutes a strict improvement over previous PI+CI based reset control strategies for SISO delayed first order plants, which consisted of treating it as a second order plant by means of a Padé approximation and applying the variable reset ratio algorithm. The benefits and drawbacks of all considered strategies have been discussed, and their performance has been shown by means of simulated examples.

Moreover, the applicability of the previous time domain-based design procedure has been shown by deriving a previously unknown extension of the SISO tuning rules to nonlinear first order systems. Some extensions to other MISO control configurations, such as the serial control architecture and a noncollaborative MISO structure (split-range control), have also been considered as well.

Finally, the benefits of the newly developed reset-based hybrid control techniques have been showcased by means of an experimental example consisting of the temperature control of a heat exchanger in a food processing pilot plant, modeled as a first order TISO control system with time delay, and controlled by PI+CI reset-and-hold controllers in a parallel configuration. The results have been satisfactory in terms of performance.

6.1 Future work

Some suggested future work lines include:

- Consider less conservative stability conditions, e.g. conditions dependent on the variable band, and on the holding time parameter in the case of reset-and-hold control, or more general conditions that do not necessarily require the stability of the base system. Another option would be trying to adapt stability conditions such as the one based on Legendre polynomials derived in [329] and used in [121], which has been shown to be more efficient than the one derived from the model transformation method, to to the (SISO and MISO) reset-and-hold case.

- Try to find design rules or algorithm for the control of higher order (SISO or MISO) systems with time delays. A possible starting approach would be to somehow combine the reset-and-hold strategy with the PI+CI ISE-minimization variable reset ratio algorithm.

- Extend the study of reset and reset-and-hold control systems to the case of nonlinear plants. A first step was made in this work through the development of a tuning rule that achieves a flat response against a certain class of first order nonlinear systems. However, a more thorough theoretical study, including well-posedness and stability, is still lacking.

- Expand to MIMO systems: the existence of asynchronicity leads one to consider compound resetting laws, and a natural next step is to consider combinations of SISO-like resetting laws associated to each independent error signal, as in [403]. It is expected that a flat response will be in general impossible to obtain, and that explicit formulas for optimized reset ratios such as (4.27) will not be available even in the simplest 2×2 case with first order plants. However, it is plausible that the algorithm (4.26) based on ISE minimization can be adapted to work with MIMO systems of any order; a similar algorithm in the context of a sector based resetting law has been developed for MIMO systems in the work [386]. A first thing to consider would be the study of hybrid variations of common MIMO strategies, such as H_∞ control [13].

- Continue to develop the application of the found techniques to heat, cold and energy generation systems, as well as in other fields (such as micro-algae bioreactors).

Bibliography

[1] W. Aangenent, G. Witvoet, W. Heemels, M. Van De Molengraft, and M. Steinbuch. Performance analysis of reset control systems. *International Journal of Robust and Nonlinear Control*, 20(11):1213–1233, 2010.

[2] W. H. Aangenent, G. Witvoet, W. Heemels, M. van de Molengraft, and M. Steinbuch. An LMI-based $\mathcal{L}_2$ gain performance analysis for reset control systems. In *2008 American Control Conference*, pages 2248–2253. IEEE, 2008.

[3] L. Acho. Nonlinear reset integrator control design: Application to the active suspension control of vehicles. In *Proceedings of the IASTED International Conference Modelling, Identification and Control (MIC 2014)*, pages 226–228. ACTA Press, 2014.

[4] E. Aguilar-Garnica, J. P. García-Sandoval, and D. Dochain. Monitoring of a biodiesel production process via reset observer. *Journal of Process Control*, 42:104–113, 2016.

[5] A. Ahmadi Dastjerdi. *Frequency-Domain Analysis of "Constant in Gain Lead in Phase (Cglp)" Reset Compensators: Application to precision motion systems*. PhD thesis, Delft University of Technology, 2021.

[6] E. Akyüz, N. Saikumar, and S. H. HosseinNia. Reset control for vibration disturbance rejection. *IFAC-PapersOnLine*, 52(15):525–530, 2019.

[7] A. K. Ali and M. M. Mahmoud. Reduced order and observer-based reset control systems with time delays. *International Journal of Robotics and Control Systems*, 2(3):448–466, 2022.

[8] J. Alvarez-Ramirez, A. Velasco, and G. Fernandez-Anaya. A note on the stability of habituating process control. *Journal of Process Control*, 14(8):939–945, 2004.

[9] F. Amato, G. Carannante, G. D. Tommasi, and A. Pironti. Finite-time control of switching linear systems: The uncertain resetting times case. *International Journal of Robust and Nonlinear Control*, 25(15):2547–2560, 2015.

[10] A. Aminzadeh and A. Khayatian. Reset observer design for time-varying dynamics: Application to WIG crafts. *Aerospace Science and Technology*, 81:32–40, 2018.

[11] J. Arcos-Legarda, J. Cortes-Romero, A. Beltran-Pulido, and A. Tovar. Hybrid disturbance rejection control of dynamic bipedal robots. *Multibody System Dynamics*, 46(3):281–306, 2019.

[12] K. J. Åström and T. Hägglund. *PID Controllers: Theory, Design, and Tuning*. ISA: The Instrumentation, Systems, and Automation Society, jan 1995.

[13] K. J. Åström, T. Hägglund, and K. J. Astrom. *Advanced PID control*, volume 461. ISA-The Instrumentation, Systems, and Automation Society Research Triangle Park, 2006.

[14] M. S. Bahnamiri, N. Karbasizadeh, A. A. Dastjerdi, N. Saikumar, and S. H. HosseinNia. Tuning of CgLp based reset controllers: Application in precision positioning systems. *IFAC-PapersOnLine*, 53(2):8997–9004, 2020.

[15] J. Bakkeheim, T. A. Johansen, Ø. N. Smogeli, and A. J. Sorensen. Lyapunov-based integrator resetting with application to marine thruster control. *IEEE Transactions on Control Systems Technology*, 16(5):908–917, 2008.

[16] J. Ban and S. W. Kim. Design of reset control for SISO linear systems using PWQ lyapunov functions. In *2019 IEEE 15th International Conference on Control and Automation (ICCA)*, pages 1253–1257. IEEE, 2019.

[17] T. Banki, F. Faghihi, and S. Soleymani. Frequency control of an island microgrid using reset control method in the presence of renewable sources and parametric uncertainty. *Systems Science & Control Engineering*, 8(1):500–507, 2020.

[18] A. Baños and A. Barreiro. *Reset Control Systems*. Springer London, 2012.

[19] A. Baños, J. Carrasco, and A. Barreiro. Reset times-dependent stability of reset control systems. *IEEE Transactions on Automatic Control*, 56(1):217–223, 2011.

[20] A. Baños and M. A. Davó. Tuning of reset proportional integral compensators with a variable reset ratio and reset band. *IET Control Theory & Applications*, 8(17):1949–1962, 2014.

[21] A. Baños and M. A. Davó. Stability of time-delay reset systems with a nonlinear and time-varying base system. *arXiv preprint arXiv:1605.09174*, 2016.

[22] A. Baños, M. A. Davó, and C. D. Cánovas. On the robustness of hybrid control systems to measurement noise and actuator disturbances. *arXiv preprint arXiv:1711.09374*, 2017.

[23] A. Baños, S. Dormido, and A. Barreiro. Stability analysis of reset control systems with reset band. *IFAC Proceedings Volumes*, 42(17):180–185, 2009.

[24] A. Baños, S. Dormido, and A. Barreiro. Limit cycles analysis of reset control systems with reset band. *Nonlinear analysis: hybrid systems*, 5(2):163–173, 2011.

[25] A. Baños and J. I. Mulero. Well-posedness of reset control systems as state-dependent impulsive dynamical systems. In *Abstract and Applied Analysis*, volume 2012. Hindawi, 2012.

[26] A. Baños, J. I. Mulero, A. Barreiro, and M. A. Davó. An impulsive dynamical systems framework for reset control systems. *International Journal of Control*, 89(10):1985, 2016.

[27] A. Baños, F. Perez, and J. Cervera. Networked reset control systems with discrete time-varying delays. In *IECON 2010-36th Annual Conference on IEEE Industrial Electronics Society*, pages 3146–3151. IEEE, 2010.

[28] A. Baños, F. Perez, and J. Cervera. Network-based reset control systems with time-varying delays. *IEEE Transactions on Industrial informatics*, 10(1):514–522, 2013.

[29] A. Banos, F. Perez, S. Tarbouriech, and L. Zaccarian. Low-complexity controllers for time-delay systems: Delay-independent stability via reset loops, advances in delays and dynamics, 2014.

[30] A. Baños, F. Pérez Rubio, S. Tarbouriech, and L. Zaccarian. Delay-independent stability via reset loops. In *Low-Complexity Controllers for Time-Delay Systems*, pages 111–125. Springer, 2014.

[31] A. Baños and A. Vidal. Definition and tuning of a PI+CI reset controller. In *2007 European Control Conference (ECC)*, pages 4792–4798. IEEE, 2007.

[32] A. Baños and A. Vidal. Design of reset control systems: The PI + CI compensator. *Journal of Dynamic Systems Measurement and Control*, 134:051003/1–11, 06 2012.

[33] A. Barreiro and A. Baños. Delay-dependent stability of reset systems. *Automatica*, 46(1):216–221, 2010.

[34] A. Barreiro and A. Baños. Sistemas de control basados en reset. *Revista Iberoamericana de Automática e Informática Industrial*, 9(4):329–346, 2012.

[35] A. Barreiro, A. Baños, and E. Delgado. Reset control of the double integrator with finite settling time and finite jerk. *Automatica*, 127:109536, 2021.

[36] A. Barreiro, A. Baños, and S. Dormido. Reset control systems with reset band: well-posedness and limit cycles analysis. In *2011 19th Mediterranean Conference on Control & Automation (MED)*, pages 1343–1348. IEEE, 2011.

[37] A. Barreiro, A. Baños, S. Dormido, and J. A. González-Prieto. Reset control systems with reset band: Well-posedness, limit cycles and stability analysis. *Systems & Control Letters*, 63:1–11, 2014.

[38] A. Barreiro and A. Baños. Delay-dependent stability of reset systems. *Automatica*, 46(1):216–221, jan 2010.

[39] A. Barreiro and E. Delgado. Reset observers alleviating the peaking and the robustness tradeoffs: A case study on force estimation in teleoperation. *ISA transactions*, 94:36–46, 2019.

[40] A. Baños and A. Barreiro. Delay-independent stability of reset control systems. In *IECON 2006-32nd Annual Conference on IEEE Industrial Electronics*, pages 665–670. IEEE, 2006.

[41] A. Baños and A. Barreiro. Delay-dependent stability of reset control systems. In *2007 American Control Conference*, pages 5509–5514. IEEE, 2007.

[42] A. Baños and A. Barreiro. Delay-independent stability of reset systems. *IEEE Transactions on Automatic Control*, 54(2):341–346, 2009.

[43] A. Baños and A. Barreiro. Reset control systems: The zero-crossing resetting law. *Nonlinear Analysis: Hybrid Systems*, 46:101259, 2022.

[44] A. Baños, J. Carrasco, and A. Barreiro. Reset times-dependent stability of reset control with unstable base systems. In *2007 IEEE International Symposium on Industrial Electronics*, pages 163–168. IEEE, 2007.

[45] A. Baños, J. Carrasco, and A. Barreiro. Reset times-dependent stability of reset system with unstable base system. In *IEEE International Symposium on Industrial Electronics*, pages 163–168. IEEE, 2007.

[46] A. Baños and M. A. Davó. Tuning rules for a reset PI compensator with variable reset. *IFAC Proceedings Volumes*, 45(3):583–588, 2012.

[47] A. Baños, F. Perez, and J. Cervera. Discrete-time reset control applied to networked control systems. In *2009 35th Annual Conference of IEEE Industrial Electronics*, pages 2993–2998. IEEE, 2009.

[48] A. Baños and A. Vidal. Design of PI+CI reset compensators for second order plants. In *2007 IEEE International Symposium on Industrial Electronics*, pages 118–123. IEEE, 2007.

[49] A. Baños and A. Vidal. Design of reset control systems: the PI+CI compensator. *Journal of Dynamic Systems, Measurement, and Control*, 134(5), 2012.

[50] R. Beerens. *Reset control and control allocation for high-precision motion systems*. PhD thesis, Eindhoven University of Technology, 2020.

[51] R. Beerens, A. Bisoffi, L. Zaccarian, W. Heemels, H. Nijmeijer, and N. van de Wouw. Reset integral control for improved settling of pid-based motion systems with friction. *Automatica*, 107:483–492, 2019.

[52] R. Beerens, A. Bisoffi, L. Zaccarian, W. P. Heemels, H. Nijmeijer, and N. van de Wouw. Hybrid PID control for transient performance improvement of motion systems with friction. In *2018 Annual American Control Conference (ACC)*, pages 539–544. IEEE, 2018.

[53] R. Beerens, A. Bisoffi, L. Zaccarian, H. Nijmeijer, M. Heemels, and N. van de Wouw. Reset PID design for motion systems with stribeck friction. *IEEE Transactions on Control Systems Technology*, 30(1):294–310, 2021.

[54] O. Beker. *Analysis of reset control systems*. PhD thesis, University of Massachussetts, 2001.

[55] O. Beker, C. Hollot, and Y. Chait. Stability of a MIMO reset control system under constant inputs. In *Proceedings of the 38th IEEE Conference on Decision and Control (Cat. No. 99CH36304)*, volume 3, pages 2780–2781. IEEE, 1999.

[56] O. Beker, C. Hollot, and Y. Chait. Forced oscillations in reset control systems. In *Proceedings of the 39th IEEE conference on decision and control*, volume 5, pages 4825–4826. IEEE, 2000.

[57] O. Beker, C. Hollot, and Y. Chait. Stability of limit-cycles in reset control systems. In *Proceedings of the 2001 American Control Conference.(Cat. No. 01CH37148)*, volume 6, pages 4681–4682. IEEE, 2001.

[58] O. Beker, C. Hollot, Y. Chait, and H. Han. Fundamental properties of reset control systems. *Automatica*, 40(6):905–915, 2004.

[59] O. Beker, C. Hollot, Q. Chen, and Y. Chait. Stability of a reset control system under constant inputs. In *Proceedings of the 1999 American Control Conference (Cat. No. 99CH36251)*, volume 5, pages 3044–3045. IEEE, 1999.

[60] O. Beker, C. V. Hollot, and Y. Chait. Plant with integrator: an example of reset control overcoming limitations of linear feedback. *IEEE Transactions on Automatic Control*, 46(11):1797–1799, 2001.

[61] E. Benalcázar, O. Camacho, and H. Leiva. Linear and nonlinear fuzzy PID reset-based controllers: An application for a chemical process with variable delay. In *2021 IEEE CHILEAN Conference on Electrical, Electronics Engineering, Information and Communication Technologies (CHILECON)*, pages 1–5. IEEE, 2021.

[62] R. Bertollo, M. Schwegel, A. Kugi, and L. Zaccarian. Reset-control-based current tracking for a solenoid with unknown parameters. *IFAC-PapersOnLine*, 54(5):199–204, 2021.

[63] A. Bisoffi, R. Beerens, W. Heemels, H. Nijmeijer, N. van de Wouw, and L. Zaccarian. To stick or to slip: A reset PID control perspective on positioning systems with friction. *Annual Reviews in Control*, 49:37–63, 2020.

[64] A. Bisoffi, F. Forni, M. Da Lio, and L. Zaccarian. Relay-based hybrid control of minimal-order mechanical systems with applications. *Automatica*, 97:104–114, 2018.

[65] A. Bisoffi, F. Forni, M. Da Lio, and L. Zaccarían. Global results on reset-induced periodic trajectories of planar systems. In *2016 European Control Conference (ECC)*, pages 2644–2649. IEEE, 2016.

[66] J. E. Bobrow, F. Jabbari, and K. Thai. An active truss element and control law for vibration suppression. *Smart Materials and Structures*, 4(4):264, 1995.

[67] H. W. Bode. Relations between attenuation and phase in feedback amplifier design. *The Bell System Technical Journal*, 19(3):421–454, 1940.

[68] S. Boyd, L. El Ghaoui, E. Feron, and V. Balakrishnan. *Linear matrix inequalities in system and control theory*. SIAM, 1994.

[69] M. C. Bragagnolo, I.-C. Morarescu, J. Daafouz, and P. Riedinger. Design of reset strategy for consensus in networks with cluster pattern. In *8th European Nonlinear Dynamics Conference, ENOC 2014*, 2014.

[70] M. C. Bragagnolo, I.-C. Morărescu, J. Daafouz, and P. Riedinger. Design and analysis of reset strategy for consensus in networks with cluster pattern. In *Delays and Networked Control Systems*, pages 217–231. Springer, 2016.

[71] I. Bras, A. C. Carapito, and P. Rocha. Stability of switched systems with partial state reset. *IEEE Transactions on Automatic Control*, 58(4):1008–1012, 2012.

[72] C. Brosilow, L. Popiel, and T. Matsko. Coordinated control. In *CPC III*, 1986.

[73] K. Brummelhuis, N. Saikumar, J.-W. van Wingerden, and S. H. HosseinNia. Adaptive feedforward control for reset feedback control systems-application in precision motion control. In *2021 European Control Conference (ECC)*, pages 2450–2457. IEEE, 2021.

[74] R. Buitenhuis, N. Saikumar, and S. H. HosseinNia. Frequency-domain modelling of reset control systems using an impulsive description. *arXiv preprint arXiv:2009.13341*, 2020.

[75] R. Bupp, D. Bernstein, V. Chellaboina, and W. Haddad. Resetting virtual absorbers for vibration control. In *Proceedings of the 1997 American Control Conference (Cat. No. 97CH36041)*, volume 5, pages 2647–2651. IEEE, 1997.

[76] R. Bupp, D. Bernstein, V. Chellaboina, and W. Haddad. Finite settling time control of the double integrator using a virtual trap-door absorber. *IEEE Transactions on Automatic Control*, 45(4):776–780, 2000.

[77] R. T. Bupp, D. S. Bernstein, V. S. Chellaboina, and W. M. Haddad. Resetting virtual absorbers for vibration control. *Journal of Vibration and Control*, 6(1):61–83, 2000.

[78] C. Cai, A. A. Dastjerdi, N. Saikumar, and S. H. HosseinNia. The optimal sequence for reset controllers. In *2020 European Control Conference (ECC)*, pages 1826–1833. IEEE, 2020.

[79] C. Cai and A. R. Teel. Characterizations of input-to-state stability for hybrid systems. *Systems & Control Letters*, 58(1):47–53, 2009.

[80] A. Campos-Rodríguez, J. García-Sandoval, V. González-Álvarez, and A. González-Álvarez. Hybrid cascade control for a class of nonlinear dynamical systems. *Journal of Process Control*, 76:141–154, 2019.

[81] C. D. Cánovas, J. I. Mulero, and A. Baños. Well-posedness of reset control systems with input delay. In *2016 20th International Conference on System Theory, Control and Computing (ICSTCC)*, pages 404–409. IEEE, 2016.

[82] J. Carrasco. *Estabilidad de sistemas de control reseteado*. PhD thesis, Universidad de Murcia, 2009.

[83] J. Carrasco and A. Baños. Reset control of an industrial in-line pH process. *IEEE transactions on control systems technology*, 20(4):1100–1106, 2012.

[84] J. Carrasco, A. Baños, and A. Barreiro. Stability of reset control systems with inputs. In *2008 16th Mediterranean Conference on Control and Automation*, pages 1496–1501. IEEE, 2008.

[85] J. Carrasco, A. Baños, and A. van der Schaft. A passivity-based approach to reset control systems stability. *Systems & Control Letters*, 59(1):18–24, 2010.

[86] J. Carrasco, A. Baños, and A. van der Schaft. A passivity approach to reset control of nonlinear systems. In *IEEE Ind. Electr. Conference (IECON)*, 2008.

[87] J. Carrasco and E. M. Navarro-López. Towards $\ell 2$-stability of discrete-time reset control systems via dissipativity theory. *Systems & Control Letters*, 62(6):525–530, 2013.

[88] J. J. Carreño-Zagarra and R. Vilamizar. Nonlinear robust control of offshore wind turbines based on flat filtering and reset compensation. In *2018 IEEE 14th*

International Conference on Control and Automation (ICCA), pages 1186–1191. IEEE, 2018.

[89] M. Cerdeira, P. Falcón, E. Delgado, and A. Barreiro. Reset controller design based on error minimization for a lane change maneuver. *Sensors*, 18(7):2204, 2018.

[90] M. Cerdeira-Corujo, A. Costas, E. Delgado, and A. Barreiro. Comparative analysis of gain-scheduled wheel slip reset controllers with different reset strategies in automotive brake systems. In *CONTROLO 2016*, pages 751–761. Springer, 2017.

[91] M. Cerdeira-Corujo, A. Costas, E. Delgado, A. Barreiro, and A. Baños. Gain-scheduled wheel slip reset control in automotive brake systems. In *2016 International Symposium on Power Electronics, Electrical Drives, Automation and Motion (SPEEDAM)*, pages 1255–1260. IEEE, 2016.

[92] M. Cerdeira Corujo, P. Falcon Oubiña, A. Barreiro Blas, M. E. Delgado Romero, M. R. Diaz Cacho Medina, et al. Control reset para maniobra de cambio de carril y validación con CarSim. In *XXXVIII Jornadas de Automática, Gijón, España, 6-8 septiembre 2017*. Enxeñaría de sistemas e automática, 2017.

[93] M. Cerdeira Corujo, P. Falcon Oubiña, M. E. Delgado Romero, A. Barreiro Blas, M. R. Diaz Cacho Medina, et al. Tuning of a reset controller via genetic algorithms for an ACC system in following mode. In *Event-Based Control, Communication and Signal Processing 2018, Perpiñán, Francia, 27-29 junio 2018*. Enxeñaría de sistemas e automática, 2018.

[94] Y. Chait and C. Hollot. On Horowitz's contributions to reset control. *International Journal of Robust and Nonlinear Control: IFAC-Affiliated Journal*, 12(4):335–355, 2002.

[95] C.-T. Chen, T.-Y. Tsai, Y.-J. Chiu, and C.-C. Wang. Sampling rate enhancement for SAR-ADCs using adaptive reset approach for fog systems. In *2019 IEEE 13th International Conference on ASIC (ASICON)*, pages 1–4. IEEE, 2019.

[96] L. Chen, N. Saikumar, S. Baldi, and S. H. HosseinNia. Beyond the waterbed effect: Development of fractional order crone control with non-linear reset. In *2018 Annual American Control Conference (ACC)*, pages 545–552. IEEE, 2018.

[97] L. Chen, N. Saikumar, and S. H. HosseinNia. Development of robust fractional-order reset control. *IEEE Transactions on Control Systems Technology*, 28(4):1404–1417, 2019.

[98] Q. Chen. *Reset control systems: Stability, performance and application*. PhD thesis, University of Massachusetts, 2000.

[99] Q. Chen, Y. Chait, and C. Hollot. Analysis of reset control systems consisting of a FORE and second-order loop. *J. Dyn. Sys., Meas., Control*, 123(2):279–283, 2001.

[100] Q. Chen, C. Hollot, and Y. Chait. BIBO stability of a class of reset control systems. In *Proceedings of the 2000 Conference on Information Sciences and Systems*, page 39, 2000.

[101] Q. Chen, C. Hollot, and Y. Chait. Stability and asymptotic performance analysis of a class of reset control systems. In *Proceedings of the 39th IEEE Conference on Decision and Control*, volume 1, pages 251–256. IEEE, 2000.

[102] Q. Chen, C. Hollot, Y. Chait, and O. Beker. On reset control systems with second-order plants. In *Proceedings of the 2000 American Control Conference. ACC*, volume 1, pages 205–209. IEEE, 2000.

[103] Y. Chen and Y. Guo. Stability of Lur'e-type discrete-time reset control systems. In *2018 13th World Congress on Intelligent Control and Automation (WCICA)*, pages 93–98. IEEE, 2018.

[104] Y. Cheng and W. Hu. A reset control approach to consensus of first-order discrete-time multi-agent systems. In *2022 IEEE 17th International Conference on Control & Automation (ICCA)*, pages 880–884. IEEE, 2022.

[105] Y. Cheng, W. Hu, Y. Guo, and Y. Xie. Reset control for leader-following consensus of multi-agent systems. *ISA transactions*, 2022.

[106] J. C. Clegg. A nonlinear integrator for servomechanisms. *Transactions of the American Institute of Electrical Engineers, Part II: Applications and Industry*, 77(1):41–42, March 1958.

[107] M. Cordioli, M. Mueller, F. Panizzolo, F. Biral, and L. Zaccarian. An adaptive reset control scheme for valve current tracking in a power-split transmission

system. In *2015 European Control Conference (ECC)*, pages 1884–1889. IEEE, 2015.

[108] A. Costas, M. Cerdeira-Corujo, A. Barreiro, E. Delgado, and A. Baños. Car platooning reconfiguration applying reset control techniques. In *2016 IEEE 21st International Conference on Emerging Technologies and Factory Automation (ETFA)*, pages 1–8. IEEE, 2016.

[109] A. Costas, M. C. Corujo, A. B. Blas, E. D. Romero, and A. B. Torrico. Control basado en reset para seguimiento de consigna en el sistema de control de crucero adaptativo. In *Actas de las XXXVII Jornadas de Automática. 7, 8 y 9 de septiembre de 2016, Madrid*, pages 85–92. Comité Español de Automática, 2021.

[110] H. Cui, G. Zhao, J. Mi, Z. Wang, and S. Liu. Convergence rate improvement for high-order nonlinear multi-agent systems by reset mechanism. In *2021 40th Chinese Control Conference (CCC)*, pages 5008–5013. IEEE, 2021.

[111] A. A. Dastjerdi, A. Astolfi, and S. H. HosseinNia. A frequency-domain stability method for reset systems. In *2020 59th IEEE Conference on Decision and Control (CDC)*, pages 5785–5791. IEEE, 2020.

[112] A. A. Dastjerdi, A. Astolfi, N. Saikumar, N. Karbasizadeh, D. Valério, and S. H. HosseinNia. Closed-loop frequency analysis of reset control systems. *IEEE Transactions on Automatic Control*, 2022.

[113] A. A. Dastjerdi and S. H. Hosseinnia. A frequency-domain tuning method for a class of reset control systems. *IEEE Access*, 9:40950–40962, 2021.

[114] A. A. Dastjerdi, N. Saikumar, and S. H. HosseinNia. Tuning of a class of reset elements using pseudo-sensitivities. In *2021 European Control Conference (ECC)*, pages 1187–1192. IEEE, 2021.

[115] M. Davanipour, A. Khayatian, and M. Dehghani. Optimal adaptive reset control with guaranteed transient and steady state tracking error bounds. *Journal of the Franklin Institute*, 354(14):5949–5963, 2017.

[116] M. Davanipour, A. Khayatian, and M. Dehghani. Transient performance improvement of model reference adaptive control: LMI-based resetting. *International Journal of Adaptive Control and Signal Processing*, 32(2):390–402, 2018.

[117] M. Davanipour, A. Khayatian, M. Dehghani, and M. Arefi. A solution for enhancement of transient performance in nonlinear adaptive control: Optimal adaptive reset based on barrier Lyapunov function. *ISA transactions*, 80:169–175, 2018.

[118] M. Davó. *Analysis and Design of Reset Control Systems*. PhD thesis, Universidad de Murcia, 2015.

[119] M. Davó and A. Baños. Reset control of integrating plus dead time processes. *Journal of Process Control*, 38:22–30, 2016.

[120] M. Davó, A. Baños, and J. Moreno. Region of attraction estimation for saturated reset control systems. In *2014 14th International Conference on Control, Automation and Systems (ICCAS 2014)*, pages 6–11. IEEE, 2014.

[121] M. Davó, F. Gouaisbaut, A. Baños, S. Tarbouriech, and A. Seuret. Stability of time-delay reset control systems with time-dependent resetting law. *IFAC-PapersOnLine*, 48(27):371–376, 2015. Analysis and Design of Hybrid Systems ADHS.

[122] M. A. Davó and A. Baños. PI+CI tuning for integrating plus deadtime systems. In *Proceedings of 2012 IEEE 17th International Conference on Emerging Technologies & Factory Automation (ETFA 2012)*, pages 1–4. IEEE, 2012.

[123] M. A. Davó and A. Baños. Delay-dependent stability of reset control systems with input/output delays. In *52nd IEEE Conference on Decision and Control*, pages 2018–2023, 2013.

[124] M. A. Davo and A. Banos. Reset control of a liquid level process. In *2013 IEEE 18th Conference on Emerging Technologies & Factory Automation (ETFA)*. IEEE, Sept. 2013.

[125] M. A. Davo, A. Baños, F. Gouaisbaut, S. Tarbouriech, and A. Seuret. Stability analysis of linear impulsive delay dynamical systems via looped-functionals. *Automatica*, 81:107–114, 2017.

[126] M. A. Davó, F. Gouaisbaut, A. Baños, S. Tarbouriech, and A. Seuret. Exponential stability of a PI plus reset integrator controller by a sampled-data system approach. *Nonlinear Analysis: Hybrid Systems*, 29:133–146, 2018.

[127] M. Á. Davó Navarro. Analyis and design of reset control systems. *Proyecto de investigación:*, 2015.

[128] B. De Schutter, W. Heemels, J. Lunze, C. Prieur, et al. Survey of modeling, analysis, and control of hybrid systems. *Handbook of Hybrid Systems Control–Theory, Tools, Applications*, pages 31–55, 2009.

[129] E. Delgado, A. Barreiro, M. Díaz-Cacho, and P. Falcón. Wheel slip reset controller in automotive brake systems. In *2014 IEEE International Electric Vehicle Conference (IEVC)*, pages 1–6. IEEE, 2014.

[130] E. Delgado, A. Barreiro, M. Díaz-Cacho, and P. Falcón. Performance analysis of wheel slip reset controller in brake systems. In *2015 International Conference on Electrical Systems for Aircraft, Railway, Ship Propulsion and Road Vehicles (ESARS)*, pages 1–6. IEEE, 2015.

[131] E. Delgado, M. Díaz-Cacho, A. Baños, and A. Barreiro. Reset control of synchronous motors with permanent magnet excitation. In *22nd Mediterranean Conference on Control and Automation*, pages 1347–1352. IEEE, 2014.

[132] J. Doktian, W. Pongyart, and P. Vanichchanunt. Development of a semi autotuning algorithm for PI+CI reset controller. In *2019 First International Symposium on Instrumentation, Control, Artificial Intelligence, and Robotics (ICA-SYMP)*, pages 155–158. IEEE, 2019.

[133] S. Dormido, A. Baños, and A. Barreiro. Interactive tool for analysis of reset control systems. In *2011 50th IEEE Conference on Decision and Control and European Control Conference*, pages 4765–4770. IEEE, 2011.

[134] Z. Echreshavi, M. Farbood, M. Shasadeghi, and M. Asemani. Reset method based unknown input observer design for continuous-time ts fuzzy system. In *2020 28th Iranian Conference on Electrical Engineering (ICEE)*, pages 1–5. IEEE, 2020.

[135] Z. Echreshavi, M. Shasadeghi, M. H. Asemani, S. Mobayen, and A. Fekih. Fuzzy reset-based $\mathcal{H}_\infty$ unknown input observer design for uncertain nonlinear systems with unmeasurable premise variables. *IEEE Access*, 9:151729–151740, 2021.

[136] E. Eitelberg. *Load sharing control*. NOYB Press, 1999.

[137] E. Eitelberg. Load sharing in a multivariable temperature control system. *Control engineering practice*, 7(11):1369–1377, 1999.

[138] K. El Rifai and O. El Rifai. Design of hybrid resetting PID and lag controllers with application to motion control. In *2009 IEEE/ASME International Conference on Advanced Intelligent Mechatronics*, pages 685–692. IEEE, 2009.

[139] L. Etienne and S. Di Gennaro. Event–triggered observation of nonlinear Lipschitz systems via impulsive observers. *IFAC-PapersOnLine*, 49(18):666–671, 2016.

[140] P. Falcón, A. Barreiro, and M. D. Cacho. Modeling of parrot ardrone and passivity-based reset control. In *2013 9th Asian control conference (ASCC)*, pages 1–6. IEEE, 2013.

[141] P. Falcón, M. Cerdeira, E. Delgado, M. Díaz Cacho, and A. Barreiro. Modelado y control reset de una planta ABS experimental. *Actas de las XXXIX Jornadas de Automática, Badajoz, 5-7 de Septiembre de 2018*, 2018.

[142] P. Falcón, M. Cerdeira, E. Delgado, M. Diaz-Cacho, J. L. Camaño, and A. Barreiro. Reset control with sector confinement for a lane change maneuver. In *IECON 2019-45th Annual Conference of the IEEE Industrial Electronics Society*, volume 1, pages 521–526. IEEE, 2019.

[143] A. Fernández, A. Barreiro, A. Baños, and J. Carrasco. Reset control for passive teleoperation. In *2008 34th Annual Conference of IEEE Industrial Electronics*, pages 2935–2940. IEEE, 2008.

[144] A. Fernández, A. Barreiro, J. Carrasco, and A. Baños. Reset control for passive bilateral teleoperation. *IEEE Transactions on Industrial Electronics*, 58(7):3037–3045, 2010.

[145] F. Ferrante and L. Zaccarian. Dynamic reset output feedback with guaranteed convergence rate. *IFAC-PapersOnLine*, 52(16):102–107, 2019.

[146] F. Fichera. *Lyapunov techniques for a class of hybrid systems and reset controller syntheses for continuous-time plants*. PhD thesis, ISAE-TOULOUSE, 2013.

[147] F. Fichera, C. Prieur, S. Tarbouriech, and L. Zaccarian. LMI-based reset $\langle_\infty$ design for linear continuous-time plants. *IEEE Transactions on Automatic Control*, 61(12):4157–4163, 2016.

[148] F. Forni, D. Nešić, and L. Zaccarian. Reset passivation of nonlinear controllers via a suitable time-regular reset map. *Automatica*, 47(9):2099–2106, 2011.

[149] J. Freudenberg, R. Middleton, and A. Stefanpoulou. A survey of inherent design limitations. In *Proceedings of the 2000 American Control Conference. ACC (IEEE Cat. No. 00CH36334)*, volume 5, pages 2987–3001. IEEE, 2000.

[150] S. Gagliano, F. Cairone, A. Amenta, and M. Bucolo. A real time feed forward control of slug flow in microchannels. *Energies*, 12(13):2556, 2019.

[151] J. Gao, H. Gu, Y. Yang, and P. Yuan. Improve supply manifold pressure of proton exchange membrane fuel cell by using of reset control. *Electrotehnica, Electronica, Automatica*, 70(2):29–36, 2022.

[152] M. Garcia-Sanz and F. Hadaegh. Load-sharing robust control of spacecraft formations: deep space and low earth elliptic orbits. *IET Control Theory & Applications*, 1(2):475–484, 2007.

[153] P. García. *Reset observers and temperature control for induction hobs*. PhD thesis, Universidad de Zaragoza, 2011.

[154] V. Ghaffari, P. Karimaghaee, and A. Khayatian. Development of a real-time model-prediction-based framework for reset controller design. *Industrial & Engineering Chemistry Research*, 53(38):14755–14764, 2014.

[155] V. Ghaffari, P. Karimaghaee, and A. Khayatian. Reset law design based on robust model predictive strategy for uncertain systems. *Journal of Process Control*, 24(1):261–268, 2014.

[156] V. Ghaffari, P. Karimaghaee, and A. Khayatian. Stability analysis and performance improvement of uncertain linear systems with designing of a suitable reset law. *IET Control Theory & Applications*, 9(17):2532–2540, 2015.

[157] V. Ghaffari, P. Karimaghaee, and A. Khayatian. A reset-time dependent approach for stability analysis of nonlinear reset control systems. *Asian Journal of Control*, 18(5):1856–1866, 2016.

[158] R. Goebel, R. G. Sanfelice, and A. R. Teel. Hybrid dynamical systems. *IEEE Control Systems Magazine*, 29(2):28–93, 2009.

[159] R. Goebel, R. G. Sanfelice, and A. R. Teel. *Hybrid dynamical systems: modeling stability, and robustness*. Princeton University Press, Princeton, NJ, 2012.

[160] J. A. González. *Hybrid reset control systems. Analysis, design and applications.* PhD thesis, Universidad de La Rioja, 2014.

[161] J. A. González, A. Barreiro, S. Dormido, and P. Falcón. Performance improvement of SISO linear control systems by hybrid state resetting and sector confinement of trajectories. *International Journal of Robust and Nonlinear Control*, 26(18):4008–4034, 2016.

[162] K. Gruntjens, M. F. Heertjes, S. Van Loon, N. Van De Wouw, and W. Heemels. Hybrid integral reset control with application to a lens motion system. In *2019 American Control Conference (ACC)*, pages 2408–2413. IEEE, 2019.

[163] C. P. Guillén-Flores, B. Castillo-Toledo, J. P. García-Sandoval, S. Di Gennaro, and V. G. Álvarez. A reset observer with discrete/continuous measurements for a class of fuzzy nonlinear systems. *Journal of the Franklin Institute*, 350(8):1974–1991, 2013.

[164] G. Guo. Joint design of reset controller and communication scheme. *International Journal of Innovative Computing, Imformation and Control*, 6(2):733–746, 2010.

[165] G. Guo, S. Yu, and Z. Ma. Some properties of networked reset control systems. *IEE Proceedings-Control Theory and Applications*, 153(1):14–20, 2006.

[166] Y. Guo. Forward completeness and stability of discrete-time reset systems. *Journal of Systems Science and Mathematical Sciences*, 36(10):1597, 2016.

[167] Y. Guo and Y. Chen. Stability analysis of delayed reset systems with distributed state resetting. *Nonlinear Analysis: Hybrid Systems*, 31:265–274, 2019.

[168] Y. Guo, W. Gui, and C. Yang. Quadratic stability of uncertain reset control systems. *IFAC Proceedings Volumes*, 44(1):6297–6300, 2011.

[169] Y. Guo, W. Gui, C. Yang, and L. Xie. On reset control systems with discrete-time triggering conditions. *IFAC Proceedings Volumes*, 44(1):6291–6296, 2011.

[170] Y. Guo, W. Gui, C. Yang, and L. Xie. Stability analysis and design of reset control systems with discrete-time triggering conditions. *Automatica*, 48(3):528–535, 2012.

[171] Y. Guo and W. He. Stability analysis of nonlinear reset control systems with smooth baseline modes. In *Proceedings of the 30th Chinese Control Conference*, pages 1190–1194. IEEE, 2011.

[172] Y. Guo, Y. Wang, and L. Xie. Mid-frequency disturbance rejection of hdd systems. In *2007 Chinese Control Conference*, pages 56–60. IEEE, 2007.

[173] Y. Guo, Y. Wang, and L. Xie. Frequency-domain properties of reset systems with application in hard-disk-drive systems. *IEEE Transactions on Control Systems Technology*, 17(6):1446–1453, 2009.

[174] Y. Guo, Y. Wang, and L. Xie. Robust stability of reset control systems with uncertain output matrix. *Automatica*, 48(8):1879–1884, 2012.

[175] Y. Guo, Y. Wang, L. Xie, H. Li, and W. Gui. Optimal reset law design of reset control systems with application to HDD systems. In *Proceedings of the 48h IEEE Conference on Decision and Control (CDC) held jointly with 2009 28th Chinese Control Conference*, pages 5287–5292. IEEE, 2009.

[176] Y. Guo, Y. Wang, L. Xie, H. Li, and W. Gui. Optimal reset law design and its application to transient response improvement of HDD systems. *IEEE transactions on control systems technology*, 19(5):1160–1167, 2011.

[177] Y. Guo, Y. Wang, L. Xie, and J. Zheng. Stability analysis and design of reset systems: Theory and an application. *Automatica*, 45(2):492–497, 2009.

[178] Y. Guo, Y. Wang, J. Zheng, and L. Xie. Stability analysis, design and application of reset control systems. In *2007 IEEE International Conference on Control and Automation*, pages 3196–3201. IEEE, 2007.

[179] Y. Guo and L. Xie. Quadratic stability of reset control systems with delays. In *Proceedings of the 10th World Congress on Intelligent Control and Automation*, pages 2268–2273. IEEE, 2012.

[180] Y. Guo, L. Xie, and Y. Wang. *Analysis and design of reset control systems*, volume 2. school of Engineering and Technology, 2015.

[181] Y. Guo and W. Zhu. A hybrid index model for discrete-time reset control systems. In *Proceedings of the 33rd Chinese Control Conference*, pages 3939–3944. IEEE, 2014.

[182] P.-O. Gutman, E. Horesh, R. Guetta, and M. Borshchevsky. Control of the aero-electric power station—an exciting QFT application for the 21st century. *International Journal of Robust and Nonlinear Control: IFAC-Affiliated Journal*, 13(7):619–636, 2003.

[183] W. M. Haddad, V. Chellaboina, and S. G. Nersesov. *Impulsive and Hybrid Dynamical Systems: Stability, Dissipativity, and Control*. Princeton University Press, 2006.

[184] W. M. Haddad, V. Chellabsina, and N. Kablar. Active control of combustion instabilities via hybrid resetting controllers. In *Proceedings of the 2000 American Control Conference. ACC*, volume 4, pages 2378–2382. IEEE, 2000.

[185] L. Hazeleger, M. Heertjes, and H. Nijmeijer. Second-order reset elements for stage control design. In *2016 American Control Conference (ACC)*, pages 2643–2648. IEEE, 2016.

[186] K. He, C. Dong, and Q. Wang. Active disturbance rejection control for uncertain nonlinear systems with sporadic measurements. *IEEE/CAA Journal of Automatica Sinica*, 9(5):893–906, 2022.

[187] W. Heemels, P. Bernard, K. Scheres, R. Postoyan, and R. Sanfelice. Hybrid systems with continuous-time inputs: subtleties in solution concepts and existence results. In *60th IEEE Conference on Decision and Control*, 2021.

[188] W. Heemels, G. Dullerud, and A. Teel. $\mathcal{L}_2$-gain analysis for a class of hybrid systems with applications to reset and event-triggered control: A lifting approach. *IEEE Transactions on Automatic Control*, 61(10):2766–2781, 2015.

[189] M. Heertjes, K. Gruntjens, S. Van Loon, N. Van de Wouw, and W. Heemels. Experimental evaluation of reset control for improved stage performance. *IFAC-PapersOnLine*, 49(13):93–98, 2016.

[190] M. F. Heertjes, K. Gruntjens, S. van Loon, N. Kontaras, and W. Heemels. Design of a variable gain integrator with reset. In *2015 American Control Conference (ACC)*, pages 2155–2160. IEEE, 2015.

[191] M. A. Henson, B. A. Ogunnaike, and J. S. Schwaber. Habituating control strategies for process control. *AIChE Journal*, 41(3):604–618, 1995.

[192] L. Hetel, J. Daafouz, S. Tarbouriech, and C. Prieur. Reset control systems: stabilization by nearly-periodic reset. *IFAC Proceedings Volumes*, 44(1):2395–2400, 2011.

[193] L. Hetel, J. Daafouz, S. Tarbouriech, and C. Prieur. Stabilization of linear impulsive systems through a nearly-periodic reset. *Nonlinear Analysis: Hybrid Systems*, 7(1):4–15, 2013.

[194] C. Hollot, O. Beker, Y. Chait, and Q. Chen. On establishing classic performance measures for reset control systems. In *Perspectives in robust control*, pages 123–147. Springer, 2001.

[195] C. Hollot, Y. Zheng, and Y. Chait. Stability analysis for control systems with reset integrators. In *Proceedings of the 36th IEEE Conference on Decision and Control*, volume 2, pages 1717–1719. IEEE, 1997.

[196] F. Hong and W. Wong. A reset PI-lead filter design with application in hard disk drives. In *Asia-Pacific Magnetic Recording Conference 2006*, pages 1–1. IEEE, 2006.

[197] I. Horowitz and P. Rosenbaum. Non-linear design for cost of feedback reduction in systems with large parameter uncertainty. *International Journal of Control*, 21(6):977–1001, 1975.

[198] I. Hosseini, M. Fiacchini, P. Karimaghaee, and A. Khayatian. Optimal reset unknown input observer design for fault and state estimation in a class of nonlinear uncertain systems. *Journal of the Franklin Institute*, 357(5):2978–2996, 2020.

[199] I. Hosseini, A. Khayatian, P. Karimaghaee, M. Fiacchini, and M. A. Davo Navarro. LMI-based reset unknown input observer for state estimation of linear uncertain systems. *IET Control Theory & Applications*, 13(12):1872–1881, 2019.

[200] S. HosseinNia. *Fractional hybrid control systems: Modeling, analysis and applications to mobile robotics and mechatronics*. PhD thesis, Universidad de Extremadura, 2013.

[201] S. H. HosseinNia, I. Tejado, D. Torres, B. M. Vinagre, and V. Feliu. A general form for reset control including fractional order dynamics. *IFAC Proceedings Volumes*, 47(3):2028–2033, 2014.

[202] S. H. HosseinNia, I. Tejado, and B. M. Vinagre. Basic properties and stability of fractional-order reset control systems. In *2013 European Control Conference (ECC)*, pages 1687–1692. IEEE, 2013.

[203] S. H. HosseinNia, I. Tejado, and B. M. Vinagre. Fractional order hybrid systems and their stability. In *Proceedings of the 14th International Carpathian Control Conference (ICCC)*, pages 128–133. IEEE, 2013.

[204] S. H. HosseinNia, I. Tejado, and B. M. Vinagre. Fractional-order reset control: Application to a servomotor. *Mechatronics*, 23(7):781–788, 2013.

[205] S. H. HosseinNia, I. Tejado, and B. M. Vinagre. Hybrid systems and control with fractional dynamics (i): Modeling and analysis. In *ICFDA'14 International Conference on Fractional Differentiation and Its Applications 2014*, pages 1–6. IEEE, 2014.

[206] S. H. HosseinNia, I. Tejado, and B. M. Vinagre. Hybrid systems and control with fractional dynamics (ii): Control. In *ICFDA'14 International Conference on Fractional Differentiation and Its Applications 2014*, pages 1–6. IEEE, 2014.

[207] S. H. HosseinNia, I. Tejado, B. M. Vinagre, and Y. Chen. Iterative learning and fractional reset control. In *International Design Engineering Technical Conferences and Computers and Information in Engineering Conference*, volume 57199, page V009T07A041. American Society of Mechanical Engineers, 2015.

[208] G. Hostetter and J. Meditch. On the generalization of observers to systems with unmeasurable, unknown inputs. *Automatica*, 9(6):721–724, 1973.

[209] X. Hou, A. A. Dastjerdi, N. Saikumar, and S. H. Hosseinnia. Tuning of 'constant in gain lead in phase (CgLp)' reset controller using higher-order sinusoidal input describing function (HOSIDF). In *2020 Australian and New Zealand Control Conference (ANZCC)*, pages 91–96. IEEE, 2020.

[210] H. Hu, Y. Zheng, Y. Chait, and C. Hollot. On the zero-input stability of control systems with clegg integrators. In *Proceedings of the 1997 American Control Conference (Cat. No. 97CH36041)*, volume 1, pages 408–410. IEEE, 1997.

[211] W. Hu, Y. Cheng, and Z. Chen. Reset control for consensus of double-integrator multi-agent systems. *Automatica*, 136:110057, 2022.

[212] B. Hunnekens, N. Wouw, and D. Nešić. Overcoming a fundamental time-domain performance limitation by nonlinear control. *Automatica*, 67:277–281, 2016.

[213] Y. Ishino, T. Mizuno, M. Takasaki, and D. Yamaguchi. Stabilization of magnetic suspension system by using first-order-reset element without derivative feedback. In *2019 12th Asian Control Conference (ASCC)*, pages 690–694. IEEE, 2019.

[214] Y. Ishino, T. Mizuno, M. Takasaki, and D. Yamaguchi. Stabilization of magnetic suspension system by using only a first-order reset element without a derivative element. In *Actuators*, volume 8, page 24. MDPI, 2019.

[215] M. Iwai. Reset control of nonlinear chaotic systems using describing function. In *2017 17th International Conference on Control, Automation and Systems (ICCAS)*, pages 647–649. IEEE, 2017.

[216] M. Iwai. Reset control of combustion oscillation in lean premixed combustor. In *2018 18th International Conference on Control, Automation and Systems (ICCAS)*, pages 207–211. IEEE, 2018.

[217] M. Iwai. Reset control of combustion oscillation model. In *2019 12th Asian Control Conference (ASCC)*, pages 1019–1023. IEEE, 2019.

[218] M. Iwai and T. Ushio. Prediction of limit cycles in nonlinear systems with reset controllers using describing function. In *2015 15th International Conference on Control, Automation and Systems (ICCAS)*, pages 913–918. IEEE, 2015.

[219] M. Iwai and T. Ushio. Reset control of pressure-drop oscillations in boiling microchannel systems. In *2016 16th International Conference on Control, Automation and Systems (ICCAS)*, pages 626–630. IEEE, 2016.

[220] O. Jaramillo, B. Castillo-Toledo, and S. Di Gennaro. Impulsive observer–based stabilization for a class of Lipschitz nonlinear systems with time–varying uncertainties. *Journal of the Franklin Institute*, 357(17):12518–12537, 2020.

[221] O. Jaramillo, B. Castillo-Toledo, and S. Di Gennaro. Impulsive observer design for a class of nonlinear Lipschitz systems with time-varying uncertainties. *Journal of the Franklin Institute*, 357(11):7423–7437, 2020.

[222] S. Jayasuriya and M. A. Franchek. A QFT-type design methodology for a parallel plant structure and its application in idle speed control. *International Journal of Control*, 60(5):653–670, 1994.

[223] Y. Jin, W. Kwon, J. Yun, and S. Lee. Dissipative reset adaptive observer for a class of singular systems. In *2017 11th Asian Control Conference (ASCC)*, pages 2095–2100. IEEE, 2017.

[224] S. Joraked, W. Pongyart, and K. Angkeaw. Design and implementation of a FPAA based PI+CI reset controller emulator. In *2018 18th International Symposium on Communications and Information Technologies (ISCIT)*, pages 266–269. IEEE, 2018.

[225] M. B. Kaczmarek, X. Zhang, and S. H. HosseinNia. Steady-state nonlinearity of open-loop reset systems. *arXiv preprint arXiv:2206.10275*, 2022.

[226] N. Karbasizadeh, A. A. Dastjerdi, N. Saikumar, and S. H. HosseinNia. Band-passing nonlinearity in reset elements. *IEEE Transactions on Control Systems Technology*, 2022.

[227] N. Karbasizadeh, A. A. Dastjerdi, N. Saikumar, D. Valério, and S. H. H. Nia. Benefiting from linear behaviour of a nonlinear reset-based element at certain frequencies. In *2020 Australian and New Zealand Control Conference (ANZCC)*, pages 226–231. IEEE, 2020.

[228] N. Karbasizadeh and S. H. HosseinNia. Complex-order reset control system. In *2022 IEEE/ASME International Conference on Advanced Intelligent Mechatronics (AIM)*. IEEE, July 2022.

[229] N. Karbasizadeh and S. H. HosseinNia. Continuous reset element: Transient and steady-state analysis for precision motion systems. *Control Engineering Practice*, 126:105232, 2022.

[230] N. Karbasizadeh and S. H. HosseinNia. Stacking integrators without sacrificing the overshoot in reset control systems. In *2022 American Control Conference (ACC)*, pages 893–899. IEEE, 2022.

[231] N. Karbasizadeh, N. Saikumar, and S. H. HosseinNia. Fractional-order single state reset element. *Nonlinear Dynamics*, 104(1):413–427, 2021.

[232] C. Karybakas. Nonlinear integrator with zero phase shift. *IEEE Transactions on Industrial Electronics and Control Instrumentation*, 24(2):150–152, 1977.

[233] B. Kieft, S. H. HosseinNia, and N. Saikumar. Reset band for mitigation of quantization induced performance degradation. In *2021 European Control Conference (ECC)*, pages 2465–2472. IEEE, 2021.

[234] B. Kieft, S. H. HosseinNia, and N. Saikumar. Time regularization as a solution to mitigate quantization induced performance degradation. In *2021 European Control Conference (ECC)*, pages 2458–2464. IEEE, 2021.

[235] K. Krishnan and I. M. Horowitz. Synthesis of a nonlinear feedback system with significant plant-ignorance for prescribed system tolerances. *International Journal of Control*, 19(4):689–706, 1974.

[236] N. M. Krylov and N. Bogoliubov. *Introduction to Nonlinear Mechanics*. Princeton University Press, Princeton, NJ, 1943.

[237] N. M. Krylov and N. N. Bogoliubov. *Introduction to non-linear mechanics. (AM-11), volume 11*. Annals of Mathematics Studies. Princeton University Press, Princeton, NJ, Dec. 1949.

[238] R. Lahee. Application of reset control to a batch reactor in the precious group metals industry. *IFAC Proceedings Volumes*, 40(12):916–921, 2007.

[239] J. H. Le and A. R. Teel. Passive soft-reset controllers for nonlinear systems. In *2021 60th IEEE Conference on Decision and Control (CDC)*, pages 5320–5325. IEEE, 2021.

[240] H. Li, C. Du, and Y. Wang. Discrete-time $\mathcal{H}_2$ optimal reset control with application to hdd track-following. In *2009 Chinese Control and Decision Conference*, pages 3613–3617. IEEE, 2009.

[241] H. Li, C. Du, and Y. Wang. Optimal reset control for a dual-stage actuator system in HDDs. *IEEE/ASME Transactions on Mechatronics*, 16(3):480–488, 2011.

[242] H. Li, C. Du, Y. Wang, and Y. Guo. Discrete-time optimal reset control for hard disk drive servo systems. *IEEE transactions on magnetics*, 45(11):5104–5107, 2009.

[243] H. Li, C. Du, Y. Wang, and Y. Guo. Discrete-time optimal reset control for the improvement of HDD servo control transient performance. In *2009 American Control Conference*, pages 4153–4158. IEEE, 2009.

[244] H. Li, C. Du, Y. Wang, and Y. Guo. Optimal reset control for a hard disk drive dual-stage actuator system. In *2009 Asia-Pacific Magnetic Recording Conference*, pages 1–2. IEEE, 2009.

[245] H. Li and Y. Wang. A unified controller design using two different types of optimal reset control laws for HDD servo systems. In *2010 11th International Conference on Control Automation Robotics & Vision*, pages 2242–2247. IEEE, 2010.

[246] L. Li, F. Wu, and X. Wang. A reset controller design method for MIMO linear systems. In *Proceedings of the 32nd Chinese Control Conference*, pages 2132–2136. IEEE, 2013.

[247] M. Li and M. Deng. Operator-based reset control for nonlinear system with unknown disturbance. *IEICE TRANSACTIONS on Fundamentals of Electronics, Communications and Computer Sciences*, 101(5):755–762, 2018.

[248] Y. Li, G. Guo, and Y. Wang. Nonlinear mid-frequency disturbance compensation in hard disk drives. *IFAC Proceedings Volumes*, 38(1):31–36, 2005.

[249] Y. Li, G. Guo, and Y. Wang. Phase lead reset control design with an application to HDD servo systems. In *2006 9th International Conference on Control, Automation, Robotics and Vision*, pages 1–6. IEEE, 2006.

[250] Y. Li, G. Guo, and Y. Wang. Reset control for midfrequency narrowband disturbance rejection with an application in hard disk drives. *IEEE Transactions on Control Systems Technology*, 19(6):1339–1348, 2011.

[251] W. Linli, S. Zhangyi, H. Mousavi, and H. Gu. A novel robust reset controller implemented through field programmable gate array for oxygen ratio regulation of proton exchange membrane fuel cell. *Computers and Electrical Engineering*, 99:107788, 2022.

[252] J. Liu and A. R. Teel. Hybrid systems with memory: Modelling and stability analysis via generalized solutions. *IFAC Proceedings Volumes*, 47(3):6019–6024, 2014.

[253] J. Liu and A. R. Teel. Hybrid systems with memory: existence and well-posedness of generalized solutions. *SIAM Journal on Control and Optimization*, 56(2):1011–1037, 2018.

[254] Y. Liu, B. Xu, and G. Wang. Ship roll reduction system based on reset control. *Electric Machines and Control*, 17(8):85–90, 2013.

[255] T. Loquen. *Some results on reset control systems*. PhD thesis, Institut National Polytechnique de Toulouse, 2010.

[256] T. Loquen, D. Nesic, C. Prieur, S. Tarbouriech, A. R. Teel, and L. Zaccarian. Piecewise quadratic Lyapunov functions for linear control systems with first order reset elements. *IFAC Proceedings Volumes*, 43(14):807–812, 2010.

[257] T. Loquen, S. Tarbouriech, and C. Prieur. Stability of reset control systems with nonzero reference. In *2008 47th IEEE Conference on Decision and Control*, pages 3386–3391. IEEE, 2008.

[258] Y.-S. Lu and Y.-C. Lee. Generalized Clegg integrator for integral feedback control systems. *Proceedings of the school of Mechanical Engineers, Part I: Journal of Systems and Control Engineering*, 227(6):556–560, 2013.

[259] M. S. Mahmoud and B. J. Karaki. Delay dependent robust stability of reset systems. In *IECON 2018-44th Annual Conference of the IEEE Industrial Electronics Society*, pages 2251–2255. IEEE, 2018.

[260] M. S. Mahmoud and B. J. Karaki. Improved stability analysis and control design of reset systems. *IET Control Theory & Applications*, 12(17):2328–2336, 2018.

[261] K. McDonough and I. Kolmanovsky. Integrator resetting for enforcing constraints in aircraft flight control systems. In *AIAA Guidance, Navigation, and Control Conference*, page 1995, 2015.

[262] X. Meng, L. Xie, and Y. C. Soh. Reset control for multi-agent systems. In *2016 American Control Conference (ACC)*, pages 3746–3751. IEEE, 2016.

[263] X. Meng, L. Xie, and Y. C. Soh. Reset control of multi-agent systems with double integrator dynamics. In *2016 35th Chinese Control Conference (CCC)*, pages 8049–8054. IEEE, 2016.

[264] X. Meng, L. Xie, and Y. C. Soh. Reset control for synchronization of multi-agent systems. *Automatica*, 104:189–195, 2019.

[265] Z. Meng, W. Zhenhua, W. Yan, and S. Yi. A fast fault diagnosis method based on reset augmented observer. In *2015 34th Chinese Control Conference (CCC)*, pages 6291–6296. IEEE, 2015.

[266] P. Mercader, J. Carrasco, and A. Baños. IQC analysis of reset control systems with time-varying delay. *International Journal of Control*, 92(9):2007–2014, 2019.

[267] P. Mercader, J. Carrasco, and A. Baños. IQC analysis for time-delay reset control systems with first order reset elements. In *52nd IEEE Conference on Decision and Control*, pages 2251–2256. IEEE, 2013.

[268] P. Mercader, M. A. Davo, and A. Baños. Performance analysis of PI and PI+CI compensation for an IPDT process. In *2015 23rd Mediterranean Conference on Control and Automation (MED)*, pages 231–236. IEEE, 2015.

[269] M. Mohadeszadeh, N. Pariz, and M. R. Ramezani-al. Exponential stability and $\mathcal{L}_2$ gain analysis of uncertain fractional reset control systems. *IMA Journal of Mathematical Control and Information*, 39(1):275–294, 2022.

[270] M. Mohadeszadeh, N. Pariz, and M. R. Ramezani-al. A fractional reset control scheme for a DC-DC buck converter. *International Journal of Dynamics and Control*, pages 1–12, 2022.

[271] M. Mohadeszadeh, N. Pariz, M. R. Ramezani-Al, et al. Stabilization of fractional switched linear systems via reset control technique. *ISA transactions*, 2022.

[272] M. Mohan, M. Kaczmarek, and S. H. HosseinNia. Resetting velocity feedback: Reset control for improved transient damping. In *2022 European Control Conference (ECC)*, pages 1421–1428. IEEE, 2022.

[273] Y. S. Moon, P. Park, W. H. Kwon, and Y. S. Lee. Delay-dependent robust stabilization of uncertain state-delayed systems. *International Journal of control*, 74(14):1447–1455, 2001.

[274] J. Moreno, J. Guzmán, J. Normey-Rico, A. Baños, and M. Berenguel. Improvements on the filtered Smith predictor using the Clegg integrator. *IFAC Proceedings Volumes*, 45(3):110–115, 2012.

[275] J. Moreno, J. Guzmán, J. Normey-Rico, A. Baños, and M. Berenguel. A combined FSP and reset control approach to improve the set-point tracking task of dead-time processes. *Control Engineering Practice*, 21(4):351–359, 2013.

[276] V. Moscardó, J. L. Díez, and J. Bondia. Parallel control of an artificial pancreas with coordinated insulin, glucagon, and rescue carbohydrate control actions. *Journal of diabetes science and technology*, 13(6):1026–1034, 2019.

[277] U. R. Nair, R. Costa-Castelló, and A. Baños. Grid voltage regulation using a reset PI+CI controller for energy storage systems. *IFAC-PapersOnLine*, 51(4):226–231, 2018.

[278] U. R. Nair, R. Costa-Castelló, and A. Baños. Reset control of boost converters. In *2018 Annual American Control Conference (ACC)*, pages 553–558. IEEE, 2018.

[279] U. R. Nair, R. Costa-Castelló, and A. Baños. Reset control for DC–DC converters: An experimental application. *IEEE access*, 7:128487–128497, 2019.

[280] D. Nesic, A. R. Teel, and L. Zaccarian. On necessary and sufficient conditions for exponential and $\mathcal{L}_2$ stability of planar reset systems. In *2008 American Control Conference*, pages 4140–4145. IEEE, 2008.

[281] D. Nesic, A. R. Teel, and L. Zaccarian. Stability and performance of SISO control systems with first-order reset elements. *IEEE Transactions on Automatic Control*, 56(11):2567–2582, 2011.

[282] D. Nešić, L. Zaccarian, and A. Teel. Stability properties of reset systems. *IFAC Proceedings volumes*, 38(1):67–72, 2005.

[283] D. Nešić, L. Zaccarian, and A. R. Teel. Stability properties of reset systems. *Automatica*, 44(8):2019–2026, 2008.

[284] S. Niculescu, C. De Souza, J. Dion, and L. Dugard. Robust stability and stabilization for uncertain linear systems with state delay: single delay case (I); multiple delay case (II). In *IFAC Workshop on Robust Control Design*, pages 469–480, 1994.

[285] E. Nikolov. Generalized reset-control with Clegg-integration - part 1. In *International Conference Automatics and Informatics*, 2018.

[286] P. Nuij. Higher-order sinusoidal input describing functions for the analysis of non-linear systems with harmonic responses. *Mechanical Systems and Signal Processing*, 20(8):1883–1904, 2006.

[287] M. Ogura and C. F. Martin. Stability analysis of positive semi-Markovian jump linear systems with state resets. *SIAM Journal on Control and Optimization*, 52(3):1809–1831, 2014.

[288] H. Padé. Sur la représentation approchée d'une fonction par des fractions rationnelles. In *Annales scientifiques de l'école Normale Supérieure*, volume 9, pages 3–93, 1892.

[289] D. Paesa, A. Baños, and C. Sagues. Optimal reset adaptive observer design. *Systems & control letters*, 60(10):877–883, 2011.

[290] D. Paesa, A. Baños, and C. Sagues. Reset observers for linear time-delay systems. a delay-independent approach. In *2011 50th IEEE Conference on Decision and Control and European Control Conference*, pages 4152–4157. IEEE, 2011.

[291] D. Paesa, J. Carrasco, O. Lucia, and C. Sagues. On the design of reset systems with unstable base: A fixed reset-time approach. In *IECON 2011-37th Annual Conference of the IEEE Industrial Electronics Society*, pages 646–651. IEEE, 2011.

[292] D. Paesa, C. Franco, S. Llorente, G. Lopez-Nicolas, and C. Sagues. Reset adaptive observers and stability properties. In *18th Mediterranean Conference on Control and Automation, MED'10*, pages 1435–1440. IEEE, 2010.

[293] D. Paesa, C. Franco, S. Llorente, G. Lopez-Nicolas, and C. Sagues. Reset observers applied to MIMO systems. *Journal of Process Control*, 21:613–619, 04 2011.

[294] A. Palanikumar, N. Saikumar, and S. H. HosseinNia. No more differentiator in PID: Development of nonlinear lead for precision mechatronics. In *2018 European Control Conference (ECC)*, pages 991–996. IEEE, 2018.

[295] F. S. Panni, D. Alberer, and L. Zaccarian. Set point regulation of an EGR valve using a FORE with hybrid input bias estimation. In *2012 American Control Conference (ACC)*, pages 4221–4226. IEEE, 2012.

[296] F. S. Panni, H. Waschl, D. Alberer, and L. Zaccarian. Position regulation of an EGR valve using reset control with adaptive feedforward. *IEEE Transactions on Control Systems Technology*, 22(6):2424–2431, 2014.

[297] F. Perez, A. Baños, and J. Cervera. Design of networked periodic reset control systems. In *2011 IEEE International Symposium on Industrial Electronics*, pages 2003–2008. IEEE, 2011.

[298] F. Perez, A. Baños, and J. Cervera. Design of networked reset control systems for reference tracking. In *IECON 2011-37th Annual Conference of the IEEE Industrial Electronics Society*, pages 2566–2571. IEEE, 2011.

[299] F. Perez, A. Baños, and J. Cervera. Periodic reset control of an in-line ph process. In *ETFA2011*, pages 1–4. IEEE, 2011.

[300] F. Pérez Rubio. *Sistemas de control reseteado discretos: aplicaciones a control en red*. PhD thesis, Universidad de Murcia, 2013.

[301] S. Polenkova, J. W. Polderman, and R. Langerak. Stability criteria for planar linear systems with state reset. In *Proceedings of the 19th International Symposium on Mathematical Theory of Networks and Systems–MTNS*, volume 5, 2010.

[302] S. Polenkova, J. W. Polderman, and R. Langerak. Stability of reset systems. In *Proceedings of the 20th International Symposium on Mathematical Theory of Networks and Systems*, pages 9–13, 2012.

[303] S. Pourdehi and P. Karimaghaee. Stability analysis and design of model predictive reset control for nonlinear time-delay systems with application to a two-stage chemical reactor system. *Journal of Process Control*, 71:103–115, 2018.

[304] S. Pourdehi and P. Karimaghaee. Reset observer-based fault tolerant control for a class of fuzzy nonlinear time-delay systems. *Journal of Process Control*, 85:65–75, 2020.

[305] J. A. G. Prieto. *Hybrid reset control systems. Analysis, design and applications.* PhD thesis, Universidade de Vigo, 2014.

[306] J. A. G. Prieto, A. Barreiro, and S. Dormido. Frequency domain properties of reset systems with multiple reset anticipations. *IET Control Theory & Applications*, 7(6):796–809, 2013.

[307] J. A. G. Prieto, A. Barreiro, S. Dormido, and S. Tarbouriech. Delay-dependent stability of reset control systems with anticipative reset conditions. *IFAC Proceedings Volumes*, 45(13):219–224, 2012.

[308] C. Prieur, I. Queinnec, S. Tarbouriech, L. Zaccarian, et al. Analysis and synthesis of reset control systems. *Foundations and Trends® in Systems and Control*, 6(2-3):117–338, 2018.

[309] C. Raimúndez, A. Barreiro, and A. Fernández. Reset control for injecting dissipation into port-Hamiltonian systems. In *2009 European Control Conference (ECC)*, pages 4919–4924. IEEE, 2009.

[310] C. Raimúndez, A. Barreiro, and A. F. Villaverde. Damping injection by reset control. *Journal of dynamic systems, measurement, and control*, 134(2), 2012.

[311] A. Reyes-Lúa and S. Skogestad. Multi-input single-output control for extending the operating range: Generalized split range control using the baton strategy. *Journal of Process Control*, 91:1–11, 2020.

[312] J. Rico. *Control robusto cuantitativo de sistemas con múltiples entradas de actuación y una salida objeto de control.* PhD thesis, Universidad de La Rioja, 2017.

[313] J. Rico-Azagra, M. Gil-Martínez, and J. Elso. Quantitative feedback control of multiple input single output systems. *Mathematical Problems in Engineering*, 2014, 2014.

[314] J. F. Sáez and A. Baños. Tuning rules for the design of MISO reset control systems. In *2020 6th International Conference on Event-Based Control, Communication, and Signal Processing (EBCCSP)*, pages 1–7. IEEE, 2020.

[315] J. F. Sáez and A. Baños. Reset control of parallel MISO systems. *Mathematics*, 9(15):1823, 2021.

[316] J. F. Sáez, A. Baños, and A. Arenas. Reset-and-hold control of systems with time delay. *IEEE Access*, 10:101803–101813, 2022.

[317] N. Saikumar, K. Heinen, and S. H. HosseinNia. Loop-shaping for reset control systems: A higher-order sinusoidal-input describing functions approach. *Control Engineering Practice*, 111:104808, 2021.

[318] N. Saikumar and H. HosseinNia. Generalized fractional order reset element (GFrORE). In *9th European Nonlinear Dynamics Conference (ENOC)*, 2017.

[319] N. Saikumar, R. K. Sinha, and S. H. HosseinNia. Resetting disturbance observers with application in compensation of bounded nonlinearities like hysteresis in piezo-actuators. *Control Engineering Practice*, 82:36–49, 2019.

[320] N. Saikumar, R. K. Sinha, and S. H. HosseinNia. "constant in gain lead in phase" element–application in precision motion control. *IEEE/ASME Transactions on Mechatronics*, 24(3):1176–1185, 2019.

[321] N. Saikumar, D. Valério, and S. H. HosseinNia. Complex order control for improved loop-shaping in precision positioning. In *2019 IEEE 58th Conference on Decision and Control (CDC)*, pages 7956–7962. IEEE, 2019.

[322] T. Samad. A survey on industry impact and challenges thereof [technical activities]. *IEEE Control Systems*, 37:17–18, 2017.

[323] A. Satoh. State feedback synthesis of linear reset control with $\mathcal{L}_2$ performance bound via LMI approach. *IFAC Proceedings Volumes*, 44(1):5860–5865, 2011.

[324] A. Satoh. Synthesis of output feedback linear reset control based on common quadratic lyapunov-like function. In *2015 European Control Conference (ECC)*, pages 2162–2167. IEEE, 2015.

[325] S. J. Schroeck, W. C. Messner, and R. J. McNab. On compensator design for linear time-invariant dual-input single-output systems. *IEEE/ASME Transactions On Mechatronics*, 6(1):50–57, 2001.

[326] I. R. Scola, M. M. Quadros, and V. J. Leite. Robust hybrid PI controller with a simple adaptation in the integrator reset state. *IFAC-PapersOnLine*, 50(1):1457–1462, 2017.

[327] A. Sebastian, N. Karbasizadeh, N. Saikumar, and S. H. HosseinNia. Augmented fractional-order reset control: Application in precision mechatronics. In *2021 IEEE/ASME International Conference on Advanced Intelligent Mechatronics (AIM)*, pages 231–238. IEEE, 2021.

[328] M. M. Seron, J. H. Braslavsky, and G. C. Goodwin. *Fundamental limitations in filtering and control*. Springer Science & Business Media, 2012.

[329] A. Seuret, C. Prieur, S. Tarbouriech, and L. Zaccarian. Event-triggered control via reset control systems framework. *IFAC-PapersOnLine*, 49(18):170–175, 2016.

[330] M. Shahbazzadeh, S. J. Sadati, and S. H. HosseinNia. Optimal reset law design based on guaranteed cost control method for lipschitz nonlinear systems. *International Journal of Robust and Nonlinear Control*, 32(8):4739–4751, 2022.

[331] A. D. Shakibjoo and M. D. Shakibjoo. 2-DOF PID with reset controller for 4-DOF robot arm manipulator. In *2015 International Conference on Advanced Robotics and Intelligent Systems (ARIS)*, pages 1–6. IEEE, 2015.

[332] A. D. Shakibjoo and N. Vasegh. Method for analytically obtaining reset ratio in non-minimum phase systems with PI+CI controller in order to improve performance. *Journal of Mechatronics, Electrical and Computer Technology*, 4(13):1880–1899., 2014.

[333] A. D. Shakibjoo, N. Vasegh, and H. HosseinNia. IMC based smith predictor design with PI+CI structure: Control of delayed MIMO systems. *MATEC Web of Conferences*, 42:01011, 2016.

[334] D. Shin, W. Kim, Y. Lee, and C. C. Chung. Nonlinear control with state-dependant reset integrator for a class of singularly perturbed interconnected nonlinear systems. *IEEE Transactions on Control Systems Technology*, 25(4):1193–1203, 2016.

[335] Y. Shizuku and Y. Ishida. Design of a PID controller based on a reset compensator using the Clegg integrator. In *2016 IEEE 12th International Colloquium on Signal Processing & Its Applications (CSPA)*, pages 74–77. IEEE, 2016.

[336] V. Simoncini. Computational methods for linear matrix equations. *SIAM Review*, 58(3):377–441, Jan. 2016.

[337] S. Skogestad. Simple analytic rules for model reduction and PID controller design. *Journal of Process Control*, 13:291–309, 2003.

[338] R. G. Subramanian and V. K. Elumalai. Discrete-time setpoint-triggered reset integrator design with guaranteed performance and stability. *ISA transactions*, 81:155–162, 2018.

[339] K. Suyama and N. Kosugi. Integrator reset strategy based on $\mathcal{L}_2$ gain analysis. *International Journal of Contemporary Mathematical Sciences*, 7(39):1947–1962, 2012.

[340] K. Suyama and N. Kosugi. Controller reset strategy for anti-windup based on l2 gain analysis. In *IECON 2013 - 39th Annual Conference of the IEEE Industrial Electronics Society*, pages 3445–3450, 2013.

[341] K. Suyama and N. Sebe. Controller reset strategy for anti-windup based on switching gain analysis. *Asian Journal of Control*, 19(6):1877–1890, 2017.

[342] S. Tarbouriech, T. Loquen, and C. Prieur. Anti-windup strategy for reset control systems. *International Journal of Robust and Nonlinear Control*, 21(10):1159–1177, 2011.

[343] A. R. Teel. Continuous-time implementation of reset control systems. *Trends in Nonlinear and Adaptive Control*, pages 27–41, 2022.

[344] V. Toochinda and A. Suwannakom. Practical discrete-time implementation of reset control systems. In *2017 2nd International Conference on Control and Robotics Engineering (ICCRE)*, pages 86–91. IEEE, 2017.

[345] H. L. Trentelman, A. A. Stoorvogel, and M. Hautus. *Control Theory for Linear Systems*. Springer London, 2001.

[346] Z. Tu, B. Fan, J. Khazaei, W. Zhang, and W. Liu. Optimal reset-control-based load frequency regulation in isolated microgrids. *IEEE Transactions on Sustainable Energy*, 2022.

[347] H. Tugal, K. Cetin, Y. Petillot, M. Dunnigan, and M. S. Erden. Manipulation at optimum locations for maximum force transmission with mobile robots under environmental disturbances. *Autonomous Robots*, 46(6):769–782, 2022.

[348] N. Vafamand and A. Khayatian. Model predictive-based reset gain-scheduling dynamic control law for polytopic lpv systems. *ISA transactions*, 81:132–140, 2018.

[349] N. Vafamand, A. Khayatian, and M. H. Khooban. Stabilisation and transient performance improvement of DC MGs with CPLs: non-linear reset control approach. *IET Generation, Transmission & Distribution*, 13(14):3169–3176, 2019.

[350] D. Valério and J. Sá da Costa. Fractional reset control. *Signal, Image and Video Processing*, 6(3):495–501, 2012.

[351] D. Valério, N. Saikumar, A. A. Dastjerdi, N. Karbasizadeh, and S. H. HosseinNia. Reset control approximates complex order transfer functions. *Nonlinear Dynamics*, 97(4):2323–2337, 2019.

[352] S. van den Eijnden, M. F. Heertjes, W. Heemels, and H. Nijmeijer. Hybrid integrator-gain systems: A remedy for overshoot limitations in linear control? *IEEE Control Systems Letters*, 4(4):1042–1047, 2020.

[353] S. van Loon. *Hybrid control for performance improvement of linear systems*. PhD thesis, Technische Universiteit Eindhoven, 2016.

[354] S. Van Loon, K. Gruntjens, M. F. Heertjes, N. van de Wouw, and W. Heemels. Frequency-domain tools for stability analysis of reset control systems. *Automatica*, 82:101–108, 2017.

[355] A. Velasco-Pérez, J. Álvarez-Ramírez, and R. Solar-González. Multiple input-single output (MISO) control of a CSTR. *Revista mexicana de ingeniería química*, 10(2):321–331, 2011.

[356] P. Vettori, J. W. Polderman, and R. Langerak. A geometric approach to stability of linear reset systems. In *21st International Symposium on Mathematical Theory of Networks and Systems, MTNS 2014*, pages 776–783. University of Groningen, 2014.

[357] A. Vidal and A. Baños. Stability of reset control systems with variable reset: Application to PI+CI compensation. In *2009 European Control Conference (ECC)*, pages 4871–4876. IEEE, 2009.

[358] A. Vidal and A. Baños. Reset compensation for temperature control: Experimental application on heat exchangers. *Chemical Engineering Journal*, 159(1-3):170–181, 2010.

[359] A. Vidal and A. Baños. QFT-based design of PI+CI reset compensators: application in process control. In *2008 16th Mediterranean Conference on Control and Automation*, pages 806–811. IEEE, 2008.

[360] A. Vidal, A. Baños, J. C. Moreno, and M. Berenguel. PI+CI compensation with variable reset: application on solar collector fields. In *2008 34th Annual Conference of IEEE Industrial Electronics*, pages 321–326. IEEE, 2008.

[361] Y. Vidal, L. Acho, I. Cifre, À. Garcia, F. Pozo, and J. Rodellar. Wind turbine synchronous reset pitch control. *Energies*, 10(6):770, 2017.

[362] A. Vidal Sánchez. *Diseño de sistemas de control reseteado: aplicaciones en control de procesos*. PhD thesis, Universidad de Murcia, 2009.

[363] N. Wada. Model predictive tracking control for constrained linear systems using integrator resets. *IEEE Transactions on Automatic Control*, 60(11):3113–3118, 2015.

[364] H. Wang and S. Zhang. Event-triggered reset trajectory tracking control for unmanned surface vessel system. *Proceedings of the school of Mechanical Engineers, Part I: Journal of Systems and Control Engineering*, 235(5):633–645, 2021.

[365] H. Wang, F. Zhu, and Y. Tian. Event-triggered optimal reset control of hard disk drive head-positioning servo systems. *Proceedings of the school of Mechanical Engineers, Part I: Journal of Systems and Control Engineering*, 233(5):582–590, 2019.

[366] L. Wang and J. Dong. Reset event-triggered adaptive fuzzy consensus for nonlinear fractional-order multiagent systems with actuator faults. *IEEE Transactions on Cybernetics*, 2022.

[367] Q. Wang, Y. Zhao, and J. Hu. Reset output feedback control of cluster linear multi-agent systems. *Journal of the Franklin Institute*, 358(16):8419–8442, 2021.

[368] S. Wang, Y. Sun, X. Li, B. Han, and Y. Luo. An optimal robust design method for fractional-order reset controller. *Asian Journal of Control*, 2022.

[369] X. Wang and J. Zhao. Logic-based reset adaptation design for improving transient performance of nonlinear systems. *IEEE/CAA Journal of Automatica Sinica*, 2(4):440–448, 2015.

[370] C. Weise, K. Wulff, and J. Reger. Extended fractional-order memory reset control for integer-order LTI systems and experimental demonstration. *IFAC-PapersOnLine*, 53(2):7683–7690, 2020.

[371] G. Witvoet, W. Aangenent, W. Heemels, M. van de Molengraft, and M. Steinbuch. $\mathcal{H}_2$ performance analysis of reset control systems. In *2007 46th IEEE Conference on Decision and Control*, pages 3278–3284, 2007.

[372] D. Wu, G. Guo, and Y. Wang. Reset integral-derivative control for HDD servo systems. *IEEE Transactions on Control Systems Technology*, 15(1):161–167, 2006.

[373] G. Wu, H. Sun, B. Zhao, S. Xu, X. Zhang, A. Egea-Alvarez, S. Wang, G. Li, Y. Li, and X. Zhou. Low-frequency converter-driven oscillations in weak grids: Explanation and damping improvement. *IEEE Transactions on Power Systems*, 36(6):5944–5947, 2021.

[374] G. Wu, S. Wang, B. Zhao, H. Hu, J. Li, L. Cao, H. Ding, L. Yu, and Q. Ma. Converter-driven low-frequency stability analysis and compensation in weak-grid-tied VSCs. In *2021 International Conference on Power System Technology (POWERCON)*, pages 1634–1639. IEEE, 2021.

[375] H. Wu, Y. Guo, W. Gui, and Z. Jiang. Reset PID control with an application to ball-beam systems. In *Proceedings of the 32nd Chinese Control Conference*, pages 986–991. IEEE, 2013.

[376] X. Xiao, J. H. Park, and L. Zhou. Stabilization of switched linear singular systems with state reset. *Journal of the Franklin Institute*, 356(1):237–247, 2019.

[377] X. Xu, X. Li, P. Dong, Y. Liu, and H. Zhang. Robust reset speed synchronization control for an integrated motor-transmission powertrain system of a connected vehicle under a replay attack. *IEEE Transactions on Vehicular Technology*, 70(6):5524–5536, 2020.

[378] Y. Xu, J. Zhou, H. Rao, R. Lu, and L. Xie. Reset moving horizon estimation for quantized discrete time systems. *IEEE Transactions on Automatic Control*, 66(9):4199–4205, 2020.

[379] H. Yan, X. Huang, M. Wang, and H. Zhang. Delay-dependent stability criteria for a class of networked control systems with multi-input and multi-output. *Chaos, Solitons & Fractals*, 34(3):997–1005, 2007.

[380] S. Yazdi and A. Khayatian. Performance improvement by optimal reset dynamic output feedback control based on model predictive strategy. *Journal of Process Control*, 88:78–85, 2020.

[381] S. Yazdi, A. Khayatian, and M. H. Asemani. Optimal robust model predictive reset control design for performance improvement of uncertain linear system. *ISA transactions*, 107:78–89, 2020.

[382] S. Yazdi, A. Khayatian, M. H. Asemani, and N. Vafamand. Designing an optimal reset controller for TS fuzzy systems. *IEEE Transactions on Systems, Man, and Cybernetics: Systems*, 52(6):4033–4044, 2021.

[383] Q. Yu, Y. Guo, and X. Zhao. Stability analysis of reset positive systems with discrete-time triggering conditions. *Applied Mathematics Letters*, 39:80–84, 2015.

[384] Q. Yu, Y. Guo, and X. Zhao. Stability analysis of reset positive systems with discrete-time triggering conditions. *Applied Mathematics Letters*, 39:80–84, 2015.

[385] C. Yuan and F. Wu. Analysis and synthesis of linear hybrid systems with state-triggered jumps. *Nonlinear Analysis: Hybrid Systems*, 14:47–60, 2014.

[386] C. Yuan and F. Wu. Output feedback reset control of general MIMO LTI systems. In *2014 European Control Conference (ECC)*, pages 2334–2339, June 2014.

[387] L. Zaccarian, D. Nesic, and A. R. Teel. First order reset element and the clegg integrator revisited. In *Proc. American Control Conference*, volume 1, pages 563–568, 2005.

[388] L. Zaccarian, D. Nesic, and A. R. Teel. Explicit lyapunov functions for stability and performance characterizations of FOREs connected to an integrator. In *Proceedings of the 45th IEEE Conference on Decision and Control*, pages 771–776. IEEE, 2007.

[389] L. Zaccarian, D. Nešić, and A. R. Teel. Analytical and numerical Lyapunov functions for SISO linear control systems with first-order reset elements. *International Journal of Robust and Nonlinear Control*, 21(10):1134–1158, 2011.

[390] S. Zaragoza, J. Sanchez, and A. Baños. Identificación de sistemas de primer y segundo orden mediante control basado en reset. *Revista Iberoamericana de Automática e Informática industrial*, 17(2):116–129, 2020.

[391] M. Zarghami and H. S. HosseinNia. Fractional order set point regulator using reset control: Application to EGR systems. In *Proceedings of the 2017 The 5th International Conference on Control, Mechatronics and Automation*, pages 35–41, 2017.

[392] J. Zhai, Y. Wang, and X. Liu. Optimal reset controller designed for induction machine drive with hardware in the loop test. In *2017 IEEE Applied Power Electronics Conference and Exposition (APEC)*, pages 506–511. IEEE, 2017.

[393] T. Zhan, S. Ma, X. Liu, and H. Chen. Impulsive observer design for a class of switched nonlinear systems with unknown inputs. *Journal of the Franklin Institute*, 356(12):6757–6777, 2019.

[394] C. Zhang, P. Dong, H. Leung, J. Wu, and K. Shen. Reset and prescribed performance approach to spacecraft attitude regulation. *Aircraft Engineering and Aerospace Technology*, 2021.

[395] J. Zhang, F. Zhu, X. Zhao, and F. Wang. Robust impulsive reset observers of a class of switched nonlinear systems with unknown inputs. *Journal of the Franklin Institute*, 354(7):2924–2943, 2017.

[396] S. Zhang, H. Wang, and Y. Tian. Event-triggered reset controller design and its application to trajectory tracking for USV system. In *2020 Chinese Control And Decision Conference (CCDC)*, pages 40–45. IEEE, 2020.

[397] S. Zhang, H. Wang, and Y. Tian. A TS fuzzy state observer-based model predictive reset control for a class of fuzzy nonlinear systems with event-triggered mechanism. *Journal of the Franklin Institute*, 2022.

[398] G. Zhao. Model-based reset control for overcoming performance limitations of linear feedback. In *2015 54th IEEE Conference on Decision and Control (CDC)*, pages 2241–2246. IEEE, 2015.

[399] G. Zhao, G. Chen, and J. Mi. Overcoming a fundamental limitation of linear systems with generalized first order reset element. In *2018 37th Chinese Control Conference (CCC)*, pages 2042–2047. IEEE, 2018.

[400] G. Zhao and H. Cui. A novel reset control approach to leader-following consensus of second-order nonlinear multi-agent systems. *Journal of the Franklin Institute*, 358(18):9678–9697, 2021.

[401] G. Zhao, H. Cui, and Z. Li. Distributed reset control for leader-following consensus of nonlinear multi-agent systems. *International Journal of Control, Automation and Systems*, 20(3):983–991, 2022.

[402] G. Zhao and C. Hua. Improved high-order-reset-element model based on circuit analysis. *IEEE Transactions on Circuits and Systems II: Express Briefs*, 64(4):432–436, 2016.

[403] G. Zhao and C. Hua. Discrete-time MIMO reset controller and its application to networked control systems. *IEEE Transactions on Systems, Man, and Cybernetics: Systems*, 48(12):2485–2494, Dec 2018.

[404] G. Zhao, C. Hua, and X. Guan. Reset control for consensus of multiagent systems with asynchronous sampling. *IEEE Transactions on Systems, Man, and Cybernetics: Systems*, 51(8):4911–4919, 2019.

[405] G. Zhao, C. Hua, and X. Guan. Reset control for consensus of multiagent systems with event-triggered communication. *IEEE Transactions on Cybernetics*, 51(11):5387–5396, 2019.

[406] G. Zhao, C. Hua, and X. Guan. Reset observer-based Zeno-free dynamic event-triggered control approach to consensus of multiagent systems with disturbances. *IEEE Transactions on Cybernetics*, 2020.

[407] G. Zhao and C.-C. Hua. Leader-following consensus of multi-agent systems via asynchronous sampled-data control: A hybrid systems approach. *IEEE Transactions on Automatic Control*, 2021.

[408] G. Zhao and J. Mi. Observer-based reset law design for linear uncertain systems based on model predictive strategy. In *2016 35th Chinese Control Conference (CCC)*, pages 2402–2407. IEEE, 2016.

[409] G. Zhao, J. Mi, J. Leng, and C. Hua. Networked reset control systems with time delays in both forward and feedback channels. In *2017 IEEE 56th Annual Conference on Decision and Control (CDC)*, pages 5985–5990. IEEE, 2017.

[410] G. Zhao, D. Nešić, Y. Tan, and C. Hua. Overcoming overshoot performance limitations of linear systems with reset control. *Automatica*, 101:27–35, 2019.

[411] G. Zhao, D. Nešić, Y. Tan, and J. Wang. Open problems in reset control. In *52nd IEEE Conference on Decision and Control*, pages 3326–3331. IEEE, 2013.

[412] G. Zhao, D. Nesic, Y. Tan, and J. Wang. Improving $\mathcal{L}_2$ gain performance of linear systems by reset control. *IFAC Proceedings Volumes*, 47(3):6400–6405, 2014.

[413] G. Zhao and J. Wang. Reset observers for linear time-varying delay systems: Delay-dependent approach. *Journal of the Franklin Institute*, 351(11):5133–5147, 2014.

[414] G. Zhao and J. Wang. Existence and design of non-overshoot reset controllers for minimum-phase linear single-input single-output systems. *IET Control Theory & Applications*, 9(17):2514–2521, 2015.

[415] G. Zhao and J. Wang. Reset control systems with time-varying delay: delay-dependent stability and gain performance improvement. *Asian Journal of Control*, 17(6):2460–2468, 2015.

[416] G. Zhao and J. Wang. Stability and stabilisation of reset control systems with uncertain output matrix. *IET Control Theory & Applications*, 9(8):1312–1319, 2015.

[417] G. Zhao and J. Wang. Stability and stabilisation of reset control systems with uncertain output matrix. *IET Control Theory & Applications*, 9(8):1312–1319, 2015.

[418] G. Zhao and J. Wang. Stability and stabilisation of reset control systems with uncertain output matrix. *IET Control Theory & Applications*, 9(8):1312–1319, 2015.

[419] G. Zhao and J. Wang. Discrete-time triggered reset law design based on model predictive strategy for linear systems. *IET Control Theory & Applications*, 10(3):282–291, 2016.

[420] G. Zhao and J. Wang. Observer-based reset law design for uncertain systems by using model predictive strategy. *Transactions of the Institute of Measurement and Control*, 38(9):1064–1072, 2016.

[421] G. Zhao and J. Wang. Observer-based reset law design for uncertain systems by using model predictive strategy. *Transactions of the Institute of Measurement and Control*, 38(9):1064–1072, 2016.

[422] G. Zhao and J. Wang. On l2 gain performance improvement of linear systems with lyapunov-based reset control. *Nonlinear Analysis: Hybrid Systems*, 21:105–117, 2016.

[423] G. Zhao, J. Wang, and K. Li. On overcoming limitations of a class of linear systems with first-order reset elements. In *Proceeding of the 11th World Congress on Intelligent Control and Automation*, pages 4218–4223. IEEE, 2014.

[424] G. Zhao, J. Wang, and K. Li. On stability analysis and synthesis of reset control systems with output uncertainties. In *Proceedings of the 33rd Chinese Control Conference*, pages 3965–3969. IEEE, 2014.

[425] G. Zhao, J. Wang, and B. Zhang. Stability analysis of periodic triggering reset control systems. *International Journal of Control, Automation and Systems*, 13(4):788–797, 2015.

[426] X. Zhao, Y. Yin, and J. Shen. Reset stabilisation of positive linear systems. *International Journal of Systems Science*, 47(12):2773–2782, 2016.

[427] X. Zhao, Y. Yin, and J. Shen. Reset stabilisation of positive linear systems. *International Journal of Systems Science*, 47(12):2773–2782, 2016.

[428] J. Zheng and M. Fu. A reset state estimator using an accelerometer for enhanced motion control with sensor quantization. *IEEE Transactions on Control Systems Technology*, 18(1):79–90, 2009.

[429] J. Zheng, Y. Guo, M. Fu, Y. Wang, and L. Xie. Improved reset control design for a pzt positioning stage. In *2007 IEEE International Conference on Control Applications*, pages 1272–1277. IEEE, 2007.

[430] J. Zheng, Y. Guo, M. Fu, Y. Wang, and L. Xie. Development of an extended reset controller and its experimental demonstration. *IET Control Theory & Applications*, 2(10):866–874, 2008.

[431] Y. Zheng. *Theory and practical considerations in reset control design*. PhD thesis, University of Massachusetts, 1998.

[432] Y. Zheng, Y. Chait, C. Hollot, M. Steinbuch, and M. Norg. Experimental demonstration of reset control design. *Control Engineering Practice*, 8(2):113–120, 2000.

[433] F. Zhu, H. Wang, and Y. Tian. Optimal law based improved reset PID control and application to hdd head-positioning systems. In *2017 32nd Youth Academic Annual Conference of Chinese Association of Automation (YAC)*, pages 258–262. IEEE, 2017.

Glossary

CI	Clegg Integrator
FO	First Order
FOPDT	First Order Plus Dead Time
FORE	First Order Reset Element
HI	Hybrid Inclusions
HO	Higher Order
IAE	Integrated Absolute Error
IAEU	Integrated Absolute Error of u_1-signal
IDS	Impulsive Dynamical Systems
ISE	Integrated Squared Error
ISEU	Integrated Squared Error of u_1-signal
LTI	Linear Time-Invariant
MIMO	Multiple-Input Multiple-Output
MISO	Multiple-Input Single-Output
PI	Proportional-Integral
PI+CI	Proportional-Integral plus Clegg Integrator
PID	Proportional-Integral-Derivative
SIMO	Single-Input Multiple-Output
SISO	Single-Input Single-Output
TISO	Two-Input Single-Output

Notation:

$\mathbb{R}$	Set of real numbers
$\mathbb{R}_{\geq 0}$	Set of nonnegative real numbers
$\mathbb{Z}$	Set of integers
$\mathbb{Z}_{\geq 0}$	Set of nonnegative integers
$\mathbb{R}^n$	n-dimensional Euclidean space
$\mathbb{R}^{n\times m}$	Set of $n \times m$ real matrices
$\mathcal{M}^{\Delta}$	Space of hybrid memory arcs with memory of size Δ
$f : A \to B$	f is a function from A to B
$f : A \rightrightarrows B$	f is a set-valued map from A to B
$\operatorname{dom} \phi$	Domain of the hybrid arc ϕ
$A^\top$	Matrix transpose of A
$A > 0$	Matrix A is positive definite
$A \geq 0$	Matrix A is positive semidefinite
$I, 0$	Identity and zero matrices (of implicit dimension)
$\lvert \cdot \rvert$	Euclidean norm on $\mathbb{R}^n$
$\lvert \cdot \rvert_{\mathcal{W}}$	Distance to the set $\mathcal{W}$
$\lvert\lvert A \rvert\rvert$	Operator norm of the matrix A
$\lvert\lvert \phi \rvert\rvert_{\mathcal{W}}$	Supremum distance to the set $\mathcal{W}$ of the hybrid arc ϕ
$\times, \setminus$	Cartesian product and set difference
$X^\circ, \overline{X}$	Interior and closure of the set X
$\operatorname{conv} X$	Convex hull of the set X
k_P	Proportional gain
T_I	Integral time
θ	Variable band
τ_H	Holding time
p_r	Reset ratio